Polymer-drug conjugates as platforms for combination therapy in the treatment of hormone-dependent breast cancer.

Coralie Deladriere

Programa Oficial de Postgrado en "Bioquímica ClinicoMédica e Inmunología"

Directores

Dra. María J. Vicent and Dra. Rut Lucas

Dr Maria Jesus Vicent Docon, PhD in Chemistry and Head of the Therapeutic Polymer Laboratory in Centro de Investigación Príncipe Felipe, Valencia, Spain.

Dr Rut Lucas Domínguez, PhD in Pharmacy and Assistant Professor in Department of History of Science and Information Science. School of Medicine. University of Valencia. Spain.

CERTIFY, that the work "**Polymer-drug conjugates as platforms for combination therapy in the treatment of homone-dependent breast cancer.**" Has been developed by Coralie Deladriere under her supervision in Centro de Investigación Príncipe Felipe in Valencia, as a thesis project in order to obtain a PhD degree in Biochemistry at University of Valencia, Biochemistry and Molecular Biology Department.

Dr. Maria J Vicent Docon   Dr. Rut Lucas Dominguez

Agradecimientos.

Una tesis es una vida dentro de la vida. Creo que he aprendido más en estos 5 años que durante los 10 últimos. Hablo de ciencia, yo soy química, y cual ha sido mi sorpresa cuando he acabado haciendo ovariectomización a los ratones y western blot (lo mejor de todo es que me gusta más que la química!!!). Además durante este período he aprendido también muchísimo de mí misma. Aprendí a gestionar un proyecto, aprendí a gestionar y aceptar tanto las victorias como las decepciones. Aprendí a tener paciencia y a conocer mis límites. Aprendí también a supervisar estudiantes, aunque seguro, me falta todavía muchísimo por descubrir, aprender y desarrollar. Todos estos pasos no hubieran sido posibles sin toda la gente que conocí aquí en Valencia y a los cuales me gustaría dar las gracias.

Primero me gustaría agradecer a mis directoras de tesis Dra María Jesús Vicent y Dra Rut Lucas sin las cuales no hubiera podido llevar a cabo esta tesis. María Jesús muchas gracias por la oportunidad que me diste de hacer la tesis en tu laboratorio y por la confianza que me diste a la hora de elegirme para la beca FPI. Gracias a tus consejos y a las soluciones que me diste pude acabar esta tesis. Muchas gracias también por darme ánimos y por tu optimismo. Rut muchas gracias por haberme apoyado durante todo el proceso y siempre animarme cuando lo necesitaba. Gracias por las discusiones. He aprendido muchísimo de vosotras.

Me gustaría también agradecer al I-36, más que un laboratorio ha sido una familia! Me fui de Francia para realizar esta tesis y ha sido toda una suerte conocer a gente como los del I-36. Primero me gustaría dar las gracias a mis dos compañeras de despacho Ana y Esther sin las cuales no hubiera podido hacer esta tesis. Gracias Ana por nuestras charlas tanto de trabajo como sobre la vida en general. Muchísimas gracias por tu apoyo y tu ayuda. Por las horas pasadas en el animalario, por las tardes que hemos pasado interpretando resultados! Sin ti no hubiera podido hacer esta tesis! Gracias también por las comidas en Algimia, los cursos de pilates y de

aerobic! Gracias Esther por todo tu apoyo, tu paciencia enseñandome los cultivos celulares! Las miles de veces que miramos los cálculos. Gracias por nuestras charlas tanto dentro como fuera del laboratorio. Las 3 semanas de curso de animales, las cenas de chicas, las risas, las fiestas en el pueblo y mucho más.

Como es lógico me gustaría también agradecer al "PhD team". Chicas, este trabajo os lo dedico a vosotras también!! En orden de llegada, Gracias Vanessa por los años compartidos, los años del despacho de las PhD. Mi pequeña Inma, muchas gracias por ser como eres!! Eres una persona grande de la cual he aprendido mucho. Gracias por tu generosidad, tus consejos, tu apoyo y tu energía que compartiste conmigo!!! Mi Gabi, gracias por tu dulzura, tu apoyo, tus ánimos!! Ahora te mando yo todo el ánimo y el apoyo que necesitas en tu última recta final!! Aroa, que decir de ti que no sepas ya! Eres una persona muy grande. Gracias por nuestras charlas, tus consejos y tus ideas. Gracias por haber compartido estos años conmigo y por tu amistad! Gracias por las cenas, los viajes, las fiestas y mucho más. No tengo palabras para exprimir todo lo que me has aportado. Amaya, gracias por tu manera de ser, siempre cuidando a los demás y preocupándote! Gracias chicas por las fondues de chocolate, estoy segura que *Haagen Dazs* se está haciendo más pobre ahora que nos vamos. Esta tesis no hubiera podido acabarla sin cada una de vosotras!!!

Quiero también dar las gracias a todos los estudiantes y personas que han pasado por el CIPF trabajando en este proyecto! habéis hecho avanzar esta tesis y me habéis hecho crecer como persona. Julie, Angela, Raoul, Antonio, Jentle, Marlies, JuanJo, David y especialmente a Helena que fue la primera persona con quien trabajé. Gracias por todo y por tu amistad!

Me gustaría también darle las gracias a María Helena, por tu apoyo, por nuestras charlas y tus consejos!! Por todos los pedidos y reclamaciones que has tenido que hacer y también por los cortes histológicos.

Me gustaría también dar las gracias a toda la gente que paso o está en el I-36, Lucile, Fabiana, Ximo, Edgard, Mathias, David, Marina, Rich, sin vosotros la aventura no hubiera sido igual y a la nueva generación del I-36, Julie, Vincent, Ismael, Juanjo, disfrutar de este I-36 y seguir haciéndolo tan especial!

Me falta una persona por nombrar, Anita sin ti seguro que no hubiera podido acabar la tesis!!! Gracias por tus masajes, eres una fisioterapeuta y amiga muy grande!!! Si no me hubieras tratado, hoy no podría girar la cabeza e iría a todos los sitios cojeando!!! Gracias también por escucharme, tus consejos, tu apoyo, y por las cenas de chicas.

Ahora voy a pasar a Francés (mi lengua materna), je voulais également remercie ma famille et ma belle famille qui ont toujours été là. Inquiet et rassurant dans les moments de doutes et de raz le bol et euphorique et présent pour partager mes victoires. Je voudrais également remercier tous mes amis de France et d'Espagne qui ont toujours été la pour me remonter le moral ou pour accompagner mes succès !!!

Et comment ne pas finir par mon mari à qui je dois cette thèse, sans lui je n'aurais surement pas réussir à surmonter tous ces mauvais moments et tous ces doutes. Merci pour m'avoir écouté milles fois te parler de mes problèmes et de partager mes joies !!! Merci d'avoir su écouter mes milliers d'essaie pour mes présentations aux divers congrès! Je pense que tu les connaissais autant que moi ! Et tout simplement merci d'être toi et d'avoir rendue ce parcourt aussi facile !!! Cette thèse est autant la tienne que la mienne, c'est la notre!!! Merci d'être dans ma vie et d'être toi.

9

Abbreviations List.

AC: Anthracycline in combination with cyclophosphamide

ACE: Angiotine II and angiotensin converting enzyme

ACN: Acetonitrile

AF-1: Activation function 1

AF-2: Activation function 2

AGM: Aminogluthetimide

Akt: Protein kinase B

ALN: Alendronate

ALP: Alkaline phosphate

ANOVA: Analysis of variance

APS: Ammonium persulfate

A.U.: Absorbance unit

Bax: Bcl2 associated X protein

Bcl2: B-cell lymphoma 2

Boc-Leu-Gly: Tert-butyl oxy carbonyl Leucine-Glycine

BSA: Bovine Serum Albumin

CAF: Cyclophosphamide, 5-fluorouracyl

Casp3: Caspase3

CHCl$_3$: Chloroform

CI: Combination Index

Conc: Concentration

CMF: Cyclophosphamide, Methotrexate, 5-Fluorouracil

CMFVP: Cyclophosphamide, Methotrexate, 5-Fluorouracil, Vincristine, Prednisone

CPT: Camptothecin

Dau: Daunorubicin

DAO: D-amino acid oxidase

DAB: Diaminobenzil

DBD: DNA binding domain

DCC: N,N'-diclyclohexyl carbodiimide

DCIS: Ductal carcinoma in situ

DIC: N,N'-Diisopropylcarbodiimide

DIEA: Diisopropyl ethyl amide

DIGE: Difference in gel electrophoresis

DMAP: 4-Dimethyl amino pyridine

DMEM: Dulbecco's Modified Eagle's Medium

DMF: Dimethylformamide

DMSO: Dimethylsufoxide

Dox: Doxorubicin

DTT: Dithiothreitol

DTX: Docetaxel

EDTA: Ethylenediaminetetraacetic acid

EGF: Epidermal growth factor

EGFR: Epidermal growth factor receptor

ELIOT: Electron Intra Operative Therapy

Epi: Epirubicin

EPR: Enhanced permeability and retention

ER: Oestrogen receptor

ERE: Oestrogen response element

Erk: Extracellular signal-regulated kinase

ESF: Science Foundation

EtAc: Ethyl acetate

FBS: Foetal bovine serum

FD: Free drug

FDA: The food and drug administration

Fmoc-Cl: Fluorenyl methyl chloride

Fmoc-Gly: Fluorenyl methyl Glycine

Gem: Gentamycin

GFLG: Glycine Phenylalanine Leucine Glycine

GlyGly: Glycine Glycine

GOT: Glutamic oxaloacetic transaminase

GPC: Gel Permeation Chromatography

GPT: Glutamic pyruvate transaminase

HER: Hypoxia response elements

HDBC: Hormone dependent breast cancer

HIF1-α: Hypoxia-inducible factor-1 alpha

HOBt: Hydroxy benzotriazole

HPLC: High Performance Liquid Chromatography

HPMA: N-(2-hydroxypropyl) methacrylamide

HTPS : High Throughput Screening

IC50: Inhibition concentration 50%

IGFR: Insulin-like growth factor receptor

iNOS: Induced nitric oxide synthase

i.v.: Intravenous

LBD: Ligand binding domain

LC3: Microtubule-associate protein light chain 3

LCIS: Lobular carcinoma in situ

LDH: Lactate dehydrogenase

LHRH: Luteinizing-hormone-releasing hormone

LS: Light Scattering

MALDI-ToF: Matrix-Assisted Laser Desorption/Ionisation- Time of flight

MßCD: Methyl-β-cytclodextrin

MeOH: Methanol

MS: Mass Spectrometry

MTD: Maximum tolerated dose

mTOR: Mammalian target of rapamycin

MTS: (3-(4,5-dimethylthiazol-2-yl)-5-(3-carboxymethoxyphenyl)-2-(4-sulfophenyl)-2H-tetrazolium)

Mw: Molecular Weigh

NO: Nitric Oxide

ONp: p-Nitrophenol

PBS: Phosphate buffer saline

PE: Phosphatidylethanolamine

PEG: Polyethylene glycol

PDEPT: Polymer directed enzyme prodrug

PELT: Polymer enzyme liposome therapy

PDI: Poly dispersion index

PFA: Paraformaldehyde

PGA: Poly-L-Glutamic acid

PGA-OS: Succinic Poly-L-Glutamic acid

PI: Propidium Iodide

PMS: Phenazine methosulfate

PR: Progesterone receptor

(P/S): Penicillin/ Streptomycin

PTX: Paclitaxel

RI: Refractive Index

RTK: Receptor Tyrosine Kinase

SD: Standard deviation

SDS: Dodecyl sulphate

SEC: Size Exclusion Chromatography

SEM: Standard error of mean

SERM: Selective oestrogen receptor modulators

TDL: Total drug loading

TEMED: Tetramethylethylenediamine

TGF α: Transforming growth factor alpha receptor

TLC: Thin Layer chromatography

Tr: Retention time

UDL: Undirected drug loading

UV: Ultraviolet

VEGF: Vascular Endothelial Growth Factor

WOR: Phosphatidyl inositol-3 kinase inhibitor wortmannin

Z: Carboxylbenzyl

Z-Gly: Carbobenzyloxy Glycine

Z-GlyGly: Carbobenzyloxy Glycine Glycine

Z-Gly-Phe: Carbobenzyloxy Glycine Phenylalanine

ZnPP: Zinc-protoporphyrin

4 OH: 4-OH-Tamoxifen

5-FU: 5-Fluorouracil

Chapter 1. General Introduction.

1.1. General Introduction.

The use of targeted drug delivery systems has become a real need in the clinic and 'Nanomedicine' has already demonstrated its key role in this field (Ferrari, 2005). Nanomedicine presents advantages to target cancer at late stages as its nanometric scale facilitates the pass through different biological barriers and could attain specifically the damaged cell more efficiently. More than 40 nanomedicines are in routine clinical use since the 90's including liposomal formulations (*i.e.* with doxorubicin (Dox)) Doxil® (Barenholz, 2012), nanocrystals or polymer therapeutics (*i.e.* PEGylated proteins) (Duncan and Gaspar, 2011).

Polymer therapeutics has emerged as the first generation of polymeric nanomedicines (Duncan, 2003). The term polymer therapeutics includes (1) water-soluble polymers with inherent activity known as polymeric drugs; (2) polymer-drug and (3) polymer-protein conjugates; (4) polymeric-micelles that contain covalently bound drugs and (5) multicomponent polyplexes used as non-viral vectors for gene delivery. Thirteen polymer therapeutics are already in routine clinical use (mostly PEGylated proteins) and many are in advanced clinical research (Duncan and Vicent, 2013).

Polymer anticancer drug conjugates are nano-sized, multi-component constructs, used both as single agents and as elements of combinations. They have the potential to improve pharmacological therapy of a variety of solid tumours mainly due to two mechanisms: (i) polymer-drug conjugation that promotes passive tumour targeting by the enhanced permeability and retention (EPR) effect and (ii) allows for lysosomotropic drug delivery following endocytic capture (Duncan, 2006, Vicent and Duncan, 2006) (see chapter 1.4.2 for more detailed explanation).

In the early 1980's, Duncan and collaborators designed the first polymer anticancer drug conjugate to enter clinical trials, N-(2-hydroxypropyl) methacrylamide (HPMA) copolymer-Dox (HPMA-Dox, PK1, FCE28068) (Vasey et al., 1999; Seymour et al., 2009). After PK1, an

exponential growing number of polymer conjugates have been transferred into the clinics bearing different anticancer agents (such as Paclitaxel (PTX) or campthotecin (CPT)) and different polymeric carriers (HPMA), polyethylenglycol (PEG) or poly-L-glutamic acid (PGA)) (Canal et al, 2011; Sanchis et al., 2010; Knop et al., 2010). Many of them have shown even more promising results mainly in combination with other therapy (Herzog et al., 2005) and for example, the most advance, Opaxio®, a PGA-PTX conjugate in Phase III has been designated as orphan drug for the treatment of glioblastoma when combined with radiotherapy (Duncan and Vicent, 2013). These facts have opened the field to a second generation of polymer drug conjugates based on combinations and to the term coined as polymer-based combination therapy (Greco and Vicent, 2009; Deladriere et al., 2010).

Breast cancer is the most common cause of cancer death in women worldwide, estimated to be responsible for around 458 500 female death in 2008 or nearly one in seven (around 14%) of all cancer deaths in women being higher after 40 years old, age of menopause (figure 1.1.) (http://www.cancer.org; http://www.cancerresearchuk.org / cancer- info / cancerstats /types / breast/ mortality/).

(a) 2010 new cancer cases   (b)

all cancers	6 234
Prostate	832
Breast	575
Brain	405
Skin	333
Lung	318
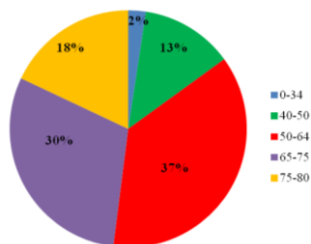
Figure 1.1. Representative cancer statistics in 2010. Panel (a) shows worldwide cancer statistics and panel (b) shows the percentage of breast cancer incidence depending on age (http://www.cancer.org; http://www.cancerresearchuk.org/cancer-info/cancerstats/types/breast/mortality/).

Moreover based on TNM classification (annexe II), breast cancer stage (annexe III) could be determined having a direct correlation with survival (figure 1.2.) in collaboration with receptor status, patient menopausal status and age.
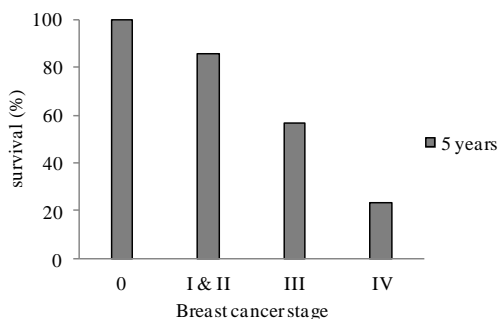
Figure 1.2. Representation of the percentage of survival at 5 years depending on disease stage (described in annexe II) (Maughan et al., 2010).

Good prognostic is achieved in the earliest stages of breast cancer thanks to the widespread use of mammographic screening, precise diagnosis and increased numbers of women receiving the adequate treatment for their conditions. However in the latter stage (III and IV) the survival is still really low and an efficient treatment is still required.

Due to the molecular complexity of cancer, the use of polymer-drug conjugates in combination therapy represents an important opportunity to enhance tumour response rates as the polymeric carrier provides an ideal platform for the simultaneous delivery of drug cocktails (Greco and Vicent, 2009; Deladriere et al., 2010). In the treatment of hormone-dependent breast cancer, it has been demonstrated that the combination of endocrine therapy with a chemotherapeutic agent may bring significant advantages (Vicent et al., 2005; Greco et al., 2007; Greco et al., 2005). This novel approach includes drug synergism and patience compliance. In this study, the conjugate containing both drugs (HPMA copolymer-AGM-Dox) showed markedly enhanced cytotoxicity compared with HPMA copolymer-Dox (Greco et al., 2005; Vicent et al.,

22

2005; Greco et al., 2007), which has already shown clinical activity in anthracycline-resistant breast cancer patients (Duncan et al., 1992).

HPMA copolymer-AGM-Dox combination conjugate is the starting point of this project and has been used as model system. The final aim of this study is to develop a new family of clinically relevant polymer-based combination conjugates for the treatment of advanced hormonal dependent breast cancer, using endocrine therapy in combination with chemotherapy. Multivalent polymeric carrier, passive tumour targeting and drug cocktail release at the same target site are advantages of the conjugate design including also lesser side effects and better patience compliance.

To accomplish this goal it was considered of importance, first, to achieve *in vivo* proof of concept of the already reported system (HPMA copolymer-AGM-Dox conjugate (Vicent et al., 2005; Greco et al., 2007). At the same time it was taken into account that the understanding of the molecular basis for synergism could provide guidance in conjugate design. As a second step, due to the fact that HPMA copolymer could present limitations in its use for chronic diseases as a result of its non biodegradability, we aim to synthesise the same combination conjugate but using a biodegradable carrier, such as PGA (Singer et al., 2003) also in advanced clinical trials. The same drug combination (AGM-Dox) was used in order to understand the carrier effect resulted from its evaluation of antitumor properties in *in vitro* and *in vivo* breast cancer models. Finally, taking into account that AGM is a first generation aromatase inhibitor not used anymore in the clinic, a High Throughput Screening (HTPS) including other endocrine therapies and cytotoxic drugs, was implemented in order to identify novel drug combinations for future design of PGA-based combination conjugates.

1.2. Hormone dependent breast cancer.

1.2.1. Breast organ development and oestrogen involvement.

Breast organ is made up mostly of fat and breast tissue, along with nerves, veins, arteries and connectives tissue. Breast tissue is a complex network of lobules (milk production) and ducts (canals that carry milk from lobules to the nipple). Breast development is well controlled by different hormones according to the different women stage.
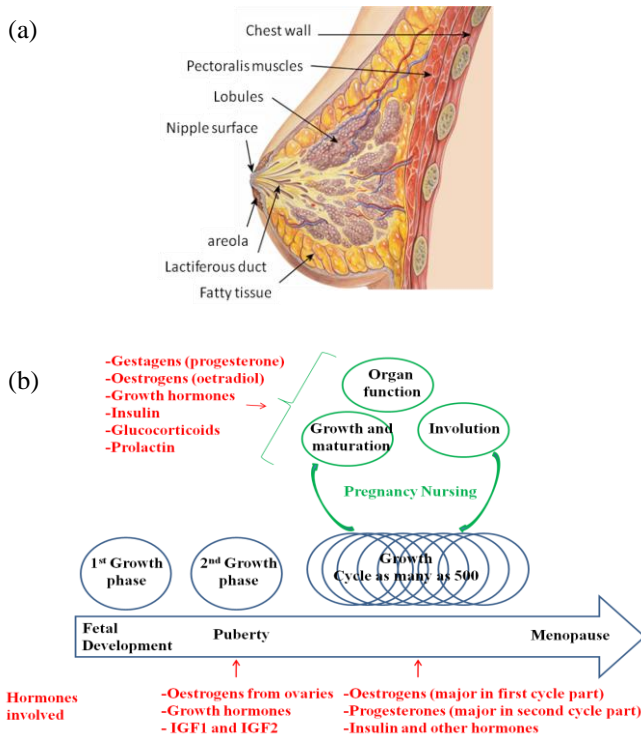
Figure 1.3. Breast organ. Panel (a) shows the breast representation (http://www.cancertreatment-wecareindia.com/breast_cancer.html). Panel (b) shows breast evolution steps and its hormones involved, adapted from (Schulz, 2005).

As described above, breast cancer is a multifactorial cancer. In this context, life style such as a late menopause, the age of the first periods, a belated pregnancy or even a fat diet can be involved in breast cancer

development (Dolle et al., 2009; Phipps et al., 2011; McNamara et al., 2012). Indeed, those life styles induce an extended exposure to oestrogens and a higher number of cell cycles that implicates a greater proportional mutation risk and longer carcinogenic cell proliferation stimulation (Schulz, 2005). On the contrary, during pregnancy, strong signals reinforce differentiation of breast ductal cell and extensive apoptosis of alveolar and ductal cells after weaning. All those cycle modifications induce an elimination of abnormal mutations and reduce breast cancer risk (Schulz, 2005; Barnes et al., 2012). Spontaneous mutation is not the only explanation for breast cancer; oxide chemical structure of oestrogen metabolites could also affect, in particular diphenolic compounds that can be partially oxidised to semiquinones and then interact with DNA triggering mutations. Semiquinones could initiate a process named quinone redox cycling that produces highly reactive oxygen species (ROS). In consequence, the cancer risk in breasts with high oestrogen concentrations may strongly depend on the individual ability to metabolise oestrogens and deals with quinone adducts to DNA and redox cycling (Samuni et al., 2003; Schulz, 2005).
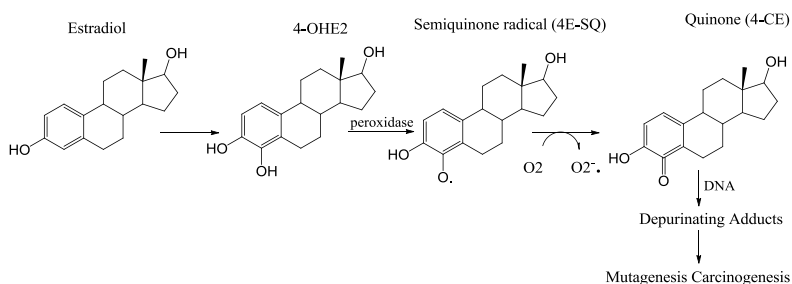
Figure.1.4. ROS species formation from oestrogen metabolite. Adapted from (Samuni et al., 2003).

Another western life style feature that could induce breast cancer is diet with high fat content. Indeed in post-menopausal women the adipose tissue is the major source of oestrogens; therefore the accumulation of this tissue could induce oestrogen overproduction (Schulz, 2005).

1.2.2. Post-menopausal hormone dependent breast cancer.

Different types of breast cancer are described depending on there stage based on TNM nomenclature (Tumour, Lymph node and metastasis state), and regarding the localisation in early stage (ductal or lobular in situ). Nevertheless the classification is more complicated and depended also on tumour cell characteristics and its cell proliferation pathways: (i) hormone dependent with oestrogen (ER) and progesterone receptor (PR) positives, named Luminal A (ER +, PR + / - , HER 2 –, low Ki67), and Lumina B (ER+, PR + / - , HER 2 +) (ii) growth factor sensitive with only HER2 receptor positive, (ER - , PR - , HER2+) and (iii) the triple negative or basal-like without any of the above-mentioned receptors (ER - , PR - , HER 2-, cytokeratine 5/6+) (Lewis-Wambi and Jordan, 2009; Schmitt, 2009; Oakman et al, 2010).

It has been described that hormone receptor positive tumours tend to respond better to chemotherapy, which is the treatment of choice for stage III and IV (Maughan et al., 2010). Therefore in this project, we develop new polymer drug conjugate treatment for luminal A breast tumours in stage III and IV mainly based on chemotherapy, (Tkaczuk, 2009) and endocrine therapy (Cheung, 2007).

In the clinics, radiotherapy and endocrine therapy are mostly used to reduce tumour size. But, so far, chemotherapy is the most efficient treatment together with surgery to significantly control breast cancer progression. However, chemotherapy related non-specific toxicity is still its major limitation (Rahman et al., 2007). In consequence, administered dose and frequency have to be well controlled in order to achieve an adequate antitumor effect with controlled side toxicities in healthy tissues. To overcome these drawbacks, the development of systems able to specifically delivery and release a bioactive drug in a control manner at the site of action is seek. The use of nanomedicine as drug delivery systems has been sought, (i) to alter drug pharmacokinetics, (ii) to increase the tumour specificity of the drugs after conjugation or

encapsulation and, consequently, (iii) to reduce side toxicities and improve therapeutic efficiency (Greco and Vicent, 2008).

1.2.3. Signalling pathways involved in proliferation and cell death.

As described above, oestradiol (E2) plays a key role in breast development but also in hormone dependent breast cancer (ER+) proliferation. The E2 fixation to the ER triggers protein cascades involved in cell proliferation.

There are three different pathways involved in the complex oestradiol-oestrogen receptor (E2-ER) described as (i) classic genomic (figure 1.5.), (ii) non-classical genomic (figure 1.6.) and (iii) non-genomic pathways (figure 1.7.).

(i) The **classic genomic pathway** takes place in the nucleus. In its inactive form, ER has to be dimerised into the nucleus. In order to achieve the translocation from the non-active ER in the cytosol to the active dimerised ER complex in the nucleus, oestradiol (E2) has to recognise the ER. The complexation of E2-ER induced the translocation and consequently the dimerization occurs. The complex is stabilised by the binding of a co-activator then is capable to recognise the oestrogen response element (ERE) inducing gene transcription directly involved in cell proliferation and ER expression. The down regulation also exists and occurs mediated by the repression of the dimer ER through a co-repressor.
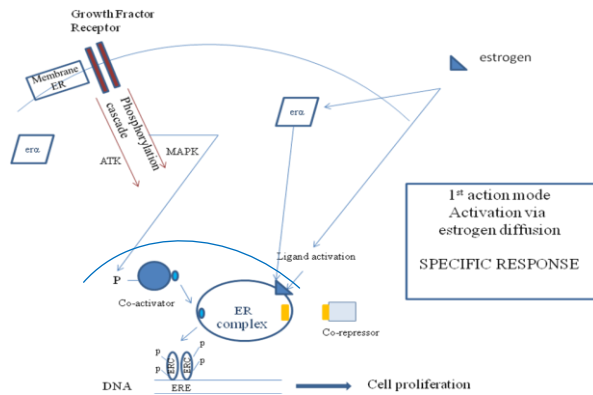
Figure 1.5. Description of the classic genomic pathway, activation via ERE.

(ii) The **Non-classical genomic pathway** does not require the E2-ER binding to ERE element. The first step of the mechanism is the same as described above. However, once the ER translocation occurs and it is stabilised with the co-activator, the complex does not recognise ERE anymore, but binds to AP1 through the Jun and Fos proteins to induce gene transcription of proliferation proteins such as cycline D1 and insulin-like growth factor I receptor (IGFR1).
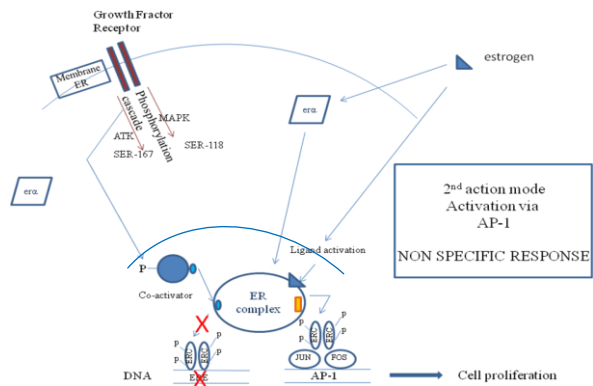
Figure 1.6. Description of the non-classical genomic pathway, activation via AP-1.

(iii) Non-genomic pathway (Platet et al., 2004; Zilli et al., 2009).
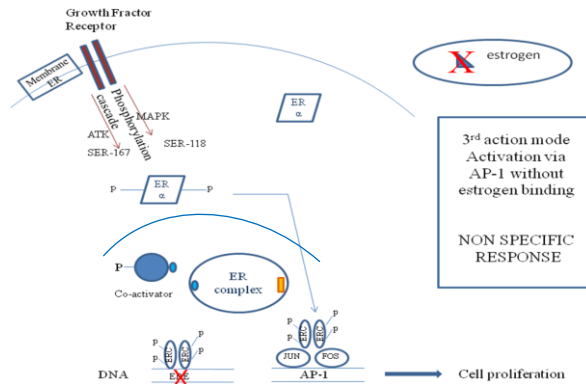
Figure 1.7. Description of the non-genomic pathway, activation via AP1 without oestrogen pathway.

The last pathway involved in cell proliferation is the growth factor pathway. The interaction with its receptor induces the activation of proteins involved in the MAPK kinase cascade and consequently the transcription of proteins involved in cell proliferation.

To control cell proliferation in a hormone dependent breast cancer ER+, oestrogen levels should be reduced. Consequently, in post-menopausal stage two options are available, (i) to block the oestrogen fixation on ER by selective oestrogen receptor modulators (SERM's) or (ii) to block the oestrogen production, inhibiting the enzyme involved in the transformation of androstenedione, to oestradiol: P450 aromatase enzyme (Jordan and Brodie, 2007). On the other hand, by means of a different pharmacological approach and in order to gain effective tumour cell death, the best option is the use of a chemotherapeutic agents acting on DNA stability or microtubule formation. The different possible targets to use are represented in figure 1.8.
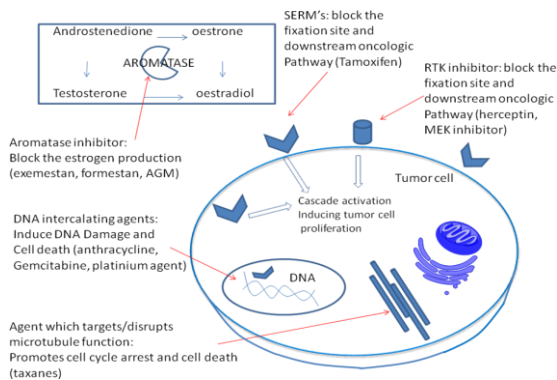
Figure 1.8. Summary of different targets for breast cancer therapy in where ⬥ is oestrogen receptor, ▮ is Receptor Tyrosine Kinase (RTK). Adapted from (Tkaczuk, 2009).

1.3. Current treatments for breast cancer.

Nowadays, there is a well-defined armoury of drugs for the treatment of breast cancer. Nevertheless the most efficient approach is tumour ablation or breast ablation in the worst scenarios. In some cases, chemotherapy and/or radiotherapy and/or hormone therapy pre-treatment are required as neoadjuvants in order to decrease tumour volume and simplify surgery. Moreover, in order to diminish the risk of tumour recurrence and death, adjuvant therapy is also administered. In hormone dependent cancers, endocrine therapy is prescribed during the 5 first years after surgery controlling the hypothetic tumour recovery and the spread of breast cancer cells (Nicholson and Gee, 2000; Dodwell et al., 2006). In tumours with high risk of recurrence or in presence of metastasis, longer cycles of chemotherapy are required. A milder or palliative treatment alternatives are seek for old patients as enhancing quality of life it is in this case more important.

1.3.1. Chemotherapy.

Anthracyclines and Taxanes are the most common options in breast cancer treatment. Both are still really important and efficient as first line breast cancer therapy.

1.3.1.a. Anthracyclines.

Dox, epirubicin (Epi) and daunorubicin (Dau) are part of the most widely used drugs in the clinics (figure 1.9.). Their exact mechanisms of action is still poorly understood (Gewirtz, 1999) and several cellular processes have been described: (i) inhibition of DNA and RNA synthesis through intercalation in nucleic acids (Goodman et al., 1974; Momparler et al., 1976); (ii) generation of reactive free radicals after Dox-redox cycling (Davies and Doroshow, 1986; Fornari et al., 1994); (iii) interference with DNA helicases (Bachur et al, 1993); (iv) induction of DNA strand breaks through type II topoisomerase inhibition (Davies and Doroshow, 1986; D'arpa and Liu, 1989; Fornari et al. 1994); (v) induction of cell death apoptosis pathway, through *tumour suppresor* p53 protein dependent or independent (Skladanowski and Konopa, 1993; Kaufmann and Earnshaw, 2000) or (vi) cell growth arrest (Ling et al., 1996). For this reason and even though anthracyclines can be considered extremely potent drugs, a number of important side toxicities have been reported, including acute and chronic cardiotoxicity and liver, kidneys and peripheral nervous system damage (Rahman et al., 2007; Carvalho et al., 2009). Consequently, the identification of a maximum tolerated dose (MTD) and an adequate dosage schedule are key issues to be considered. Dox MTD has been set at 80 mg/m^2 in patients (Singal and Iliskovis, 1998; Duncan, 2007; Roca-Alonso et al., 2012).
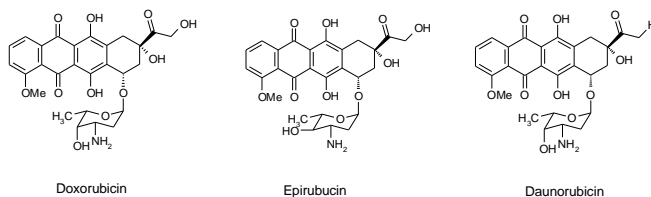
Figure 1.9. Examples of anthracycline chemical structures (Bachur et al, 1993).

Besides, it is interesting to note that patients which have any of the following conditions should not be treated with Dox: (i) baseline

31

neutrophil count < 1500 cells/mm^3; (ii) severe hepatic impairment; (iii) recent myocardial infarction; (iv) severe myocardial insufficiency; (v) severe arrhythmias; (vi) previous treatment with complete cumulative doses of Dox, Dau and/or other anthracyclines and anthracenediones; or (vii) hypersensitivity to Dox, any of its excipients, or other anthracyclines or anthracenediones.

1.3.1.b. Taxanes.

Paclitaxel (PTX) (Taxol) and Docetaxel (DTX) can be considered the most used taxanes for breast cancer treatment. They are known to interfere with microtubules and block the microtubule flexibility necessary for cell division (mitosis) (Whelan, 2002). As a consequence, the mitosis cannot be properly achieved and death signalling pathways trigger tumour cell death.
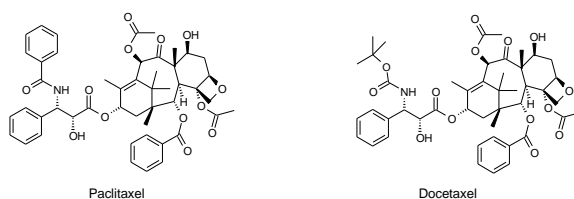
Figure 1.10. Examples of taxanes chemical structure.

1.3.1.c. Chemotherapy-based Combination Therapy.

Due to the molecular complexity of cancer, combination therapy is becoming increasingly important for a better long-term prognosis and to decrease side effects. Combination therapy refers to either simultaneous administration of two or more pharmacologically active agents but also to the combination of different therapies (such as chemotherapy and radiotherapy). The advantage of the multi-agent therapy is the possibility to modulate different signalling pathways in tumour cells, maximising the therapeutic effect and, possibly, overcoming mechanisms of resistance (Broxterman and Georgopapadakou, 2005).

32

The use of combination therapy for cancer treatment is well established (Gee et al., 2005). Whereas chemotherapeutic drugs are normally associated with severe side effects, administration of agents hitting different targets and decreasing different toxicity profiles can improve the therapeutic index. Even if the MTD of Dox is 80 mg/m^2, (Duncan, 2007) in combination therapy the administered dose is much lower due to the combination with other toxic drug. Presently, some well-known combinations are used for cancer treatment. For example, Dox (60 mg/m^2) in combination with cyclophosphamide (600 mg/m^2) is administrated i.v. (intravenously) each 21 d (day) (AC), (Fisher et al., 1997), also the cocktail cyclophosphamide (500 mg/m^2, i.v. d 1), 5-fluorouracyl (500 mg/m^2, i.v., d 1) and Dox (50 mg/m^2, i.v., d 1) each 21 d (CAF) is commonly used (Stewart et al., 1997; Hortobagyi, 2002). In the last few years, new combinations of anthracyclines plus taxanes are being tested with promising results. Firstly, PTX was added to existing combinations such as ACT. ACT is known as AC (Dox 60 mg/m^2 i.v. d 1 + cyclophosphamide 600 mg/m^2 i.v. d 1 each 21 days 4 times) regime followed by PTX (175 mg/m^2) during 3h d 1 each 21 days 4 times (Parnes et al., 2003). Combination of Dox and taxanes has been also reported, such as, Dox (50 mg/m^2 i.v 15 min. D 1) and DTX (75 mg/m^2 i.v. 1 h d 1) each 21 d or Dox (50 mg/m^2 i.v. d 1) followed by PTX (200 mg/m^2 i.v. 3 h d 2) 24 h after each 21 d (Jassem et al., 2001). In the 1980's, the combination of chemotherapeutic agent with an endocrine agent was firstly reported for hormone-dependent breast and prostate cancer (Pearson et al., 1989). More recently, the use of endocrine therapy with adjuvant bisphosphonate therapy (zoledronic acid) has been shown to be effective in breast cancer preventing bone loss in postmenopausal women with breast cancer (Greco and Vicent, 2009). Combination therapy seems, therefore, to be a good opportunity to achieve a more effective treatment with better patience compliance.

1.3.2. Endocrine therapy.

For hormone dependent breast cancer, endocrine therapy has been described as an indispensable tool to modulate cell proliferation. Two options are used, the blockage of the ER by SERM's or the decrease in the oestrogen production by aromatase enzyme inhibition (important in postmenopausal population) (Jordan, 2003; Jordan and Brodie, 2007).

1.3.2.a. SERM's therapy.

The selective oestrogen receptor modulators (SERM's) are competitive antagonists of oestrogens. They bind to the ER preventing its activation and consequently cell growth. Representative examples of SERM's are shown in figure 1.11.

The most widely used in breast cancer therapy is tamoxifen discovered by ICI Pharmaceuticals in the early 1970's (Jordan, 2006). The food and drug administration (FDA) approved the use of tamoxifen in June 1990 for a major additional use to help prevent the recurrence of cancer in "node negative" patients. It is administrated orally and daily. Liver metabolisation leads to the active compound: 4-OH-Tamoxifen , which shows a ten-folds more interaction with the ER than Tamoxifen (Jordan, 2003; Cheung, 2007). The treatment is used for women pre- o post-menopausal for a maximum of 5 years. Another interesting SERM is Fulvestrant known as Falsodex. It received the FDA approval in April 2002 for hormone receptor positive metastatic breast cancer in postmenopausal women whose disease has progressed after receiving anti-oestrogen therapy such as Tamoxifen. Instead of blocking ER, this compound targets and degrades the ER present in breast cancer blocking ER transcription. The Falsodex therapy is given as a once-a-month intramuscular injection (Tang et al., 2008; http://www.fda.gov).
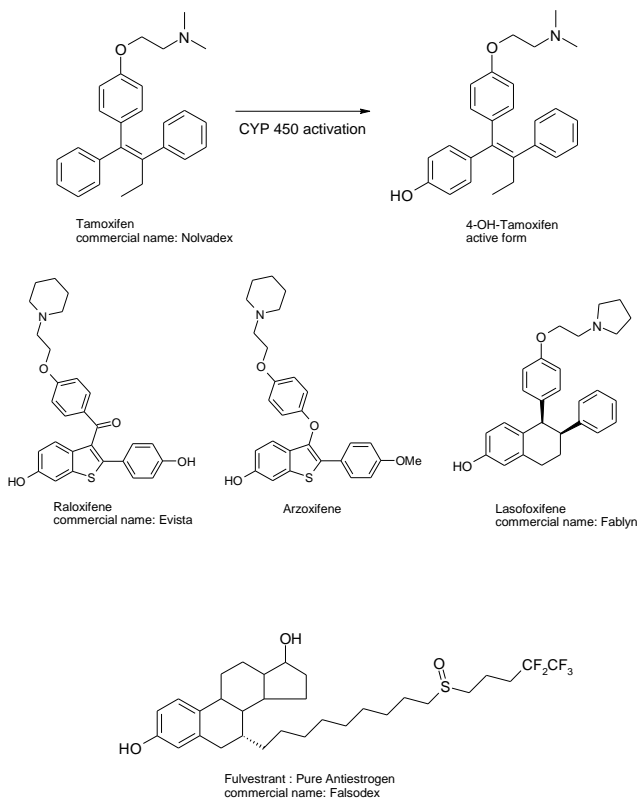
Figure 1.11. SERM's chemical structures (Jordan, 2003).

.

1.3.2.b. Aromatase inhibitors.

The other strategy followed to limit the oestrogen-induced cell proliferation is to diminish the oestrogen flow. The oestrogen biosynthesis is involved in the last step of cholesterol degradation, the aromatisation of the androstenedione steroid A-ring. Once androstenedione fixes the aromatase enzyme (cytochrome P450) through its haeme centre, serial reactions occur involving NADPH, NADP mechanisms to achieve the A ring aromatisation (figure 1.12.) (Jordan, 2007).
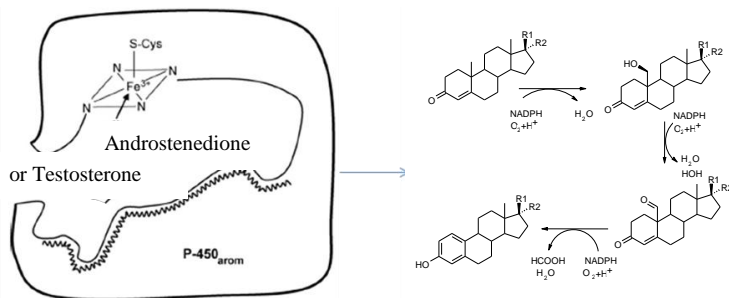
Figure 1.12. Last step of oestrogen biosynthesis adapted from (Jordan and Brodie, 2007).

Aromatase inhibitors act on the haeme nucleus arresting the oestrogen production. This treatment is orally available but it could be only administered for post-menopausal women due to the oestrogen need in pre-menopausal women. Aminoglutethimide (AGM), marketed under the name ORIMETEN[®] was the first aromatase inhibitor used clinically in the treatment of postmenopausal breast cancer for 20 years with a modest response rate. AGM is a non-steroidal, nonspecific, reversible and competitive aromatase inhibitor with very low potency (Lombardi, 2002). For example, it was observed that women treated with AGM could develop osteoporosis, thereof cortisol had to be administrated as adjuvant therapy (Kelloff et al., 1998). Since AGM, research has devoted to develop new aromatase inhibitors with better pharmacological profile. Currently two families of inhibitors are indexed, (i) Irreversible Inhibitors and (ii) Reversible inhibitors (figure 1.13.) (Cheung, 2007; Jordan, 2007).

Aromatase inhibitors, such as AGM, Fadrozole, Letrozole and Anastrozole act by reversibly binding to the enzyme and by interfering with the haeme-iron group of the cytochrome P-450 moiety of the enzyme (Lombardi, 2002). A variety of pathways involve cytochrome P-450, therefore, a carefully design of the aromatase inhibitor have to be done. Furthermore, due to their reversibility, the oestrogen deprivation highly depends on the presence of the drug, thus posing potential toxicity issues.

36
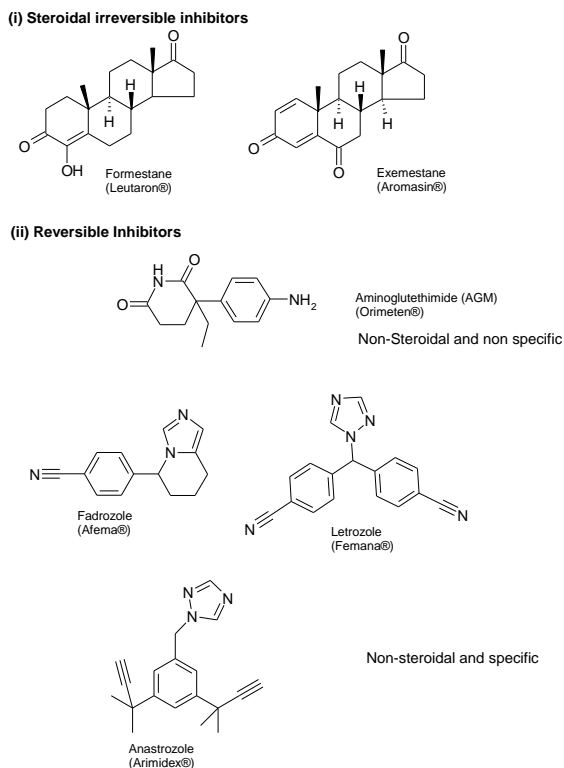
Figure 1.13. Representative example of aromatase inhibitors (Jordan, 2003).

The irreversible inhibitors also known as suicide inactivators, such as Formestane and Exemestane interact with the substrate-binding site of the enzyme. They must have an androstenedione-like structure to be transformed by the normal catalytic action of the target enzyme. A covalent bond formation then occurs with its nucleophilic site, leading to the irreversible inactivation of the aromatase enzyme (Lombardi, 1995). Due to its irreversibility, the biosynthesis of new aromatase enzymes is required to achieve oestrogen production (Miller, 1996).

Regarding clinical trials in postmenopausal women with hormone dependent breast cancer (ATACC trial), letrozole and anastrozole were more effective than tamoxifen with lesser side effects, as consequence

these aromatase inhibitors are considered first line treatment in postmenopausal patients (Goss and Strasser, 2002; Howell et al., 2005).

1.3.3. Tyrosine Kinase Inhibitors.

As described above, growth factor pathways are also involved in cell proliferation and thereof could be an interesting target. The downstream signalling pathway begins with the interaction between growth factors and their receptors situated on the plasma membrane. The receptor triggered by the ligand, activates kinase cascade, including the receptor's intrinsic tyrosine kinase activity and the mitogen-activated protein (MAP) cascade involved in cell proliferation (Dancey and Sausville, 2003). However, in normal cells a balance between activation and inhibition of these pathways is highly regulated and well-balanced. In the development of cancer pathology, those pathways could be altered in several ways. For example, growth factor receptors such as epidermal growth factor (EGF) receptor (EGFR) and/or insulin-like growth factor (IGF) receptor (IGFR) can be overexpressed. Consequently, the blockage of the growth factors downstream signalling pathways at any level should theoretically be beneficial in several types of cancer.

Some studies have shown that the EGF and oestrogen signalling are strictly connected (Nicholson et al., 2001). In fact, not only are EGFRs over-expressed in cells previously treated with anti-hormonal drugs, but there is an active crosstalk between oestrogen and growth factor signalling pathways (Nicholson and Gee, 2000). The crosstalk can be summarised as follows (Nicholson and Gee, 2000). Growth factors like EGF, Transforming growth factor (TGF-α) and IGF are able to phosphorylate the serine 118 residue of ER and activate the receptor without previous oestrogen fixation.

- Oestrogens are able to trigger positive elements involved in growth factors signalling cascade.

- The ER enhances the activity of nuclear transcription factors induced by growth factors.

In addition, oestrogen deprivation has been correlated with up-regulation of growth factor receptors such as EGFR. The tyrosine kinase inhibitor (TKI) drug most used clinically is Trastuzumab (Herceptin®) for HER-2/neu receptor (Gschwind et al., 2004; Nielsen et al., 2009; Normanno et al., 2009). The standard clinical administration is Trastuzumab 4 mg/kg i.v. d 1, then 2 mg/kg i.v. per week followed by PTX (175 mg/m^2) during 3 h i.v d 1 each 21 d.

1.3.4. Surgery.

Breast conservation is currently the most popular treatment as most carcinomas have a restricted size and large primary tumours could be reduced in size by primary chemotherapy. In most breast-cancer centres, conservative surgery represents 75–80 % of all operations. However, surgeons are advised to undertake mastectomies in the same operative sessions as reconstruction of the breast. Moreover the resection of the axillaries nodes closely depends on the results of the sentinel lymph-node biopsy (Veronesi et al., 2005[a]; Veronesi et al., 2005[b]).

1.3.5. Radiotherapy.

As described above, in most developed countries the current standard of care for patients with early-stage breast cancer consists of breast conserving surgery, followed by 5-6 weeks postoperative radiotherapy. Three different approaches are described, whole breast irradiation, partial breast irradiation and intraoperative radiotherapy.

In daily practice, radiotherapy is used on the whole breast. Probabilities of adequate local control rates are high with this conventional fractionation. Some data support the effectiveness of an additional dose applied to the tumour bed (*i.e.* boost irradiation). The traditional schedule is 42,5 Gy in 16 fractions for 22 days in patients with negative lymph node. For patients younger than 48 years who received an intraoperative

boost dose of 12 Gy, a rapid course of external radiotherapy is used (13 fractions of 2,85 Gy each).

In parallel, the rationale for the use of partial breast irradiation instead of the conventional approach is based on the finding that most recurrences arise near the primary tumour location. And concerning intraoperative radiotherapy, it corresponds to the application of a high dose of radiation during surgical intervention after removal of the tumour. ELIOT (Electron Intra Operative Therapy) is currently used in early stage breast cancer as the only treatment at the European Institute of Oncology and prospective randomised trial is ongoing (Veronesi et al., 2005[a]; Leonardi et al., 2012).

1.4. Polymer Therapeutics.

It could be said that the beginning of polymer therapeutics was established in the 70's when the concept of polymer-drug conjugates (Duncan, 2003) and the first PEGylated proteins (Davis, 2002) were developed to achieve in 1994 the first anticancer PEG-protein conjugate, PEG-L-Asparaginase (Oncaspar[®]) approved by FDA. However, it was 20 years ago when the known term 'Polymer Therapeutics' was coined by Prof. Ruth Duncan to define a family of new chemical entities (NCEs) considered the first polymeric nanomedicines (Duncan, 2003; Duncan and Gaspar, 2011). After the 70's, the field has been in permanent evolution. The term 'Polymer Therapeutics' includes different complex macromolecular systems, in which a water-soluble polymeric carrier (with or without inherent activity) and the bioactive molecule(s) are covalently bond (figure 1.14.). Drug conjugation to a polymer not only enhances its aqueous solubility but also changes drug pharmacokinetics at the whole organism and even subcellular level with the possibility to clearly enhance drug therapeutic value (Duncan, 2006; Vicent and Duncan, 2006). This family can be subdivided in five general categories (figure 1.14.): polymeric drugs, polymer-protein conjugates, polyplexes, polymeric micelles and polymer-drug conjugates (Duncan, 2003; Duncan, 2006).

In our purpose, we focus on polymer-drug conjugates. With 16 conjugates already transferred to clinical trials (Table 1.1.) (Vicent et al., 2009; Duncan and Vicent, 2013), the new research trends in this field are focused on four main strategies: 1) design of innovative polymer conjugates targeted to new molecular targets, 2) the search for better physico-chemical characterisation methods paying special attention to conformational issues in solution, 3) the synthesis of new polymeric carriers with defined architecture and, 4) the use of polymer conjugates as a platform for the simultaneous administration of more than one drug, strategy known as polymer-based combination therapy.
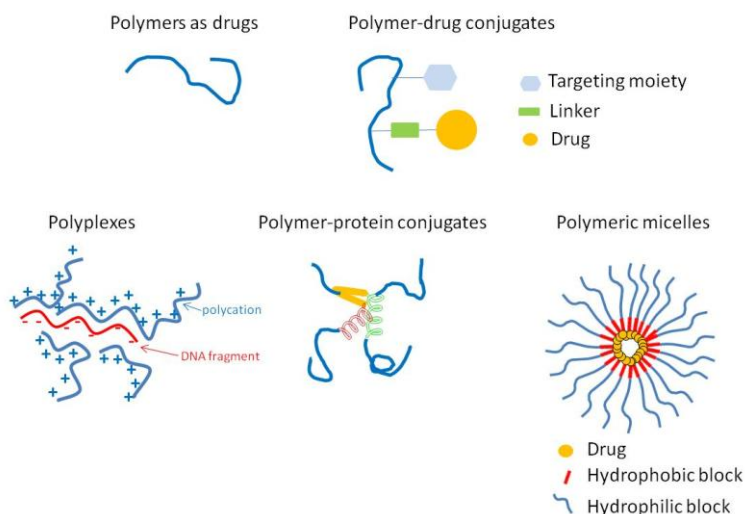
Figure 1.14. Polymer Therapeutics family adapted from (Duncan, 2003).

1.4.1. Polymer-drug conjugates.

With the vision of Ringsdorf and De Duve the concept of polymer anticancer drug conjugates (1975) was born (Ringsdorf, 1975). The first polymer-drug conjugate, an HPMA copolymer-anticancer drug conjugate (HPMA copolymer–Dox conjugate, FCE28068 known as PK1) was transferred to clinical trials in the 90's (Duncan et al., 1998). Currently, the most advanced is the PGA paclitaxel conjugate known as Opaxio®

41

(previously Xyotax[TM] or PPX (paclitaxel polyglumex)) from Cell Therapeutics Inc. (CTI, Seattle (USA)) (Singer et al., 2003; Singer, 2005; Singer et al., 2005) in phase III trials for several cancers (ovarian, prostate, stomach, etc.) alone or in combination. In fact, last September Opaxio in combination with radiotherapy was designated by the FDA as Orphan drug for the treatment of glioblastoma (figure 1.15.).
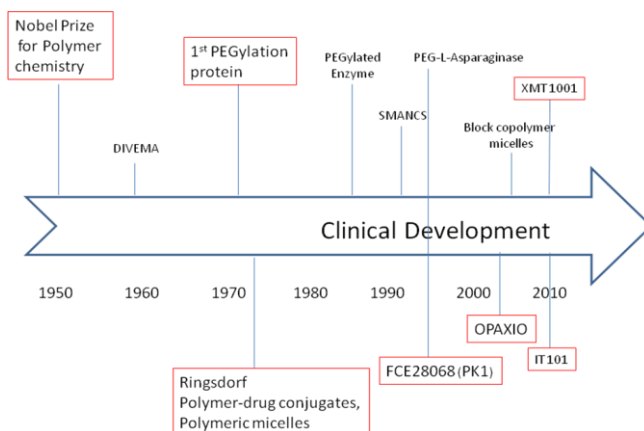
Figure 1.15. From polymer chemistry to Polymer Therapeutics (Duncan, 2006).

What is a polymer-drug conjugate?

A polymer-drug conjugate is a new "chemical" entity in which a drug is covalently bound to a polymer through a bioresponsive linker. Each part (polymer, drug and linker) has to fulfil exigencies related to the molecular target, way of administration, pharmacokinetics, etc... Therefore, the use of a biological rational is key prior to the design of an efficient polymer anticancer drug conjugate.

The **polymer backbone** has to be non-toxic, non immunogenic and water-soluble to allow i.v. administration. In order to achieve a better pharmacological profile, the use of biodegradable carriers allows us to always use a polymer size with safe renal excretion. However, in the case

of non-biodegradable polymers, a maximum weight of 40 kDa should be used to allow renal clearance. The most widespread polymers in the last 20 years were the non-biodegradable HPMA, PEG and the biodegradable PGA (Singer et al., 2003; Vicent and Duncan, 2006) nevertheless new polymers are currently appearing (Tong et al., 2010).

The **drug** is chosen according to the target, but it has also to fulfil some prerequisites. Apart from bearing adequate functionalities and a high potency, our drug has to be stable under lysosomal conditions in order to preserve its therapeutic activity as once the polymer drug conjugate reach the tumour, the conjugate is internalised generally by endocytosis.

The **linke**r is a bioresponsive spacer used to attach drugs to the polymer backbone. This spacer has to be design in order to be degraded under specific conditions to release the cargo, which usually remains inactive when attached to the polymer backbone. Intracellularly, release should be triggered within the lysosomes to achieve a lysosomotropic drug delivery (Duncan, 1992). Consequently, the linker should be responsive in presence of lysosomal enzymes such as cathepsin B and/or hydrolytically labile at acidic pH. Two strategies are generally developed, a peptidic substrate as linker or a pH labile linker. It should be noted the importance of enzyme levels in patients receiving this type of treatments. For example, during clinical studies with Opaxio[®] it was demonstrated that patient cathepsin B levels were directly correlated with the oestrogen levels and since then oestrogen levels are considered as biomarker to indicate the possible effectiveness of this treatment. Concerning the treatment of a hormone dependent breast cancer in post-menopausal women, cathepsin B levels could represent a limitation in the use of nanomedicines bearing PGA as carrier or linkers based on peptides substrate for cathepsin B (Devetzi et al., 2009).

A **target moiety** is an optional part of the nanoconjugate. It is used to actively target and to directly and specifically deliver the drug to the targeted cell or tissue. Nevertheless, of the conjugates transferred to

clinical trials only one bears a targeting group. This is the HPMA copolymer-Dox-galactosamine conjugate (also known as FCE28069 or PK2) and was designed to achieve liver targeting by selective binding to the asialoglycoprotein receptor in the hepatocytes and therefore, to be used as treatment for hepatocellular carcinoma (Seymour et al., 2002).

It could be summarised that, the main benefits of polymer-drug conjugates compared to the parent free drug are: (a) passive tumour targeting by the enhanced permeability and retention (EPR) effect, which can be utilised for tumour targeting and polymer-drug conjugate accumulation (Maeda, 1994), (b) a decrease of toxicity (Vasey et al., 1999), (c) an increase of solubility in biological fluids (Meerum et al., 2001), (d) an ability to overpass some mechanisms of drug resistance (Minko et al., 1998) and (e) an ability to elicit immunostimulatory effects (Rihova et al., 2003; Sirova et al., 2007).

Table 1.1. Polymer-drug conjugates in clinal trials (Duncan and Vicent., 2013; Sanchis et al., 2010).

conjugate	Name	Trial Phase
HPMA copolymer-Dox	PK1	II
HPMA copolymer-Dox-galactosamine	PK2	I
OxDetran-Dox	AD-70	I/disc.
PGA-CPT	CT-2106	I/II
Cyclodextrin-CPT	IT-101	I
Polyacetal-CPT	XMT-1001	I
HPMA copolymer-CPT	MAG-CPT	I
PEG-CPT	pegamotecan	II/disc.
Carboxymethyl-dextran-exatecan	DE-310	I
PEG-irinotecan	NKTR-102	II
HPMA copolymer-PTX	PNU166945	I/disc.
PGA-PTX	CT-2103 (Opaxio)	III
PEG-docetaxel	NKTR-105	I
HPMA copolymer-malonato-platinate	AP5280	I
HPMA copolymer-DACH-platinate	AP5346 (Prolindac[TM])	II
PEG-naloxone	NKTR-118	III

1.4.2. Enhance-permeability and retention (EPR) effect represents an indispensable tool to target solid tumours.

The EPR effect offers a passive targeting to solid tumour tissues after i.v. administration of a macromolecular conjugate. The cancerous cells are rapidly growing and creating its own vessels to support its significant growth. This process is known as **angiogenesis**, a biological mechanism regulated by many different growth factors (Folkman and Shing, 1992; Segal and Satchi-Fainaro, 2009). The new vessels created by the cancerous mass, possess its own characteristics (e.g. lack of smooth muscle layer cells, looser endothelial cell-cell junctions, incomplete basement membrane). This leads to an <u>enhanced permeability</u> of the cancerous capillaries for macromolecules (Duncan et al., 1987; Maeda et al., 2001). Moreover, solid tumours lack effective lymphatic drainage, leading to lower clearance ability from the tumours, and consequently an <u>enhanced retention</u> of the macromolecular drug within the tumour. The EPR effect allows a discrimination of healthy tissues. This passive and selective targeting present in tumour tissues allows an increased accumulation of the macromolecular constructs. Due to the different pharmacokinetics of macromolecular anticancer drugs, chemotherapy side effects can be minimised. It was reported that the ideal size for take profit of EPR effect is a molecular size larger than 40 kDa (Maeda, 2001; Maeda, 2010). However some other characteristics and limitation have to be taking into account (Maeda et al., 2012). The macromolecule cannot interact with blood components or blood vessels, the total surface charges have to be weakly negative to near neutral and ideal time required to achieve the EPR have to be larger than several hours in systemic circulation in mice (Maeda et al., 2012).

It is extremely important to note that, EPR effect is heterogeneous and highly depends on the tumour type and cancer stage. Recent studies demonstrate that it is possible to enhance the EPR effect by using molecules such as brakylin, NO and prostaglandins to facilitate extravasation. In addition combination of small drug, such as Angiotine II

and angiotensin converting enzyme (ACE), induce hypertension and consequently increase tumour blood flow (Maeda et al., 2012).
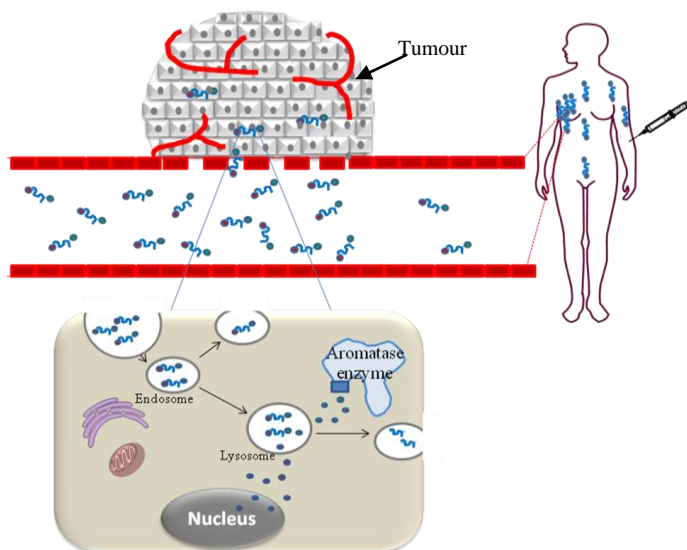
Figure 1.16. Enhance permeability and retention (EPR) effect adapted from (Duncan, 2006; Peer et al., 2007) where ● is Dox, ● is AGM, ∿° is the conjugate, ⌐ is an angiogenic vessel and ▬ is an epithelial cell.

Once present in the tumour interstitium, polymer-drug conjugates can be act either extracellularly or after being uptaken by the cells via endocytosis (Duncan, 2003). It has been demonstrated that cellular uptake of macromolecules is limited to endocytosis, and this process would lead to a "lysosomotropic" drug delivery (De Duve et al., 1974). Endocytosis involves cell membrane invagination for the capture and vesicular internalisation of extracellular molecules. Once internalised, macromolecules are transferred via endosomes (pH 6,0–6,5) to lysosomal compartments, which contain hydrolytic enzymes and a lower pH (pH 5,0-5,5) (Duncan, 2003; Duncan, 2006). Conjugation of therapeutic agents to macromolecules through a linker that only degrades when exposed to these specific lysosomal conditions would allow intracellular release of the drug, which would then passively diffuse through the

lysosomal membrane to reach its pharmacological target in the cell (figure 1.16.).

1.5. Polymer-based combination therapy.

The term "polymer-drug conjugates for combination therapy" is a general phrase that comprises at least four families of systems (figure 1.17.).

1) Family I: polymer-drug conjugate plus free drugs. This concept was developed based on the combination of a polymer-drug conjugate carrying a single drug administered with a low molecular weight drug or a different type of therapy (e.g. radiotherapy).

2) Family II: polymer-drug conjugate plus polymer-drug conjugate. In this approach the strategy developed is the combination of two different polymer-drug conjugates each containing a single therapeutic agent.

3) Family III: single polymeric carrier carrying a combination of drugs. In contrast to the other families, this approach involves only one polymer mainchain in which two or more single drugs are conjugated.

4) Family IV: polymer-directed enzyme prodrug therapy (PDEPT) and polymer enzyme liposome therapy (PELT). PDEPT relies on the combination of polymer drug conjugate with a polymer-enzyme conjugate capable of the selective release of the drug at the tumour site. PELT is a comparable strategy where a polymer enzyme conjugate is administered in combination with the liposome to induce its degradation allowing the release of the encapsulated drug.
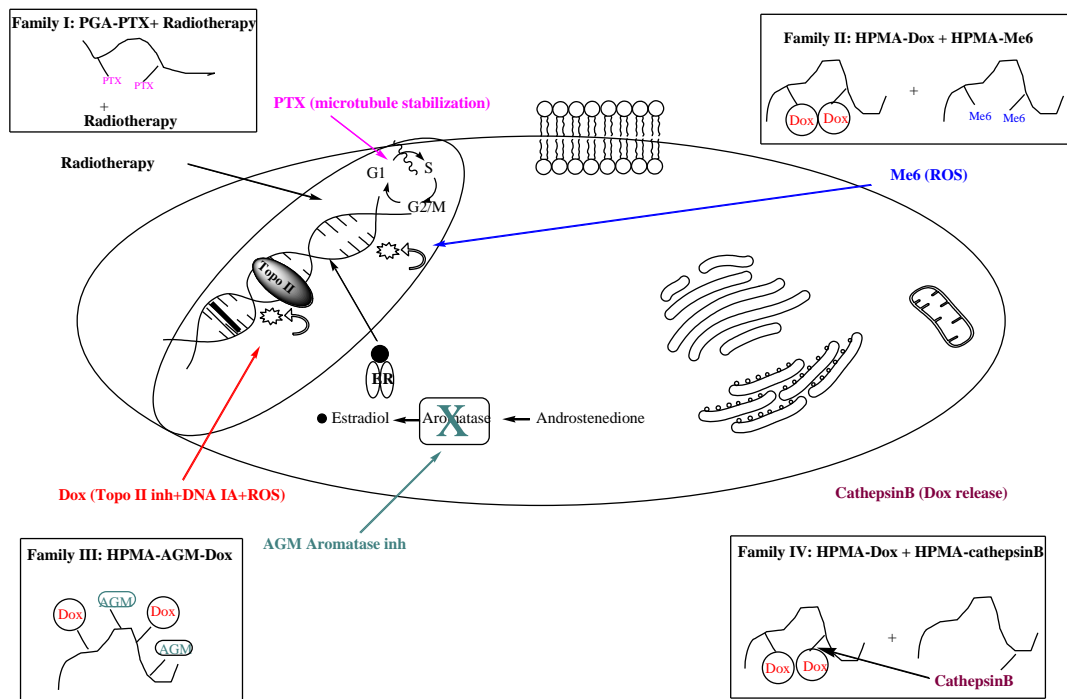
Figure 1.17. Schematic representation of the different types of polymer-based combination therapy with representative examples and their target sites. Family I: PGA-PTX+radiotherapy; Family II: HPMA-Dox + HPMA-Me6; Family III: HPMA-AGM-Dox; Family IV: PDEPT approach, HPMA-Dox + HPMA-Cathepsin B (Deladriere et al., 2010).

1.5.1. Challenges and Opportunities associated with the use of polymer-based combination therapy.

Due to the intra-tumour heterogeneity of the tumour tissue and the complex molecular mechanism of tumour progression, the presence of two or more therapeutic agents on a single polymeric chain opens new therapeutic possibilities, but also new challenges to be overcome. Therefore, several issues should be considered in order to develop polymer-drug conjugates for combination therapy.

1.5.1.a. Identification of appropriate drug combinations and drug ratios.

Most drug combinations are based on the assumption that by targeting different cellular pathways there is an enhancement in the therapeutic benefit and a decrease in toxicity. Several studies confirmed this statement while others did not reach their expectative (Jones, 2009). Indeed, two important and not trivial points have to be considered, firstly the identification of the drugs to be combined that will be subsequently released together, and secondly, the determination of the optimal drug ratio.

In order to achieve the maximum clinical benefit in patients, clinicians usually combine drugs that do not have overlapping toxicities at their individual maximum tolerated dose (MTD). However, this assumption is not correct in many cases as a different ratio of the selected drugs may be synergistic (greater effect than the sum of the individual drugs), additive (equal activity to the sum of the individual drugs) or antagonistic (less anti-cancer effect than the sum of the individual drugs). In order to evaluate the possible synergism of both drugs a Combination index (CI) have to be determined using the method described by Chou (2006).

$$CI = \frac{D1}{(Dm)1} + \frac{D2}{(Dm)2}$$

D1 and D2 are the corresponding concentrations determined to achieve 50% of cell death (IC 50) when drug 1 and 2 are tested in combination. Dm is the IC50 of drug 1 and 2 when they are tested as single drug.

When CI < 1, this indicates synergism,
When CI = 1, this indicates an additive effect
When CI > 1 this indicates an antagonism

Moreover drug ratios can play a critical role when combining drugs. The results of multiple *in vitro* and preclinical studies have demonstrated that the molar ratios of drugs used can have a significant impact on the overall efficacy and safety of combination chemotherapy (Mayer and Janoff, 2007). The full understanding of this concept has been the key of the successful technology developed by the Canadian company Celator Technologies Inc. (www.celator.ca, 01 November 2010). Ideally, it is hoped that a similar approach will be applied to the development of polymer-drug combination conjugates. In this context, further studies investigating the impact of different drug ratios on biological activity of polymer-drug conjugate should be carried out.

1.5.1.b. Kinetics of drug release.

This is another important parameter to control when developing polymer-drug combination conjugates that confers clear benefits to this platform technology when compared to other nanopharmaceuticals. The presence of bioresponsive polymer-drug(s) linker(s) offers the possibility of finely tuning drug release ratio(s) that could be directly translating in an enhancement of the therapeutic output. However, achieving a successful drug(s) release rate is not a trivial issue.

It is well established that the drug release rate from the polymer to the target site is an essential requirement for polymer-drug conjugates to reach its activity.

Therefore, the ideal linker has to be stable in blood but readily cleaved at the target site. Meticulous research carried out in the 1980s comparing peptidyl linkers for selective cleavage in the lysosomal compartment led to the development and clinical assessment of HPMA copolymer-GFLG-Dox (Gly-Phe-Leu-Gly) conjugate (Duncan, 2005). These early studies showed that the different peptidyl linkers displayed a different release rate. It was also observed that the biodegradability of the linker also depended on the conjugated drug. Indeed, the linker –GlyGly- is non-biodegradable when it is designed in the conjugate HPMA copolymer-GlyGly-Dox. However, when it is used in the conjugate HPMA copolymer-GlyGly-melphalan, the drug release is achieved (Duncan et al., 1991). In addition, when more than one drug is linked to the carrier, drug release can be clearly affected by the presence of the second bioactive agent, mainly due to changes in hydrophobicity, pH or conjugate conformation in solution. Also, for conjugates combining more than one agent, relative drug release rate (which drug is released faster) and sequential drug release (which drug is released first) can further increase the complexity of the system and become key factors for activity (Vicent et al., 2005; Greco et al., 2007).

1.5.1.c. Loading capacity.

In order to design polymer-based combinations a multifunctional carrier should be used. Ideally with a loading capacity adequate to ensure delivery of sufficient amount of drugs to the tumour site, very important if multi-agent therapy is used. For instance, cyclodextrins (Davis, 2009), polyacetals (Yurkovetskiy and Fram, 2009) or PGA can theoretically carry one drug molecule per monomer and indeed, conjugates based on these platforms have a high drug loading (10 w% Cyclodextrin-CPT (Davis, 2009), 10 wt% poly (1-hydroxymethylene hydroxymethyl formal) (Fleximer®)-CPT (XMT-1001) (Yurkovetskiy and Fram, 2009) or 37 wt % PGA-PTX. It is important to note that, to achieve an efficient polymer combination system it is required to get the best drug ratio that will provide an optimal therapeutic output, whilst maintaining water solubility (Bhatt et al., 2003; Duncan, 2005; Singer et al., 2005; www.celator.ca, 01 November 2010). In addition to linear polymers, novel branched polymeric

architectures that display a good carrying capacity together with other interesting characteristics are also being explored (Duncan and Izzo, 2005; Vicent et al., 2008).

1.5.2. Correlation of *in vitro* studies with behaviour *in vivo*.

The main limitation here is the lack of preclinical models for combination therapy neither *in vitro* (*i.e.* screening cell models to examine combinations) nor *in vivo* models standardised for use with targeted combinations.

Preliminary screening of the anticancer activity of newly synthesised polymer-drug conjugates is normally carried out *in vitro* against cancer cells using standard cell viability assays. The usefulness of such *in vitro* screening is debatable as, polymer-drug conjugates relay on accumulation in the tumour tissue via the EPR effect, which can be observed only *in vivo*. In addition, and due to the different cell trafficking mechanisms, the free drug is normally more active *in vitro* than the conjugated drug but *in vivo* studies show opposite trends (Duncan, 2005). Based on these considerations, the significance of *in vitro* tests and their relevance to predict *in vivo* behaviour are difficult issues. Ethical considerations and cost are obvious reasons in favour of *in vitro* pre-screening but there are additional advantages, particularly in the case of polymer based combination therapy. First, *in vitro* testing allows a comparison of the relative activity of different polymer-drug conjugates, possible benefits of combining two agents within a single drug carrier can be highlighted at this early stage. Second, an extensive evaluation of different drug ratios can be carried out, which would not be feasible at a later stage. Finally, specific experiments can be designed to elucidate the mechanism of action of these systems including drug release mechanisms and their ability to trigger or block specific cell processes.

1.5.3. Clinical Development.

Transfer of these combination products into the clinic is extremely challenging, since it calls for additional measures to unequivocally prove their clinical benefit. In particular, there is the need to demonstrate that clinical benefits are due to the advanced drug delivery strategy rather than simply the additive/synergistic effects of the parent compounds administered as separate

therapeutic entities. In other words, there is the need to demonstrate that the combination of two or more agents within a single delivery system provides advantages over the simple administration of the free drugs. Due to the complexity in designing such clinical trials and the consequent ethical issues, it is envisaged that the development costs for such combination products might be significantly more than the development of current pharmaceutical preparations. However, if the therapeutic output of the developed combination is clinically valuable, it would be always possible to accelerate this process asking FDA to recognise the combination compound as a single entity, this is the case for Combiplex® technology (www.celator.ca, 01 November 2010).

Representative examples of each family system are described and classified below following their clinical status. It is important to note that the combination therapy based on polymer-drug conjugate plus free drug (family I) is already in clinical trials, and families II, III and IV are mainly in preclinical status and few of them are still under early *in vitro* evaluation (Table 1.2.).

Table 1.2. Summary of polymer–drug conjugates based on combination therapy classified by its clinical status.

	Name	Family	Carrier	Drugs	Drug types	Ref
In Vitro	CPT–PEG-LHRH + CPT –PEG-BH3	II	PEG	CPT LHRH BH3	Chemotherapeutic Targeting residue Proapoptotic protein	(Khandare et al., 2006)
	HPMA copolymer-Dox-DEX	III	HPMA copolymer	Dox DEX	Chemotherapeutic Antiinflammatory	(Krakovicova et al., 2009)
	HPMA copolymer-AGM-Dox	III	HPMA copolymer	AGM Dox	Endocrine therapy Chemotherapeutic	(Vicent et al., 2005; Greco et al., 2007)
	PEG-poly(aspartate hydrazide) block copolymer-Dox-WOR	III	PEG-poly(aspartate hydrazide)	Dox WOR	Chemotherapeutic Phosphotidylinositol-3kinase inhibitor	(Bae et al., 2007)
Preclinical	HPMA copolymer-Dox + HPMA copolymer Mscl e6	II	HPMA copolymer	Dox Mscl e6	Chemotherapeutic Phototherapy	(Krinick et al., 1994; Shiah et al., 2001)
	PEG-(ZnPP) + PEG-(DAO)	II	PEG	ZnPP DAO	Hemeoxigenase inhibitor enzyme oxidative chemotherapeutic type	(Fang et al., 2004)
	HPMA copolymer-TNP-470-ALN	III	HPMA copolymer	ALN TNP 470	Bone targeting - antiangiogenic agent Anti angiogenic agent	(Satchi-Fainaro et al., 2004; Satchi-Fainaro et al., 2005)
	HPMA copolymer-PTX-ALN	III	HPMA copolymer	PTX ALN	Chemotherapeutic Bone targeting – antiangiogenic agent	(Miller et al., 2009)

Preclinical	HPMA copolymer-Gem-Dox	III	HPMA copolymer	Gem Dox	Chemotherapeutic Chemotherapeutic	(Lammers et al., 2009)
	PEG-NO-EPI	III	PEG	NO EPI	signalling molecule Chemotherapeutic	(Santucci et al., 2006) (Santucci et al., 2007)
	CPT-PEG-LHRH-BH3	III	PEG branched	CPT LHRH BH3	Chemotherapeutic Targeting residue Proapoptotic protein	(Khandare et al., 2006) Chandna et al., 2007)
	HPMA copolymer-Dox + HPMA copolymer-cathepsin B	IV	HPMA copolymer	Dox Cathepsin B	Chemotherapeutic Proteolytic enzyme	(Satchi-Fainaro et al., 2003)
	HPMA copolymer-Dox + HPMA copolymer-β-lactamase	IV	HPMA copolymer	Dox β-lactamase	Chemotherapeutic Proteolytic enzyme	(Satchi-Fainaro et al., 2002)
Clinical Phase I	PGA-PTX + cisplatium	I	PGA	PTX Cisplatium	Chemotherapeutic Chemotherapeutic	(Verschraegen et al., 2009)
Phase I	PGA-PTX + radiotherapy	I	PGA	PTX Radiotherapy	Chemotherapeutic Radiotherapy	(Dipetrillo et al., 2006) (Orphan drug for Glioblastoma)
Phase III	PGA-PTX + carboplatinum	I	PGA	PTX Carboplatinum	Chemotherapeutic Chemotherapeutic	(Langer et al., 2008)

1.5.4. HPMA copolymer-AGM-Dox conjugate: First described combination conjugate for the treatment of breast cancer.

The use of polymer-drug conjugates has been traditionally limited to the delivery of a single therapeutic agent. However, the multivalency of polymeric carriers allows their use to deliver cocktails of different drugs. This is a huge therapeutic opportunity as it is becoming increasingly clear that multi-agent therapy as opposed to single agent therapy is warranted for diseases such as cancer. At present, only few groups have suggested the use of a polymeric carrier for delivery of drug combinations. Dr Vicent in collaboration with Prof Duncan and Dr Greco (Vicent et al., 2005) developed the first conjugate that combined endocrine therapy and chemotherapy on a single polymeric chain; an HPMA copolymer carrying the aromatase inhibitor AGM and the chemotherapeutic agent Dox. The observations that HPMA copolymer-Dox (FCE28068, PK1) showed activity in chemotherapy refractory breast cancer patients in Phase I clinical trials (Vasey et al., 1999), and that aromatase inhibitors can act synergistically with chemotherapy (Johnston and Dowsett, 2003), led them to synthesise HPMA copolymer-AGM-Dox as a novel particular combination conjugate (figure 1.18.) (Vicent et al., 2005).
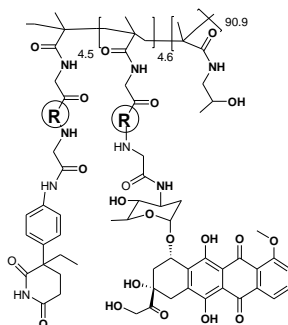
Figure 1.18. Structure of HPMA copolymer-AGM-Dox combination conjugate.

This combination conjugate showed markedly enhanced cytotoxicity in MCF7 breast cancer cells compared to HPMA copolymer-Dox whose activity has been proven clinically (Vasey et al., 1999) and to any other combination of single agents (namely, AGM + Dox or HPMA copolymer-AGM conjugate + HPMA

copolymer-Dox conjugate or HPMA copolymer-Dox conjugate + AGM) (Vicent et al., 2005; Greco et al., 2007) (figure 1.19.).
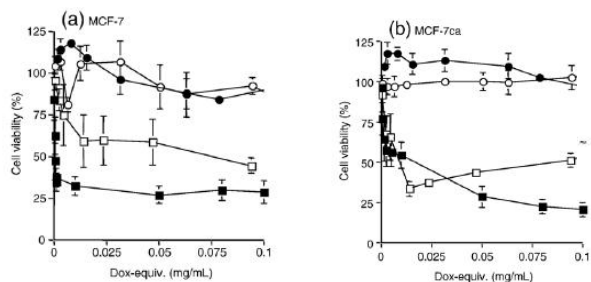
Figure 1.19. Comparison of the cytotoxicity HPMA copolymer-AGM-Dox and conjugate mixture in MCF7 and MCF7 Ca cells. Panel (a) shows cytotoxicity in MCF7; panel (b) shows cytotoxicity in MCF7 Ca (Greco et al., 2007).

Furthermore, experiments studying a library of HPMA copolymer conjugates containing AGM alone (the first conjugates to contain endocrine therapy), confirmed aromatase inhibition *in vitro*, and also that AGM liberation was a requirement for activity (Greco et al., 2005). To further investigate the mechanism of enhanced cytotoxicity of HPMA copolymer-AGM-Dox, particularly in comparison with HPMA copolymer-Dox, the possible different mechanisms or rates of endocytic uptake, the differences in the rate of release of the bioactive drug(s) and the differences in the molecular mechanisms of cell death were studied. Flow cytometry and live-cell imaging were used to evaluate cell binding (4 °C) and endocytic uptake (37 °C). In addition, studies in the presence of methyl-β-cyclodextrin (MßCD) (inhibits clathrin-mediated and clathrin- and caveolin-independent endocytosis), chlorpromazine (inhibits clathrin-mediated endocytosis) and cytochalasin B (inhibits macropinocytosis) were undertaken to proof the mechanism of endocytic internalisation. The rate of Dox and AGM release from the conjugates was measured *in vitro* in the presence of rat liver lysosomal enzymes (tritosomes).

HPMA copolymer-AGM-Dox and HPMA copolymer-Dox conjugate showed a similar pattern of cell binding and endocytic uptake (via cholesterol dependent

57

pathway). However, marked differences on drug release profile were found. Dox was released with time from HPMA copolymer-Dox showing a linear trend whereas the release of Dox from HPMA copolymer-AGM-Dox did not (figure 1.20.).
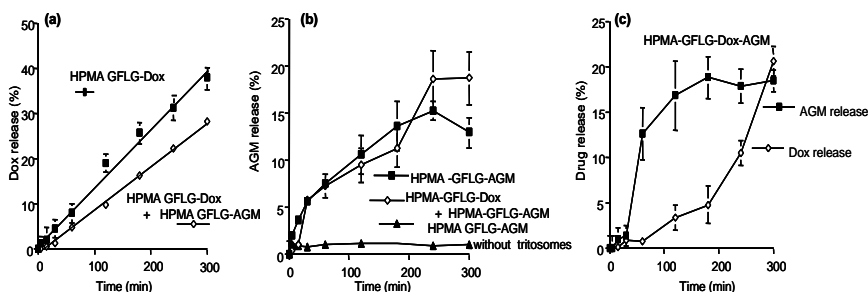
Figure 1.20. Drug release from HPMA copolymer conjugates. Panel (a) shows the release of Dox from the conjugates in presence of tritosomes. Panel (b) shows the release of AGM from conjugate in presence and absence of tritosomes and the panel (c) shows the release of Dox and AGM from HPMA copolymer-AGM-Dox conjugate (Vicent et al., 2005).

Finally, immunocytochemistry was used to assess the effect of both conjugates on the proliferation marker ki67 and the anti-apoptotic protein B-cell lymphoma 2 (Bcl-2). The preliminary immunocytochemical studies showed decreased expression of ki67 following incubation of MCF7 and MCF7 Ca cells with HPMA copolymer-Dox and HPMA copolymer-AGM-Dox. This effect was higher for the combination polymer. As ki67 is a well-described marker for the proliferating fraction of a cell population this was consistent with the higher cytotoxicity obtained with the combination polymer. More importantly, HPMA copolymer-Dox had no effect on Bcl-2 protein expression whereas a marked Bcl-2 down-regulation was induced after MCF7 treatment with the combination conjugate, suggesting that combined AGM and Dox leads to a synergistic effect which induces a different cell death mechanism, hence the increased activity of the combination polymer.

As a conclusion it is possible to say that these early studies highlighted that the conjugate conformation in solution and the drug release rates are key parameters for the activity (Greco et al., 2007). However, further studies are still needed to

58

investigate these effects and define both therapeutic potential of HPMA copolymer-AGM-Dox conjugate and to establish the exact mechanism of action. It is clear that this approach offers a new opportunity for the treatment of chemoresistant metastatic breast cancer. Apart from enhancing the cytotoxic activity, this technological platform is intravenously administered (adequate for a systemic treatment of metastasis with enhanced angiogenesis) and its cellular internalisation mechanism is different, avoiding mechanism of resistance such as the overexpression of p-glycoprotein in cell membrane.

1.6. Bibliography.

Bachur, N.R., Johnson, R., Yu, F., Hickey, R., Applegren, N., and Malkas, L.. (1993). "Antihelicase action of DNA-binding anticancer agents: relationship to guanosine-cytidine intercalator binding." Mol Pharmacol 44(5): 1064-1069.

Bae, Y., Diezi, T.A., Zhao, A., and Kwon, G.S. (2007). "Mixed polymeric micelles for combination cancer chemotherapy through the concurrent delivery of multiple chemotherapeutic agents." J Control Release 122(3): 324-330.

Barenholz, Y. (2012). "Doxil(R)--the first FDA-approved nano-drug: lessons learned." J Control Release 160(2): 117-134.

Barnes, N. L. and Ooi, J. L. (2012). "Ductal carcinoma in situ of the breast." BMJ 344: e797.

Bhatt, R., de Vries, P., Tulinsky, J., Bellamy, G., Baker, B., Singer, J.W. and Klein, P. (2003). "Synthesis and in vivo antitumor activity of poly(l-glutamic acid) conjugates of 20S-camptothecin." J Med Chem 46(1): 190-193.

Broxterman, H. J. and Georgopapadakou N. H. (2005). "Anticancer therapeutics: "Addictive" targets, multi-targeted drugs, new drug combinations." Drug Resist Updat 8(4): 183-197.

Canal, F., Sanchis, J., and Vicent, M.J. (2011). "Polymer-drug conjugates as nano-sized medicines." Curr Opin Biotech 22(6): 894-900.

Carvalho, C., Santos, R.X., Cardoso, S., Correia, S., Oliveira, P.J., Santos, M.S., Moreirab P.I.. Carvalho, C., and Santos, R. X. (2009). "Doxorubicin: the good, the bad and the ugly effect." Curr Med Chem 16(25): 3267-3285.

Chandna, P., Saad, M., Wang, Y., Ber, E., Khandare, J., Vetcher, A.A., Soldatenkov, V.A. and Minko, T. (2007). "Targeted proapoptotic anticancer drug delivery system." Mol Pharm 4(5): 668-678.

Cheung, K. L. (2007). "Endocrine therapy for breast cancer: an overview." Breast 16(4): 327-343.

Chou, T. C. (2006). "Theoretical basis, experimental design, and computerized simulation of synergism and antagonism in drug combination studies." Pharmacol Rev 58(3): 621-681.

D'Arpa, P. and Liu, L.F. (1989). "Topoisomerase-targeting antitumor drugs." Biochim Biophys Acta 989(2): 163-177.

Dancey, J. and Sausville, E.A. (2003). "Issues and progress with protein kinase inhibitors for cancer treatment." Nat Rev Drug Discov 2(4): 296-313.

Davies, K. J. and Doroshow, J.H. (1986). "Redox cycling of anthracyclines by cardiac mitochondria. I. Anthracycline radical formation by NADH dehydrogenase." J Biol Chem 261(7): 3060-3067.

Davis, F. F. (2002). "The origin of pegnology." Adv Drug Deliv Rev 54(4): 457-458.

Davis, M. E. (2009). "Design and development of IT-101, a cyclodextrin-containing polymer conjugate of camptothecin." Adv Drug Deliv Rev 61(13): 1189-1192.

De Duve, C., De Barsy, T., Poole, B., Trouet, A., Tulkens, P., and Van Hoof, F. (1974). "Lysosomotropic agents." Biochemical Pharmacology 23(18): 2495-2531.

Deladriere, C., Lucas, R. and Vicent, M.J. (2011) "Future Trends, Challenges, and Opportunities with Polymer-Based Combination Therapy in Cancer." Dr. Felix Kratz, Dr. Peter Senter PhD, Dr. Henning Steinhagen (Ed), Wiley Philadelphia.: 805-838.

Devetzi, M., Scorilas, A., Tsiambas, E., Sameni, M., Fotiou, S., Sloane, B.F., and Talieri, M. (2009). "Cathepsin B protein levels in endometrial cancer: Potential value as a tumour biomarker." Gynecol Oncol 112(3): 531-536.

Dipetrillo, T., Milas, L., Evans, D., Akerman, P., Ng, T., Miner, T., Cruff, D., Chauhan, B., Iannitti, D., Harrington, D., and Safran, H. (2006). "Paclitaxel poliglumex (PPX-Xyotax) and concurrent radiation for esophageal and gastric cancer: a phase I study." Am J Clin Oncol 29(4): 376-379.

Dodwell, D., Wardley, A. and Johnston, S. (2006). "Postmenopausal advanced breast cancer: options for therapy after tamoxifen and aromatase inhibitors." Breast 15(5): 584-594.

Dolle, J. M., Daling, J. R., White, E., Brinton, L.A., Doody, D.R., Porter, P.L. and Malone, K.E. (2009). "Risk factors for triple-negative breast cancer in women under the age of 45 years." Cancer Epidemiol Biomarkers Prev 18(4): 1157-1166.

Duncan, R. (2003). "The dawning era of polymer therapeutics." Nat Rev Drug Discov 2(5): 347-360.

Duncan, R. (2005). N-(2-hydroxypropyl) methacrylamide copolymer conjugate. Polymeric Drug Delivery System. G. S. Kwon. New york, Marcel Dekker Inc.: 1-92.

Duncan, R. (2006). "Polymer conjugates as anticancer nanomedicines." Nat Rev Cancer 6(9): 688-701.

Duncan, R. (2007). "Designing polymer conjugates as lysosomotropic nanomedicines." Biochem Soc Trans 35(1): 56-60.

Duncan, R. (2009). "Development of HPMA copolymer-anticancer conjugates: clinical experience and lessons lernt." Adv Drug Deliv Rev 61(13): 1131-1148.

Duncan, R. (2011). "Polymer therapeutics as nanomedicines: new perspectives." Curr OPin Biotech 22(4): 492-501.

Duncan, R., Coatsworth, J. K. and Burtles, S. (1998). "Preclinical toxicology of a novel polymeric antitumour agent: HPMA copolymer-doxorubicin (PK1)." Hum Exp Toxicol 17(2): 93-104.

Duncan, R. and Gaspar, R. (2011). "Nanomedicine(s) under the microscope." Mol Pharm 8(6): 2101-2041.

Duncan, R., Hume, I.C., Kopeckova, P., Ulbrich, K., Strohalm, J., and Kopecek. (1991). "Macromolecular prodrugs for use in targeted cancer chemotherapy: melphalan covalently coupled to N-(2-hydroxypropyl) methacrylamide copolymers." J. Control. Release 16: 121-136.

Duncan, R. and Izzo, L. (2005). "Dendrimer biocompatibility and toxicity." Adv Drug Deliv Rev 57(15): 2215-2237.

Duncan, R., Kopecková-Rejmanová, P., Strohalm, J., Hume, I., Cable, H.C., Pohl, J., Lloyd, J.B. and Kopecek, J. (1987). "Anticancer agents coupled to N-(2-hydroxypropyl)methacrylamide copolymers. I. Evaluation of daunomycin and puromycin conjugates in vitro." Br J Cancer 55(2): 165-174.

Duncan, R. and Vicent, M.J. (2010). "Do HPMA copolymer conjugates have a future as clinical useful nanomedicines? A critical overview of current status and future opportunities." Adv Drug Deliv Rev 62(2): 272-282.

Duncan, R. and Vicent, M.J. (2013). "Polymer therapeutics-prospects for 21st century: The end of the beginning." Adv Drug Deliv Rev 65(1): 60-70.

Fang, J., Sawa, T., Akaike, T., Greish, K. and Maeda, H. (2004). "Enhancement of chemotherapeutic response of tumor cells by a heme oxygenase inhibitor, pegylated zinc protoporphyrin." Int J Cancer 109(1): 1-8.

Ferrari M. (2005). "Cancer nanotechnology: opportunities and challenges." Nat. Rev. Cancer 5(3): 161-171.

Fisher, B., Anderson, S., Wickerham, D.L., DeCillis, A., Dimitrov, N., Mamounas, E., Wolmark, N., Pugh, R., Atkins, J.N., Meyers, F.J., Abramson, N., Wolter, J., Bornstein, R.S., Levy, L., Romond, E.H., Caggiano, V., Grimaldi, M., Jochimsen, P. and Deckers, P., (1997). "Increased intensification and total dose of cyclophosphamide in a doxorubicin-cyclophosphamide regimen for the treatment of primary breast cancer: findings from National Surgical Adjuvant Breast and Bowel Project B-22." J Clin Oncol 15(5): 1858-1869.

Folkman, J. and Shing, Y., (1992). "Angiogenesis." The Journal of Biological Chemistry 267: 10931-10934.

Fornari, F.A., Randolph, J.K., Yalowich, J.C., Ritke, M.K. and Gewirtz, D.A. (1994). "Interference by doxorubicin with DNA unwinding in MCF-7 breast tumor cells." Mol Pharmacol 45(4): 649-656.

Gee, J.M., Howell, A., Gullick, W.J., Benz, C.C., Sutherland, R.L., Santen, R.J., Martin, L.A., Ciardiello, F., Miller, W.R., Dowsett, M., Barrett-Lee, P., Robertson, J.F., Johnston, S.R., Jones, H.E., Wakeling, A.E., Duncan, R. and Nicholson, R.I. (2005). "Consensus statement. Workshop on therapeutic resistance in breast cancer: impact of growth factor signalling pathways and implications for future treatment." Endocr Relat Cancer 12 Suppl 1: S1-7.

Gewirtz, D. A. (1999). "A critical evaluation of the mechanisms of action proposed for the antitumor effects of the anthracycline antibiotics adriamycin and daunorubicin." Biochem Pharmacol 57(7): 727-741.

Goodman, M.F.,Bessman, M.J. and Bachur, N.R. (1974). "Adriamycin and daunorubicin inhibition of mutant T4 DNA polymerases." Proc Natl Acad Sci U S A 71(4): 1193-1196.

Goss, P. E. and Strasser, K., (2002). "Tamoxifen resistant and refractory breast cancer: the value of aromatase inhibitors." Drugs 62(6): 957-966.

Greco, F. and Vicent, M. J., (2008). "Polymer-drug conjugates: current status and future trends." Front Biosci 13: 2744-2756.

Greco, F. and Vicent, M. J., (2009). "Combination therapy: opportunities and challenges for polymer-drug conjugates as anticancer nanomedicines." Adv Drug Deliv Rev 61(13): 1203-1213.

Greco, F., Vicent, M. J., Gee, S., Jones, A.T., Gee, J., Nicholson, RI., and Duncan, R. (2007). "Investigating the mechanism of enhanced cytotoxicity of HPMA copolymer-Dox-AGM in breast cancer cells." J Control Release 117(1): 28-39.

Greco, F., Vicent, M.J., Penning, N.A., Nicholson, R.I. and Duncan, R. (2005). "HPMA copolymer-aminoglutethimide conjugates inhibit aromatase in MCF-7 cell lines." J Drug Target 13(8-9): 459-470.

Gschwind, A., Fischer O.M., and Ullrich, A. (2004). "The discovery of receptor tyrosine kinases: targets for cancer therapy." Nat Rev Cancer 4(5): 361-370.

Herzog, T., Barret, R.J., Edwards, R. and Oldham, F. B. (2005). "Phase II study of paclitaxel (PPX) / Carboplatin (c) for the 1st line induction and maintenance therapy of stage III/IV ovarian or primary peritoneal carcinoma." J. Clin. Oncol. 23(16): 458S-458S.

Hortobagyi, G. N. (2002). "The status of breast cancer management: challenges and opportunities." Breast Cancer Res Treat 75 Suppl 1: S61-65; discussion S57-69.

Howell, A., Cuzick, J., Baum, M., Buzdar, A., Dowsett, M., Forbes, J.F., Hoctin-Boes, G., Houghton, J., Locker, G.Y., and Tobias, J.S. (2005). "Results of the ATAC (Arimidex, Tamoxifen, Alone or in Combination) trial after completion of 5 years' adjuvant treatment for breast cancer." Lancet 365(9453): 60-62.

http://www.fda.gov.

http://www.cancer.org

http://www.cancertreatment-wecareindia.com/breast_cancer.html

http://www.celator.ca (01 november 2010).

http://www.ucsf.edu/news/2011/09/10704/breast-cancer-month-time-take-stock-ucsf-advances.

Jassem, J., Pieńkowski, T., Płuzańska, A., Jelic, S., Gorbunova, V., Mrsic-Krmpotic, Z., Berzins, J., Nagykalnai, T., Wigler, N., Renard, J., Munier, S. and Weil, C. (2001). "Doxorubicin and paclitaxel versus fluorouracil, doxorubicin, and cyclophosphamide as first-line therapy for women with metastatic breast cancer: final results of a randomized phase III multicenter trial." J Clin Oncol 19(6): 1707-1715.

Johnston, S.R. and Dowsett, M., (2003). "Aromatase inhibitors for breast cancer: lessons from the laboratory." Nat Rev Cancer 3(11): 821-831.

Jones, D. (2009). "Avastin-Tarceva combination fails in lung cancer." Nat Biotechnol 27(2): 108-109.

Jordan, V.C. (2003). "Antiestrogens and selective estrogen receptor modulators as multifunctional medicines. 2. Clinical considerations and new agents." J Med Chem 46(7): 1081-1111.

Jordan, V.C. (2006). "Tamoxifen (ICI46,474) as a targeted therapy to treat and prevent breast cancer." Br. J. Pharmacol 147: 5269-5276.

Jordan, V.C. (2007). "New insights into the metabolism of tamoxifen and its role in the treatment and prevention of breast cancer." Steroids 72(13): 829-842.

Jordan, V. C. and Brodie, A.M., (2007). "Development and evolution of therapies targeted to the estrogen receptor for the treatment and prevention of breast cancer." Steroids 72(1): 7-25.

Kaufmann, S. H. and Earnshaw, W.C., (2000). "Induction of apoptosis by cancer chemotherapy." Exp Cell Res 256(1): 42-49.

Kelloff, G.J., Lubet, R.A., Lieberman, R., Eisenhauer, K., Steele, V.E., Crowell, J.A., Hawk, E.T., Boone, C.W. and Sigman, C.C. (1998). "Aromatase inhibitors as potential cancer chemopreventives." Cancer Epidemiol Biomarkers Prev 7(1): 65-78.

Khandare, J.J.,Chandna, P., Wang, Y., Pozharov, V.P. and Minko, T. (2006). "Novel polymeric prodrug with multivalent components for cancer therapy." J Pharmacol Exp Ther 317(3): 929-937.

Knop, K., Hoogenboom, R., Fischer, D. And Schubert, U.S. (2010) "Poly(ethylene glycol) in drug delivery: Pros and Con s as well as potential alternatives." Angew Chem 49 (36): 6288-6308.

Krakovicova, H., Etrych, T., and Ulbrich, K. (2009). "HPMA-based polymer conjugates with drug combination." Eur J Pharm Sci 37(3-4): 405-412.

Krinick, N. L., Sun, Y., Joyner, D., Spikes, J.D, Straight, R.C., and Kopecek, J. (1994). "A polymeric drug delivery system for the simultaneous delivery of drugs activatable by enzymes and/or light." J Biomater Sci Polym Ed 5(4): 303-324.

Lammers, T., Subr, V., Ulbrich, K., Peschke, P., Huber, P.E., Hennink, W.E., and Storm, G. (2009). "Simultaneous delivery of doxorubicin and gemcitabine to tumors in vivo using prototypic polymeric drug carriers." Biomaterials 30(20): 3466-3475.

Langer, C.J., O'Byrne, K.J., Socinski, M.A., Mikhailov, S.M., Leśniewski-Kmak, K., Smakal, M., Ciuleanu, T.E., Orlov, S.V., Dediu, M., Heigener, D., Eisenfeld,

A.J., Sandalic L, Oldham, F.B., Singer J.W. and Ross, H.J. (2008). "Phase III trial comparing paclitaxel poliglumex (CT-2103, PPX) in combination with carboplatin versus standard paclitaxel and carboplatin in the treatment of PS 2 patients with chemotherapy-naive advanced non-small cell lung cancer." J Thorac Oncol 3(6): 623-630.

Leonardi, M.C., Ivaldi, G.B., Santoro, L., Lazzari, R., Ferrari, A., Morra, A., Caldarella, P., Burgoa, L., Bassi, F.D., Sangalli, C., Rotmensz, N., Luini, A., Veronesi, U. and Orecchia, R. (2012). "Long-term side effects and cosmetic outcome in a pool of breast cancer patients treated with intraoperative radiotherapy with electrons as sole treatment." Tumori 98(3): 324-330.

Lewis-Wambi, J. S. and Jordan, V.C., (2009). "Estrogen regulation of apoptosis: how can one hormone stimulate and inhibit?" Breast Cancer Res 11(3): 206.

Ling, Y.H., el-Naggar, A.K., Priebe, W., and Perez-Soler, R., (1996). "Cell cycle-dependent cytotoxicity, G2/M phase arrest, and disruption of p34cdc2/cyclin B1 activity induced by doxorubicin in synchronized P388 cells." Mol Pharmacol 49(5): 832-841.

Lombardi, P. (1995). "The irreversible inhibition of aromatase (oestrogen synthetase) by steroidal compounds." Curr. Pharm. Des. 1: 23-50.

Lombardi, P. (2002). "Exemestane, a new steroidal aromatase inhibitor of clinical relevance." Biochim Biophys Acta 1587(2-3): 326-337.

Maeda, H. (1994). Polymer conjugated macromolecular drugs for tumour-specific targeting. Polymeric site-specific Pharmacotherapy. J. W. a. S. Ltd. USA: 96-116.

Maeda, H. (2001). "The enhanced permeability and retention (EPR) effect in tumor vasculature: the key role of tumor-selective macromolecular drug targeting." Adv Enzyme Regul 41: 189-207.

Maeda, H. (2010). "Tumor-selective delivery of macromolecular drugs via the EPR effect: background and future prospects." Bioconjug Chem 21(5): 797-802.

Maeda, H., Nakamura, H. and Fang, J. (2012). "The EPR effect for macromolecular drug delivery to solid tumors: Improvement of tumor uptake, lowering of systemic toxicity, and distinct tumor imaging in vivo." Adv Drug Deliv Rev. 65(1): 71-79.

Maeda, H., Sawa, T. and Konno, T. (2001). "Mechanism of tumor-targeted delivery of macromolecular drugs, including the EPR effect in solid tumor and clinical overview of the prototype polymeric drug SMANCS." J Control Release 74(1-3): 47-61.

Maughan, K. L., M. A. Lutterbie, and Ham, P. (2010). "Treatment of breast cancer." Am Fam Physician 81(11): 1339-1346.

Mayer, L. D. and Janoff, A.S. (2007). "Optimizing combination chemotherapy by controlling drug ratios." Mol Interv 7(4): 216-223.

McNamara, K.M., Yoda, T., Takagi, K., Miki, Y., Suzuki, T., and Sasano, H. (2012). "Androgen receptor in triple negative breast cancer." J Steroid Biochem Mol Biol 133C: 66-76.

Meerum Terwogt, J.M., Bokkel Huinink, W.W., Schellens, J.H., Schot, M., Mandjes, I.A., Zurlo, M.G., Rocchetti, M., Rosing, H., Koopman, F.J.,and Beijnen, J.H. (2001). "Phase I clinical and pharmacokinetic study of PNU166945, a novel water soluble polymer conjugated prodrug of paclitaxel." Anticancer Drugs Des 12: 315-323.

Miller, K., Erez, R., Segal, E., Shabat, D., and Satchi-Fainaro, R. (2009). "Targeting bone metastases with a bispecific anticancer and antiangiogenic polymer-alendronate-taxane conjugate." Angew Chem Int Ed Engl 48(16): 2949-2954.

Miller, W. R. (1996). "Aromatase inhibitors " Endocr Relat Cancer 3: 65-79.

Minko, T., Kopecková, P., Pozharov, V., and Kopecek, J. (1998). "HPMA copolymer bound adriamycin overcomes MDR1 gene encoded resistance in a human ovarian carcinoma cell line." J Control Release 54(2): 223-233.

Momparler, R.L., Karon, M., Siegel, S.E., and Avila, F. (1976). "Effect of adriamycin on DNA, RNA, and protein synthesis in cell-free systems and intact cells." Cancer Res 36(8): 2891-2895.

Mondragón, L., Orzáez, M., Sanclimens, G., Moure, A., Armiñán, A., Sepúlveda, P., Messeguer, A., Vicent, M.J., and Pérez-Payá, E. (2008). "Modulation of cellular apoptosis with apoptotic protease-activating factor 1 (Apaf-1) inhibitors." J Med Chem 51(3): 521-529.

Nicholson, R. I. and Gee, J.M. (2000). "Oestrogen and growth factor cross-talk and endocrine insensitivity and acquired resistance in breast cancer." Br J Cancer 82(3): 501-513.

Nicholson, R.I., Hutcheson, I.R., Harper, M.E., Knowlden, J.M., Barrow, D., McClelland, R.A., Jones, H.E., Wakeling, A.E., and Gee, J.M. (2001). "Modulation of epidermal growth factor receptor in endocrine-resistant, oestrogen receptor-positive breast cancer." Endocr Relat Cancer 8(3): 175-182.

Nielsen, D.L., Andersson, M., and Kamby, C. (2009). "HER2-targeted therapy in breast cancer. Monoclonal antibodies and tyrosine kinase inhibitors." Cancer Treat Rev 35(2): 121-136.

Njar V.C.O. and Brodie A.M.H. (1999). "Comprehensive pharmacology and clinical efficacy of aromatase inhibitors." Drugs 58(2): 233-255.

Normanno, N., Morabito, A., De Luca, A., Piccirillo, M.C., Gallo, M., Maiello, M.R., and Perrone, F. (2009). "Target-based therapies in breast cancer: current status and future perspectives." Endocr Relat Cancer 16(3): 675-702.

Oakman, C. and Viale, G.. (2010). "Management of triple negative breast cancer." Breast. 19(5): 312-321.

Parnes, H.L., Cirrincione, C., Aisner, J., Berry, D.A., Allen, S.L., Abrams, J., Chuang, E., Cooper, M.R., Perry, M.C., Duggan, D.B., Szatrowski, T.P., Henderson, I.C., and Norton, L. (2003). "Phase III study of cyclophosphamide, doxorubicin, and fluorouracil (CAF) plus leucovorin versus CAF for metastatic breast cancer: Cancer and Leukemia Group B 9140." J Clin Oncol 21(9): 1819-1824.

Pearson, O.H., Hubay, CA., Gordon, N.H., Marshall, J.S., Crowe, J.P., Arafah, B.M., and McGuire, W. (1989). "Endocrine versus endocrine plus five-drug chemotherapy in postmenopausal women with stage II estrogen receptor-positive breast cancer." Cancer 64(9): 1819-1823.

Peer, D., Karp, J.M., Hong, S., Farokhzad, O.C., Margalit, R. and Langer, R. (2007). "Nanocarriers as an emerging platform for cancer therapy." Nature technology 2: 751-760.

Phipps, A.I., Chlebowski, R.T., Prentice, R., McTiernan, A., Wactawski-Wende, J., Kuller, L.H., Adams-Campbell, L.L., Lane, D., Stefanick, M.L., Vitolins, M., Kabat, G.C., Rohan, T.E., and Li, C.I. (2011). "Reproductive history and oral contraceptive use in relation to risk of triple-negative breast cancer." J Natl Cancer Inst 103(6): 470-477.

Platet, N., Cathiard, A.M., Gleizes, M., and Garcia, M. (2004). "Estrogens and their receptors in breast cancer progression: a dual role in cancer proliferation and invasion." Crit Rev Oncol Hematol 51(1): 55-67.

Rahman, A.M., Yusuf, S.W., and Ewer, M.S. (2007). "Anthracycline-induced cardiotoxicity and the cardiac-sparing effect of liposomal formulation." Int J Nanomedicine 2(4): 567-583.

Ríhová, B., Strohalm, J., Prausová, J., Kubácková, K., Jelínková, M., Rozprimová, L., Sírová, M., Plocová, D., Etrych, T., Subr, V., Mrkvan, T., Kovár, M., and

Ulbrich, K. (2003). "Cytostatic and immunomobilizing activities of polymer-bound drugs: experimental and first clinical data." J Control Release 91(1): 1-16.

Ringsdorf, H. (1975). "Structure and proprieties of pharmacologically active polymer." J. Polymer Sci. Polymer Symp. 51: 135-153.

Roca-Alonso, L., Pellegrino, L., Castellano, L., and Stebbing, J. (2012). "Breast cancer treatment and adverse cardiac events: what are the molecular mechanisms?" Cardiology 122(4): 253-259.

Samini, A.M., Chuang, E.Y., Krishna, M.C., Stein, W., DeGraff, W., Russo, A., and Mitchell, J.B. (2003). "Semiquinone radical intermediate in catecholic estrogen-mediated cytotoxicity and mutagenesis: Chemo prevention strategies with antioxidants" PNAS 100(9): 5390-5395.

Sanchis, J., Canal, F., Lucas, R., and Vicent, M.J. (2010) "Polymer-drug conjugates for novel molecular targets." Nanomedicine 5(6): 915-935.

Santucci, L., Mencarelli, A., Renga, B., Ceccobelli, D., Pasut, G., Veronese, FM., Distrutti, E. and Fiorucci, S. (2007). "Cardiac safety and antitumoral activity of a new nitric oxide derivative of pegylated epirubicin in mice." Anticancer Drugs 18(9): 1081-1091.

Santucci, L., Mencarelli, A., Renga, B., Pasut, G., Veronese, F., Zacheo, A., Germani, A., and Fiorucci, S. (2006). "Nitric oxide modulates proapoptotic and antiapoptotic properties of chemotherapy agents: the case of NO-pegylated epirubicin." FASEB J 20(6): 765-767.

Satchi-Fainaro, R., Hailu, H., Davies, JW., Summerford, C., and Duncan, R. (2003). "PDEPT: polymer-directed enzyme prodrug therapy. 2. HPMA copolymer-beta-lactamase and HPMA copolymer-C-Dox as a model combination." Bioconjug Chem 14(4): 797-804.

Satchi-Fainaro, R., Mamluk, R., Wang, L., Short, S.M., Nagy, J.A., Feng, D., Dvorak, A.M., Dvorak, H.F., Puder, M., Mukhopadhyay, D., and Folkman, J. (2005). "Inhibition of vessel permeability by TNP-470 and its polymer conjugate, caplostatin." Cancer Cell 7(3): 251-261.

Satchi-Fainaro, R., Puder, M., Davies, J.W., Tran, HT., Sampson, D.A., Greene, AK., Corfas, G., and Folkman, J.. (2004). "Targeting angiogenesis with a conjugate of HPMA copolymer and TNP-470." Nat Med 10(3): 255-261.

Satchi-Fainaro, R., Wrasidlo, W., Lode, H.N., and Shabat, D. (2002). "Synthesis and characterization of a catalytic antibody-HPMA copolymer-Conjugate as a tool for tumor selective prodrug activation." Bioorg Med Chem 10(9): 3023-3029.

Schmitt, F. (2009). "HER2+ breast cancer: how to evaluate?" Adv Ther 26 Suppl 1: S1-8.

Schulz, W. A. (2005). Molecular biology of human cancers. An advanced student's textbook. dusseldorf, Springer.

Segal, E., and Satchi-Fainaro, R. (2009). "Design and development of polymer conjugates as anti-angiogenic agents." Adv. Drug Deliv. Rev. 61(13): 1159-1176.

Seymour, L.W., Ferry, D.R., Anderson, D., Hesslewood, S., Julyan, P.J., Poyner, R., Doran, J., Young, A.M., Burtles, S., and Kerr, D.J. (2002). "Hepatic drug targeting: phase I evaluation of polymer-bound doxorubicin." J Clin Oncol 20(6): 1668-1676.

Seymour, L.W., Ferry, D.R., Kerr, D.J., Rea, D., Whitlock, M., Poyner, R., Boivin, C., Hesslewood, S., Twelves, C., Blackie, R., Schatzlein, A., Jodrell, D., Bissett, D., Calvert, H., Lind, M., Robbins, A., Burtles, S., Duncan, R., and Cassidy, J. (2009). "Phase II studies of polymer-doxorubicin (PK1, FCE28068) in the treatment of breast, lung and colorectal cancer." Int J Oncol 34(6): 1629-1636.

Shiah, J.G., Sun, Y., Kopecková, P., Peterson, C.M., Straight, RC. and Kopecek, J. (2001). "Combination chemotherapy and photodynamic therapy of targetable N-(2-hydroxypropyl)methacrylamide copolymer-doxorubicin/mesochlorin e(6)-OV-TL 16 antibody immunoconjugates." J Control Release 74(1-3): 249-253.

Singal, P. K. and Iliskovic, N. (1998). "Doxorubicin-induced cardiomyopathy." N Engl J Med 339(13): 900-905.

Singer, J. W. (2005). "Paclitaxel poliglumex (XYOTAX, CT-2103): a macromolecular taxane." J Control Release 109(1-3): 120-126.

Singer J.W., Baker B., De Vries, P., Kumar, A., Shaffer, S., Vawter, E., Bolton, M., and Garzone, P. (2003). "Poly-(L)-glutamic acid-paclitaxel (CT-2103) [XYOTAX], a biodegradable polymeric drug conjugate: characterization, preclinical pharmacology, and preliminary clinical data." Adv Exp Med Biol 519: 81-99.

Singer, J.W., Shaffer, S., Baker, B., Bernareggi, A., Stromatt, S., Nienstedt, D., and Besman, M. (2005). "Paclitaxel poliglumex (XYOTAX; CT-2103): an intracellularly targeted taxane." Anticancer Drugs 16(3): 243-254.

Sirova, M., Strohalm, J., Subr, V., Plocova, D., Rossmann, P., Mrkvan, T., Ulbrich, K., and Rihova, B. (2007). "Treatment with HPMA copolymer-based doxorubicin conjugate containing human immunoglobulin induces long-lasting systemic anti-tumour immunity in mice." Cancer Immunol Immunother 56(1): 35-47.

Skladanowski, A. and Konopa, J. (1993). "Adriamycin and daunomycin induce programmed cell death (apoptosis) in tumour cells." Biochem Pharmacol 46(3): 375-382.

Stewart, D.J., Evans, W.K., Shepherd, F.A., Wilson, K.S., Pritchard, K.I., Trudeau, M.E., Wilson, J.J., and Martz, K. (1997). "Cyclophosphamide and fluorouracil combined with mitoxantrone versus doxorubicin for breast cancer: superiority of doxorubicin." J Clin Oncol 15(5): 1897-1905.

Tang, J. Y., Rampaul, R.S., and Cheung, K.L. (2008). "The use of fulvestrant, a parenteral endocrine agent, in intestinal obstruction due to metastatic lobular breast carcinoma." World J Surg Oncol 6: 128.

Tkaczuk, K. H. (2009). "Review of the contemporary cytotoxic and biologic combinations available for the treatment of metastatic breast cancer." Clin Ther 31 Pt 2: 2273-2289.

Tong, J., R. Luxenhofer, Xiang, Y., Rainer, J. and Kabanov, AV. (2010) "Protein Modification with Amphiphilic Block Copoly(2-oxazoline)s as a New Platform for Enhanced Cellular Delivery." Mol Pharm. 7(4): 984-992.

Vasey, P.A., Kaye, S.B., Morrison, R., Twelves, C., Wilson, P., Duncan, R., Thomson, A.H., Murray, L.S., Hilditch, T.E., Murray T., Burtles, S., Fraier, D., Frigerio, E., and Cassidy, J. (1999). "Phase I clinical and pharmacokinetic study of PK1 [N-(2-hydroxypropyl)methacrylamide copolymer doxorubicin]: first member of a new class of chemotherapeutic agents-drug-polymer conjugates. Cancer Research Campaign Phase I/II Committee." Clin Cancer Res 5(1): 83-94.

[a]Veronesi, U., Goldhirsch, A., Boyle, P., Orecchia, R., and Viale, G. (2005). "Breast cancer." Discov Med 5(27): 271-277.

[b] Veronesi, U., Orecchia, R., Zurrida, S., Galimberti, V., Luini, A., Veronesi, P., Gatti, G., D'Aiuto, G., Cataliotti, L., Paolucci, R., Piccolo, P., Massaioli, N., Sismondi, P., Rulli, A., Lo Sardo, F., Recalcati, A., Terribile, D., Acerbi, A., Rotmensz, N., and Maisonneuve, P. (2005). "Avoiding axillary dissection in breast cancer surgery: a randomized trial to assess the role of axillary radiotherapy." Ann Oncol 16(3): 383-388.

Verschraegen, C.F., Skubitz, K., Daud, A., Kudelka, A.P., Rabinowitz, I., Allievi, C., Eisenfeld, A., Singer, J.W., and Oldham, F.B. (2009). "A phase I and pharmacokinetic study of paclitaxel poliglumex and cisplatin in patients with advanced solid tumors." Cancer Chemother Pharmacol 63(5): 903-910.

Vicent, M. J. (2007). "Polymer-drug conjugates as modulators of cellular apoptosis." Aaps J 9(2): E200-207.

Vicent, M. J., Dieudonne, L., Carbajo, R.J., and Pineda-Lucena, A. (2008). "Polymer conjugates as therapeutics: future trends, challenges and opportunities." Expert Opin Drug Deliv 5(5): 593-614.

Vicent, M. J. and Duncan, R. (2006). "Polymer conjugates: nanosized medicines for treating cancer." Trends Biotechnol 24(1): 39-47.

Vicent, M. J., Greco, F., Nicholson, R.I., Paul, A., Griffiths, P.C., and Duncan, R. (2005). "Polymer therapeutics designed for a combination therapy of hormone-dependent cancer." Angew Chem Int Ed Engl 44(26): 4061-4066.

Vicent, M. J. and Perez-Paya, E. (2006). "Poly-L-glutamic acid (PGA) aided inhibitors of apoptotic protease activating factor 1 (Apaf-1): an antiapoptotic polymeric nanomedicine." J Med Chem 49(13): 3763-3765.

Vicent, M. J., Ringsdorf, H., and Duncan, R. (2009). "Polymer therapeutics: clinical applications and challenges for development." Adv Drug Deliv Rev 61(13): 1117-1120.

Whelan, J. (2002). "Targeted taxane therapy for cancer." Drug Discov Today 7(2): 90-92.

Yurkovetskiy, A. V. and Fram, R.J. (2009). "XMT-1001, a novel polymeric camptothecin pro-drug in clinical development for patients with advanced cancer." Adv Drug Deliv Rev 61(13): 1193-1202.

Zilli, M., Grassadonia, A., Tinari, N., Di Giacobbe, A., Gildetti, S., Giampietro, J., Natoli, C., and Iacobelli, S. (2009). "Molecular mechanisms of endocrine resistance and their implication in the therapy of breast cancer." Biochim Biophys Acta 1795(1): 62-81.

Chapter 2. Aims and Objectives.

2.1. Aims and objectives.

Based on the *in vitro* evaluation of HPMA copolymer-AGM-Dox conjugate, it seems that the combination of the AGM with Dox in the same polymeric backbone induces a synergistic effect against human breast cancer cells. However *in vitro* tests are not taken into account the *in vivo* complexity, therefore, the first aim of this PhD thesis is to achieve *in vivo* proof of concept for HPMA copolymer-AGM-Dox conjugate synergism followed by a fully understanding of the molecular mechanism of action for our combination conjugate, HPMA copolymer-AGM-Dox conjugate.

Additionally, HPMA copolymer is known as a non-biodegradable polymer, which induces an unfavourable pharmacological profile for long-term treatment (Duncan et al., 2010). Therefore in order to improve the structure and also to know if the carrier chosen could influence drug synergism, a new family of PGA conjugates will be developed. The design of an effective PGA-AGM-Dox conjugate family and its comparison with the model conjugate will be the main objective in order to understand the basis for synergism that would allow us a better design of a future combination therapy.

The therapeutic potential of polyglutamates as drug delivery systems is based on the successful development of Xyotax^{TM} now named as Opaxio® (Singer et al., 2005) (from Cell Therapeutics Inc.) the first polymer-drug conjugate that is expected to come to market as anticancer treatment alone and in combination with radiotherapy. Moreover, Dr Vicent's group, in collaboration with Dr Pérez-Payá and Dr Messeguer, has developed the first antiapoptotic medicine, PGA-peptoid conjugate, currently in preclinical development (Vicent and Perez-Paya, 2006; Vicent, 2007; Mondragon et al., 2008).

Although it is important to keep the same combination of drugs in order to evaluate the influence of the carrier, AGM is a first generation aromatase inhibitor already removed from the market. Therefore, new drug cocktails should be identified. In this sense, as a final chapter in this thesis, a high throughput screening (HTPS) has been developed with 4 chemotherapeutic agents and 3 endocrine agents looking for new efficient combinations including

current drugs in the market with better therapeutic profile, such as second generation of aromatase inhibitors (*i.e.* Exemestane, Formestane).

2.2. Bibliography.

Duncan, R. and Vicent, M.J. (2010). "Do HPMA copolymer conjugates have a future as clinical useful nanomedicines? A critical overview of current status and future opportunities." Adv Drug Deliv Rev 62(2): 272-282.

Singer, J.W., Shaffer, S., Baker, B., Bernareggi, A., Stromatt, S., Nienstedt, D., and Besman, M. (2005). "Paclitaxel poliglumex (XYOTAX; CT-2103): an intracellularly targeted taxane." Anticancer Drugs 16(3): 243-254

Vicent, M. J. and Perez-Paya, E. (2006). "Poly-L-glutamic acid (PGA) aided inhibitors of apoptotic protease activating factor 1 (Apaf-1): an antiapoptotic polymeric nanomedicine." J Med Chem 49(13): 3763-3765.

Vicent, M. J. (2007). "Polymer-drug conjugates as modulators of cellular apoptosis." Aaps J 9(2): E200-207.

Chapter 3. Materials and General Methods.

3.1. Equipment.

Gel Permeation Chromatography (GPC) analysis was carried out with Two Waters pumps mixer using Two TSK-gel columns in series G25000PWXL (200-12000) and G3000 PWXL (1000-250000). The detection was performed with a quadruple detector Viscotek TDA^{TM}; Ultraviolet (UV), Light Scattering (LS), Refractive Index (RI) and Viscosimetry.

Mass Spectrometry was used for metabolite identification with a MALDI-ToF bruker for weight higher than 500 kDa and Waters HPLC-MS quadruple system for the weight lesser than 500 kDa.

NMR: The NMR was performed with a 300 MHz Bruker equipment.

High Performance Liquid Chromatography (HPLC) analysis was performed with three Waters pumps mixer 515 using RP18 column (125x4mm). The 717 autosampler was from Waters and the HPLC was provided of two detectors, a diode array (2996 Waters) and a multi wavelength detector (2475 Waters). The chromatograms were recorded and analysed by Empower Software.

Size Exclusion Chromatography (SEC) was carrying out with Sephadex G25 for waters soluble sample and with Sephadex LH20 for organic soluble sample.

Thin Layer chromatography (TLC) was performed on Merck silica gel plates (TLC silica gel 60 F_{254}) and on Merck C18 gel plates (TLC silica gel 60 RP-18 F_{254} S)

Ultraviolet (UV-Vis) spectra were measured by a Jasco V630 spectrophotometer.

Small Angle Neutron Scattering (SANS) experiments were carried out in ILL Grenoble (France) in collaboration with Dr Paul (Cardiff Univ., UK).

3.1.1. Cell Culture and equipment for biological tests.

Cell experiments were performed in Laminar flow hood. Cell cultures were grown in tissue culture sterile plates (P100, 55cm^2) from Falcon (353003) and

maintained in incubator at 37°C with or without 5% of CO_2 depending of the cell line culture conditions. For cell experiments, tissue culture sterile plates (96 wells and P60, 21cm^2) from costar (3596) were used. For cell passaging, alive cell number was counted in a Neubauer camera following previous trypan blue staining. Sterile pipette were from costar. Centrifuge tubes were from ependorf (5702).

Microtome. Histological slides were performed/prepared with MICROM international model HM 340E.

Ultraturrax. The animal samples were processed by means of IKA T 25 digital ultraturrax.

IVIS Spectrum Optical Imaging System. Pre-clinical In Vivo Imaging System (Perkin Elmer).

3.2. Materials.

3.2.1. Chemical reagents.

Dimethylformamide (DMF), Hydroxybenzotriazole (HOBt), N,N'-diclyclohexylcarbodiimide (DCC), N,N'-Diisopropylcarbodiimide (DIC), 4-Dimethyl amino pyridine (DMAP), Aminoglutethimide (AGM), Diisopropyl ethyl amide (DIEA), 5-fluorouracil (5 FU), Oestradiol, Daunorubicin, Fluorenyl methyl chloride (Fmoc-cl), 4-OH-Tamoxifen (4 OH-T), tert-butyl oxy carbonyl Leucine-Glycine (Boc-Leu-Gly), Carbobenzyloxy Glycine Phenylalanine (Z-Gly-Phe), Glycine Glycine (GlyGly), camptothecin were provided by Sigma (ES). Methanol (MeOH), acetonitrile (ACN), Acetone, O-phosphoric acid, Ethyl acetate (EtAc) were supplied from VWR (SP). Carbobenzyloxy Glycine Glycine (Z-GlyGly), Carbobenzyloxy Glycine (Z-Gly) were bought in Bachem (Sp). Fluorenyl methyl Glycine (Fmoc-Gly) was from Iris Biotech Gmb (DE). Paclitaxel (P) was from Shaanxi sciphar (China). Doxorubicin (Dox) and exemestane (E) were from Sinoapex pharm (CN).

3.2.2. Polymeric carriers.

N-(2-hydroxypropyl) methacrylamide (HPMA) copolymer precursors, carrying either a Gly-Gly-p-nitrophenol ester (ONp) (5 mol%; Mw~30.000 g/mol and Mw/Mn = 1,3-1,5) or Gly-Phe-Leu-Gly-ONp (either 5 or 10 mol%; Mw~30.000 g/mol and Mw/Mn = 1,3-1,5) were from Polymer Laboratories Ltd, Shropshire, U.K. The bound ONp content of polymeric precursors was calculated using ε274 nm = 9500 L.mol-1.cm-1 (in DMSO). Poly-L-Glutamic acid (PGA) were provided by Cell Therapeutics Europe s.r.l. or synthesised as reported elsewhere (Conejos-Sánchez et al., 2013).

3.2.3. Chemical reagents for biological analysis.

Dimethylsufoxyde (DMSO), Charcoal A, Dextran, Bradford reagent, Sodium Dodecilsulfate (SDS), Tris, borate acid and phenazine methosulfate (PMS) were supplied by Sigma (Sp). Dulbecco's Modified Eagle's Medium (DMEM), Leibovitz, Phosphate buffer saline (PBS), Foetal bovine serum (FBS) and Trypsin, were provided from Gibco. Penicillin/ Streptomycin (P/S) and Bovine Serum Albumin (BSA) were from Invitrogen. (3-(4,5-dimethylthiazol-2-yl)-5-(3-carboxymethoxyphenyl)-2-(4-sulfophenyl)-2H-tetrazolium) (MTS) was supplied by Promega (Sp). Ammonium Persulfate, Tetramethylethylenediamine (TEMED) and tween 20 were provided by VWR.

The acrylamide/bis was supplied by BioRad (Sp) and non-fat dry milk was bought in Carrefour. For histological analysis, eosine, hematoxyline and sodium azide were from Sigma, SuperFrost Plus slide from Menzel-Glaser, Thermo Fisher Scientific Inc. UK, formaldehyde and Eukitt were bought in Panreac (Sp) and paraffin was purchased from ParaPlast Plus, Tyco Healthcare (UK).

For *in vivo* models, sevofluorane, buprex and morfine were provided by the animal house keeping office. The androstenedione and Evans blue were purchased from sigma. Matrigel was bought in BD (Sp).

3.3. Experimental Methods.

3.3.1. Synthesis of conjugates and derivatised linker drugs.

3.3.1.a. Synthesis of linker-drugs.

   G-AGM: Fluorenylmethyloxycarbonyl glycine (Fmoc-G) (0,65 mmol, 193,24 mg) was dissolved in DMF anhydrous (5 mL), DIC (0,975 mmol, 153 µL) activation was done during 5 min then 1-hydroxybenzotriazole (HOBt) (0,975 mmol, 132 mg) was added. After 10min, AGM (0,65 mmol, 147 mg) was finally added. The pH was controlled and adjusted with DIEA to pH8. The reaction was left to react for 36 h at room temperature (RT). The DMF was evaporated by high vacuum and Fmoc-G-AGM was purified by liq/liq extraction. Fmoc-G-AGM was dissolved in AcOEt (10 mL) and extracted with sat NaHCO$_3$ (3 x 10 mL). Synthesis and characterisation of Fmoc-G-AGM was performed by NMR. ^{1}H NMR (300MHz,DMSO) 10, (s, 1H, NH Gly), 11,(s, 1H, NH AGM), 7,85 (d9d3, 1H, arom. Fmoc), 7,65(d9d3, 1H, arom. Fmoc), 7,53 (t7, 1H, arom. Fmoc), 7,5 (d9, 1H, arom. AGM), 7,37 (t9d3, 1H, arom. Fmoc), 7,18 (d9, 1H, arom. AGM). 4,2 (m, 2H, CH, CH2 Fmoc), 3,7 (d7, 2H, CH2 Gly), 2-2,3 (m, 2H, CH AGM), 1,8 (q7, 2H, CH2 AGM) and 0,7 (t7, 3H, CH3 AGM). ^{13}C NMR 300 MHz, 176 (1C, C=O AGM), 173 (1V, C=O Gly), 168 (1C, C=O AGM), 157 (2C, C=O Fmoc), 144 (2C, Cq Arom. Fmoc), 141 (2C, Cq Arom. Fmoc), 139 (1C, Cq Arom. AGM), 136 (1C, Cq Arom. AGM), 128 (2C, CH Arom. Fmoc), 127 (2C, CH Arom. Fmoc), CH Arom. AGM), 125 (125 (2C, CH Arom. Fmoc), 120 (2C, CH Arom. Fmoc), 119 (2C, CH Arom. AGM), 70 (1C, CH2, Fmoc) 50 (1C, Cq AGM), 47 (1C, CH, Fmoc), 32 (1C, CH2, AGM), 29 (2C, CH2, AGM), 26 (2C, CH2, AGM), 10 (1C, CH3, AGM).

Then the organic phase was washed with acid chloride (HCl) 1M (3 x 10 mL), dried on sodium sulphate (Na$_2$(SO$_4$)) and evaporated to yield 90% of a white product. Afterwards, a deprotection step was performed using piperidine 20% in AcOEt during 1 h. Product purification was carried out by RP-chromatography with a C18 Porous resin. The starting chromatographic conditions were water (H$_2$O)/acetonitrile (ACN) (30:70). After 30 mL of elution, further ACN (10 mL) was also poured. The purification was monitored by TLC (G-AGM Rf:0, Fmoc

Rf: 0,83 with Hexane:AcOEt 1:4). A double detection protocol was used: UV and Nihindrin staining. The reaction yield was 70% (0,46 mmol, 125 mg). Characterisation of G-AGM was performed by NMR. ^{1}H NMR (300 MHz, DMSO)): 7,6 (d9, 2H, Arom. AGM), 7,22 (d9, 2H, Arom. AGM), 3 (t7, 2H, CH2 Gly), 2-2,3 (m, 4H, 2 CH AGM), 1,8 (q7, 2H, CH2 AGM) and 0,64 (t7, 3H, CH3 AGM). ^{13}C NMR 300MHz 174 (1C, Cq, C=O AGM), 172 (1C, C=O Gly), 169 (1C, C=O AGM), 138 (1C, Cq, AGM), 135 (1C, Cq, AGM), 127 (2C, CH, Arom. AGM), 119 (2C, CH, Arom. AGM), 50 (1C, Cq, AGM), 44 (1C, CH2, Gly), 32 (1C, CH2, AGM), 29 (1C, CH2, AGM), 22 (1C, CH2, AGM), 10 (1C, CH3, AGM).

GG-AGM: In order to synthesise GG-AGM a previous step was required, the Fmoc protection of GG.

Fmoc-GG (Tomlinson et al., 2002) : GG (0,28 mmol, 37,8 mg) was dissolved in a $NaHCO_3$ solution (10%) (1,6 mL), then dioxane was added (0,9 mL) and the reaction was cooled down in ice. Once the right temperature was achieved, fluorenylmethyloxycarbonyl chloride (Fmoc-Cl) (0,28 mmol, 80 mg) was carefully added dropwise. The reaction was left to react for 4 hours on an ice bath and overnight at room temperature. Fmoc-GG was purified by liq/liq extraction, 3x H_2O (3 mL) was added and the aqueous phase was extracted with AcOEt (3x5 mL). The aqueous phase was acidified with HCl (1 M) up to pH 2 and extracted with AcOEt (3x5 mL). The organic phase was collected, dried on $Na_2(SO_4)$ and evaporated to yield 81% of a white product. Characterisation of Fmoc-G-G was performed by NMR. ^{1}H NMR (300 MHz, DMSO): 8,2 (t7, 1H NH Gly), 7,85 (d9d3, 2H, CH, Arom. Fmoc), 7,65(d9d3, 2H, CH, Arom. Fmoc), 7,53 (t7, 1H NH Fmoc), 7,37 (t9d3 2H, CH, Arom. Fmoc) 7,25 (t9d3, 2H, CH, Arom. Fmoc), 4,2 (m, 3H, CH CH2, Fmoc), 3,7 (d7, 2H, CH2, Gly) and 3,4 (d7, 2H, CH2, Gly).

Then the GG-AGM synthesis was carried out following the same procedure described above for G-AGM.

G-Dox: Benzyl chloroformate glycine Bz-G (0,083 mmol, 31,8 mg) was dissolved in DMF anhydrous (5 mL), then DIC (0,124 mmol, 20 μL) was added

and after 5 min HOBt (0,124 mmol, 22 mg) was also added as solid. After 10 min activation, Dox.HCl (0,083 mmol, 45,5 mg) was finally incorporated to the reaction mixture. The pH was controlled and adjusted with DIEA to obtained pH = 8. The reaction was left to react for 36 h at RT. DMF was then evaporated at high vacuum. The dry pellet was dissolved in MeOH and the purification was carried out by RP-chromatography (C_{18}) with 10 mL of 2-propanol/H_2O (12:88) (v/v), 10 mL of 2-propanol/H_2O (29:71) (v/v) and then 20 mL of MeOH (pH3,2). The purification procedure was monitored by TLC through a double detection system set at λ= 254 nm and λ= 366 nm. Z-GG-Dox was identified by Maldi-Tof. Then, the deprotection was carried out in H_2 Pd/C_{act} overnight. The solution was filtrated through celite and with a filter of 0,2 µm. After the MeOH removal, a yield of 50% was achieved and GG-Dox was identified by Maldi-Tof.

GG-Dox: The synthesis of GG-Dox was performed following the same protocol above-described for G-Dox.

3.3.1.b. Single conjugates synthesis.

PGA-OSucc synthesis and purification: For PGA-AGM synthesis, previous carboxylic group activation was necessary. Indeed due to the poor reactivity of the AGM aromatic amine, classic diimide activation was not enough for the coupling. The PGA carboxylic groups were activated first by succinic group. PGA (3,55 mmol, 471.4 mg) was dissolved in DMF anhydrous (5 mL), N-hydroxy succinimid (2,33 mmol, 268.4 mg) was added to reach a maximum of 60% of carboxylic group activation. When the solution was totally transparent, DIC (2.33 mmol, 350 µL) and a catalytic amount of DMAP were added. The reaction was left for 36 h. The DMF was evaporated by high vacuum and the PGA-OSucc was precipitated in Chloroform ($CHCl_3$)/Acetone (4/1). The product was purified by ether wash (x3) in ultrasonic bath (5 min each). The yield was 77% and the activation rate was 41%. The product was characterised by ^{1}H NMR (300 MHz, δ(ppm)). δ8, (s, CH, main chain PGA), δ4,3 (m, CH2, lateral chain of PGA), δ 2 (m, CH2, lateral chain of PGA), δ 2,35 (m, 4H, CH2 Succ).

PGA-AGM synthesis and purification: PGA-OSucc (0,52 mmol, 91,3 mg) was dissolved in DMF anhydrous (5 mL), then AGM (0,026 mmol, 6 mg) and a catalytic amount of DMAP were added. The pH was controlled and adjusted with DIEA to pH 8. The reaction was left to react for 40 h at RT. The DMF was evaporated by high vacuum and the conjugate was precipitated with AcOEt/Acetone 4/1 at 4°C. PGA-AGM sodium salt was made by the addition of $NaHCO_3$ 1M (0,58 mmol, 285 μL). A purification step by SEC was carried out in order to remove the salt excess and the rest of unreacted products. If free DMAP is still detected by UV, dialysis against H_2O should be performed. After lyophilisation, the reaction yield was 65% (65 mg).

PGA-G-AGM synthesis and purification: The synthesis of PGA-G-AGM was performed using the following protocol. PGA (0,51 mmol, 80,3 mg) was dissolved in DMF anhydrous (5 mL), DIC (0,808 mmol, 126,2 μL) was added and after 5 min HOBt (0,808 mmol, 109 mg). After the activation of the carboxylic acid groups by DIC and HOBt, G-AGM (0,0269 mmol, 7,8 mg) was added. The pH was controlled and adjusted with DIEA to pH8. The reaction was monitored by TLC and was left to react for 36 h at RT. The DMF was evaporated by high vacuum and the polymer drug conjugate was precipitated by $CHCl_3$/Acetone 4/1 at 4°C by stirring 30 min followed by a further 30 min without stirring. PGA-G-AGM sodium salt was obtained by the addition of $NaHCO_3$ 1M (0,51 mmol, 250 μL). Two purification steps (dialysis against water (membrane Mw cut off 3500 Da) and G25 column) were carried out in order to remove the excess of salt and any remaining impurities including free drug. After lyophilisation, the reaction yield was 60%.

PGA-GG-AGM synthesis and purification: PGA-GG-AGM was synthesised following the same approach as described for PGA-G-AGM.

PGA-DOX synthesis and purification: PGA (0,51 mmol, 80,3 mg) was dissolved in DMF anhydrous (5 mL), then DIC (0,808 mmol, 126,2 μL) was added and after 5 min HOBt (0,808 mmol, 109 mg) was also added as solid. After 10 min, Dox.HCl (0,0269 mmol, 14 mg) was incorporated to the reaction mixture and the pH adjusted with DIEA to 8. The reaction was monitored by TLC and left to

react for 36 h at RT. DMF was evaporated under high vacuum and the conjugate precipitated with a CHCl$_3$:Acetone 4:1 solution at 4°C by stirring 30 min followed by a further 30 min without stirring. PGA-Dox sodium salt was obtained by addition of NaHCO$_3$ 1M (0,51 mmol, 250 μL). Two purification steps (dialysis against water (membrane Mw cut off 3500 Da) and G25 column) were carried out in order to remove the excess of salt and any remaining impurities including unreacted drug (yield 60% (60mg)).

PGA-G-Dox and PGA-GG-Dox synthesis and purification: The PGA-G-Dox and PGA-GG-Dox were performed following the same procedure used for PGA-Dox.

3.3.1.c. Combination Conjugates synthesis.

PGA-AGM-Dox: PGA-OSucc (0,259 mmol, 85,45 mg) was dissolved in DMF anhydrous (5 mL). A catalytic amount of DMAP was added and pH was adjusted to 8 with DIEA. Then, AGM (0,027 mmol, 6,3 mg) was added. The reaction was monitored by TLC and was left to react for 36h at RT. Then DIC (0,036 mmol, 5,7 μL) was added and after 5 min HOBt (0,036 mmol, 4,9 mg). After the activation of the carboxylic acid groups by DIC and HOBt, Dox (0,024 mmol, 13.6 mg) was then added, the pH was adjusted to 8 with DIEA and the reaction was left to react for 36h more at room temperature. The DMF was evaporated by high vacuum and polymer conjugate precipitated by adding 5 mL of CHCl$_3$: Acetone (1:1). PGA-AGM-Dox sodium salt was obtained by the addition of NaHCO$_3$ 1 M (0,51 mmol, 250 μL). Two purification steps (dialysis against water (membrane Mw cut off 3500 Da) and G25 column) were performed to finally yield after lyophilisation the desired conjugate (60%).

PGA-X-AGM-Y-Dox: PGA was dissolved in DMF anhydrous (5 mL). DIC (1,5 eq) was added and after 5 min HOBt (1,5 eq) as solid. After the activation of the carboxylic acid groups by DIC and HOBt, X-AGM (1 eq) was then added and the pH was adjusted to 8 with DIEA. The reaction was left to react for 36 h at RT. Afterwards, DIC (1,5 eq) was again added and after 5 min HOBt (1,5 aq). After the activation of the remaining free carboxylic acid groups, Y-Dox (1 eq)

was then added, the pH was adjusted to 8 with DIEA and the reaction was left to react for further 36 h at RT. The DMF was evaporated under high vacuum and the polymer conjugate precipitated by adding 5 mL of $CHCl_3$: Acetone (1:1). PGA-X-AGM-Y-Dox sodium salt was obtained by the addition of $NaHCO_3$ 1M (0,51 mmol, 250 µL). Two purification steps (dialysis against water (membrane Mw cut off 3500 Da) and G25 column) were carried out in order to remove the excess of salt and any remaining impurities including unreacted drug (yield 60% (60mg)).

3.3.2. Physico-chemical characterisation of conjugates synthesised.
3.3.2.a. Determination of Total AGM loading and Free AGM content.

Determination of total AGM content by UV Spectroscopy: AGM or an aminoacid-AGM derivative X-AGM were first prepared for use as calibration standards. A stock solution of <u>AGM derivative</u> in HPLC grade MeOH was prepared (1 mg/mL). To obtain a calibration curve samples were diluted using MeOH to give a concentration range of 0-50 µg/mL for AGM or 0-130 µg/mL for X-AGM. The total drug loading of the conjugates was determined by measuring the optical density at 254 nm in milliQ H_2O. PGA in the same concentration range as the conjugates analysed (0-5 mg/mL) was used as blank.

Determination of total AGM content by HPLC, indirect analysis: The dried residue obtained from the conjugation reactions was dissolved in CH_2Cl_2 and all remaining precipitate was filtered off. AGM is completely soluble in CH_2Cl_2. The solvent was evaporated under reduced pressure and MeOH (10 mL) was added to make the stock solution. 3 different concentrations were injected to the HPLC (after filtered through 0,45 µm). The free amount of drug in the conjugate residues was determined by HPLC using a RP_{18} column (125x4 mm), with a flow rate of 1 mL/min and using a gradient elution [A: H_2O milliQ+0,1%TFA, solvent B: ACN+0,1%TFA]. Total run time 25 min and the gradient profile was: t=0 A 90%, t=4 A 90%, t=19 A 10%, t=21 A=90%, t=25 A=90%, t=40 A 0%, t=42 A 0%. Oestradiol (1 µg/mL) was used as internal standard. A UV-Vis diode array (DAD) was used as detector. The retention time was 2 min for GG-AGM, 6 min for G-AGM and 5 min for AGM.

Determination of free AGM content by HPLC: To evaluate the free drug loading, 100 µL of a known concentration of polymer conjugate was added with 100 µL of sodium bicarbonate and 100 µL of oestradiol (1 µg/mL) as internal standard. Free X-AGM and oestradiol were thoroughly extracted with a mixture (5 mL) of AcOEt : Isopropyl alcohol 4:1 (3x10 s). The upper organic layer was carefully removed and dried through N_2 flow. The dried residue was dissolved in 100 µL of HPLC grade ACN. In parallel to construct a standard curve, the same concentrations used for the determination of the total drug loading were used to obtain an HPLC standard curve. 100 µL of each concentration was added to a mixture of 100 µL of bicarbonate, 100 µL of oestradiol and 700 µL of milliQ H_2O and thoroughly extracted as described above. The amount of free drug was determined by HPLC using the same HPLC protocol described for the determination of the total drug loading by HPLC (indirect measurement). The retention time was 2 min for GG-AGM, 6 min for G-AGM, 5 min for AGM and 12 min for oestradiol.

3.3.2.b. Determination of Total and Free Dox by HPLC.

Determination of total Dox content by HPLC: Aqueous solutions of PGA-Y-Dox conjugates (1 mg/mL) were prepared, and an aliquot (100 µL) was added to a polypropylene tube and made up to 1 mL with water. Then 1 mL of 2 M HCl was added and the tubes were heated at 80°C for 30 min in order to get Dox aglycone. After cooling down to RT. 1 mL 2 M NaOH and the pH of the samples was adjusted to 8,5 with ammonium formate buffer (100 µL, 1 M, pH 8,5). In parallel the same procedure was carried out for the parent compound Y-Dox (using 100 µL of a 1 mg/mL stock aqueous solution). Daunorubicin (Dau) was used here as internal standard; 100 µL of a 1 µg/mL stock aqueous solution was added to each sample. Samples were then thoroughly extracted by vortexing (3x10 sec). The upper aqueous layer was carefully removed and the solvent was evaporated under N_2. The dry residue was dissolved in 100 µL of HPLC grade methanol. In parallel the same procedure was carried out for the parent compound Y-Dox (using 100 µL of a 1 mg/mL stock aqueous solution). Addition of 1 µL of methanol to redissolve the product gave a 100 µg/mL stock

from which a range of concentrations were prepared (2-60 µg/mL). The amount of total drug was determined by HPLC using RP18 column (125x4 mm), with a flow rate of 1 mL/min and using a gradient elution [A: 2-propanol/H_2O 12:88 (v/v), solvent B: 2-propanol/H_2O 29:71 (v/v)] adjusted to pH 3,2 with o-phosphoric acid. The total run time was 25 min and the gradient profile was: t = 0 A 0%, t = 1 A 60%, t = 3 A 60%, t = 8 A 0%, t = 18 A 0%, t = 20 A 100%, t = 20 A 100%. To monitor Dox and Dau standard a fluorescence detection at λ = 485 nm for excitation and λ = 560 nm for emission was used. The retention time (tr) was 15 min for Dox aglycone and 20 min for Dau aglycone.

Determination of free Dox content by HPLC: 100 µL of a known concentration of PGA-Y-Dox conjugate was added with 100 µL of $NaHCO_3$ and 100 µL of Dau (1 µg/mL) as internal standard. The free Dox and Dau were thoroughly extracted with $CHCl_3$:Isopropyl alcohol 4:1 (3x30 sec). The upper aqueous layer was carefully removed and the organic phase dried through N_2 flow. The dry residue was dissolved in 100 µL of HPLC grade MeOH. In parallel the same process was also carried out with a mixture of Dox and Dau to construct a standard curve. The standards were dissolved in 1 mL of HPLC grade MeOH to give us a 100 µg/mL stock solution from which a range of concentration were prepared (5-100 µg/mL). The amount of free drug was determined by HPLC using RP18 column (125x4 mm), with a flow rate of 1 mL/min and using a gradient elution [A: 2-propanol/H_2O 12:88 (v/v), solvent B: 2-propanol/H_2O 29:71 (v/v)] adjusted to pH 3,2 with o-phosphoric acid. Total run time was 42 min and the gradient profile was: t = 0 A 0%, t = 1 A 0%, t = 26 A 100%, t = 27 A 50%, t = 37 A 50%, t = 40 A 0%, t = 42 A 0%. To monitor Dox and Dau standard, a fluorescence detection at λext = 485 nm for excitation and λem = 560 nm for emission was used. The tr was 20 min for Dox and 30 min for Dau.

3.3.2.c. Molecular Weight (MW) determination by GPC.

To evaluate the mass of the conjugates, 100 µL of 3 mg/mL conjugate solution in PBS was injected in the GPC using two TSK Gel columns in series G2500 PWXL and G3000 PWXL with a Viscoteck TDA^{TM} 302 triple detector

with UV detection coupled. The mobile phase using is PBS 0,1 M, flow 0,8 mL/min.

3.3.2.d. Small angle neutron scattering (SANS).

Small-angle neutron scattering experiments were performed on the D11 instrument at the Institute Laue-Langevin, Grenoble, France. Scattering data are expressed in terms of the scattering vector, Q, which is given by $Q=4\pi/\lambda\ sin(\theta/2)$ where λ is wavelength and θ the angle at which the neutrons are scattered. The incident neutron wavelengths were 6 ±1 Å and 12 Å, giving accessible Q-ranges of 0,0017 to 0,42 Å^{-1} using four different sample-detector distances. Sample solutions were prepared at a conjugate concentration of 0,5-2 wt% on a 1g scale in D_2O (pH 5,5, 0,1M phosphate buffer) and placed in 2 mm path length quartz cells, mounted in a sample changer thermostatted at 37 °C (± 0,2). These conditions allowed the study of the conjugates at a pH, temperature and ionic strength that mimic those physiologically encountered. Data were corrected for transmission intensity, electronic background and normalised against a flat scatter according to the standard procedures for the instrument. The obtained scattering profiles I(Q) vs. Q were analysed according to I(Q) $\propto$ ϕVp P(Q) S(Q) + Binc where ϕ is the volume fraction and Vp the particle volume. The FISH modelling suite was used for the analysis. FISH incorporates parameterised form factors, P(Q) and structure factors, S(Q), to describe the dimensions of the scattering particle and inter-particle interactions (Heenan, R.K.. 1989).

3.3.3. Stability in plasma of conjugate and Kinetics of drug release in presence of cathepsin B.

3.3.3.a. Kinetics of drug release in presence of cathepsin B.

Cathepsin B (5 U) was added last to a solution of 3 mg PGA-X-AGM, PGA-Y-Dox or PGA-X-AGM-Y-Dox in 1 mL of a pH 6 buffer composed by 20 mM sodium acetate, 2 mM EDTA and 5 mM DTT. Incubation was carried out at 37°C. Aliquots (150 μL) were taken at times up to 96 h, immediately frozen in liquid nitrogen, and stored frozen in the dark until assayed by HPLC (analysis of

100 μL aliquots after extraction procedure, as described above for free drug analysis) and/or GPC (direct analysis of 30 μL aliquots). In control experiments polymers were incubated in buffer alone (without addition of cathepsin B) to assess non-enzymatic hydrolytic cleavage. In addition, free drug (0,75 mg/mL) was also incubated under same conditions and later used as the reference control.

GPC Evaluation of Polymer Mw loss: The 30 μL aliquots were diluted up to 200 μL with buffer (PBS) and the Mw determined by GPC. Generally degradation profiles for biomedical polymers are obtained under constant sink conditions and the results correlated with mass loss of the polymer. Since PGA polymers are water soluble, the relative peak areas used in the GPC derived molecular weight calculations provided a suitable alternative to indicate the relative amount of the polymer that remained at each time point. As the polymer degraded there was a loss of PGA conjugates molecular weight. Therefore, the loss with time of the area under the curve (AUC) for PGA conjugates was considered to evaluate the rate of backbone degradation.

3.3.3.b. Plasma stability.

Conjugates (3 mg/mL) were incubated at 37°C in freshly extracted serum from Balb/c mice for up to 24h. At scheduled times, aliquots (100 μL) were collected. 10 μL of 100 μg/mL solution of oestradiol in MeOH was added as internal standard and then 110 μL of MeOH in order to precipitate serum proteins. Following centrifugation (12000 g, 5 min), supernatants were analysed by HPLC as reported above.

3.3.3.c. Metabolite identification by MS.

The X-AGM metabolites were identified using a UPLC-MS system from Waters. The mass method optimised was capillary (kV) 3,50, cone (V) 20, Extractor (V) 6, RF Lens (V) 0,2. The source temperature was set at 120°C and the desolvation temperature at 380°C. Gas desolvation and the gas cone were 950 and 50 L/H, respectively. The analyser and detector parameter were the normal one for this kind of ZQ mass. The UPLC method was 90/10 H_2O+0,1%

formic acid /ACN+0,1% formic acid to 10/90 H_2O+0,1% formic acid /ACN +0,1% formic acid in 15 min. The initial conditions were recovered in 2 min and the system was equilibrated in 4 min. After filtration, 20 µL of the sample was injected. A double detection system was employed, UV (DAD, $\lambda = 268$ nm) and the total ion count (TIC) of mass.

For the Y-Dox metabolites, the Mw were higher consequently a MALDI-Tof experiment was performed. The matrix used was α-cyano-4-hydroxisucinnamic acid, it was extracted with a laser pulsed at 337 nm. The acquisition was performed in reflection mode.

3.3.4 Cell culture assays.

3.3.4.a. Cell maintenance and passaging.

For cell culture assays MCF7, MCF7 Ca, 4T1 and MDA-MB231 immortalised breast cancer cell lines were used. Human oestrogen-dependent, breast carcinoma cell lines MCF7 and MCF7 Ca (human aromatase-transfected) were from the Tenovus Centre for Cancer Research at Cardiff University. 4T1 is a metastatic breast cancer murine cell line and the MDA MB 231 is a non-oestrogen dependent human breast cancer cell line (ER-) and used here as control. Cell culture conditions are specified for the different breast cancer cell lines utilised in table 2.1. Cells were cultured in P100 plates with the appropriate medium supplemented with 10% of foetal bovine serum (FBS) as standard tissue culture conditions (37ºC and 5% CO_2). In order to maintain the transfected strain, the culture medium of MCF7 Ca was always (for routine tissue culture and for all the experiments) further supplemented with 0,75 mg/mL of geneticin. Steroid-deprived FBS (SFBS) was used and prepared as described below. In order to mimic post-menopausal conditions, an aliquot of oestradiol was added at a final concentration of 10^{-9} M for MCF7 and MCF7 Ca cell cultures. In all cases, cell medium was changed every two days to induce cell growth. Once 70-90% cell confluence was reached, the medium was removed and the cells were washed with 10 mL PBS. Trypsin (1 mL) was then added and left 5 min at 37°C (until detached), 9 mL of free medium was added and cells were collected in universal container and centrifuged for 5 min at 200

rcf at RT. Supernatant medium was carefully removed and the cells resuspended in fresh medium. After cell counting using a Neubauer camera, cells were seeded in P100 plates at 40 000 cell/mL or at 20 000 cell/mL to reach confluence after one or two weeks, respectively.

3.3.4.b. Preparation of Steroid-deprived FBS (SFBS).

500 mL of FBS was first deactivated at 56°C during 30 min. Once at RT, were adjusted to a pH of 4,2 adding HCl 5 M and equilibrated to a temperature of 20°C. A charcoal solution was prepared adding 18 mL of ddH_2O, 0,2 g of Norit A charcoal and 0,01 g of dextran T-80. 25 mL of the charcoal solution were added to the acidic FBS and the suspension was stirred for 16 h at 4 °C. Then, the suspension was centrifuged and coarsely filtrated with celite to remove the charcoal. The pH was adjusted to 7,2 with NaOH 5 M, the suspension was filtered with millipore filters 0,2 μm and stored in appropriate containers at -20°C.

Table 2.1. Summary of breast cancer cell lines culture conditions.

Cell line	Medium	%FBS*	Incubator condition	source
MCF7 Ca	DMEM	10%**	37°C with 5% CO_2	Cardiff university
4T1	RPMI	10%	37°C with 5%CO_2	ATCC
MCF7	DMEM	10%**	37°C with 5%CO_2	ATCC
MDA MB 231	Leibovitz	10% **	37°C without CO_2	ATCC

*: Foetal Bovine Serum (FBS) **: treated foetal bovine serum

3.3.4.c. MTS assay for cell viability determination.

In order to perform cell viability assays, a prior step based on the development of a growth cell curve for each breast cancer cell line used was performed, and the cell concentrations needed for the cytotoxic assays were determined. Cytotoxicity of free drugs (AGM and Dox), and their conjugates was evaluated using the MTS cell viability assay (72 h incubation). Both cell lines were seeded

in sterile 96-well microtitre plates (4×10^3 cells/well for MCF7 Ca, 2×10^3 cells/well for 4T1 and 10×10^3 cells/well for MDA MD 231) in the adequate medium as reported in Table 2.1. Plates were incubated for 24 h and compounds (0,2 μm filter sterilised) were then added to give a final concentration of 0-1 mg/mL drug-equiv. After 72 h of incubation, [3 - (4,5-dimethylthiazol-2-yl) – 5 - (3-carboxymethoxyphenyl) – 2 - (4-sulfopheyl)2H - tetrazolium] (MTS) (10 μL of manufacturer solution) was added to each well, and the cells were incubated for a further 2 h. Mitochondrial dehydrogenase enzymes of viable cells converted MTS tetrazolium into a coloured formazan product. The optical density of each well was measured at 490 nm. For High Throughput Screening (HTPS) studies, MCF7 and MDA MB 231 cell lines were cultured with the antibiotic P/S (1%) in order to avoid any possible contaminations while using TECAN robot for compounds dispensing under non-controlled sterile conditions. Cell viability was expressed as a percentage of the viability of untreated control cells.

3.3.5. *In vivo* Tumour Model.

3.3.5.a. MCF7 Ca athymic mice model.

All the animal experiments were performed in accordance with the guidelines established by the European Communities Council Directive (86/609/ECC) and by Spanish Royal Decree 1201/2005. All the experimental procedures were approved by the institutional Animal Care and Use Committee. Female Balb/c athymic mice 4-6 weeks of age were purchased from Harlan (Europe). The animals were housed in a pathogen-free environment under control condition. Ovarectomy was performed under sevofluorane 1 week before cell inoculation. MCF7 Ca cells were resuspended in matrigel and an aliquot (100 μL, 10 million cells) was then injected in each animal in the third mammary pad. Beginning one day after cell inoculation, animals received subcutaneously 100 μL of androstenedione (0,1 mg/mouse/day). Tumour Growth was followed twice a week by measuring tumour volume and calculating the tumours with a calliper. Once the tumour reached the maximum size authorised (1 cm^3), mice were

sacrificed and tumour removed to perform histological and vascularisation studies.

Following *in vivo* model optimisation, polymer conjugates were tested in order to evaluate antitumor activity. Then, 10^6 MCF7 Ca cells were injected in the third mammary pad. Once the tumour size reached 0,2 cm^3, the conjugates were injected intravenously 3 times every 3 days and the tumour size was followed twice a week. When the tumour achieved the maximum size authorised, heart, liver, kidney and spleen were extracted, weighed and fixed for histological studies. Tumours were also frozen for western blot analysis.

3.3.5.b. 4T1 mice model.

Balb/c female 4-6 weeks mice were purchased in Harland (EU). The animals were housed in a pathogen-free environment under control condition. Two different concentrations ($5x10^5$ and 10^6 cells) of 4T1 cells were injected in the right third mammary pad. The tumour growth was followed every day. Once the tumour reached the maximum size authorised (1 cm^3), mice were sacrificed and tumour removed in order to perform histological and vascularisation studies.

Finally, in order to test polymer conjugates antitumour activity on 4T1 model mice, $5x10^5$ cells were injected in the third mammary pad. After 8 days the tumour size reached 0,1 cm^3 then the conjugates were injected intravenously 3 times every 3 days and the size was followed every day. When the tumour achieved the maximum size authorised, heart, liver, kidney and spleen were extracted, weighed and fixed for histological studies. Tumours were frozen instead for western blot analysis.

3.3.5.c. Polymer Conjugates treatment selection for in vivo models.

Conjugates were injected at 5 mg/kg intravenously three times every three days and Dox at 3 mg/kg. The tumour growth was followed twice a week for MCF7 Ca model and each day for 4T1 model. After 90 days for MCF7 Ca and 2 weeks for 4T1, the mice were sacrificed, heart, liver, kidney and spleen were extracted, weighed and fixed for histological studies experiment. Tumours were frozen

instead for western blot analysis and blood was removed to perform hepatic analysis.

3.3.5.d. Tumour vascularisation analysis.

This experiment was conducted to visualize and also quantitate the behaviour of macromolecules at tissue level. A solution of Evans blue was injected into the tail vein of the tumour-bearing mice at a dose of 10 mg/kg. (Matsumura and Maeda, 1986; Wu et al., 1998; Maeda, 2001). One hour after the injection, solid tumours were removed, weighed and immersed in 3 mL of formamide followed by incubation at 60°C for 48 h to extract the dye. Then the quantification was performed spectrophotometrically at 620 nm.

3.3.5.e. Toxicological analysis.

Hepatic evaluation in blood: Extracted blood from heart was centrifuged at 4 000 g during 10 min to obtain the plasma. Plasma was sent to 'Analitíca clínica veterinaria Lab (ACVLAB)' to evaluate the levels of the different enzymes involved in hepatic damage such as Glutamic oxaloacetic transaminase (GOT), Glutamic pyruvate transaminase (GPT), Lactate dehydrogenase (LDH) and Alkaline phosphate (ALP).

3.3.5.f. Histological analysis.

Tumour was removed from control animal after the model optimisation, washed in PBS and fixed in paraformaldehyde (PFA) overnight. Then the excess of PFA was removed by washing with PBS through a strong agitation (200 rpm) during 20 min 3 times. Finally, samples were stored in a solution of PBS with 0,05% of sodium azide. In order to include the sample in paraffin, a previous dehydration of the sample through 2 min incubation in increased degree of alcohol solutions (30%, 50%, 70%, 96% and 2 baths of 100%) was performed, followed by 2 xylene washes of 1 min to finally include the sample in paraffin. Then the paraffin block was cut in 4 µm slide and set up in superfrost plus glass slide to haematoxylin-eosin staining.

Haematoxylin has a deep blue-purple colour and stains nucleic acids of cells by a complex, incompletely understood reaction. Eosin is pink and stains proteins non-specifically. In a typical tissue, nuclei are stained blue, whereas the cytoplasm and extracellular matrix have varying degrees of pink staining. For haematoxylin-eosin staining, previously tissue slides were deparaffinized with xylene and then rehydrated with decreasing battery ethanols (100%, 95%, 70%, 50%, 30%, water) and later samples were immersed in 2 water baths (5 min) followed by haematoxylin 2 min bath and 2 water washes (5 min). Then the slides were incubated 3 min in Lithium carbonate and HCl 0,25% in ethanol 70% in order remove the haematoxylin staining excess. After 2 washes in water for 5 min, the incubation of the tissue slides in a fresh eosin-floxin solution was performed (0,35% of eosin, 1,1% of floxin at 2%, 83 mL of absolute alcohol, 3,3 mL of distilled water and 450 µL Acetic acid) for 6 minutes. To finish, a last water bath was done (5 min) followed by a dehydration with increase alcohol degrees (5 min alcohol 70°, 2x 5 min 96°, 2x 10 min 100° and 2x Xylene), and finally the slide was mounted with Eukitt.

3.3.5.g. Western Blot analysis.

Western blot analysis was performed to evaluate key protein expressions from removed tumours of mice after 8 and 16 days of treatment in the 4T1 model. Extracted tumours were homogenised in RIPA buffer (150 mM NaCl, 1% NP40, 0,5% Sodium deoxycholate, 0,1% SDS, 50 mM Tris PH8, 50 mM NaF, 100 µM Na_3VO_4 and protease inhibitor cocktail tablet). After 15 min in agitation at 4°C, a series of 3x5 sec sonication and vortex was performed before leaving 1h at 4°C in agitation. Then the solution was centrifuged 20 min at 13 500 g, 4ºC and supernatant protein was determined by Bradford assay. 30 µg protein was then mixed with 5x SDS sample buffer, boiled for 7 min at 95°C to denaturised the protein, and separated through 8% to 15% SDS-PAGE gels. After electrophoresis, the proteins were transferred to PVDF membranes (Amersham Pharmacia Biotech, UK) by electrophoretic transfer. The membranes were blocked in 5% skim milk for 2 h, rinsed, and incubated overnight at 4ºC with the following primary antibodies: beta-Actin α-tubulin (Sigma), BAX, and VEGF (Santa Cruz Biotechnology), caspase 3, Beclin , LC3B, pAKt, and Bcl2 (Cell

Signalling), iNos (Cayman chemical), HIF1α (BD Biosciences Pharmigen). Excess antibody was then removed by washing the membrane in PBS/0,1% Tween 20, and the membranes were incubated for 1 h with horseradish peroxidase-conjugated secondary antibodies: goat anti-mouse IgG, donkey anti-rabbit IgG or rabbit anti goat IgG (1:5000) (Santa Cruz Biotechnology Inc., Santa Cruz, CA, USA). After washes in PBS/0,1% Tween 20, immunodetection was performed with the use of the ECL Western blotting detection system (Amersham Pharmacia Biotech, UK), according to the manufacturer´s instructions. Relative protein levels were quantified by densitometry with Scion Image programme. Results were standardised using β-Actin as the reference.

3.4. Statistical analysis.

In vitro experiment results were expressed as mean ± SD where at least n = 3 experiments per group and *in vivo* experiment results were expressed as mean ± SEM where at least n = 4 experiments per group. Statistical analysis was performed using GraphPad Prism 5 (Graph Pad Software, Inc., San Diego, http://www.graphpad.com).

Values obtained from the experiments were analyzed using ANOVA and simple method of Dunnett's t for multiple comparisons. In all cases, we considered differences to be significant when p*** < 0,001; p** < 0,01; p*< 0,05; ns: non-significant and NA non-applicable.

3.5. Bibliography.

Dolle, J.M., Daling, J.R., White, E., Brinton, L.A., Doody, D.R., Porter, P.L., and Malone, K.E. (2009). "Risk factors for triple-negative breast cancer in women under the age of 45 years." Cancer Epidemiol Biomarkers Prev 18(4): 1157-1166.

Heenan, R.K. (1989). FISH dara analysis program. Rutherford Appleton Laboratory Report RAL-89-129, CCLRC, didcot.UK

Maeda, H. (2001). "The enhanced permeability and retention (EPR) effect in tumor vasculature: the key role of tumor-selective macromolecular drug targeting." Adv Enzyme Regul 41: 189-207.

Matsumura, Y. and Maeda H. (1986). "A new concept for macromolecular therapeutics in cancer chemotherapy: mechanism of tumoritropic accumulation of proteins and the antitumor agent smancs." Cancer Res 46(12 Pt 1): 6387-6392.

Maughan, K.L., Lutterbie, M.A., and Ham, P.S. (2010). "Treatment of breast cancer." Am Fam Physician 81(11): 1339-1346.

McNamara, K.M., Yoda, T., Takagi, K., Miki, Y., Suzuki, T., and Sasano, H. (2012). "Androgen receptor in triple negative breast cancer." J Steroid Biochem Mol Biol 133C: 66-76.

Tomlinson, R., Klee, M., Garrett, S., Heller, J., Duncan, R., and Brocchini, S. (2002). Pendent chain functionalized polyacetals that display pH-dependent degradation: a platform for the development of novel polymer therapeutics, Macromolecules 35(2): 473-480.

Wu, J., Akaike, T., and Maeda, H. (1998). "Modulation of enhanced vascular permeability in tumors by a bradykinin antagonist, a cyclooxygenase inhibitor, and a nitric oxide scavenger." Cancer Res 58(1): 159-165.

Chapter 4. *In vivo* **evaluation of HPMA copolymer-AGM-Dox combination conjugate.**

4.1. Introduction.

The aim of this study was to achieve *in vivo* proof of concept for antitumour activity synergism with HPMA copolymer-AGM-Dox combination conjugate in breast cancer animal models. As already described in the introduction chapter, Vicent *et al.* (2005) showed that HPMA copolymer-AGM-Dox induced a markedly enhanced *in vitro* cytotoxicity compared to the HPMA copolymer–Dox (FCE28068, PK1), a conjugate that had already demonstrated activity in chemotherapy refractory breast cancer patients during early clinical trials (Vasey et al., 1999). It should be emphasised that mixtures of polymer conjugates containing only AGM or only Dox did not show any synergistic benefit when tested in MCF7 cells *in vitro* (Vicent et al., 2005; Greco et al., 2007). This result was even more remarkable as the PK1 conjugate that has demonstrated clinical benefits typically shows ~ 100 fold lower cytotoxicity *in vitro* than free Dox. This is due to their different cell pharmacokinetics *i.e.* endocytosis of the polymer-Dox conjugate followed by lysosomal cathepsin B mediated Dox release compared to cellular entry by diffusion for free Dox (Duncan, 2009; Duncan and Vicent, 2010). These preliminary *in vitro* results suggested for the first time that the combination of AGM and Dox in the same carrier would lead to a synergistic effect, and hence the increased activity of the combination polymer. Following these promising findings, the aim of the present study was to demonstrate if the previous *in vitro* results would extrapolate into an *in vivo* animal model. More specifically the following studies were performed:

i) In order to investigate the reproducibility of the earlier studies IC 50 values were determined for HPMA copolymer-Dox and HPMA copolymer-Dox-AGM in MCF7 Ca and 4T1 cells. The activity of both compounds (as single agents or as combination) against both immortalised cell lines was evaluated in order to confirm drug synergism. ii) Two orthotopic breast cancer animal models were established (MCF7 Ca and 4T1) and the conjugates were evaluated to determine their pharmacokinetic profile and antitumour activity.

4.2. *In vitro* analysis of HPMA copolymer-AGM-Dox and HPMA copolymer-Dox conjugates.

The protocol used to synthesise the combination conjugate was based on previous studies (Vicent et al., 2005; Greco et al., 2007). After conjugate synthesis using a carbodiimide mediated coupling reaction for HPMA copolymer-AGM-Dox and aminolysis for HPMA copolymer-Dox, the total drug loading and the free drug content were determined for both conjugates (see Table 4.1).

Table 4.1. Conjugate characteristics.

	Total drug loading (wt%) [a]		Free Drug content (wt% of total drug) [a]	
Product	**AGM**	**Dox**	**AGM**	**Dox**
HPMA copolymer-AGM-Dox	6,20	6,10	0,45	0,35
HPMA copolymer-Dox	NA	5,60	NA	0,25

[a] determined by HPLC. Free drug content expressed as a percentage of total drug; NA- not applicable

4.2.1. *In vitro* cell viability analysis against MCF7 Ca and 4T1 cells.

In order to determine the HPMA conjugate and free Dox concentration required to inhibit 50% of cell viability (IC50) under our experimental conditions, previous cell growth curves were performed with MCF7 Ca and 4T1 cells to determine the adequate cell seeding density (figure 4.1.).
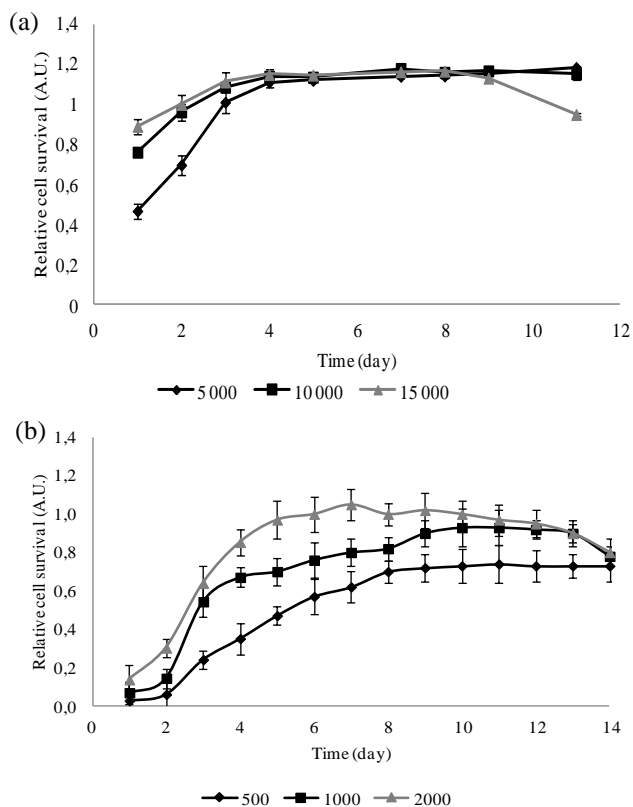
Figure 4.1. Optimisation of cell seeding density for future cytotoxicity tests. Panels (a) shows MCF7 Ca cells and panel (b) shows 4T1 cells. Symbols relating to number of cells per well seeded are shown in the graphs. Data is expressed as mean ± SD, n = 3. A.U. means absorbance unit.

To evaluate the effect of the conjugates on cell viability, serial dilutions of both conjugates were tested (0,01 µg/mL to 0,01 mg/mL Dox-equiv.) (n = 4). Conjugates were solubilised directly into the medium, added to the cells and incubated for 72 h at 37ºC as described in detail in Chapter 3.

(a)

(b)

HPMA copolymer-AGM-Dox   HPMA copolymer-Dox   Dox
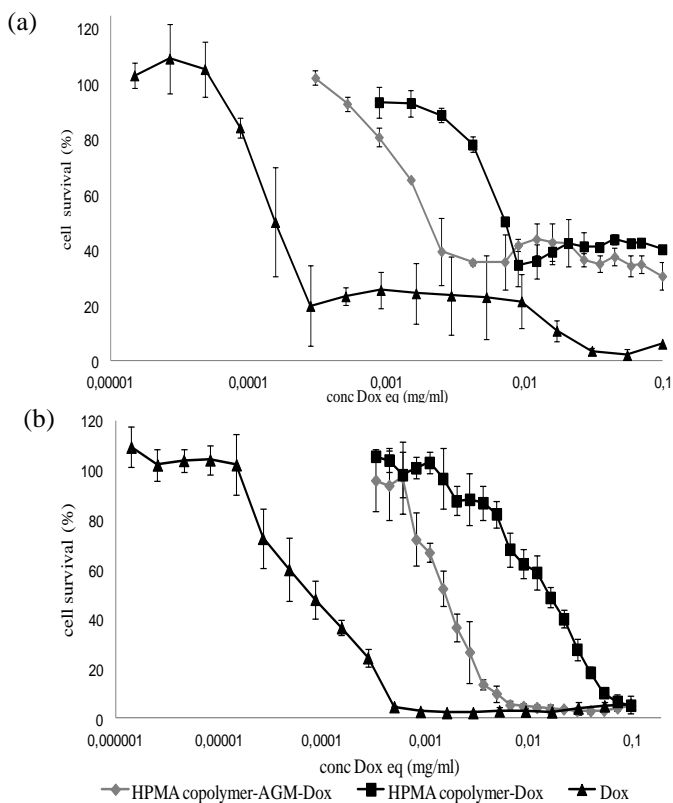
Figure 4.2. Cell viability of Dox and HPMA copolymer conjugates; Panel (a) MCF7 Ca cell and Panel (b) 4T1 cell in presence of 10^{-9} M oestradiol. Cell viability was measured by a MTS assay after 72h incubation. Data expressed as mean ± SD, n = 4 experiments per treatment.

The serum used was previously deprived from oestrogens (see details in Chapter 3) to avoid uncontrolled cell growth. A known oestrogen concentration was added mimicking the levels found in post-menopausal women (as described in Vicent et al., 2005) then MTS assay was performed (always n = 4).

Table 4.2. Determination of the IC50 value (µg/mL) for HPMA copolymer conjugate and free Dox in MCF7 Ca and 4T1 breast cancer cell lines.

	IC50[a] (µg/mL)			
	MCF7 Ca cells		4T1 cells	
	AGM-equiv.	Dox equiv.	AGM-equiv.	Dox-equiv.
Dox	NA	0,2 ± 0.1	NA	0,08 ± 0,02
HPMA copolymer- AGM-Dox	2,3 ± 1,6	2,0 ± 1,0	1,75 ± 1,3	1,5 ± 0.4
HPMA copolymer- Dox	NA	8,0 ± 2,0	NA	15,0 ± 5,9
HPMA copolymer-AGM	> 100	NA	> 100	NA

[a] Mean value ± SD (n = 4).

The IC50 value determined for HPMA conjugate and free Dox against MCF7 Ca and 4T1 cell is shown in table 3.2. As it can be seen, the IC50 value of HPMA copolymer-AGM-Dox was significantly lower than that obtained for HPMA copolymer-Dox, showing higher cytotoxicity for the combination conjugate (2 µg/mL vs. 8 µg/mL for the combination and HPMA-Dox conjugate, respectively). To evaluate the synergistic effect between AGM and Dox in HPMA copolymer-AGM-Dox, a combination index (CI) was determined using the method described by Chou (2006). The CI is defined as follows

$$CI = \frac{\text{IC50 Dox in HPMA-AGM-Dox}}{\text{IC50 HPMA-Dox}} + \frac{\text{IC50 AGM in HPMA-AGM-Dox}}{\text{IC50 HPMA-AGM}}$$

When CI < 1, this indicates synergism,

When CI = 1, this indicates an additive effect

When CI > 1 this indicates an antagonism (Chou, 2006; Peer et al., 2007; Rodea-Palomares et al., 2010; Chou, 2010)

In **MCF7 Ca** cells, the CI obtained for HPMA copolymer-AGM-Dox was **0,26**, therefore, a strong synergistic effect was clearly observed with the

combination conjugate. The CI value in **4T1** cells was **CI = 0,109**, even better than that observed in MCF7 Ca cells suggesting a greater cytotoxic activity for this conjugate in the metastatic murine cell line.

After cell analysis and to investigate whether HPMA copolymer-AGM-Dox could display synergism *in vivo* two orthotopic mouse models were established, (i) the human MCF7 Ca cell line was established in ovarectomised nude mice to mimic a post menopausal breast cancer; and (ii) the murine cell line 4T1 was inoculated into Balb/c mice to establish an aggresive tumour model in a mouse having a functional immunological system. Moreover, the 4T1 cells being cells extracted from a spontaneously arising Balb/c mammary tumour (Tao et al., 2008) are capable of metastasis preferentially to the lungs, liver, bone and brain and thus give rise to a tumour model more closely resembling the behaviour of metastatic breast cancer in human patients (Gao et al., 2011). However before evaluating any of our conjugates, the aromatase enzyme levels were evaluated in 4T1 tumor by western blot to ratify the suitability of this cell line for our studies. Levels in MCF7 Ca were already reported in (Greco et al., 2007)
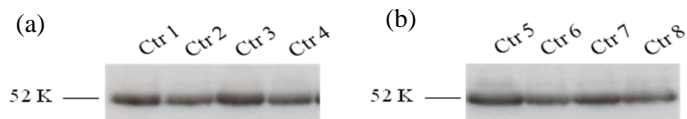
Figure.4.3. Determination of aromatase expression in 4T1 tumour by Western blot. Panel (a) after 16 days of cell inoculation. Panel (b) after 24 days of the cell inoculation.

4.3. *In vivo* evaluation of HPMA conjugate and free Dox.

4.3.1. Optimisation of the MCF7 Ca and 4T1 tumour models.

To optimise the selected tumour models the host animals were inoculated with different tumour cell numbers into the mammary fat pad, for MCF7 Ca $5,0 \times 10^6$ and $10,0 \times 10^6$ cells, and for 4T1 $0,5 \times 10^6$ and $1,0 \times 10^6$ cells. The comparison between the two models in terms of tumour volume growth with time is shown in figure 4.3.
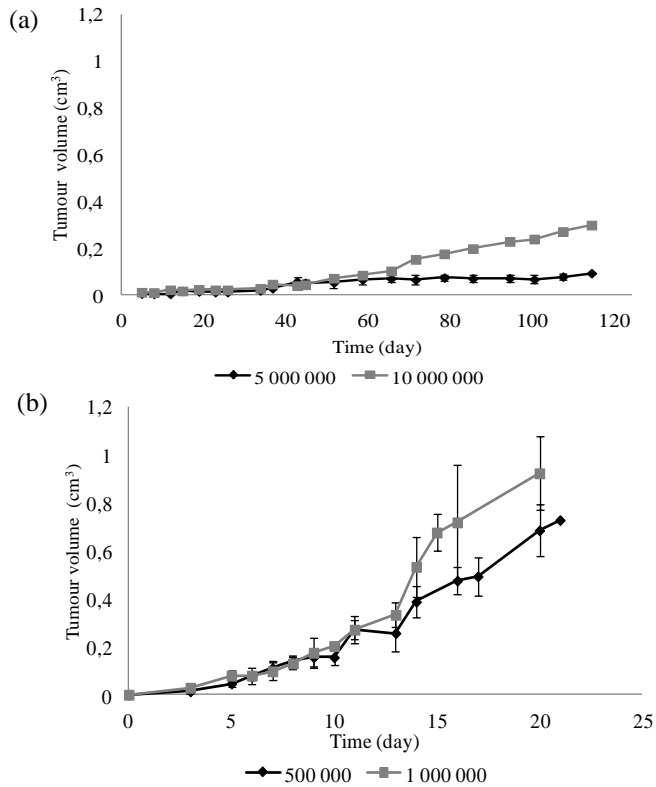
Figure 4.3. Determination of the optimum cell number required for tumour formation. Panel (a) shows MCF7 Ca in ovarectomised nude mice and Panel (b) shows 4T1 cells in Balb/c mice. Results are expressed as mean ± SEM, n = 4 animals per group. Symbols relating to number of cells per animal are shown in the graphs.

As can be seen in figure 4.3., 4T1 is a more aggressive tumour model, and only 0.5×10^6 cells were needed to reach a tumour volume of 1 cm^3 in 20 days. In contrast, for the MCF7 Ca model, 10.0×10^6 cells were necesary to reach 0,3 cm^3 after 110 days. MCF7 Ca can be considered then a more heterogeneous and time consuming model to be established and used than 4T1. MCF7 Ca is hormone dependent tumour, and in our proposal it was used to mimic post menauposal breast cancer patients as described in the literature (Yue et al., 1994; Brodie et al., 1999; Brodie et al., 2001). To compare the morphological differences between both tumours, a tumour histological study was performed.

104

(a)

Tumour core

(b)

Tumour core

→ Neovasculation   ▶ Erythrocyte   ➤ Necrosis area

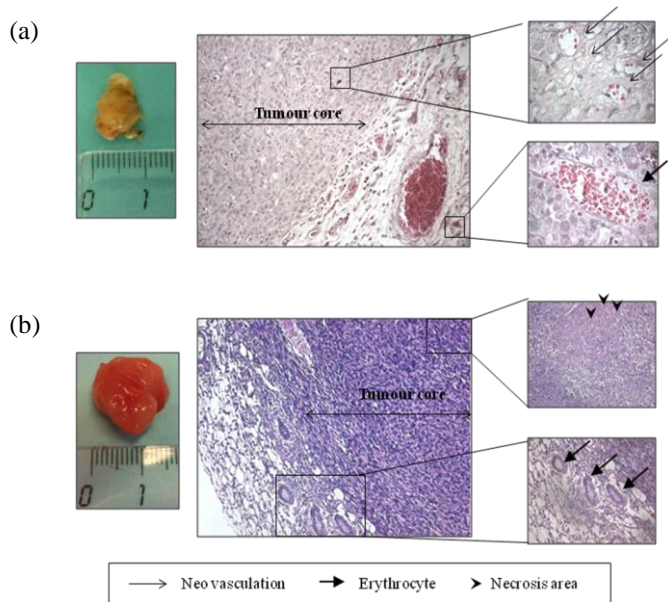Figure 4.4. Tumour histological study. Panel (a) orthotopic MCF7 Ca tumour model (b) orthotopic 4T1 tumour model.

In both models, the tumour core exhibited lower vessel density surrounded by a peripheral area with bigger vessels, which may be involved in the angiogenesis process. The MCF7 Ca tumour, perhaps due to the slower tumour growth rate, appeared as a more compact and solid tumour than 4T1 model. The 4T1 is a murine model isolated from spontaneous breast tumours occurred in Balb/c mice and it is also known to metastasise as occurs in breast human cancer spreading mainly in bone, liver and lungs. Accordingly, three weeks after orthotopic injection of the 4T1 cells into the mammary fat pad, primary tumours displayed large areas of necrosis into which neutrophils and other inflammatory cells showed infiltrated blood vessels. In addition, tumour cells were observed at the surfaces of the blood vessels indicating metastasis (figure 4.4.b.).

As tumour vascular permeability, the EPR effect (Matsumura and Maeda, 1986; Wu et al., 1998; Maeda, 2001), is a key factor in the clinical performance of polymer drug conjugates it was important to define the vascular permeability of both *in vivo* tumour models at different stages. Evans blue dye was used as

probe to quantify tumour permeability, and the effect of tumour Evans blue dye accumulation (doses (%)/tumour (g)) was determined.

In the case of the MCF7 Ca tumours higher permeability was seen for very small tumours (size lower than 0,08 cm^3). These tumours were almost undetectable, so due to experimental limitations when determining reliable tumour volume changes it was necessary to select a more easily detectable starting tumour size. Thus, the selected tumour volume used to start conjugate antitumour evaluation was ~ 0,1 cm^3 for 4T1 model, and ~ 0,2 cm^3 for the MCF7 Ca model, to allow in both cases starting with the same dose(%)/tumour(g) (~6%). It is noteworthy that up to a volume of 0,23 cm^3 the 4T1 tumour displayed slightly more vascular permeability than MCF7 Ca model.
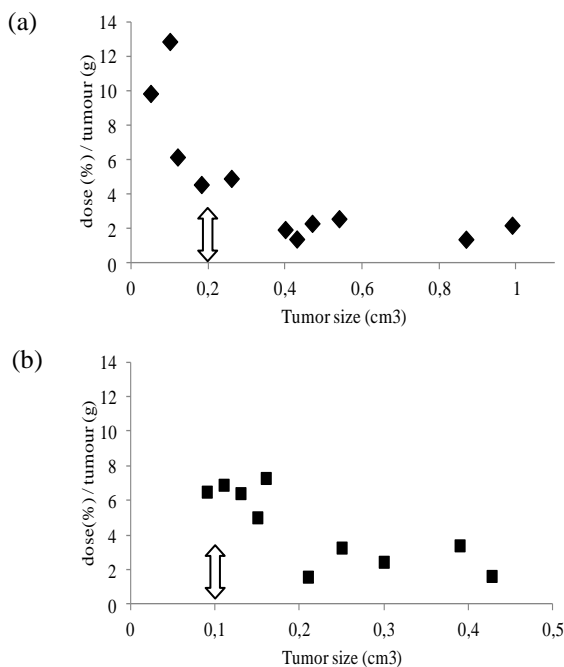

Figure 4.5. Characterisation of tumour EPR effect depending on tumour size by means of Evans blue dye. Panel (a) shows MCF7 Ca tumour model permeability and panel (b) shows 4T1 tumour model permeability. The tumour size selected for conjugate i.v. administration is remarked.

4.3.2. Biodistribution of HPMA conjugate and free Dox in 4T1 induced *in vivo* tumour model.

In order to better understand the behaviour of both conjugates *in vivo*, new studies based on tumour accumulation and biodistribution were performed. Due to the experimental requirements (time length) with the MCF7 Ca *in vivo* model, the pharmacokinetics of HPMA conjugates and free Dox was carried out in the 4T1 induced *in vivo* tumour model.
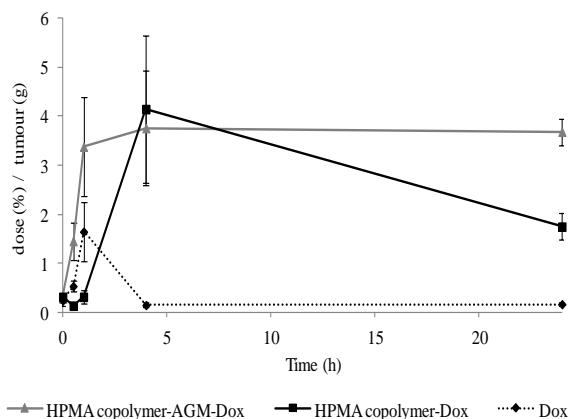
Figure 4.6. Tumour accumulation with time of HPMA conjugates and free Dox in 4T1 induced tumours. The total Dox content was used to calculate dose (%) (see Chapter 3). Results are expressed as mean ± SEM where n = 4 animals per group.

Table 4.3. Statistical analysis of tumour accumulation data with the HPMA conjugates and free Dox.

	1h	4h	24h	
P value	**1**	**3**	**2**	**3**
1	NA	***	*	***
2	*	**	NA	***
3	ns	NA	***	NA

1- HPMA copolymer-AGM-Dox conjugate, **2-** HPMA copolymer-Dox conjugate and **3-** Dox. Significances calculated by one-way ANOVA. P*** < 0,001, P* *< 0,01, P* < 0,05, ns: non-significance and NA: non applicable. Statistics at T = 0 and 30 min showed non-significance.

In good agreement with already reported data (Duncan, 2009), whereas free Dox tumour accumulation was faster than HPMA copolymer-Dox, its retention in the tumour was much lower than that observed with the conjugates. Dox highest accummulation was achieved at 1 h representing only 1,5% of the total administered dose. Regarding the conjugates, although the maximum % dose/g of tumour was similar in both cases, around 4,5%, HPMA copolymer-AGM-Dox tumour accumulation seemed to be faster than HPMA copolymer-Dox and showed a different kinetic profile. Whereas the combination conjugate reach a plateau after 1 h that was maintained after 24 h, HPMA copolymer-Dox accumulation in the tumour started to decrease after 5 h post-injection. Summarising, with the conjugates approximately 5% of the injected dose reached the tumour after 24 h and as expected, this value was much greater than the 1% identified for free Dox.

In order to understand better the whole conjugate body bioditribution, a quantitative analysis was performed at 1 h and 24 h in several organs including, heart, liver, kidney, spleen and tumour (figure 4.7.). As it can be observed in figure 4.7.a., the conjugation of Dox to HPMA copolymer completely changes its whole body biodistribution. At 1 h post-injection the highest accumulation of Dox was found in heart. This result is in good agreement with already reported data and explains the cardiotoxicity associated to this molecule. Upon conjugation, accumulation in heart was almost diminished. This decrease in the toxicity could allow us to increase the dose and its schedule. On the other hand, a clear renal filtration was observed for both conjugates but with different clearance rate as seen at 24 h profile. Differences in conjugate behaviour were also observed with time for liver and spleen as a significantly different accumulation of HPMA copolymer-AGM-Dox conjugate in the liver was observed at 1 h when compared with HPMA copolymer-Dox conjugate. Therefore, even if the quantity observed was low in the liver (4% of the dose (%)/ tissue (g)), a toxicology study was performed to ensure the safety of the combination conjugate not only in 4T1 but also in MCF7 Ca model (figure 4.8.)

(a)

dosis (%) / tissue (g)

Liver Kidney Heart Spleen Tumour

(b)

dosis (%) / tissue (g)

Liver Kidney Heart Spleen Tumour

□ HPMA copolymer-AGM-Dox   ■ HPMA copolymer-Dox   ■ Dox

(c)

Ctr HPMA-AGM-Dox Ctr HPMA-Dox Ctr Dox

Liver
Kidney
Spleen
Heart
Tumour

(d)

Ctr HPMA-AGM-Dox Ctr HPMA-Dox Ctr Dox
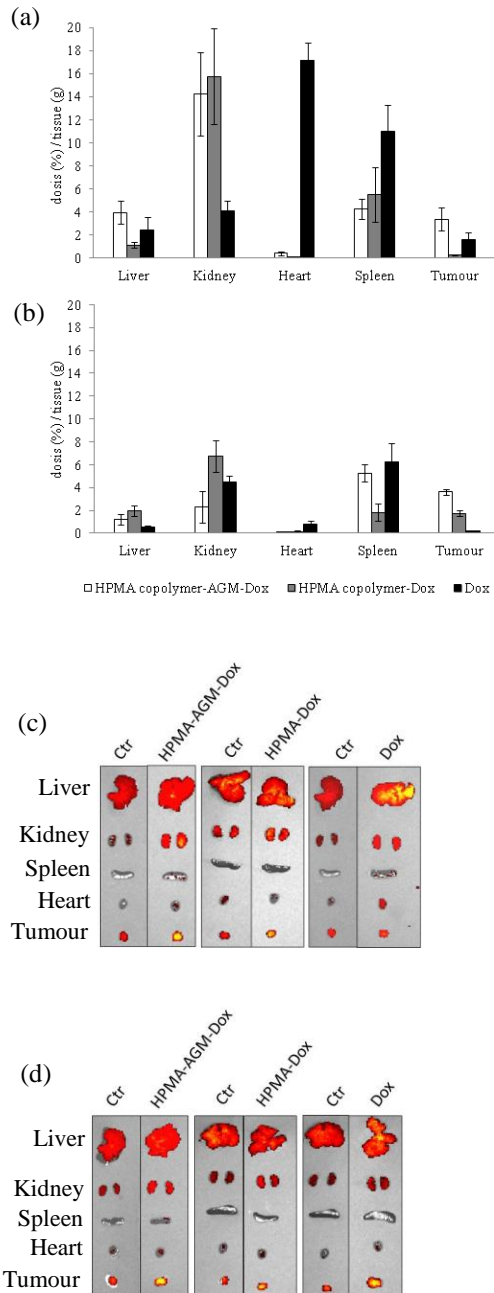
Liver
Kidney
Spleen
Heart
Tumour

Figure 4.7. Biodistribution study of HPMA conjugates and free Dox in 4T1 *in vivo* tumour model (n = 4 animals per group of treatment). Panel (a) shows Conjugates

and Dox quantification by HPLC at 1 h. Panel (b) shows quantification by HPLC at 24 h post-administration. Results are expressed as mean ± SEM where n = 4 animals per group and significances calculated by one-way ANOVA. P*** < 0,001, P**< 0,01, P* < 0,05. Panel (c) and (d) show fluorescence comparison of target organs with the different treatments by IVIS Spectrum® at (c) 1 h post-administration and (d) 24 h post-administration.

Table.4.4. Statistical analysis of the biodristribution data with the HPMA conjugates and free Dox depending of the organs. Panel (a) show the statistique analysis at 1h and panel (b) shows the statistique analysis at 24h.

(a)	Liver	Kidney	Heart	Spleen	Tumour
P value	1	3	3	3	2
1	NA	**	***	*	*
2	**	**	***	ns	NA
3	ns	NA	NA	NA	ns

(b)	Liver	Kidney	Spleen	Tumour	
P value	3	2	2	1	3
1	*	*	*	NA	***
2	*	NA	NA	*	***
3	NA	ns	*	***	NA

1- HPMA copolymer-AGM-Dox, 2- HPMA copolymer-Dox and 3- Dox. The total Dox content was represented (HPMA conjugate + free Dox, analysed by HPLC looking at aglycone, see Materials and Methods) (n = 6). Significances calculated by one-way ANOVA. P*** < 0,001, P* *< 0,01, P* < 0,05, ns: non significance. Statistics at of the other combination showed non significance.

In MCF7 Ca animal model, blood analysis was performed after 60 days in order to better evaluate a possible long-term effect, and in the 4T1 model the analysis was performed 16 days after the administration of treatments, reproducing a short-term evaluation of therapies. In all cases non-significant differences were observed between both treatments in comparison to the control (figure 4.8.).

Importantly, GOT, GPT, LHD and ALP for the combination conjugate showed basal levels in all cases indicating its safety.

Additionally, organ weight was also monitored 8 days post-injection as this was the time when all treatments were more efficient looking further for any toxicological sign. Two types of controls were used, a control group in non-tumour bearing animal, and a control group in the 4T1 model (figure 4.8.).
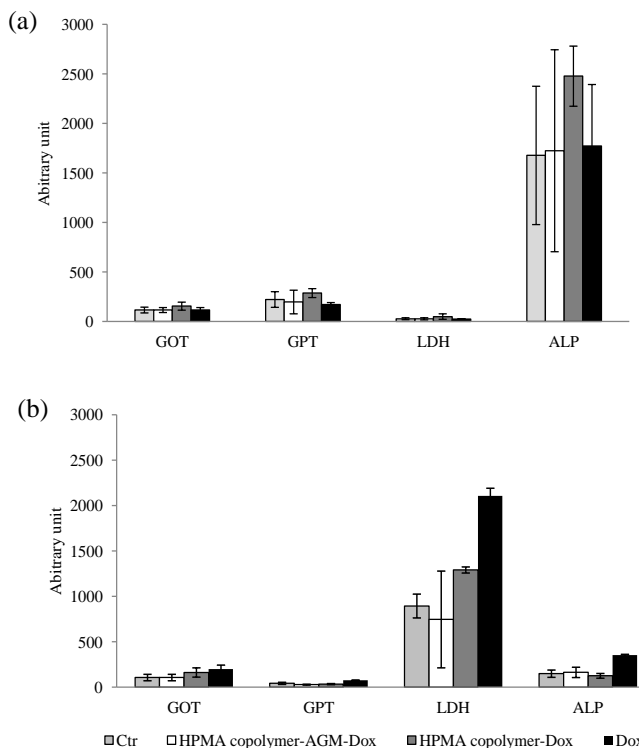
Figure 4.8. Biochemical evaluation of treatments on liver toxicity from plasma samples. Panel (a) shows plasma extracted from 4T1 tumour mice model 16 days treatment post-administration. Panel (b) shows plasma extracted from the MCF7 Ca tumour mice model 60 days treatment post-injection. Results are expressed as mean ± SEM where n = 4 animals per group.

Regarding liver and kidney, a significant weight decreased was observed once tumour was present in the animals. On the other hand, the spleen was found to be much smaller in healthy animals than in those bearing tumour cells. This fact

has been already reported in the literature as splenomegaly caused by the growth factors stimuli triggered by tumour growth (DuPre et al., 2007). The differences in spleen size were directly correlated with tumour size (figure 4.10.) and indirectly correlated to the efficiency of each treatment, as it is shown in the figures 4.9. and 4.10.
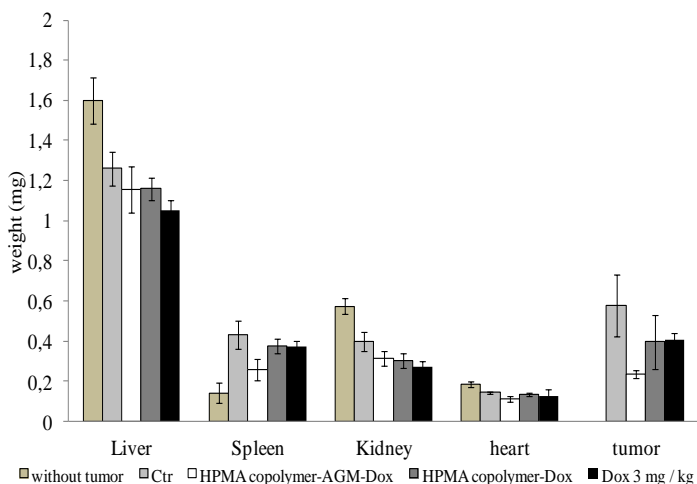
Figure 4.9. Effect of the treatment on the organ weight after 8 days post-administration. Results are expressed as mean ± SEM where n = 6 animals per organs.

Table.4.5. Statistical analysis data of organ weigh evolution after treatment administration.

	Liver	Kidney	Spleen			tumour	
P value	5	5	4	5	1	1	2
1	**	**	*	***	NA	NA	ns
2	**	**	ns	ns	*	*	NA
3	**	**	ns	ns	*	*	ns
4	**	**	NA	***	ns	ns	**
5	NA	NA	ns	NA	ns	ns	ns

1- HPMA copolymer-AGM-Dox, 2- HPMA copolymer-Dox and 3- Dox, 4-Ctr with tumour and 5-Ctr without tumour. (n = 6). Significances calculated by one-way ANOVA. P*** <

0,001, P* *< 0,01, P* < 0,05, ns: non significance. Statistics at of the other combination showed non significance. N.A. non applicable.

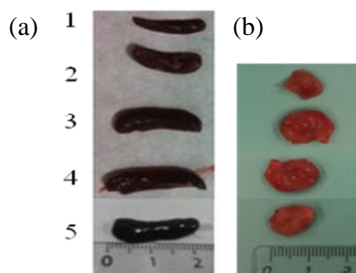Figure 4.10. Representative images of spleen size in direct correlation with tumour growth from the different animal groups. Panel (a) shows spleen images and panel (b) shows tumour images. **1**: Ctr without tumour, **2:** HPMA copolymer-AGM-Dox conjugate, 3: HPMA copolymer-Dox conjugate, 4: Ctr and 5: Dox.

In conclusion, the conjugation of Dox to a polymer carrier induces a safer biodistribution in comparison to the free Dox, markedly decreasing Dox heart accumulation and enhancing tumour accumulation. Moreover, even if a slightly greater accumulation in liver was observed for HPMA copolymer-AGM-Dox conjugate, this fact did not trigger any associated toxicity either at short- or at long-term post-injection.

4.3.3. Evaluation of the antitumour activity of HPMA conjugates and free Dox in the ovarectomised nude mice MCF7 Ca tumour orthotopic model.

Initially based on literature data (St'astny et al., 2002) a Dox-equiv. dose of 5 mg/kg was chosen and this was administered 3 times at intervals of 3 days. Dox toxicity was seen in mice after the third injection reflected by a rapid weight loss (figure 4.11.a.). Therefore, in a second experiment a lower Dox dose of 3 mg/kg was used, again administered 3 times at intervals of 3 days (Talelli et al., 2013). In contrast, the HPMA copolymer conjugates showed less toxicity compared to free drug and a higher dose could be used without any signs of toxicity. In summary, only the control group (no treatment) and the Dox 5 mg/kg treated group induced animal deaths before 90 days (figure 4.11.b.).

113

(a)

(b)

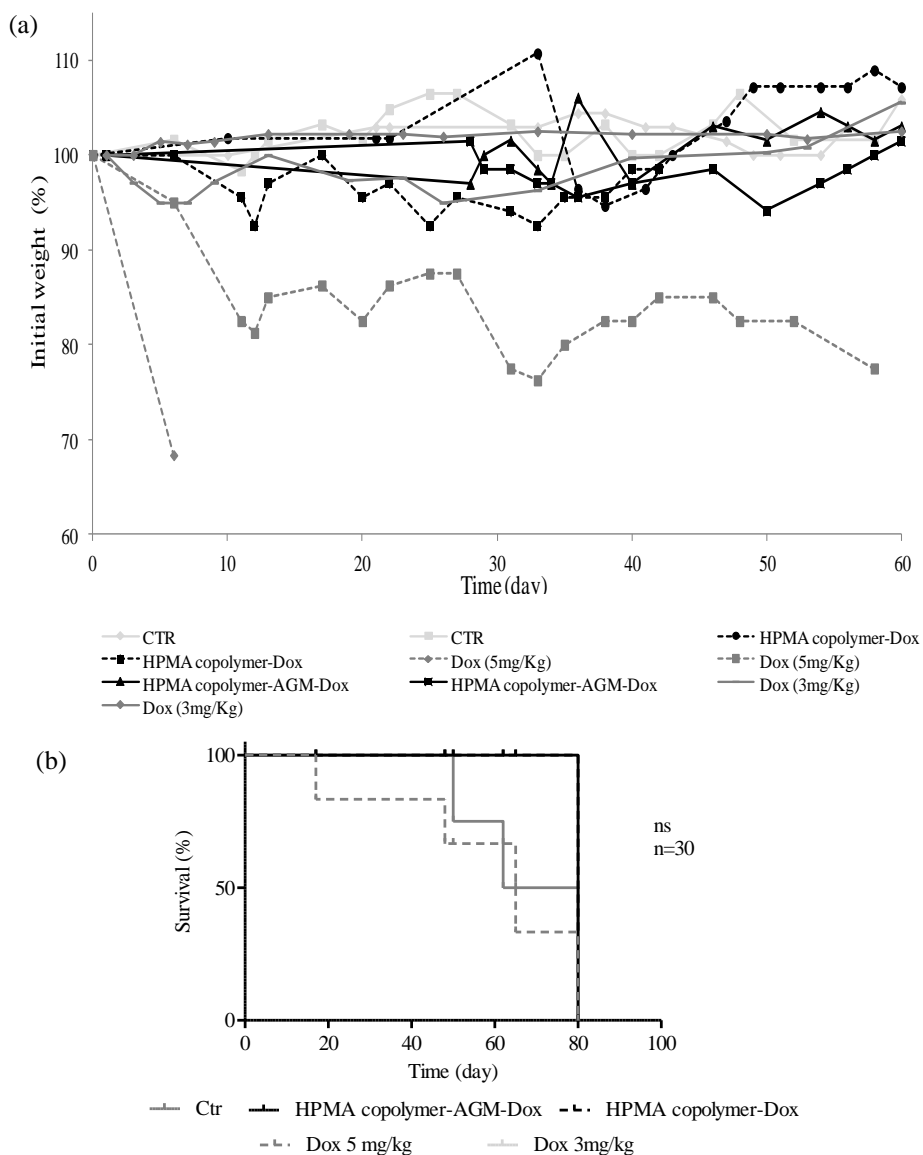Figure 4.11. Effect of HPMA conjugates and free Dox in animal weight and overall survival. Panel (a) shows the compound effect on animal weight lose over 60 days, 2 animals are shown as example; and panel (b) shows the Kaplan–Meier survival analysis, (n = 30, ns), in a MCF7 Ca orthotopic breast cancer model. The injection of treatments was performed on days 0, 3 and 6 as indicated by the arrows.

Table 4.6. Summary of treatment toxicity and long term survival effect.

Treatment	Dose	T/C[b]	Toxic death[c]	Long term survival [c]
Ctr			0/6	0/6
HPMA copolymer-AGM-Dox	5 mg/kg	100	0/6	6/6
HPMA copolymer-Dox	5 mg/kg	100	0/6	6/6
Dox 1	5 mg/kg	50	4/6	0/6
Dox 2	3 mg/kg	100	0/6	5/6

b: determined at 40 days, c: determined at 80 days.
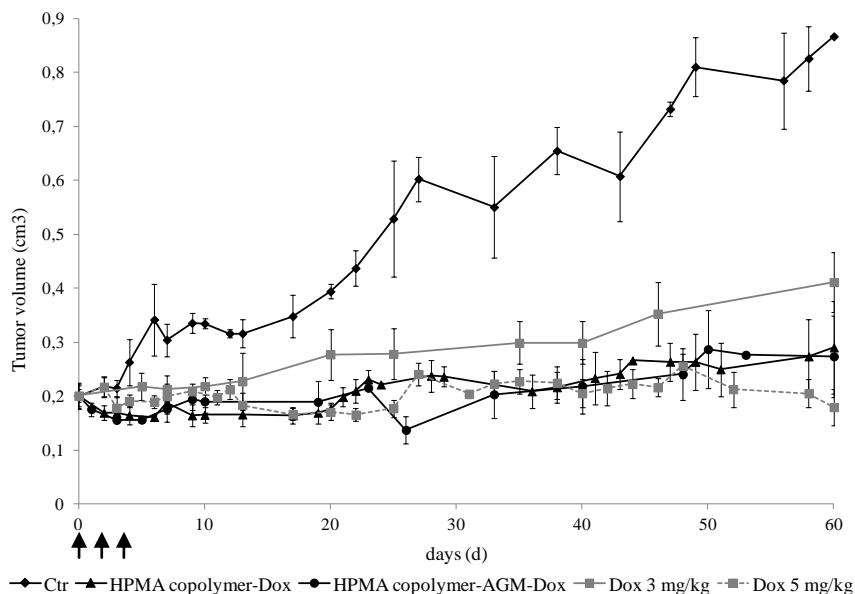

Figure 4.12. Evaluation of HPMA copolymer-AGM-Dox, HPMA copolymer-Dox and Dox in MCF7 Ca induced tumour model. Both conjugates were administered at 5 mg/kg and Dox at 5 and 3 mg/kg, injected 3 times every 3 days. Results are expressed as mean ± SEM where n = 6 animals per group. The injection of treatments was performed on days 0, 3 and 6 as indicated by the arrows.

Both conjugates, HPMA copolymer-AGM-Dox and HPMA copolymer-Dox, achieved a complete tumour regression compared to the control group with non-significant differences between them after 60 days. Figure 4.12. also shows the effect of Dox at 5mg/kg and 3mg/kg. The 3 doses of 5 mg/kg inhibited the tumour growth in the same manner as the conjugates, however this effect was certainly due to the Dox-related toxicity induced in the animals.

Importantly, if we focus on the 10 first days post-injection only when the conjugates were used, a significant tumour regression was achieved (figure 4.13.). This could be explained by the greater accumulation due to the EPR effect and and efficient drug releae kinetics in the tumour tissue.
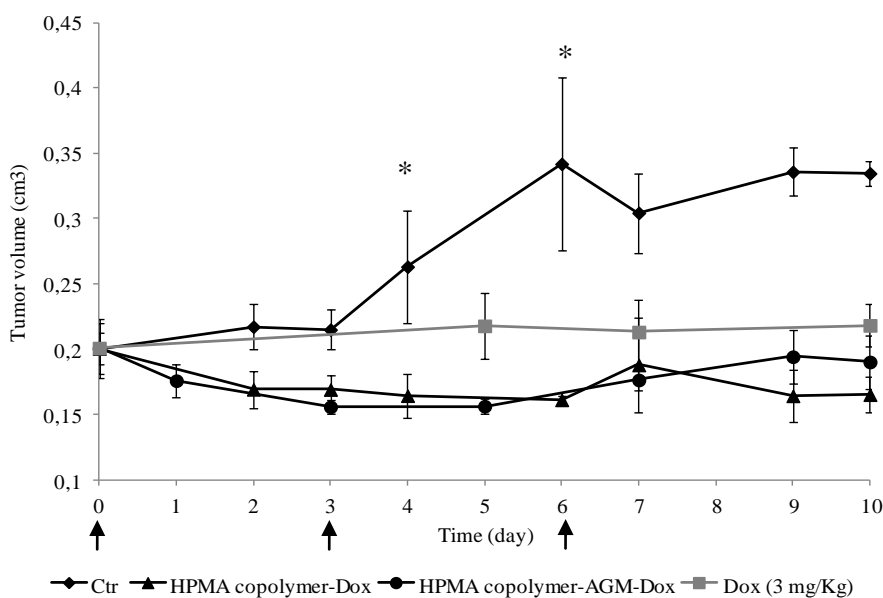
Figure 4.13. Zoom of figure 4.12. HPMA conjugates (5 mg/kg) and free Dox (3 mg/kg) activity in MCF7 Ca *in vivo* model. Results are expressed as mean ± SEM where n = 6 animals per group and significances calculated by one-way ANOVA and P* < 0,05. The injection of treatments was performed on days 0, 3 and 6 as indicated by the arrows.

In conclusion, MCF7 Ca tumour model has been established and characterised as a slow-growth tumour. Both conjugates showed after the 3 first injections a

significant decrease in tumour growth in comparison with the control followed by a complete remission of the tumour with non-significant differences between them but with greater activity than the parent free drug together with an absence of toxicity. Although the MCF7 Ca model could be considered an important and clinically relevant model, it grows so slowly that it would be difficult to use it in future studies devoted to define differences in molecular mechanism associated to the combination therapy. For this reason, after demonstration of antitumour activity, 4T1 model was used for all future studies (Chapter 5).

4.3.4. Evaluation of HPMA conjugate and free Dox in Balb/c mice 4T1 induced tumour orthotopic model.

As it was previously described, in the 4T1 model only after 8 days following cell inoculation the tumour reached the selected 0,1 cm^3 size. Treatments were then administrated 3 times every 3 days following the same strategy used with the MCF7 Ca *in vivo* model.
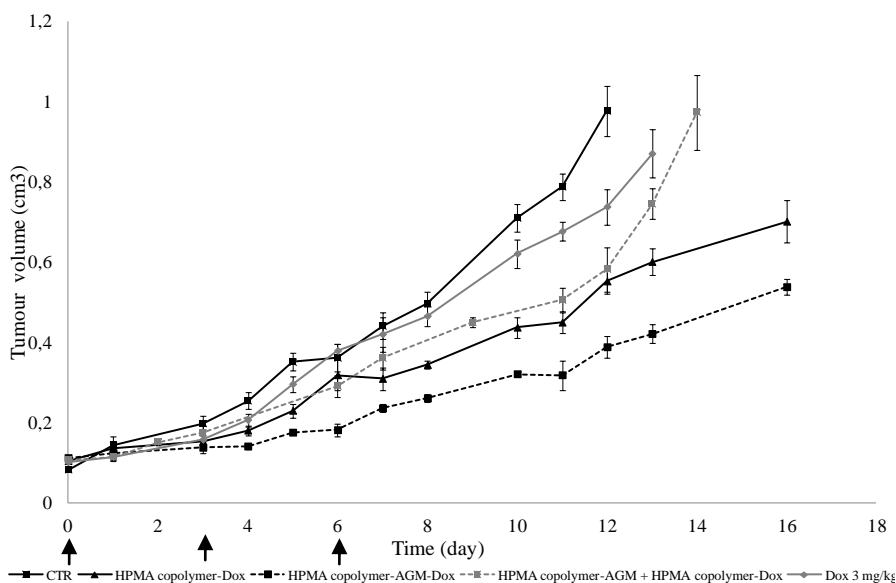

Figure 4.14. Evaluation of the antitumour activity of HPMA conjugates and free Dox in a 4T1 orthotopic mice model. Arrows indicate injection schedule and results

are expressed as mean ± SEM where n = 7 animals per group. The injection of treatments was performed on days 0, 3 and 6.

The statistic analysis was performed with the non-parametric ANOVA one-way test and it is summarised in table 4.7.

Table 4.7. Significance of HPMA conjugates and free Dox treatments on tumor growth in the 4T1 murine model.

P value	1	2	3	4
1	NA	*	**	**
2	*	NA	**	**
3	**	**	NA	*
4	**	**	*	NA

1- HPMA copolymer-AGM-Dox 5 mg/kg, **2-** HPMA copolymer-Dox 5mg/kg, **3-** Dox 3mg/kg and **4-** Control. Significances were carried out by one-way ANOVA; $P^{***} < 0,001$, $P^{**} < 0,01$, $P^{*} < 0,05$. Significant differences were obtained 10 day after the first injection. NA: non applicable.

Both conjugates significantly diminished tumour growth in comparison to the Dox and control groups. Moreover, after the second injection, the antitumour activity of HPMA copolymer-AGM-Dox conjugate compared to HPMA copolymer-Dox conjugate was significantly greater, increasing with time up to day 16 (end of experiment). Therefore, *in vivo* proof of anticancer activity for the combination conjugate was achieved. Remarkably, the combination of both single conjugates (HPMA copolymer-Dox + HPMA copolymer-AGM) showed similar effect as HPMA copolymer-Dox up to day 12 (figure 4.14.), afterthat this combination lost efficiency. The results obtained ratify the importance of conjugating both drugs in the same polymer backbone.

During the experiment, any animal weight loses or abnormal behaviour was monitored as shown in figure 4.15.a.

(a)

(b)
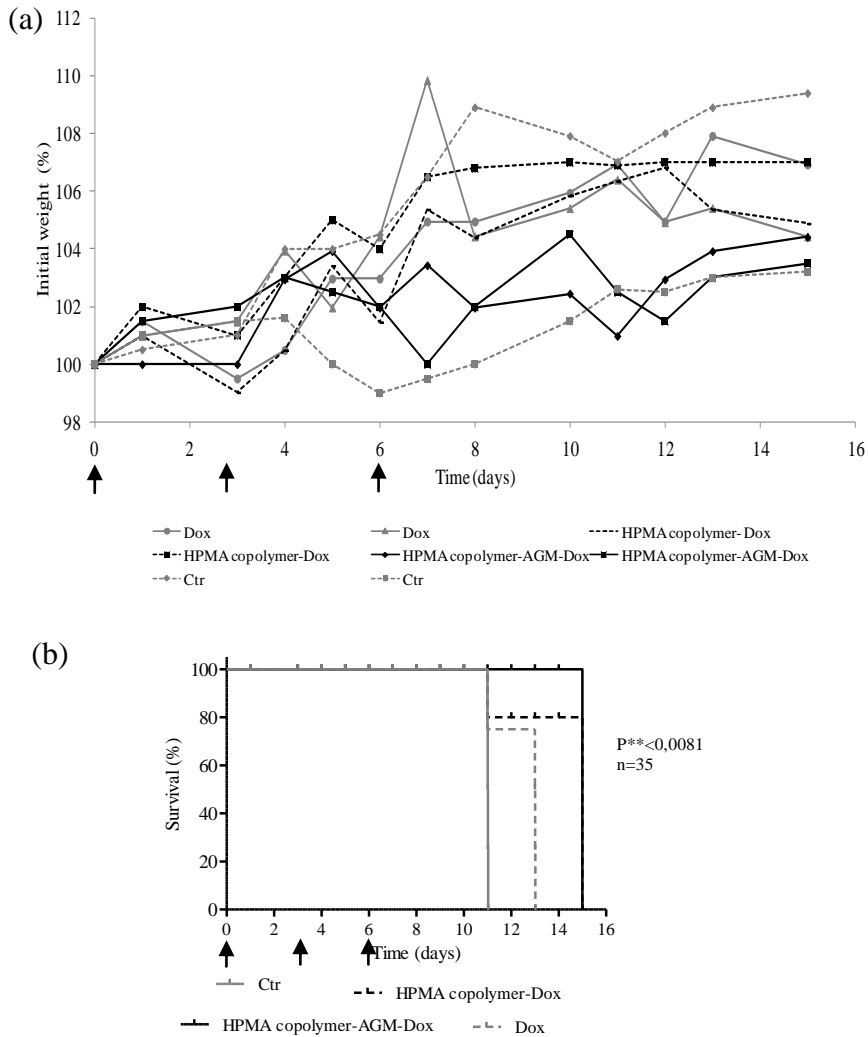
Figure 4.15. Effects of HPMA copolymer-AGM-Dox, HPMA copolymer-Dox conjugates and Dox on survival in a 4T1 orthotopic breast cancer model. Panel (a) shows the evolution of animal weight after the administered treatment. The weight progression of 2 animals is shown as example. Panel (b) shows the Kaplan–Meier survival analysis (n=35, P** < 0,0081). The injection of treatments was performed on days 0, 3 and 6 as indicated by the arrows.

Table 4.8. Summary of treatment toxicity and long-term survival effect.

Treatment	Dose (mg/kg)	T/C[b]	Toxic death[c]	Long term death[c]
Ctr			0/7	7/7
HPMA copolymer-AGM-Dox	5 mg/kg	100	0/7	2/7
HPMA copolymer-Dox	5 mg/kg	100	0/7	2/7
Dox	3 mg/kg	71	0/7	5/7

b: determined at 8 days, c determined at 16 days.

In conclusion, HPMA copolymer-Dox and HPMA copolymer-AGM-Dox conjugates were evaluated in two different orthotopic breast cancer animal models, MCF7 Ca and 4T1, showing always better therapeutic effect than free Dox in terms of toxicity and efficacy. Importantly, in the 4T1 model, a significant difference was observed with HPMA copolymer-AGM-Dox conjugate in terms of antitumour efficacy when compared with HPMA copolymer-Dox or HPMA copolymer-Dox+HPMA copolymer-AGM combination ratifying the importance of having both drug in same polymer mainchain (family 3 combination therapy described in chapter 1.5.).

Molecular mechanism studies were subsequently performed in cell models as well as in 4T1 tumour tissues as the next step towards the understanding the benefits of combination therapy. Looking at the possible reasons for the greater tumour growth inhibition observed with HPMA copolymer-AGM-Dox combination conjugate (see chapter 5). The conjugation of more than one drug in the same polymer backbone secures their release within the same cell and, therefore, synergism could be achieved if drug ratio and the kinetics of drug release are adequately designed (further discussion on this topic will be found in Chapter 6).

4.4. Discussion.

The HPMA copolymer-AGM-Dox combination conjugate was first described by Vicent *et al.* in 2005 showing very promising results in human breast cancer cell models in comparison to HPMA copolymer-Dox conjugate. In this context and to move to a step further, HPMA conjugate and free drug *in vitro* evaluation was not only performed in MCF7 Ca breast cancer human cell line but also in 4T1 breast cancer murine cell line. The CI was calculated from the IC50 as described previously showing a clear synergic effect of the HPMA copolymer-AGM-Dox in comparison to HPMA copolymer-Dox. Vicent et al. reported CI = 0,114 in MCF7 Ca cells (Vicent et al., 2005) in comparion with the CI here obtained of CI = 0,26; this difference could be justified by the use of a different cell passaging number. The CI value in 4T1 cells (CI = 0,109) was even better than that observed in MCF7 Ca cells suggesting a greater cytotoxic activity for this conjugate in the murine cell line *in vivo* model.

In order to confirm those *in vitro* results, two different orthotopic *in vivo* tumour models, established from human MCF7 Ca and murine 4T1 cells, were optimised and fully characterised. The Evans blue experiment allowed us to understand the permeability for both systems and choose the appropriate experimental conditions to take profit of the EPR effect (described in chapter 1.4.2.). Moreover in this study a higher permeability, 12% of Evans blue, was observed in very small tumour sizes (0,08 cm^3) in MCF7 Ca model when in palpable tumour (0,2 cm^3) only 7% of Evans blue was quantified. Therefore, this confirms the opportunity for polymer drug conjugate to target especially small tumours as occurred in metastatic cancers.

Both conjugates showed much lower toxicity and a significant delay in tumour growth in the MCF7 Ca mice model in comparison to free Dox. Moreover a significant tumour regression was also observed during the first days only for both conjugates. This result could be explained based on tumour accumulation (by the EPR effect), the drug release and uptake rates. Greco et al (2007) described a similar uptake for both HPMA conjugate starting after 1 h in MCF7 Ca. And once inside the lysosome, 20% of the Dox is released in 5 h for HPMA copolymer-AGM-Dox and 40% for HPMA copolymer-Dox. Therefore

the schedule of 3 injections each 3 days take profit of the time course needed in endocytosis and drug release occurred only with polymer drug conjugate in comparison to Dox diffusion inside the cell (Decorti et al., 1989). Therefore after the conjugate injection, Dox is progressively released during the 3 days and consequently induce a greater decrease in tumour growth than that observed for the free drug. After the 3rd injection, this decrease was not further observed. However, MCF7 Ca was not an adequate model to differentiate the performance between the conjugates and, therefore, a murine model established from 4T1 metastatic cell line was also optimised. The 4T1 model was chosen as a representative metastatic and aggressive model that closely resemble to human breast cancer inducing metastasis in lung, bone, liver and brain. In this scenario, both conjugates showed better performance than free Dox and more importantly, significant tumour inhibition was observed for HPMA copolymer-AGM-Dox conjugate in comparison to HPMA copolymer-Dox conjugate.

In order to fully evaluate both conjugates and to explain these differences a full pharmacokinetics study was performed. Whole body biodistribution showed that the conjugation of Dox to a polymer backbone significantly reduced Dox accumulation in heart, in good agreement with already reported data. Renal excretion was observed for the conjugates but with a different pharmacokinetic profile showing faster clearance for HPMA copolymer-Dox versus HPMA copolymer-AGM-Dox. Tumour accumulation was also evaluated showing an increase tumour targeting for both conjugates in comparison to free Dox and possible differences on the endocytic mechanism in 4T1 tumour cells was clearly observed with HPMA copolymer-Dox showing non-detectable Dox levels in the tumour before 1 h. A slight liver accumulation was also observed with the conjugates in comparison to free Dox being more important for HPMA copolymer-AGM-Dox. Consequently, a biochemical blood analysis was performed, including key proteins such as GOT, GPT, LDH, ALP, trying to identify any possible liver-related toxicity that would compromise the possible clinical benefit for the combination conjugate. No signs of toxicity were observed in any case.

4.5. Bibliography.

Brodie, A. and Long, B. (2001). "Aromatase inhibition and inactivation." Clin Cancer Res 7(12 Suppl): 4343s-4349s; discussion 4411s-4412s.

Brodie, A., Lu, Q., Liu, Y., and Long, B. (1999). "Aromatase inhibitors and their antitumor effects in model systems." Endocr Relat Cancer 6(2): 205-210.

Chou, T. C. (2006). "Theoretical basis, experimental design, and computerized simulation of synergism and antagonism in drug combination studies." Pharmacol Rev 58(3): 621-681.

Chou, T. C. (2010). "Drug combination studies and their synergy quantification using the Chou-Talalay method." Cancer Res 70(2): 440-446.

Decorti, G., Klugmann, F. B., Candussio, L., Furlani, A., Scarcia, V. and Baldini, L. (1989). "Uptake of adriamycin by rat and mouse mast cells and correlation with histamine release." Cancer Res 49(8): 1921-1926.

Duncan, R. (2009). "Development of HPMA copolymer-anticancer conjugates: clinical experience and lessons learnt." Adv Drug Deliv Rev 61(13): 1131-1148.

Duncan, R. and Vicent, M.J. (2010). "Do HPMA copolymer conjugates have a future as clinically useful nanomedicines? A critical overview of current status and future opportunities." Adv Drug Deliv Rev 62(2): 272-282.

DuPre, S. A. and Hunter, K.W.Jr. (2007). "Murine mammary carcinoma 4T1 induces a leukemoid reaction with splenomegaly: association with tumor-derived growth factors." Exp Mol Pathol 82(1): 12-24.

Gao, Z. G., Tian, L., Hui, J., Park, I. and Han Bae, Y. (2011). "Prevention of metastasis in a 4T1 murine breast cancer model by doxorubicin carried by folate conjugated pH sensitive polymeric micelles." J Control Release 152(1): 84-89.

Greco, F., Vicent, M.J., Gee, S., Jones, A.T., Gee, J., Nicholson, R. and Duncan, R. (2007). "Investigating the mechanism of enhanced cytotoxicity of HPMA copolymer-Dox-AGM in breast cancer cells." J Control Release 117(1): 28-39.

Greco, F., Vicent, M.J., Penning, N.A., Nicholson, R.I. and Duncan, R. (2005). "HPMA copolymer-aminoglutethimide conjugates inhibit aromatase in MCF-7 cell lines." J Drug Target 13(8-9): 459-470.

Maeda, H. (2001). "The enhanced permeability and retention (EPR) effect in tumor vasculature: the key role of tumor-selective macromolecular drug targeting." Adv Enzyme Regul 41: 189-207.

Matsumura, Y. and Maeda H. (1986). "A new concept for macromolecular therapeutics in cancer chemotherapy: mechanism of tumoritropic accumulation of proteins and the antitumor agent smancs." Cancer Res 46(12 Pt 1): 6387-6392.

Peer, D., Karp, J.M., Hong, S., Farokhzad, O.C., Margalit, R. and Langer, R. (2007). "Nanocarriers as an emerging platform for cancer therapy." Nat Nanotechnol 2(12): 751-760.

Rodea-Palomares, I., Petre, A.L., Boltes, K., Leganés, F., Perdigon-Melon, J.A., Rosal, R. and Fenandes-Pinas, P. (2010). "Application of the combination index (CI)-isobologram equation to study the toxicological interactions of lipid regulators in two aquatic bioluminescent organisms." Water Res 44(2): 427-438.

St'astny, M., Plocova, D., Etrych, T., Ulbrich, K. and Rihova B. (2002). "HPMA-hydrogels result in prolonged delivery of anticancer drugs and are a promising tool for the treatment of sensitive and multidrug resistant leukaemia." Eur J Cancer 38(4): 602-608.

Talelli, M., Oliveira, S., Rijcken, C.J., Pieters, EH., Etrych, T., Ulbrich, K., Van Nostrum, R.C., Storm, G., Hennink, W.E., and Lammers, T. "Intrinsically active nanobody-modified polymeric micelles for tumor-targeted combination therapy." Biomaterials 34(4): 1255-1260.

Tao, K., Fang, M., Alroy, J., and Sahagian, G.G. (2008). "Imagable 4T1 model for the study of late stage breast cancer." BMC Cancer 8: 228.

Vasey, P.A., Kaye, S.B., Morrison, R., Twelves, C., Wilson, P., Duncan, R., Thomson, A.H., Murray, L.S., Hilditch, T.E., Murray, T., Burtles, S., Fraier, D., Frigerio, E. and Cassidy, J. (1999). "Phase I clinical and pharmacokinetic study of PK1 N-(2- hydroxypropyl)methacrylamide copolymer doxorubicin : First member of a new class of chemotherapeutic agents - Drug-polymer conjugates." Clin Cancer Res 5(1): 83-94.

Vicent, M.J., Greco, F., Nicholson, R.I., Paul, A., Griffiths, P.C. and Duncan, R. (2005). "Polymer therapeutics designed for a combination therapy of hormone-dependent cancer." Angew Chem Int Ed 44(26): 4061-4066.

Wu, J., Akaike, T., and Maeda, H. (1998). "Modulation of enhanced vascular permeability in tumors by a bradykinin antagonist, a cyclooxygenase inhibitor, and a nitric oxide scavenger." Cancer Res 58(1): 159-165.

Yue, W., Zhou, D., Chen, S., and Brodie, A. (1994). "A new nude mouse model for postmenopausal breast cancer using MCF-7 cells transfected with the human aromatase gene." Cancer Res 54(19): 5092-5095.

Chapter 5. Study of the mechanism of action for HPMA conjugates in comparison with Dox in a 4T1 orthotopic breast cancer model.

5.1. Introduction.

Following these promising *in vivo* findings, the aim of the present study was to obtain a better understanding of the molecular mechanisms for synergism observed *in vivo* as this could help in the design of improved polymer-based combination conjugates in the future. Based on previous *in vitro* studies, Vicent *et al.* (2005) and Greco *et al*. (2007) tried to determine the molecular mechanisms underlying this improved activity (Vicent et al., 2005, Greco et al., 2007). When HPMA conjugate and free Dox were compared differences in drug release kinetic profile were observed due to their different solution conformation. Immunocytochemistry studies were also carried out to assess the effect of both conjugates on the proliferation marker ki67 and the anti-apoptotic protein Bcl-2 (Greco et al., 2007). A down regulation of ki67 protein expression following incubation of MCF7 and MCF7 Ca cells with both conjugates was observed but this was more pronounced with the combination polymer. As ki67 is a well-described marker for the proliferating fraction of a cell population, this result was consistent with the higher cytotoxicity obtained with the combination polymer in cell viability assays. More importantly, HPMA copolymer-Dox had no effect on Bcl-2 anti-apoptotic protein expression, whereas a marked down regulation of Bcl-2 was achieved after incubation of MCF7 with the combination conjugate. Moreover Bcl-2 is described as a dual regulator involved in both apoptosis and autophagy cell death pathway, (Levine et al., 2008). It was consequently proposed here to study the effect of HPMA conjugate and free Dox in both pathways. More specifically the following studies were performed:

(i)   The reproducibility of the earlier studies, Bcl-2 expression was evaluated for HPMA conjugates and free Dox in MCF7 Ca cell by western blot. And to move a step further cell cycle analysis in MCF7 Ca cells for HPMA conjugates and free Dox was studied by flow cytometry.

(ii)   New studies to better understand *in vivo* tumour growth inhibition (Chapter 4), including autophagy and apoptosis cell death mechanism as well as tumour proliferation pathways by means of the modulation of several key proteins by western blot analysis. [Protein kinase B (Akt), microtubule-associate

protein light chain 3 (<u>LC3</u>), caspase3, <u>Bcl2</u>, Bcl2 associated X protein (<u>Bax</u>), hypoxia-inducible factor-1 alpha (<u>HIF1-α</u>) induced nitric oxide synthase (<u>iNOS</u>) and vascular endothelial growth factor (<u>VEGF</u>)].

5.2. Evaluation of HPMA conjugates and free Dox in MCF7 Ca cell line.

As follow up of the previous reported results and in order to evaluate the conjugates effect on cell cycle, the conjugates and free Dox were incubated in MCF7 Ca cells for 72 h and the modulation on apoptosis markers and cell cycle analysed by flow cytometry.
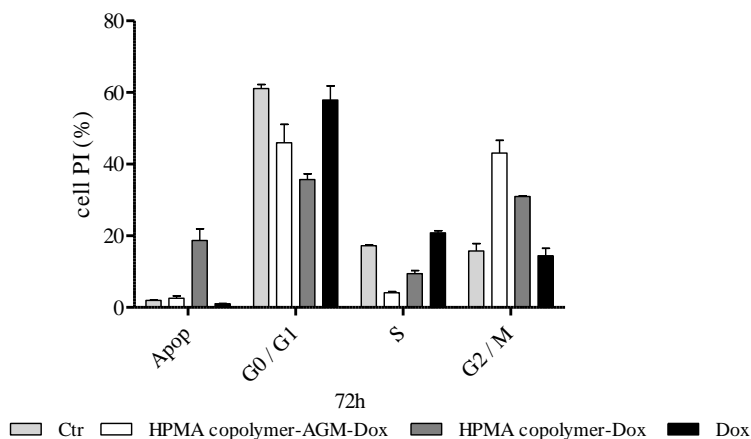

Figure 5.1: Cell cycle analysis after 72 h incubation of conjugates and free Dox in MCF 7 Ca cell line at each compound IC50 value. Data expressed as mean ± SD where n = 3. PI means Propidium Iodide and Apop means apoptosis.

Table.5.1. Statistical analysis data of cell cycle study in MCF7 Ca cell line.

	Apop.	G0/G1		S		G2/M	
P value	2	4	2	4	2	4	3
1	**	ns	*	**	**	**	**
2	NA	***	NA	**	NA	**	**
3	**	ns	**	ns	**	ns	NA
4	**	NA		NA	ns	NA	ns

1- HPMA copolymer-AGM-Dox conjugate, **2-** HPMA copolymer-Dox conjugate and **3-** Dox and **4-**Ctr. (n = 3). Significances calculated by one-way ANOVA. P*** < 0,001, P* *< 0,01,

P* < 0,05, ns: non significance. Statistics at of the other combination showed non significance. NA: non applicable.

Whereas a significant apoptosis was observed only for HPMA copolymer-Dox in comparison with the other compounds tested, a stop in G2/M phase for both conjugates was achieved in contrast to free Dox. Western blot analysis was also carried out to ratify these studies looking at proteins involved in cell cycle as well as cell death mechanism. However due to the difficulty to achieve reproducible data, it was decided to performed a deeper analysis using tumour tissue from the 4T1 model activity experiment instead of cells. In this way it would be possible to correlate the activity graphs with the actual molecular mechanism responsible for antitumor activity as EPR-mediated targeted effects could be also taken into account.

5.3. Evaluation of HPMA conjugates and free Dox by western blot.

5.3.1. Evaluation of protein expression modulation involved in autophagy by HPMA conjugates and free Dox.

Differences between both conjugates regarding possible cell death pathways were analysed at two different times points, 8 days after 1st injection (48 h after the last injection trying to keep the 72 h timeframe studied so far) and 16 days after 1st injection (end of the experiment).

Based on literature, different mechanisms of cell death including autophagy (Kondo and Kondo, 2006) or apoptosis (Kaufmann and Earnshaw, 2000) need of Bcl2 as regulator protein. Autophagy is the basic catabolic mechanism that involves cell degradation of unnecessary or dysfunctional cellular components through the lysosomal machinery (from the Greek words, *auto* "self" and *phagein*" to eat") (Lin et al., 2012). At the beginning of autophagy, portions of the cytoplasm, as well as intracellular organelles, are sequestered in autophagosomes (figure 5.3.a.). Then, autophagosomes fuse with lysosomes to form autolysosomes, and the sequestered contents are degraded by lysosomal hydrolases (Kondo et al., 2005). Numerous proteins such as Kinases,

mammalian targets of rapamycin (mTOR), (Akt), Beclin, (LC3) (Kondo et al., 2005; Kondo and Kondo, 2006; Noda et al., 2009; Chen and Karantza, 2011) are involved in this mechanism of action, therefore they could be used as molecular targets to evaluate autophagy under specific conditions (figure 5.3.a.). It is important to note that, Bcl-2 is a cross-talk protein involved in both autophagy and apoptosis (Hoyer-Hansen et al., 2007; Levine et al., 2008). mTOR has been described as a major protein in the autophagy signalling pathway but it also regulates many other aspects of cell function, including transcription, translation, cell size and cytoskeletal organisation (Schmelzle and Hall, 2000). Due to the lack of selectivity, mTOR was not considered a good molecular marker to evaluate autophagy in our tumour models. mTOR study was replaced by p-Akt protein expression analysis, the activated form of p-Akt is involved in the down regulation of mTOR and consequently in the formation of the pre-autophagosome through beclin-1. Beclin-1 is the first molecule that has been demonstrated to have a direct link between tumorigenesis and disruption of autophagy and has also been described to be involved in the autophagosome formation. Exogenous expression of beclin-1 in MCF7 cells, which do not express beclin-1 endogenously, resulted in induction of autophagy, decreased cell proliferation and tumorigenesis inhibition (Kondo et al., 2005; Kondo and Kondo, 2006; Esclatine et al., 2009). Beclin-1 was down-regulated by different co-repressors as for example Bcl-2. Finally, it is well-known the key role of LC3 in the autophagosome closure (Noda et al., 2009). LC3 became proteolytically activated, thereby generating a cytosolic LC3-I that subsequently conjugates with phosphatidylethanolamine (PE) to form the membrane associated LC3-II (Juenemann and Reits, 2012). LC3-II persists in the autophagosomal membrane even after fusion with the lysosomes and therefore can be considered as a key maker for autophagosome monitoring. The number of autophagosomes present in the cell is a key parameter to confirm an autophagic cell death mechanism. In terms of LC3 analysis by western blotting, it is important to note that the immunoreactivity of LC3-B I and II considerably differs. The increase in LC3-B II expression is usually greater than the decrease in LC3-B I levels. Therefore, LC3-B II/LC3-B I ratio could be considered a good marker for autophagy (Mizushima and Yoshimori, 2007). The levels of p-Akt, Bcl-2, Beclin-1 and

129

LC3 proteins in control tumours were found to be in good agreement with literature (Kondo et al., 2005; Levine et al., 2008; Chen and Karantza, 2011).
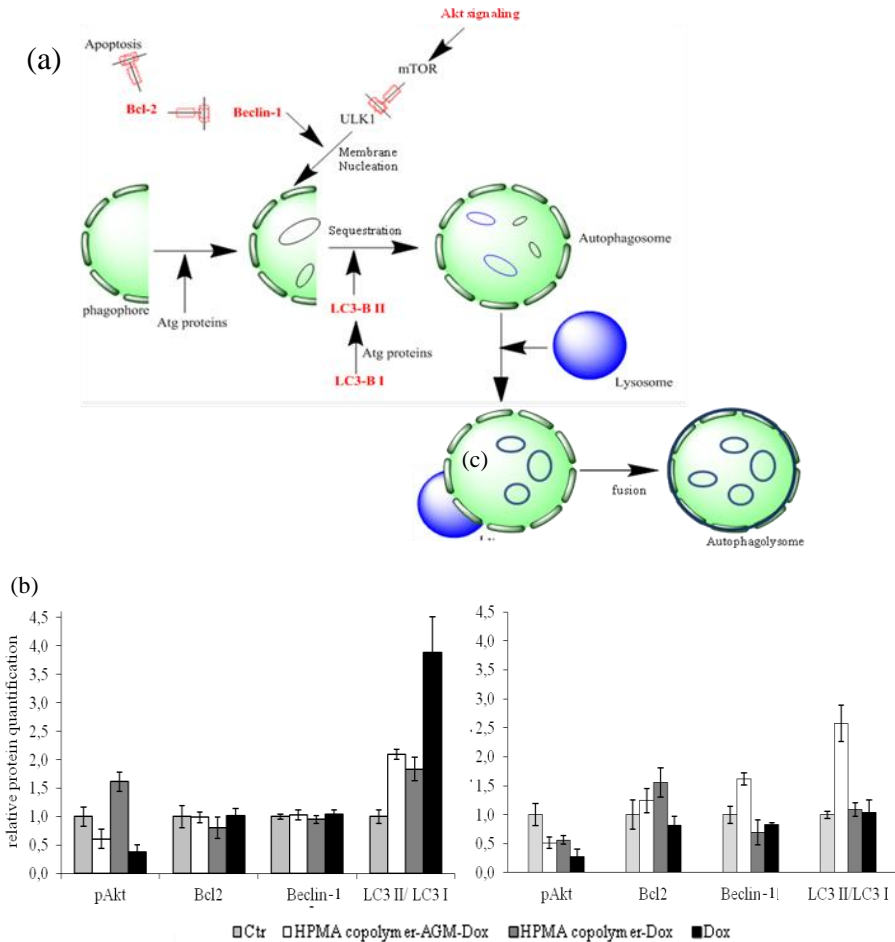

Figure 5.3. Evaluation of the autophagic protein cascade triggered by the HPMA copolymer-AGM-Dox conjugate, HPMA copolymer-Dox conjugate and Dox treatments in 4T1 animal model. Panel (a) shows a schematic diagram with target proteins involved in autophagy. Panel (b) and (c) shows the quantification of autophagy-related protein; (b) 8 days after the first treatment injection (n = 4 animals per group) and (c) 16 days after the first treatment injection (n = 6 animals per group). Mean values ± SEM.

Table.5.2. Statistical analysis data of protein expression involved in autophagy.

	pAkt 8 d		pAkt 16d	LC3 II/ LC3 I 8 d		LC3 II/ LC3 I 16 d	Beclin-1 16 d
P value	2	4	4	4	3	1	1
1	**	ns	*	**	*	NA	NA
2	NA	*	*	*	*	**	**
3	**	*	*	**	NA	**	**
4	ns	NA	NA	NA	**	**	**

1- HPMA copolymer-AGM-Dox conjugate, **2-** HPMA copolymer-Dox conjugate and **3-** Dox and **4-**Ctr. (n = 3). Significances calculated by one-way ANOVA. P*** < 0,001, P* *< 0,01, P* < 0,05, ns: non significance. Statistics with tother combinations showed non significance. NA: non applicable.

As it can be seen in figure 5.3., 8 days after the first treatment injection both conjugates showed a significant increased in LC3-B II/LC3-B I ratio. Moreover free Dox presented a significant increased in comparison to control and the conjugates. This result was confirmed by a decrease in pAkt expression with HPMA copolymer-AGM-Dox conjugate and free Dox. However, an unexpected increased in pAkt expression for HPMA copolymer-Dox conjugate was obtained together with the non-significant changes observed for beclin-1. On the other hand, 16 days after the first treatment injection, HPMA copolymer-AGM-Dox conjugate showed a significant increased in LC3-B II/LC3-B I whereas this effect was not observed either with HPMA copolymer-Dox conjugate or free Dox. This differential result was confirmed by the down-regulation of p-Akt and a significant overexpression in beclin-1 in the HPMA copolymer-AGM-Dox conjugate treated mice.

5.3.2. Evaluation of protein modulation involved in apoptosis by HPMA conjugates and free Dox.

To complement the study on death mechanisms, apoptosis, known as programmed cell-death, was also explored. Apoptosis is a fundamental mechanism of programmed cell death regulated physiologically and genetically that plays a central role in development, normal cell turnover and immune

131

system function. Moreover, abnormal apoptotic processes are important and influence the severity of disease progression in a number of pathologies. The mechanism of apoptosis is executed by a family of highly conserved proteases known as caspases, which in a cascade of sequential initiator and effector members dismantle the cell. Different cell death stimuli can initiate the mechanism. In particular, defined apoptotic signals activate the mitochondria-mediated or intrinsic pathway that utilizes caspase-9 as its initiator. Caspase-9 activation is triggered by the release to the cytoplasm of proapoptotic proteins from the mitochondrial inter-membrane space, in particular cytochrome *c* and Smac/Diablo. The formation of the macromolecular complex named apoptosome is a key event in this pathway. The apoptosome is a holoenzyme multiprotein complex formed by cytochrome *c*-activated Apaf-1 (apoptosis protease-activating factor), dATP and procaspase- 9 activating caspase 3 and 7 and inducing cell death. It was also described an extrinsic pathway induced by ligation of death receptors (TNF receptor) and through the formation of the oligomerisation of the adapter molecule FADD, caspase-8 and 10 were trigged and finally induced cell death through caspase 3 activation. (Douglas et al., 2005). Key proteins involved and studied in this cascade are Bcl2, Bax, and caspase 3 (figure 5.4.a.).

As it can be seen in figure 5.4., 8 days after the first injection, an increase in caspase 3 expresion was observed for both conjugates and free Dox. However, after 16 days only HPMA copolymer-Dox conjugate was capable of up-regulating caspase 3 expresion in comparison to the control group, suggesting that HPMA copolymer-Dox conjugate triggers cell death through an apoptotic pathway. Nevertheless, the protein expressions of Bcl2 and Bax were kept unchanged, therefore it could be hypothesised that the extrinsic pathway of apoptosis is the one taking place.

Altogether, it could be hypothesised that at the beginning a mix mechanism of cell death is taken place in all treatments. However, at long-term a differenciation in cell death mechanisms occur and HPMA copolymer-AGM-Dox combination conjugate was mostly involved in autophagy when solely

132

apoptosis was modulated by HPMA copolymer-Dox conjugate in good agreement with already reported data (Minko et al., 2000; Malugin et al., 2007).
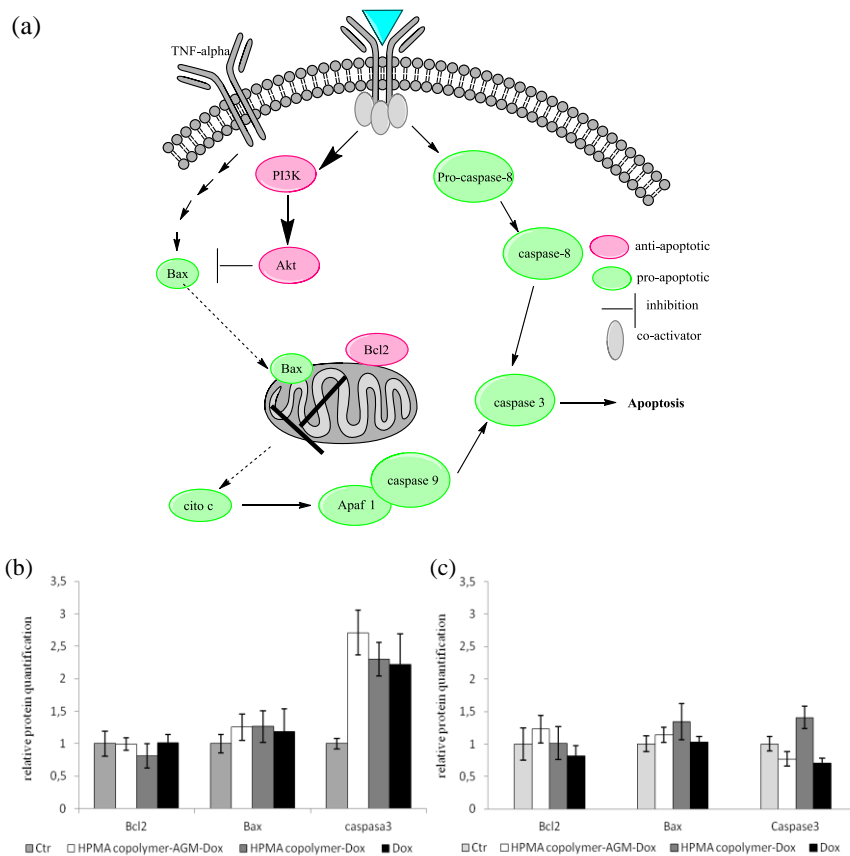

Figure 5.4. Evaluation of the apoptosis-related protein expression in 4T1 tumour tissue after treatment with Dox-derivatives. Panel (a) shows a schematic diagram showing the target proteins involved in apoptosis. Panel (b) and (c) show the quantification of proteins involved in apoptosis mechanism (Bcl2, Bax, casp3) after (b) 8 days of treatment and (c) 16 days of treatment. The experiment was performed with n = 6 animals per group. Mean values ± SEM.

Table.5.3. Statistical analysis data of protein expression involved in apoptosis cell death.

	Caspase3 8 d	Caspase3 16d
P value	4	2
1	*	*
2	*	NA
3	*	*
4	NA	*

1- HPMA copolymer-AGM-Dox conjugate, **2-** HPMA copolymer-Dox conjugate and **3-** Dox and **4-**Ctr. (n = 3). Significances calculated by one-way ANOVA. P* < 0,05, ns: non significance. Statistics at of the other combination showed non significance. NA: non applicable.

5.3.3. Evaluation of protein modulation involved in angiogenesis pathways by HPMA conjugates and free Dox.

Solid tumour malignancies including breast, lung and prostate carcinomas are considered to be angiogenesis dependent. Tumour angiogenesis could be induced by different mechanism but always depending of VEGF. VEGF is one of the most widely studied hypoxia-inducible proteins. It is often observed that the hypoxia encountered in the tumour core induced tumour growth and activates oncogenic protein signalling cascades. Both mechanisms result in an increased expression of the hypoxia-inducible factor (HIF)-1α and its transcriptional target VEGF (Ellis et al., 2009). HIF-1α is an heterodimeric transcription factor composed of HIF-1α which dimerises with a constitutively expressed β subunit and subsequently binds to hypoxia response elements (HRE) in the promoters of target genes (Semenza, 2003; Semenza, 2012). HIF-1α regulates the expression of numerous genes involved in various cellular signalling pathways, including angiogenesis, via the increased expression of VEGF. Moreover two distinc pathways by which VEGF expression is regulated have been identified, one through HIF-1α translation already decribed and one HIF independent, both involving Akt. VEGF is one of the genes under control of HIF-1α in hypoxic conditions but it is also activated in normoxic conditions through the PI3-K/Akt pathways by growth factor receptors and estrogen receptors activation targeting the proximal transacting transcription factor 1

(SP1)-binding sites on proximal core of *VEGF* promoter (Pore et al., 2004; Pore et al., 2006; Kazi and Koos, 2007; Curry et al.,2008; Kazi et al., 2009).
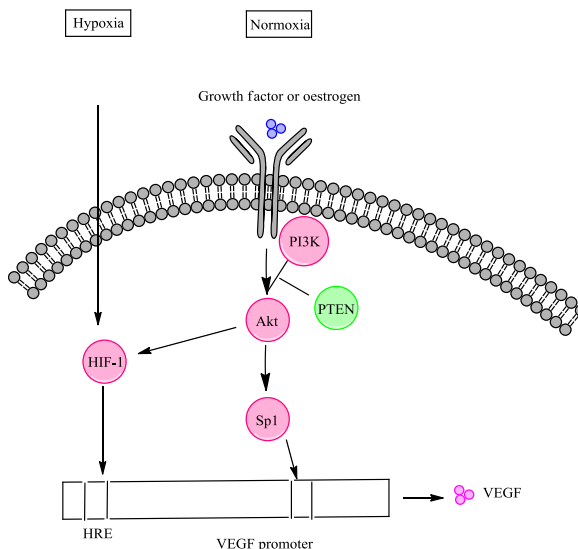

Figure 5.5. Mechanism of VEGF transcription in normoxia and hypoxia.

After VEGF induction, a down-stream cascade of proteins involved in vascular permeability (iNOS), cell proliferation (Extracellular signal-regulated kinase Erk), survival (PI3K, pAkt) and migration (MAPK) are also activated. All those mechanisms have been reported in tumour growth, dissemination and metastasis (Semenza, 2003; Semenza, 2012). In addition, it has also been described that HRE are present in NOS promoter, triggering the transcription of (iNOS) under hypoxia (Tendler et al., 2001; Singh and Gupta, 2011). In this context, it was reported that breast tumours showed predominantly localised iNOS expression in tumour cells differentiating them from normal tissues with no detectable iNOS activity. This suggests a clear relationship between iNOS and malignancy (Thomsen et al. 1994; Singh and Gupta, 2011). Moreover, a study carried out in 1997 based on the iNOS expresion in primary breast tumours, suggested that iNOS played a key role in the facilitation of tumour metastasis (Duenas-Gonzalez et al., 1997).

In order to study the different expression of proteins involved in tumour angiogenesis, tumours were isolated after 8 and 16 days treatment and proteins were extracted for western blot analysis.
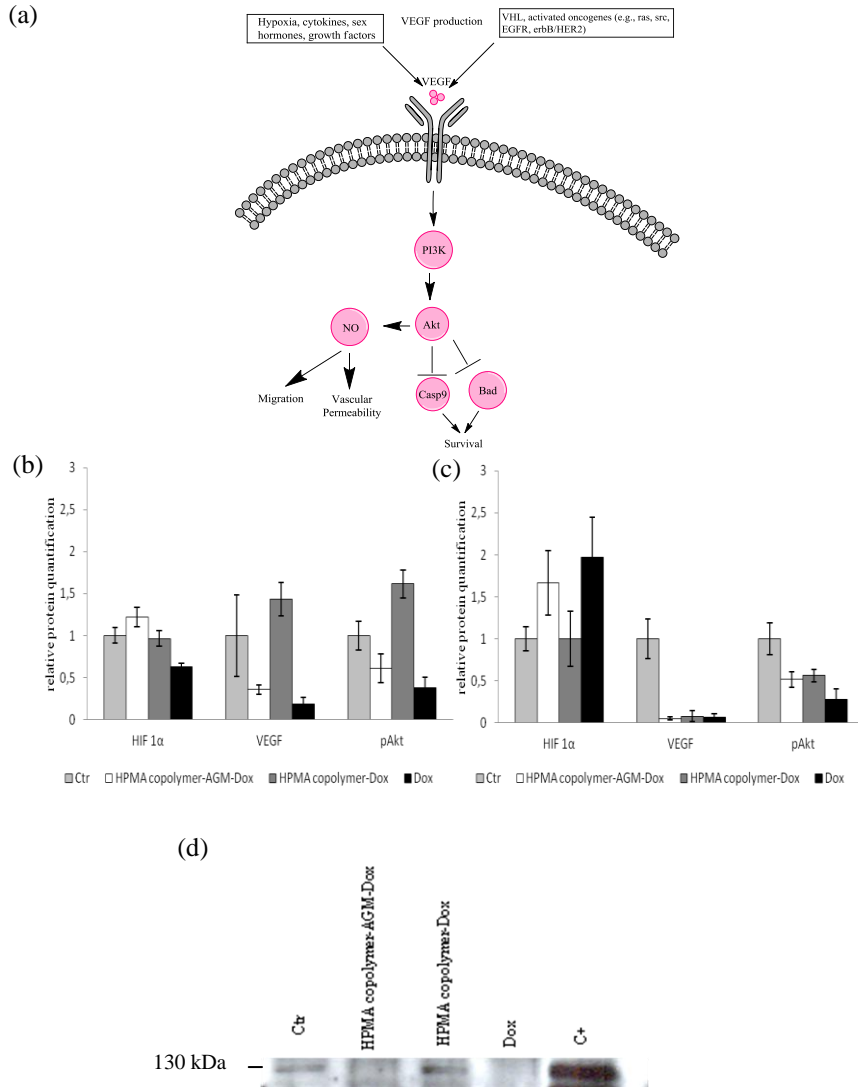
(a)

(b)

(c)

(d)

130 kDa —

Figure 5.6. Protein expression analysis of HIF-1α, VEGF and iNOS in 4T1 tumour tissue after 8 and 16 days treatment post-administration. Panel (a) shows the schematic diagram showing a possible mechanism of action with the target proteins involved in angiogenesis. Panel (b) and (c) show the protein quantification done by densitometry analysis protein expression showing the effect of different treatments;

(b) 8 days after the first injection and (c) 16 days after the first injection. β-Actin was included as a loading control. Panel (d) shows a representative Western blot of iNos protein. The experiment was performed with n = 4 animals per group for the 8 days and n = 6 for the 16 days. C+ is an extract of MCF7 cell used as positive control in our study. Mean values ± SEM.

Table.5.4.Statistical analysis data of protein expression involved in angiogenesis.

	HIF 1α 8d	HIF 1α 16d	VEGF 8d	VEGF 16d	pAkt 8d		pAkt 16d
P value	3	3	2	4	2	4	4
1	*	*	**	**	ns	ns	*
2	*	*	*	**	NA	*	*
3	NA	NA	**	**	**	*	*
4	*	*	NA	NA	ns	NA	*

1- HPMA copolymer-AGM-Dox conjugate, **2-** HPMA copolymer-Dox conjugate and **3-** Dox and **4-**Ctr. (n = 3). Significances calculated by one-way ANOVA. P*** < 0,001, P* *< 0,01, P* < 0,05, ns: non significance. Statistics with other combinations showed non significance. NA: non applicable.

Interestingly, two different behaviours were observed at 8 and 16 days. At 8 days after the first injection, a significant decrease in VEGF protein expression was observed only for free Dox and HPMA copolymer-AGM-Dox conjugate. A decrease in HIF-1α was only observed for Dox, however, the same protein expression profile of HIF-1α was obtained for pAkt. After 16 days, an inhibition of VEGF in all treatments was observed and confimed by pAkt showing the same expression profile. However, non expected protein expression modulation was obtained for HIF-1α, as none of the treatments achieved any effect. Unfortunately, due to the limitation of the iNOS antibody or its expresion levels in tissue, quantification of iNOS could not be performed although a clear trend was observed with iNOS inhibition levels by HPMA copolymer-AGM-Dox combination conjugate and free Dox in comparison to HPMA copolymer-Dox. More studies need to be carried out in order to evaluate the effects of these conpounds on migration and metastasis.

5.4. Discussion.

In order to better understand the molecular mechanisms responsible for antitumour drug synergism, first Bcl-2 expression was studied by western blot (in order to corroborate previously reported data) together with cell cycle analysis by flow cytometry in MCF7 Ca cells for HPMA conjugates and free Dox. Whereas a significant apoptosis was observed only for HPMA copolymer-Dox in comparison with the other compounds tested, a stop in G2/M phase for both conjugates was achieved in contrast to free Dox. Western blot analysis was also carried out to ratify these studies looking at proteins involved in cell cycle as well as cell death mechanism. However, due to the difficulty to achieve reproducible data in cells, a deeper analysis using tumour tissue from the 4T1 model activity experiment was instead performed. In this way it would be possible to correlate the activity graphs with the actual molecular mechanism responsible for antitumor activity as EPR-mediated targeted effects could be also taken into account.

Firstly, differences between both conjugates regarding possible cell death pathways were analysed at two different time points, 8 days after 1st injection (48 h after the last injection trying to keep the 72 h timeframe studied so far) and 16 days after 1st injection (end of the experiment). Whereas a mix mechanism of apoptosis and autophagy was observed at short-term for both conjugates, at long-term (16 days) only autophagy was observed with HPMA copolymer-AGM-Dox and an apoptotic death mechanism for HPMA copolymer-Dox conjugate. This fact was one of the major differences between both conjugates. Then, the effect of our conjugates in tumor proliferation and angiogenesis was also studied mainly focusing on VEGF expression. Two days after the last injection, and contrarily from the HPMA copolymer-Dox conjugate, a strong difference was obtained in the tumour angiogenesis pathways for the combination conjugate. Indeed HPMA copolymer-AGM-Dox conjugate triggered significant inhibition of VEGF mainly due to two phenomena 1) the oestrogen reduction induced by AGM (Kazi and Koos, 2007; Koss, 2010; Koos, 2011) and 2) the inhibition of p-Akt protein expression that triggered the down-regulation of VEGF (Pore et al., 2004). However, at the end of the experiment

(16 days after the first injection), a decrease of VEGF was observed with all treatments. This pharmacokinetic effect on VEGF inhibition could be explained first by differences observed in tumour accumulation, HPMA copolymer-AGM-Dox was accumulated faster in the tumour than HPMA copolymer-Dox conjugate although the accumulated Dox dose in the tumour is very similar. After tumour accumulation, drug release kinetics would also play a key role. As described by Vicent *et al.*, 2005, in the combination conjugate the presence of AGM induce dramatic changes in Dox release profile due to a different solution conformation of the conjugate as demonstrated by Small Angle Neutron Scattering (SANS) (Vicent et al., 2005). AGM was first released followed by an exponential Dox release up to 20% of drug in both cases after 5 h.

Importantly, together with the pk differences and as described before (chapter 1), AGM blocked the aromatase enzyme involved in oestrogen production. It has been described that oestrogen triggered VEGF expression and therefore a down-regulation in the oestrogen levels could induced a down-regulation on VEGF expression (Kazi and Koos, 2007; Kazi et al., 2009; Koss, 2010; Koss, 2011).

Based on VEGF modulation, cell migration and metastatic processes were evaluated in a first approach by means of iNOS expression. Unfortunately, due to the limitation of the iNOS antibody or its expresion levels in tissue, quantification of iNOS could not be performed. However a clear trend of iNOS expression inhibition was observed by HPMA copolymer-AGM-Dox combination conjugate and free Dox in comparison to HPMA copolymer-Dox. Therefore other experiments are currently perfomed to complete and confirm the effect of HPMA copolymer-AGM-Dox on cell migration and metastases.

Regarding the results obtained with free Dox, it is clear that the pharmacokinetics play an important role. Indeed it was described in literature that Dox was evaluated with single dose (Kimberley et al., 2013) or other schedule injection (Woessner et al., 2000). However in our experiment, Dox was injected at 3 mg/kg each 3 days. Based on the 4T1 activity model, Dox showed significant lower efficacy in comparison to the HPMA conjugates. However,

when tumour tissue protein expression was evaluated, greater levels of cell death markers were observed at short-term in comparison with the conjugates, this levels significantly decreased at long-term. Dox is accumulated rapidly inside the tumour but not retained (chapter 4). On the contrary, Dox effect on angiogenesis was conserved even at the end of the experiment.

As conclusion it could be said that, the antitumour activity observed for both conjugates in comparison with Dox was mainly relating to the pharmacokinetic and the capacity of the conjugate to accumulate an get retained in the tumour (EPR effect) (Maeda, 2001; Maeda, 2010). When both conjugates are compared there are also pharmacokinetic parameters influencing their different antitumour behaviour. However, we believe that the differences observed in cell death mechanisms and VEGF modulation are the key factors inducing a greater antitumour effect for the combination conjugate.

5.5. Bibliography.

Chen, N. and Karantza, V. (2011). "Autophagy as a therapeutic target in cancer." Cancer Biol Ther 11(2): 157-168.

Curry JM, Eubank TD, Roberts RD, Wang Y, Pore N, Maity A and Marsh CB. (2008) "M-CSF signals through the MAPK/ERK pathway via Sp1 to induce VEGF production and induces angiogenesis in vivo." Plosone 3(10):e3405.

Douglas, R.G. and Kroemer, G. (2005). "Pharmacological manipulation of cell death: clinical applications in sight?" The J. Clin. Invest. 115(10): 2610-2617.

Dueñas-Gonzalez, A., Isales, C.M., del Mar Abad-Hernandez, M., Gonzalez-Sarmiento, R., Sangueza, O., Rodriguez-Commes, J. (1997). "Expression of inducible nitric oxide synthase in breast cancer correlates with metastatic disease." Mod Pathol 10(7): 645-649.

Ellis, L., Hammers, H., and Pili, R. (2009). "Targeting tumor angiogenesis with histone deacetylase inhibitors." Cancer Lett 280(2): 145-153.

Esclatine, A., Chaumorcel, M., and Codogno, P. (2009). "Macroautophagy signaling and regulation." Curr Top Microbiol Immunol 335: 33-70.

Greco, F., Vicent, M.J., Gee, S., Jones, A.T., Gee, J., Nicholson, R.I., and Duncan, R. (2007). "Investigating the mechanism of enhanced cytotoxicity of HPMA copolymer-Dox-AGM in breast cancer cells." J Control Release 117(1): 28-39.

Hoyer-Hansen, M., Bastholm, L., Szyniarowski, P., Campanella, M., Szabadkai, G., Farkas, T., Bianchi, K., Fehrenbacher, N., Elling, F., Rizzuto, R., Mathiasen, I.S., and Jäättelä, M. (2007). "Control of macroautophagy by calcium, calmodulin-dependent kinase kinase-beta, and Bcl-2." Mol Cell 25(2): 193-205.

Juenemann, K. and Reits, E. A. (2012). "Alternative macroautophagic pathways." Int J Cell Biol 2012: 189794.

Kaufmann, S. H. and Earnshaw, W. C. (2000). "Induction of apoptosis by cancer chemotherapy." Exp Cell Res 256(1): 42-49.

Kazi, A.A., Molitoris, K.H. and Koos, R.D. (2009) "Estrogen rapidly activates the PI3K/AKT pathway and hypoxia-inducible factor 1 and induces vascular endothelial growth factor A expression in luminal epithelial cells of the rat uterus." Biol Reprod. 81(2):378-387.

Kazi, A. A. and Koos, R. D. (2007). "Estrogen-induced activation of hypoxia-inducible factor-1alpha, vascular endothelial growth factor expression, and edema in the uterus are mediated by the phosphatidylinositol 3-kinase/Akt pathway." Endocrinology 148(5): 2363-2374.

Kondo, Y., Kanzawa, T., Sawaya, R., and Kondo, S. (2005). "The role of autophagy in cancer development and response to therapy." Nat Rev Cancer 5(9): 726-734.

Kondo, Y. and Kondo, S. (2006). "Autophagy and cancer therapy." Autophagy 2(2): 85-90.

Koos, R.D. (2010). "HIF-1's role in estrogen-induced VEGF expression : Implications for both normal and pathological cell proliferation." Bio of reprod. 83: 199.

Koos R.D. (2011). "Minireview: Putting physiology back into estrogens' mechanism of action." Endocrinology. 152(12):4481-8.

Laginha K.M., Verwoert S., Charrois G.J., and Allen T.M. (2005) "Determination of doxorubicin levels in whole tumor and tumor nuclei in murine breast cancer tumors." Clin. Cancer Res. 11(19):6944-6949.

Levine, B., Sinha, S., and Kroemer, G. (2008). "Bcl-2 family members: dual regulators of apoptosis and autophagy." Autophagy 4(5): 600-606.

Lin, N.Y., Beyer, C., Gießl, A., Kireva, T., Scholtysek, C., Uderhardt, S., Munoz, L.E., Dees, C., Distler, A., Wirtz, S., Krönke, G., Spencer, B., Distler, O., Schett, G., and Distler, J.H. (2012). "Autophagy regulates TNFalpha-mediated joint destruction in experimental arthritis." Ann Rheum Dis.

Maeda, H. (2001). "The enhanced permeability and retention (EPR) effect in tumor vasculature: the key role of tumor-selective macromolecular drug targeting." Adv Enzyme Regul 41: 189-207.

Maeda, H. (2010). "Tumor-selective delivery of macromolecular drugs via the EPR effect: background and future prospects." Bioconjug Chem 21(5): 797-802.

Malugin, A., Kopecková, P., and Kopecek, J. (2007). "Liberation of doxorubicin from HPMA copolymer conjugate is essential for the induction of cell cycle arrest and nuclear fragmentation in ovarian carcinoma cells." J Control Release 124(1-2): 6-10.

Minko, T., Kopecková, P., and Kopecek, J. (2001). "Preliminary evaluation of caspases-dependent apoptosis signaling pathways of free and HPMA copolymer-bound doxorubicin in human ovarian carcinoma cells." J Control Release 71(3): 227-237.

Mizushima, N. And Yoshimori, T. (2007). "How to interpret LC3 immunoblotting." Autophagy 3(6): 542-545.

Noda, T., Fujita, N., and Yoshimori, T. (2009). "The late stages of autophagy: how does the end begin?" Cell Death Differ 16(7): 984-990.

Pore N, Jiang Z, Gupta A, Cerniglia G, Kao GD and Maity A. (2006) "EGFR tyrosine kinase inhibitors decrease VEGF expression by both hypoxia-inducible factor (HIF)-1-independent and HIF-1-dependent mechanisms." Cancer Res. 66(6):3197-3204.

Pore N, Liu S, Shu HK, Li B, Haas-Kogan D, Stokoe D, Milanini-Mongiat J, Pages G, O'Rourke DM, Bernhard E and Maity A. (2004) "Sp1 is involved in Akt-mediated induction of VEGF expression through an HIF-1-independent mechanism." Mol Biol Cell. 15(11):4841-4853.

Schmelzle, T. and Hall M.N. (2000). "TOR, a central controller of cell growth." Cell 103(2): 253-262.

Semenza, G. L. (2003). "Targeting HIF-1 for cancer therapy." Nat Rev Cancer 3(10): 721-732.

Semenza, G. L. (2012). "Hypoxia-inducible factors: mediators of cancer progression and targets for cancer therapy." Trends Pharmacol Sci 33(4): 207-214.

Singh, S. and Gupta, A. K. (2011). "Nitric oxide: role in tumour biology and iNOS/NO-based anticancer therapies." Cancer Chemother Pharmacol 67(6): 1211-1224.

Tendler, D.S., Bao, C., Wang, T., Huang, E.L., Ratovitski, E.A., Pardoll, D.A., and Lowenstein, C.J. (2001). "Intersection of interferon and hypoxia signal transduction pathways in nitric oxide-induced tumor apoptosis." Cancer Res 61(9): 3682-3688.

Thomsen, L.L., Lawton, F.G., Knowles, R.G., Beesley, J.E., Riveros-Moreno, V., and Moncada, S. (1994). "Nitric oxide synthase activity in human gynecological cancer." Cancer Res 54(5): 1352-1354.

Vicent, M.J., Greco, F., Nicholson, R.I., Paul, A., Griffiths, P.C., and Duncan, R. (2005). "Polymer therapeutics designed for a combination therapy of hormone-dependent cancer." Angew Chem Int Ed Engl 44(26): 4061-4066.

Woessner, R., An, Z., Li, W., Hoffman, R.M., Dix, R. and Bitonti, A., (2000), "Comparison of three approaches to doxorubicin therapy: free Doxorubicin, Liposomal doxorubicin and β-glucuronidase-actived prodrug (HMR 1826)". 20(4): 2289-2296.

Chapter 6. PGA-based combination conjugates. Optimisation of PGA-X-AGM-Y-Dox conjugates.

6.1. Introduction.

As already described in the introduction section, in an adequate design of a polymer-drug conjugate, the selection of the polymer carrier is a key factor. The polymer has to be non-toxic, non immunogenic, water-soluble to allow i.v. administration and ideally multivalent to allow high drug loading. The most widespread polymers transferred to the clinic in the last 20 years have been the non-biodegradable HPMA copolymer, PEG and the biodegradable polyglutamic acid (PGA) (Deladriere et al., 2011; Duncan and Gaspar, 2011). Biopersistent carriers (PEG, HPMA) present disadvantages if chronic parenteral administration and/or high doses are required as there is the potential to generate lysosomal storage disease syndrome. Preclinical evidence of intracellular vacuolation with certain PEG-protein conjugates is raising awareness of the potential advantage of biodegradable polymers regarding safety benefit apart from the possibility to use higher molecular weight (Mw) carriers allowing PK optimisation (Barz et al., 2011). Taking this into account and aiming to move a step further with our polymer-based combination strategy, the aim in this study was to substitute the non-biodegradable HPMA by the multivalent, biodegradable PGA. Due to its intrinsic characteristics, PGA presents a more favourable pharmacological profile as already demonstrated in the clinics with Opaxio[TM] (PGA-Paclitaxel conjugate, Cell Therapeutics Inc.) in phase III clinical trial and recently designated as orphan drug in combination with radiotherapy for glioblastoma (Singer et al., 2003; Oldham et al., 2006; http://www.celltherapeutics.com/pdf/OPAXIO_facts-4pg.pdf.2008).

For this purpose, a family of PGA-AGM-Dox conjugates was synthesised to be directly compared with the previously synthesised HPMA copolymer-AGM-Dox model conjugate, investigating the maintenance of the synergistic effect. Moreover, as drug release kinetics is thought to be a possible reason of these phenomena, we proposed to evaluate its influence on cell cytotoxicity.

The first objective was to confirm that AGM and Dox was in fact a synergistic drug combination independently of the polymer carrier, therefore, we aimed to reproduce at least the same *in vivo* results obtained with HPMA copolymer-AGM-Dox conjugate in the 4T1 model. Secondly, by means of PGA carrier we

would like to demonstrate the possible advantages provided by the use of a multivalent, biodegradable carrier. The development of this study was divided in two phases, firstly, linker optimisation for PGA-AGM and PGA-Dox families were performed separately. Drug release profile studies and cell toxicity were carried out with the single conjugates to systematically determine the blocks to conform theoretically the best PGA-AGM-Dox combination conjugate.

For a lysosomotropic drug delivery two types of linkers could be developed, (i) a pH labile linker, or (ii) an enzymatic sensitive linker. Following the same strategy used for HPMA copolymer-AGM-Dox, the linker optimisation was first based on an enzymatic cleavage (*i.e.* -G-, -GG-, no linker). The peptidic linkers were bound to the drug through an amide bond.

In this chapter, it is reported the synthesis, characterisation and biological evaluation of the families PGA-X-AGM, PGA-Y-Dox and PGA-X-AGM-Y-Dox. The appropriate linkers have been selected from the kinetics of drug release in presence of cathepsin B together with the cell viability data gained against MCF7 Ca cells. After the selection of the best candidates from *in vitro* cytotoxicity assays, the evaluation of their antitumour activity was also performed in the 4T1 breast cancer murine model.

6.2. Synthesis and characterisation of PGA-X-AGM.

6.2.1. Synthesis of X-AGM.

The first linker used was Glycine (-G-) as mono- and dipeptide, as it is simple and has previously demonstrated its value as cathepsin B labile sequence with other hydrophobic drugs (Vicent and Pérez-Payá, 2006). The 9-fluorenyl methyl-oxy carbonyl (Fmoc)-based peptide synthesis approach was followed to avoid any side reactions. G-AGM synthesis was finalised by a deprotection step with piperidine as described in figure 6.1. all intermediates as well as the final product were characterised by NMR as shown in Figure 6.2.
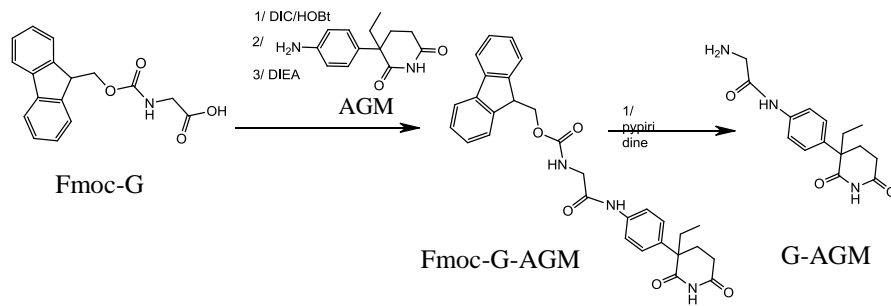
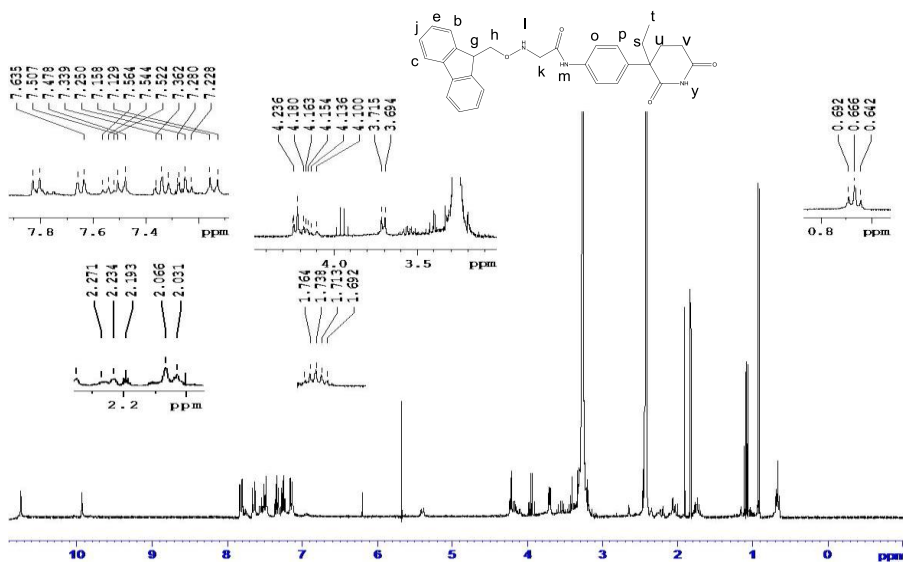Figure 6.1. Synthetic scheme of the G-AGM reaction.

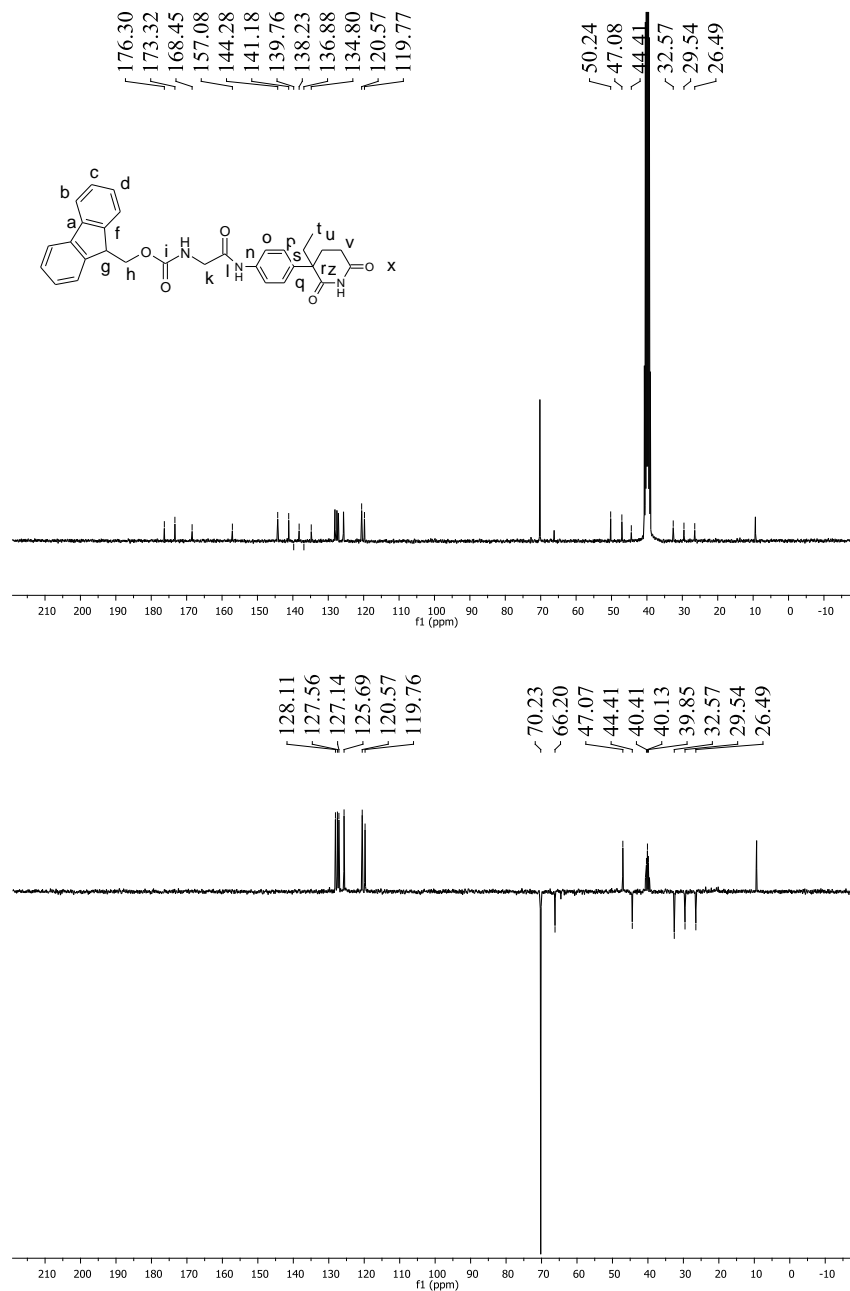Figure 6.2. ^{1}H-NMR spectrum of Fmoc-G-AGM, 300Hz, DMSO.

Figure 6.3. ^{13}C and DEPT$_{135}$ NMR spectrum of Fmoc-G-AGM, 300Hz, d$_6$-DMSO.

^{1}H and ^{13}C/ DEPT$_{135}$ NMR analysis confirmed the identity of Fmoc-G-AGM. A shift from 3 ppm to 8 ppm was observed corresponding to the amide bond formation. Furthermore, AGM aromatic protons showed greater chemical shifts in Fmoc-G-AGM than in the parent AGM due to the electron delocalisation induced by the Fmoc group (from 7 to 7,5 ppm).
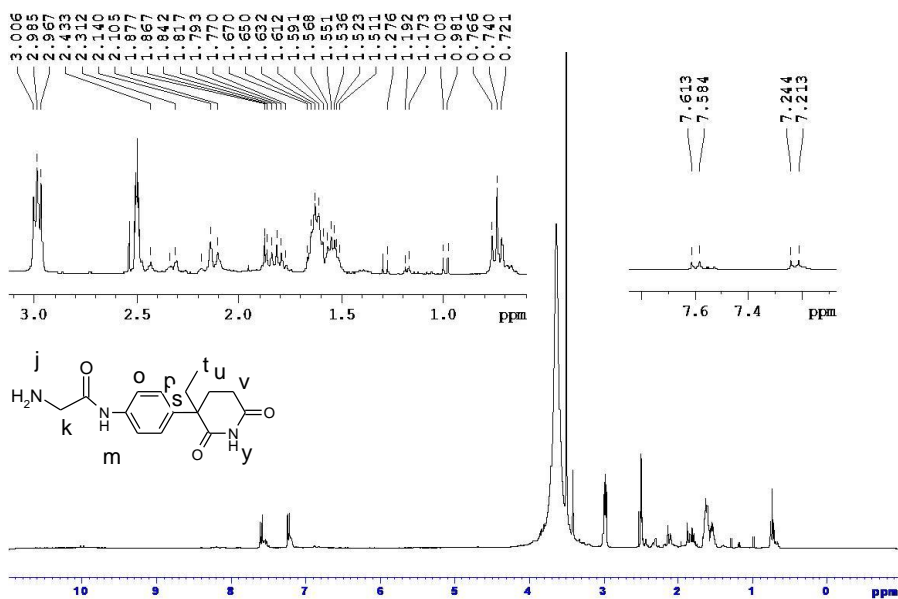

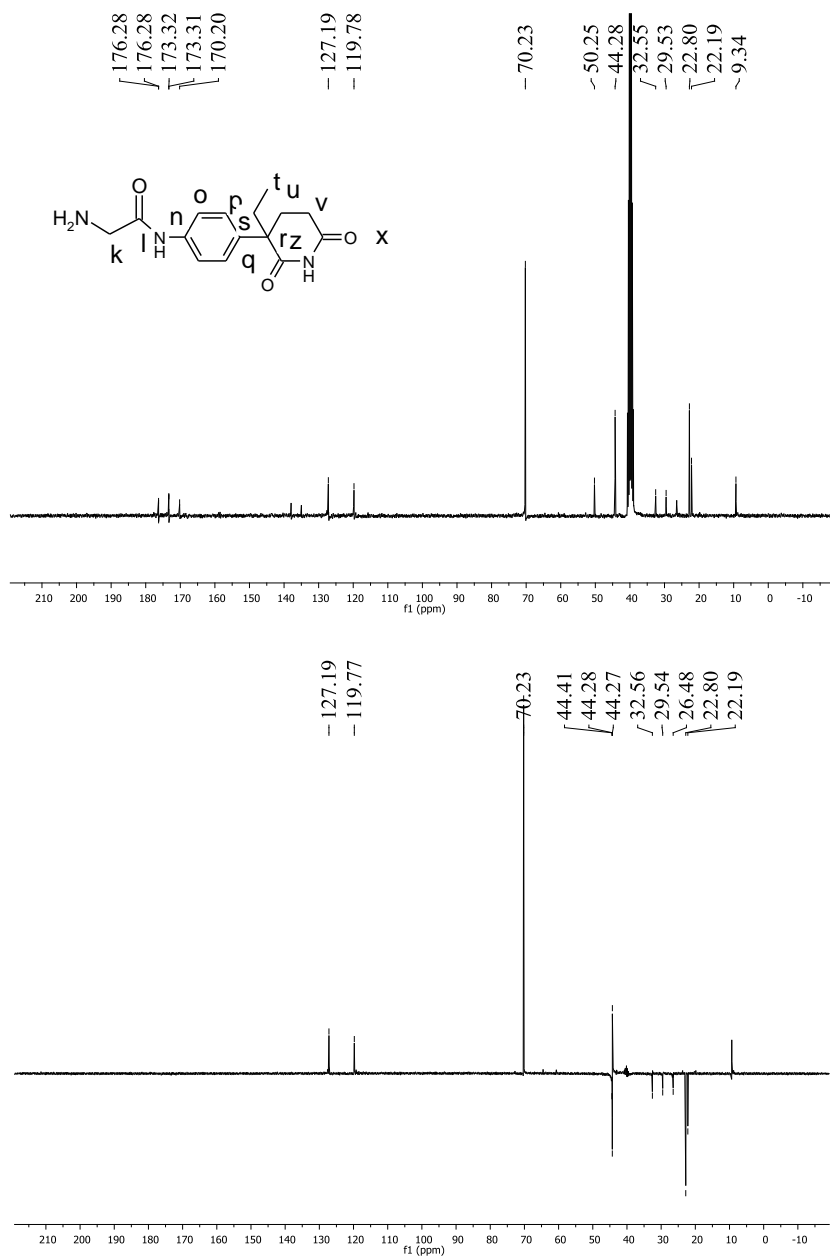Figure 6.4. ^{1}H-NMR spectrum of G-AGM, 300Hz, d$_6$-DMSO.

Figure 6.5. ^{13}C and DEPT$_{135}$ NMR spectrum of G-AGM, 300Hz, d$_6$-DMSO.

As mentioned above, Fmoc deprotection was carried out with piperidine and product identity and purity was also confirmed by ^{1}H-NMR by the disappearance of the Fmoc aromatic peaks at 7, 7,8 and 8 ppm. The aromatic ^{1}H corresponding to AGM remained (at 7,2 and 7,6 ppm) (figure 6.5.).

The same synthetic protocol was used to synthesise G-G-AGM. It is important to note that in this case, a previous protection step for G-G with the Fmoc moiety had to be carried out.
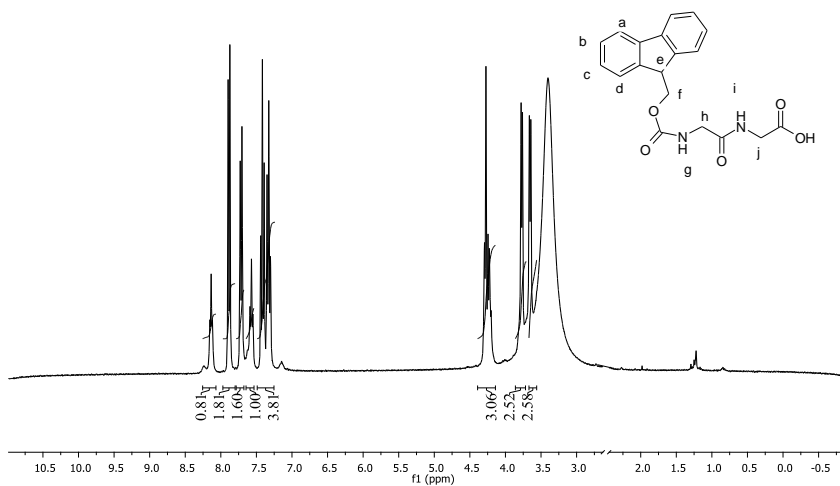

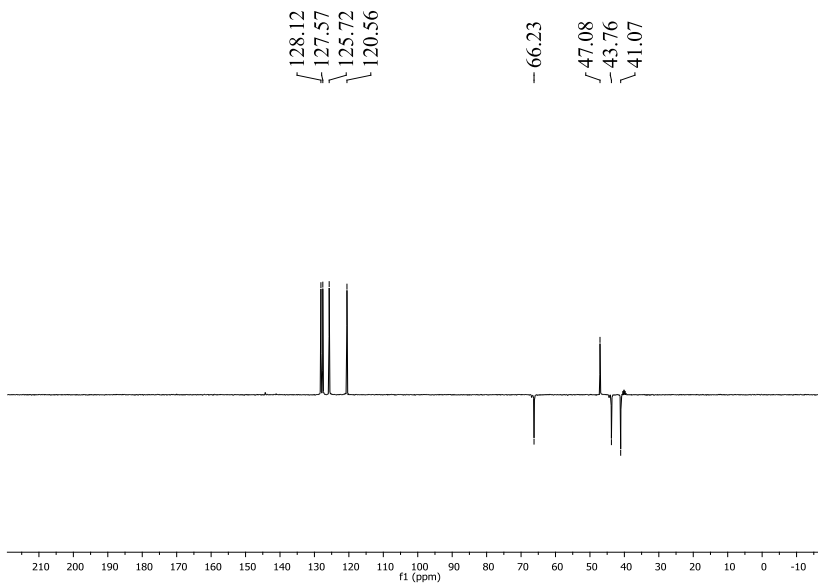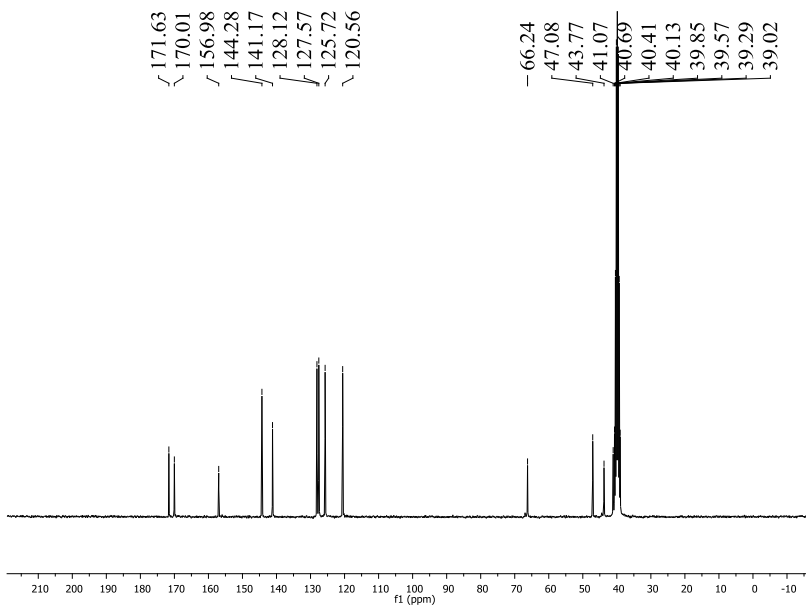Figure 6.6. ^{1}H-NMR spectrum of Fmoc-GG, 300Hz, d_6-DMSO.

Figure 6.7. ^{13}C and DEPT $_{135}$ NMR spectrum of Fmoc-GG, 300Hz, d$_6$-DMSO.

Based on ^{1}H-NMR analysis, the protection of GG with Fmoc was successfully achieved with the appearance of the Fmoc aromatic peak (7,2, 7,3, 7,7 and 7,8 ppm) in good relation with the Gly -CH$_2$- corresponding peak (3,5 and 3,7 ppm). Then, the synthesis of GG-AGM followed the procedure as described above.

To conclude, two AGM derivatives bearing a peptidic chain were successfully synthesised, purified and characterised, G-AGM and GG-AGM. Then, their polymer conjugations to PGA were successfully performed as described in the next section.

6.2.2. Synthesis of PGA-X-AGM.

The synthetic strategy used for PGA-X-AGM family was based on carbodiimide coupling reactions. The mechanism of the reaction was divided in three different steps. First, the activation of PGA carboxyl group with N,N'-diisopropylcarbodiimide (DIC) and the stabilisation of the complex with hydroxybenzotriazole (HOBt) to favour the nucleophilic substitution reaction with amino-terminated X-AGM derivative. Reaction pH was adjusted to 8 with di-isopropyl ethylamine (DIEA) (figure 5.7. and 5.8.).
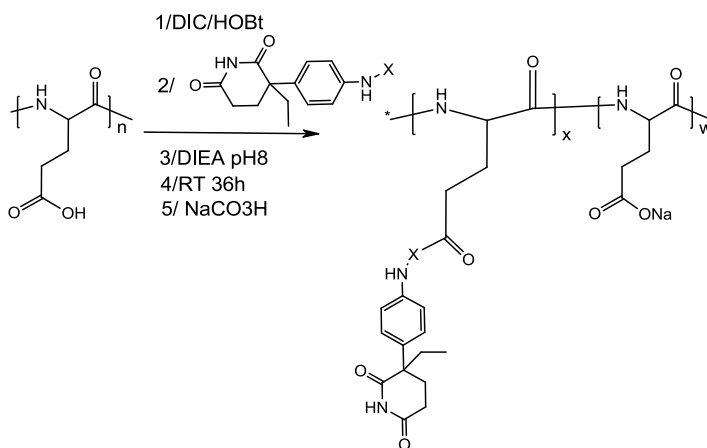

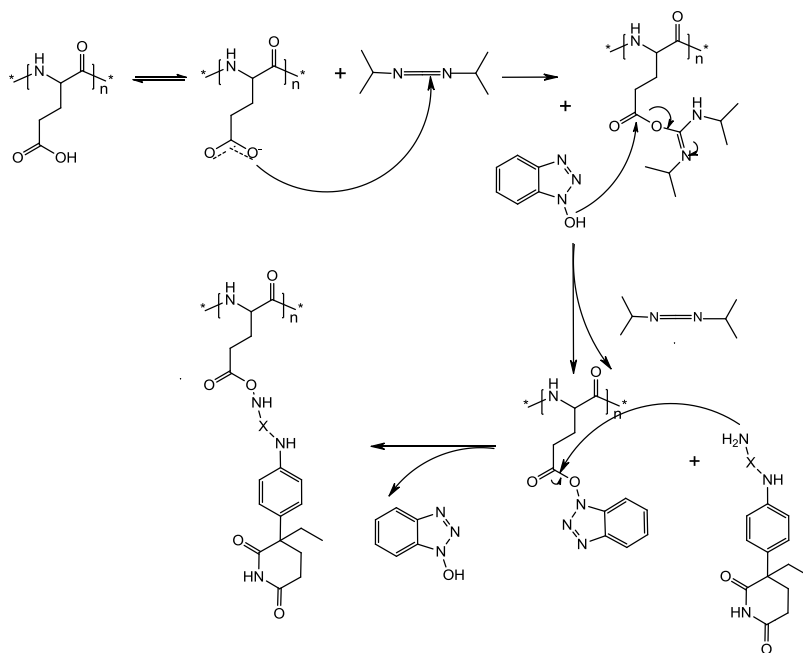Figure 6.7. Synthetic scheme followed to obtain PGA-X-AGM conjugates.

Figure 6.8. Carbodiimide activation mechanism taking place during PGA-X-AGM synthesis.

Once the conjugate was obtained, purification and full characterisation was performed with the determination of the total drug loading and the possible free drug still entrapped inside the conjugate after purification.

PGA-AGM conjugate was achieved by direct conjugation of AGM to the PGA mainchain. AGM bears an aromatic amine group with poor reactivity due to the electronic delocalisation. The activation of the –COOH with DIC/ HOBt did not allow an appropriate drug loading, therefore, a previous PGA activation strategy by means of succinimide (NHS) was used before AGM conjugation and its mechanism of activation is described in figure 6.9.
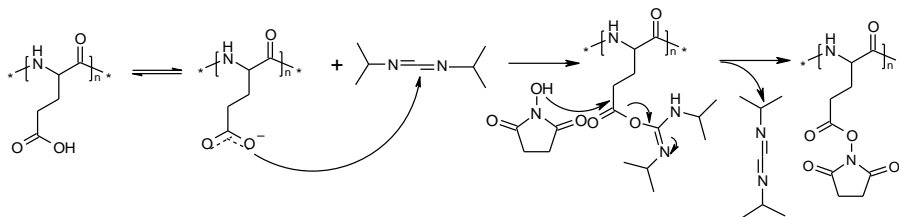
Figure 6.9. Activation of PGA using N-hydroxy succinimide to obtain PGA-OSuc.

In order to limit the side reactions during AGM conjugation, PGA-OSuc was previously purified and the percentage of activated carboxylic groups determined by ^{1}H-NMR.
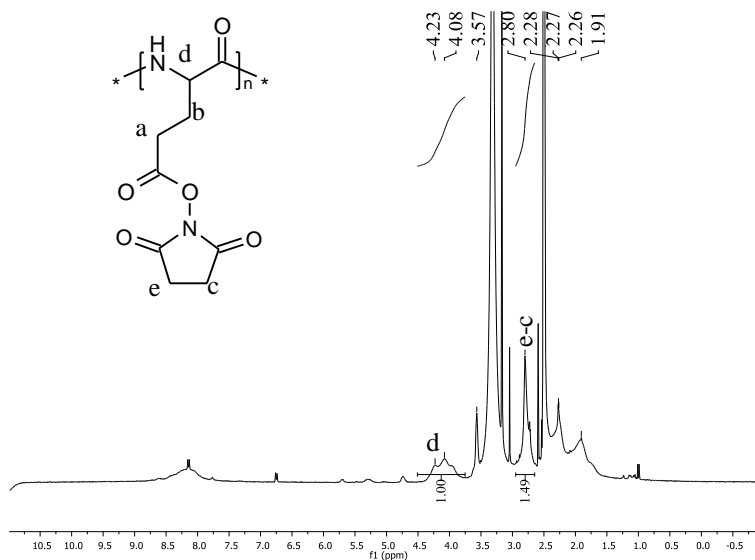

Figure 6.10. Determination of PGA-OSuc activation rate by ^{1}H-NMR.

The succinimide activation rate was determined by the relation with the e-c integral peak and the theoretical protons (x4) corresponding to 100% activation.

$$\text{Activation rate} = \frac{\text{e-c integral peak}}{\text{4 protons}} \times 100$$

155

The activation rate in this case was 37%. NHS-activated PGA was then allowed to react with AGM in the presence of catalytic amounts of DMAP during 36 h at RT in order to achieve PGA-AGM conjugate as described in figure 6.11.
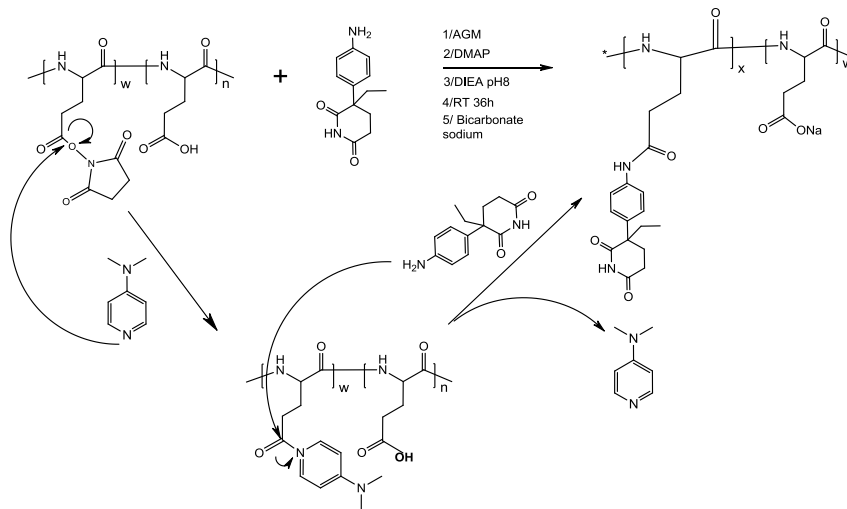
Figure 6.11. Reaction mechanism followed in NHS mediated PGA-AGM conjugate synthesis.

The conjugate reaction conditions were optimised regarding temperature and concentration. The conjugate was then purified as described in chapter 3.

6.3. Synthesis and characterisation of the PGA-Y-Dox family.

6.3.1. Synthesis of Y-Dox.

The strategy used to synthesise Y-Dox was the same as described before for the protected group. Indeed Carboxybenzyl (Cbz, Z) was selected in this case instead of Fmoc- as amino-protecting groups allowed deprotection by hydrogenation avoiding any basic/acid media during the synthesis in order to protect the Dox structure.
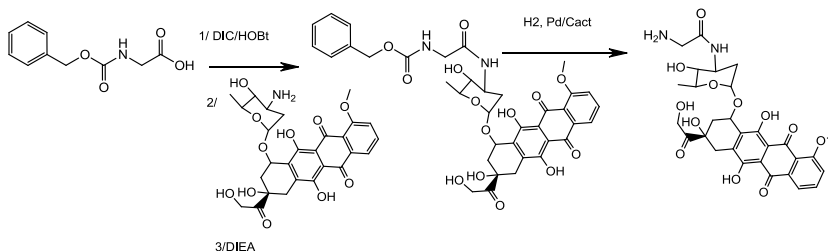
Figure 6.12. Synthetic scheme for the obtention of G-Dox.

The GG-Dox synthesis followed the same strategy as shown above for G-Dox.

6.3.2. Synthesis of PGA-Y-Dox family.

As in the case of X-AGM conjugates, PGA-Y-Dox conjugates were achieved by a carbodiimide-mediated coupling of a previously synthesised amino-termiated –Y-Dox derivative.

Figure 6.13. Synthetic approach followed with PGA-Y-Dox conjugate.

Due to the instability of Dox in basic media at RT or even in acid environment at high temperatures (figure 6.13.), the synthetic approach used for Dox derivatives (Y-Dox) was different from that reported for X-AGM. The following side-reactions occurred deactivating Dox.
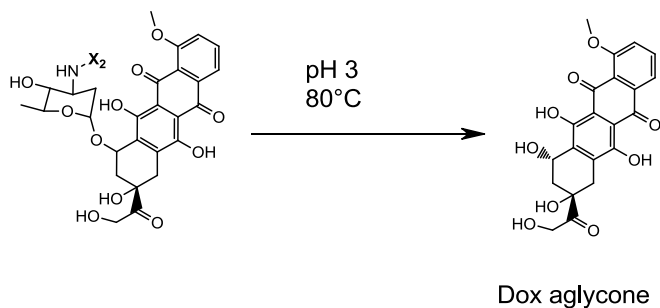
Figure 6.14. Dox hydrolysis under acidic pH.

6.4. Synthesis of PGA-X-AGM-Y-Dox combination conjugates.

The synthesis of X-AGM and Y-Dox described above were used to synthesise the combination conjugates.
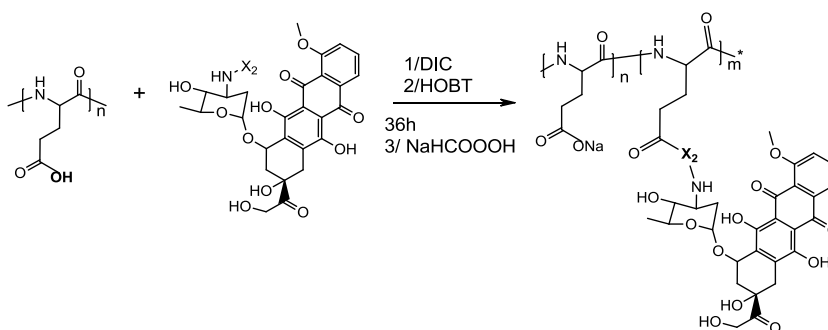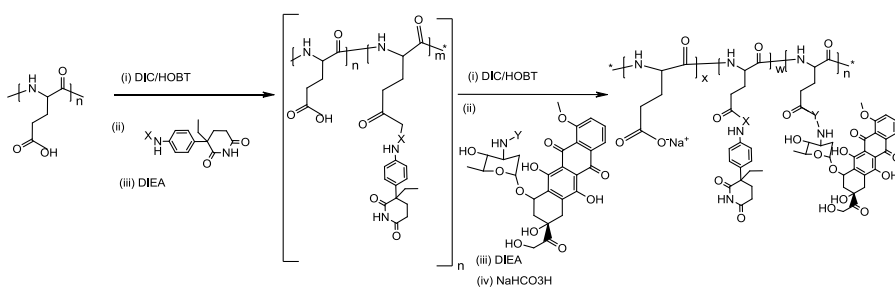

Figure 6.15. Synthetic scheme used for PGA-X-AGM-Y-Dox combination conjugate.

The PGA-X-AGM-Y-Dox synthetic approach was based on subsequent carbodiimine couplings similar to those described above (figure 6.8.).

6.5. Physico-chemical characterisation of the synthesised conjugates.

PGA-X-AGM, PGA-Y-Dox and PGA-X-AGM-Y-Dox families were design in order to have a total drug loading around 5 mol% to allow direct comparison with the model HPMA-AGM-Dox combination conjugate. To fully characterise our polymer-drug conjugates several parameters were determined, including: (i) total drug loading, (ii) free drug content, (iii) Mw and polydispersity (Mw/Mn)

158

and (iv) conjugate solution conformation (size and shape) by small angle neutron scattering (SANS). The results obtained are summarised in the following table.

Table 6.1. Characteristics of PGA-X-AGM, PGA-Y-Dox and PGA-AGM-Dox conjugates. P (PGA), A (AGM), D (Dox), G (Glycine).

	Yield (%)	Total drug[a] (%w/w)		Free drug [b] (%w/w of total drug)		Mw [c] (Da)	PDI[d]
Conjugates		A	D	A	D		
P	-	-	-	-	-	18 000	1,2
P-A	68	6,8	-	1.12	-	18 200	1,2
P-G-A	48	9,1	-	0,92	-	18 500	1,2
P-GG-A	62	10,8	-	0,92	-	22 200	1,2
P-D	68	-	14,2		0,14	19 000	1,2
P-GG-D	50	-	2,5		0,24	20 600	1,2
P-A-D	68	8,1	15,8	0,89	0,18	23 104	1,2
P-G-A-D	65	7,8	20,1	1,14	0,32	23 510	1,2
P-A-GG-D	70	7,6	4,2	0,82	0,36	23 960	1,2
P-GG-A-D	64	7,6	18,9	0,87	0,22	23 958	1,2
P-G-A-GG-D	65	7,1	3,1	0,78	0,28	26 135	1,2

a. Total drug and free drug content determined by HPLC expressed in [%w/w]. b. Free drug content expressed as a percentage of total drug [%w/w total drug]. c. Mw determinated by Gel permeation chromatography (GPC) expressed in Da. d. Polydispersity (PDI) determined by GPC.

The total drug loading was determined by HPLC after a hydrolytic protocol as described above (Chapter 3). In the clinical setting, the control on any residual impurity in synthesised polymer conjugates is a critical issue that could compromise its safety. Therefore, any traces of residual solvent or entrapped free drug are parameters to carefully control in order to ensure an effective and reproducible therapy. It has been reported that free drug content should be always less than 2 wt% of the total drug loading (Gaspar and Duncan, 2009). When conjugating potent drugs such as Dox, free drug content is a key parameter to control as the different pharmacokinetics (diffusion vs. endocystosis) could mask the real benefits obtained upon conjugation.

As it can be seen in table 3.2., free drug content was lower than 0,5 wt% in all conjugates synthesised.

6.5.1. Conjugate characterisation by GPC.

Other important features in polymer conjugate design is the control on polymer molecular weight (Mw) and polydispersity index (PDI), important challenges when synthesising polymeric carriers. A high PDI in a conjugate could be the reason of a lower therapeutic efficacy due to an un-controlled pharmacokinetics. For this reason, in the Polymer Therapeutics laboratory a versatile and simple methodology for the preparation of well-defined polyglutamate nanocarriers has been recently reported (Conejos-Sánchez et al., 2013). For the first time ammonium salts with non-nucleophilic tetrafluoroborate anions has used as initiators for the ring opening polymerisation of α-N-carboxyanhydrides (NCAs) allowing a large scale polyglutamate synthesis with defined Mw (up to 800 units), low PDI (< 1,2), controlled chain end functionality, adequate stereoselectivity and absence of any toxic impurity required for biomedical applications.

Applying this novel methodology a well-defined PGA of Mw = 17 000Da and PDI = 1,2 was achieved and used in the present work as our selected polymeric carrier. Although only post-polymerisation modifications have been carried out here, Mw and PDI of the final conjugates were also confirmed by GPC to ensure conjugate integrity. A Viscotek[TDA] triple detection system was used bearing a

Refractive Index (RI), Light Scattering (LALS and MALS) and Viscosimetry. As an example, a spectrum of PGA-GG-AGM is presented below (figure 6.16.). As expected, in all cases the conjugation of the drug(s) did not dramatically change the PDI of the starting PGA carrier.

Finally, it is important to consider that polymer conjugate composition clearly influence the final solution conformation in terms of size, shape, and the dynamic changes that occur in response to physiological microenvironment. Therefore, not only conjugate identity but also solution conformation are key parameters to determine. In the laboratory we pioneered the use of advanced physico-chemical techniques, such as Small Angel Neutron Scattering (SANS) to explore conjugate solution conformation (Vicent et al, 2005; Giménez et al., 2012). In this work, SANS together with circular dichroism (CD) have been also used to determine solution conformation of the different conjugates synthesised and to try to understand/identify predictors that could help in polyglutamate-based combination therapy design.
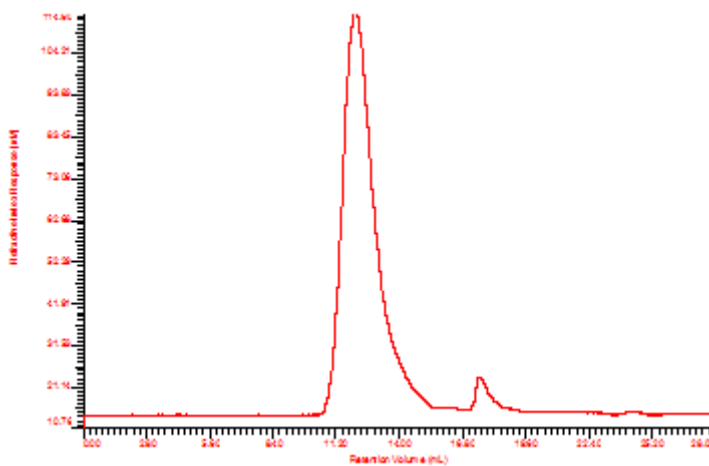
Figure 6.16. Refractive Index (RI) of PGA-GG-AGM GPC spectrum.

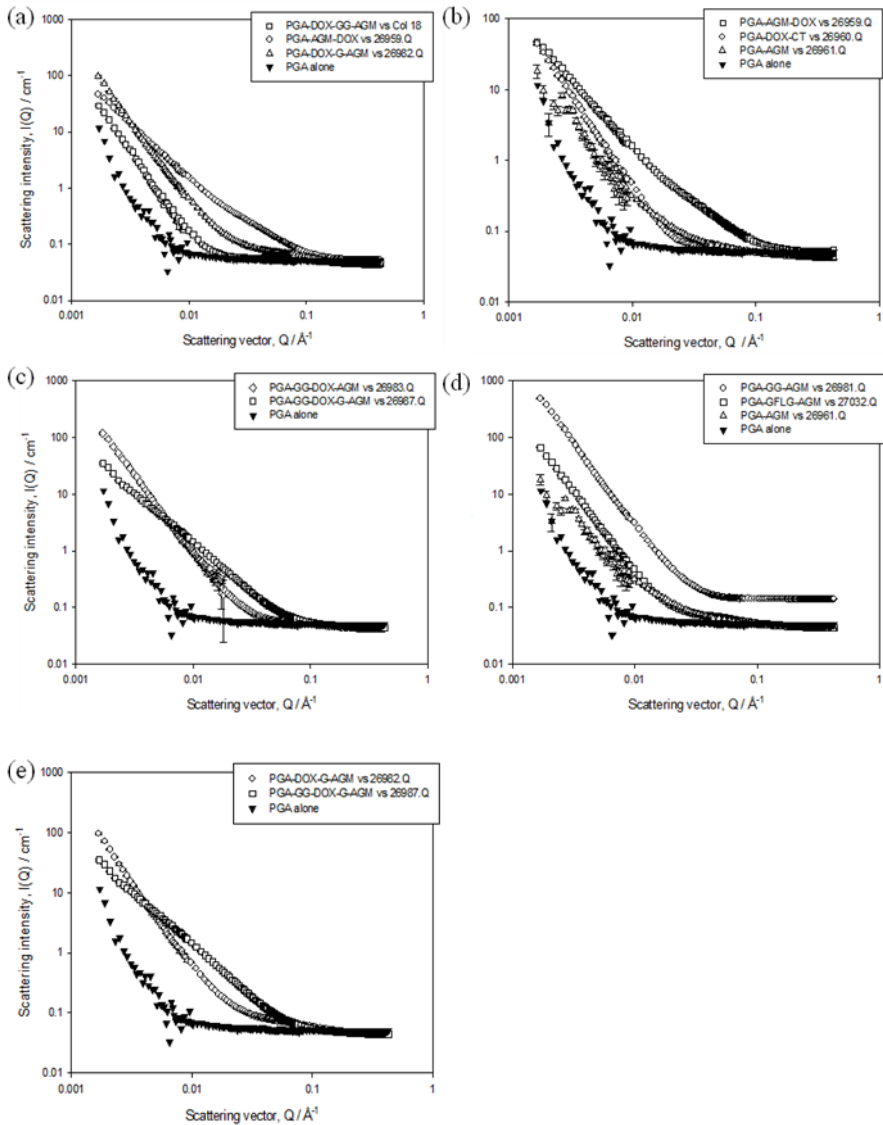## 6.5.2. Characterisation of the conjugate by SANS.

Figure 6.17. SANS curve effect of the drug conjugation on the PGA size and shape. Panel (a-c) show the effect of the AGM Linker with Dox on PGA. Panel (b) shows the effect of the drug combination on PGA. Panel (d) shows the effect of AGM linker on the PGA. Effect of Dox linker on the combination therapy shape and size

when the linker chosen for AGM was –G-. Panel (e) shows the effect of Dox linker on PGA shape and size when AGM was linked through –G-.

The final determination of the size and the shape has not been achieved yet as difficult mathematical calculations are required. These studies are performed in collaboration with Dr Paul at Cardiff University and the calculation of PGA based conjugate came to be new and more complex than expected due to different conformational arrangements observed. Therefore, more time would be needed to achieve the concrete size and shape of our polyglutamates. However, comparing the shape and the slope of the different conjugate curves, some comparisons and the first conclusions could be already drawn. Based on panel (d) comparisons, it could be clearly seen that the AGM linker had an influence on the conjugate conformation and on the PGA conformation. Also with the graphic (a) and (c), it was clearly demonstrated that the AGM linker changed drastically the conformation of the conjugate when Dox was either directly linked or through a –GG- linker. However, based on the panel (d) and only regarding to the single AGM conjugate, it was demonstrated that AGM linker had no strong effect on the PGA conjugate nevertheless a change was achieved in comparison to PGA conformation. Moreover based on panel (b) observations, it could be said that the most important change on the scatter curves was observed when both drugs were linked to the PGA. Therefore, Dox played an important role on the conformational changes maybe due to a strong π-π staking effect. Nevertheless, in combination with AGM, PGA conformation changes are induced from both drugs as observed in panel (b). These results suggest that, each drug alone had an effect on the PGA conformation but this effect clearly becomes much stronger when both drugs are conjugated together in the same polymeric backbone.

Summarising, data from SANS experiments demonstrated that the combination of both drugs in the same PGA carrier induced a much stronger effect on its solution conformation than the single counterparts. The influence of Dox on conjugate solution conformation is much stronger than that triggered by AGM due to its more hydrophobic and planar structure. It is expected that changes in

conjugate solution conformation would influence conjugate therapeutic output (see next section for detailed cell and *in vivo* data).

6.6. Linker evaluation and drug release kinetics.

In order to evaluate the linker, a simulation of the drug release as occurred in lysosomes was performed. Polymer drug conjugates were incubated with the lysosomal enzyme cathepsin B up to 1 week. The kinetics of drug release was monitored by HPLC and the polymer conjugate degradation followed by the % Mw loss as determined by GPC (figure. 6.18. and 6.19.).

6.6.1. Kinetics of drug release of single conjugates and identification of the main metabolites.

6.6.1.a. Drug release study.
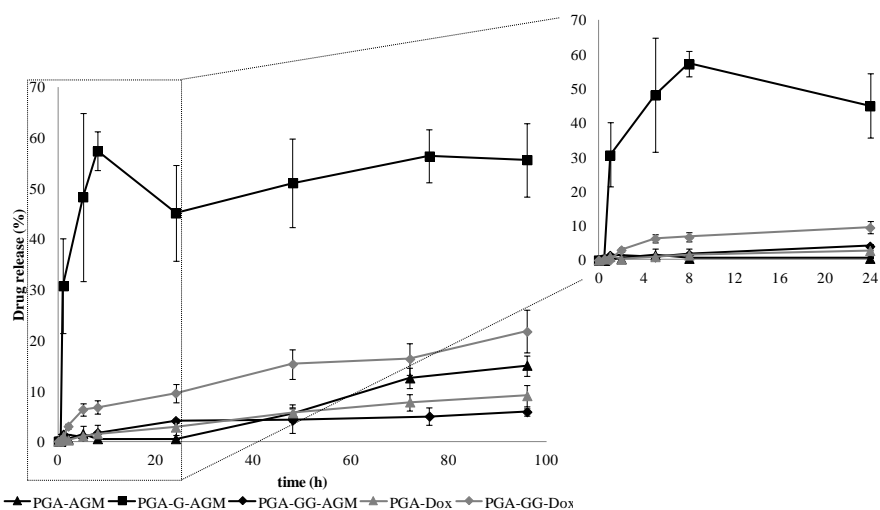
Figure 6.18. Kinetics of drug release from the conjugates synthesised in presence of Cathepsin B. Measured by HPLC. Data are expressed as mean ± SD where n = 3.
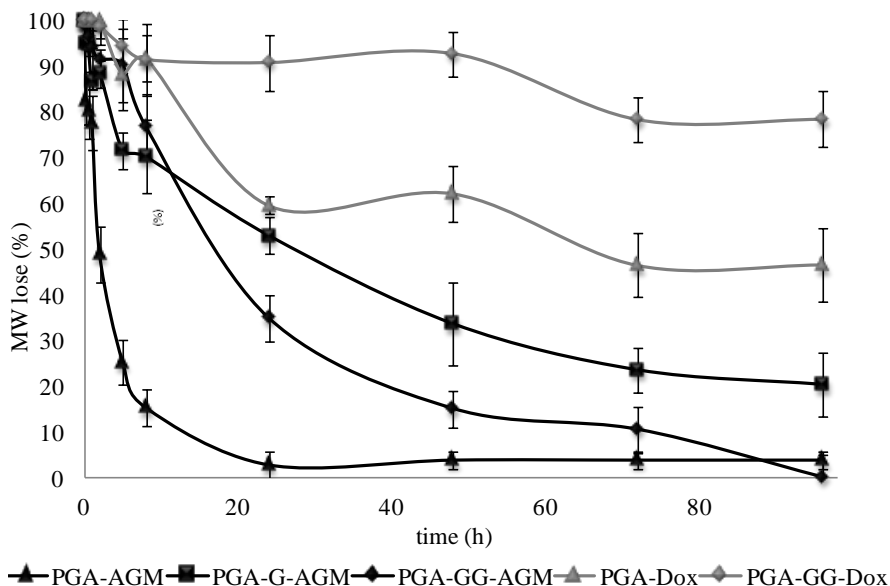
Figure 6.19. Mw loss of the polymer conjugates synthesised in presence of cathepsin B. Measured by GPC. Data are expressed as mean ± SD where n = 3.

6.6.1.b. Identification by LC-MS of the main metabolites released in presence of cathepsin B.

Apart from the rate of drug release, other important task to performed was the identification of the main metabolites released from the conjugates in order to identify any possible inactivation effects. Therefore, LC-MS experiments were performed for the PGA-X-AGM family and MALDI-Tof analyses for PGA-Y-Dox conjugate. Only a MALDI-Tof experiment was performed for the combination therapies.

The metabolite identification was first carried out for PGA-X-AGM family. The samples injected were PGA-AGM after 48 h incubation with cathepsin B, PGA-G-AGM after 24 h incubation with cathepsin B and PGA-GG-AGM after 24 h incubation in presence of cathepsin B.

Figure 6.20. PGA-AGM conjugate metabolite identification after 48 h in presence of cathepsin B. Panel (a) shows the chromatogram of PGA-AGM degradation extract after 48 h in presence of cathepsin B. The retention time (tr) of AGM is 5 min and 7 min for 7 min. Panel (b) shows the mass spectrum corresponding to the AGM peak tr. Peak m/z 233,1, AGM [M+H$^+$]. Panel (c) shows the mass spectrum

corresponding to the Glutamic acid peak retention time. Peak m/z 130,4, Glutamic acid [M+H$^+$].

LC-MS confirmed the release of AGM after 24 h, Glutamic acid units were also identified. However, different peaks were observed in the chromatogram although any correspondence was identified with any PGA fragments or other parts of our system.

Figure 6.21. PGA-G-AGM metabolite identification after 24h in presence of cathepsin B. Panel (a) shows the chromatogram of PGA-G-AGM degradation extract after 24h in presence of cathepsin B. The tr for AGM is 5 min, 6 min for G-AGM and 7 min for glutamic acid is. Panel (b) shows the mass spectrum corresponding to the AGM peak retention time. Peak m/z 233,1, AGM [M+H$^+$]. Panel (c) shows the mass spectrum corresponding to the G-AGM peak retention time. Peak m/z 264,3, G-AGM [M+H$^+$]. Panel (d) shows the mass spectrum corresponding to the Glutamic acid peak retention time. Peak m/z 130,4, Glutamic acid [M+H$^+$].

The HPLC and LC-MS analysis confirmed that G-AGM was first released and finally converted to AGM after 5 h. Glutamic acid units were also observed.
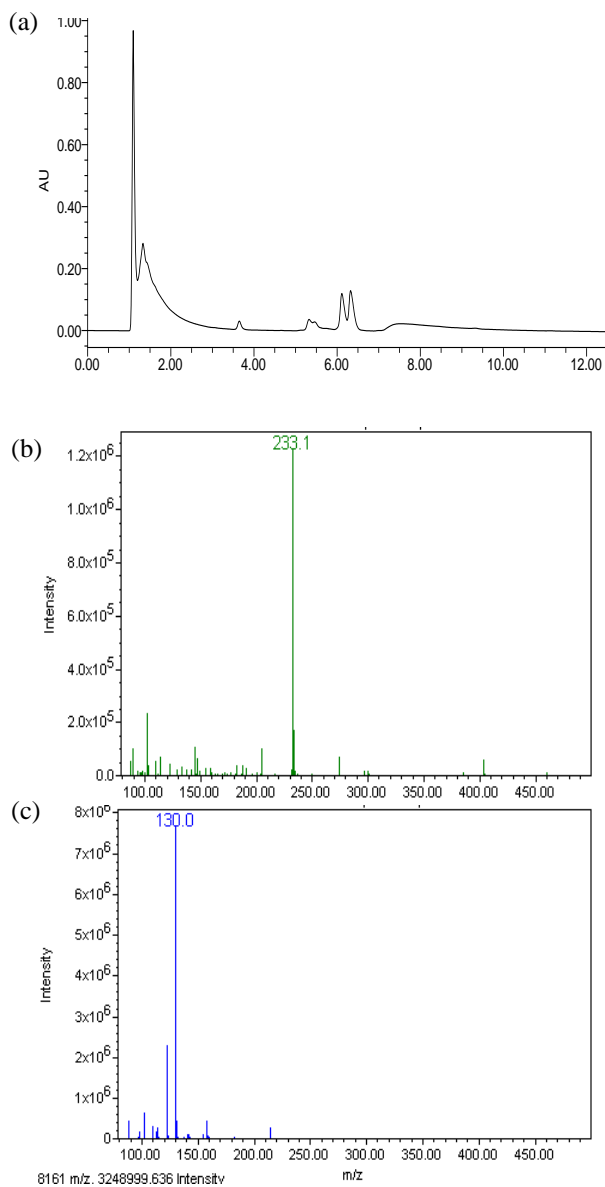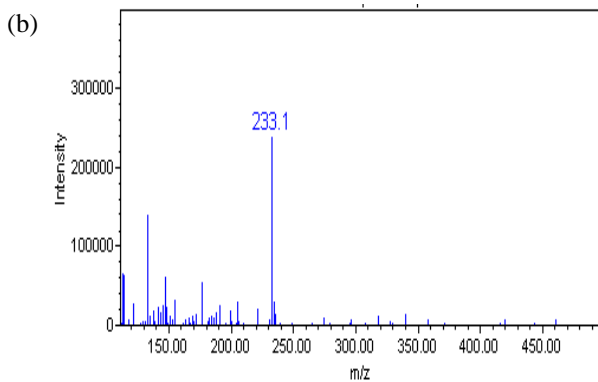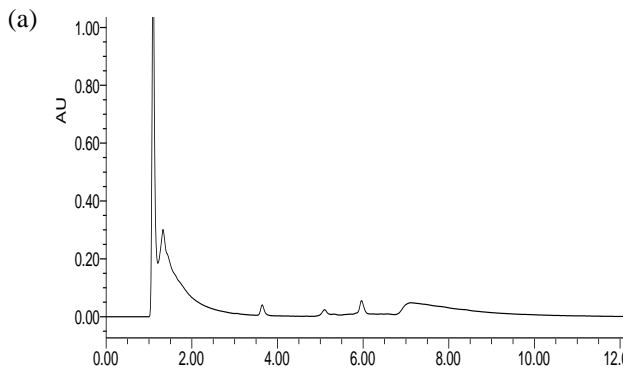
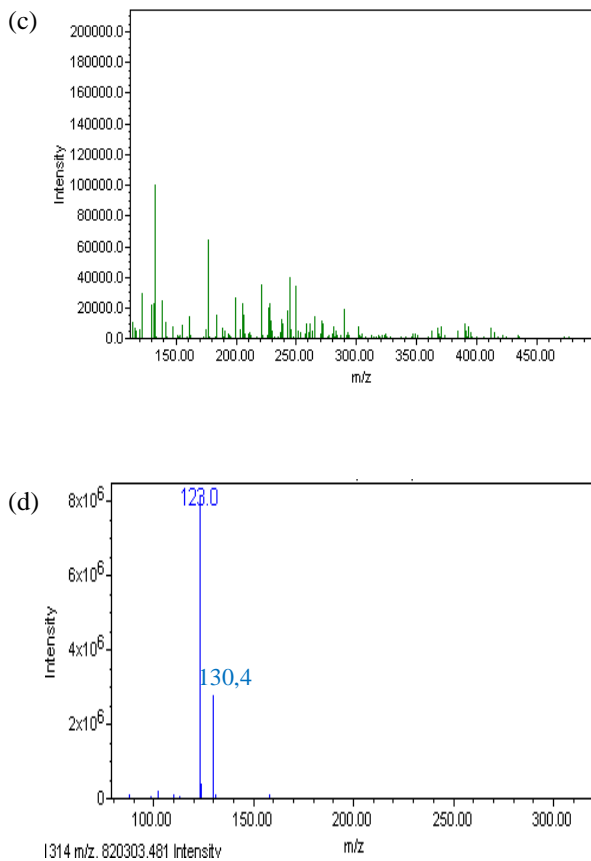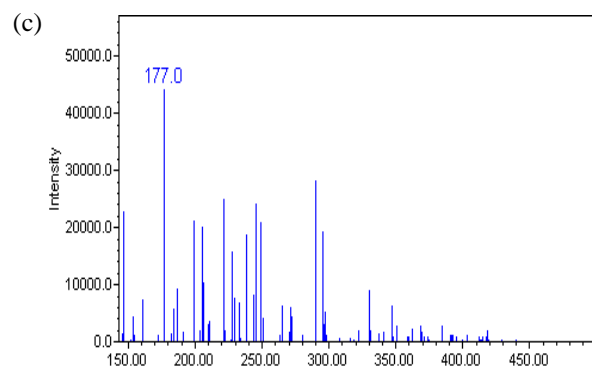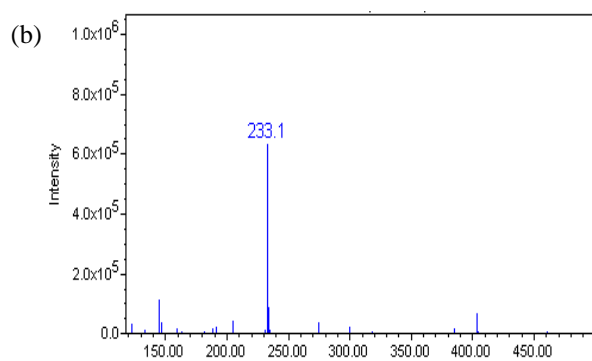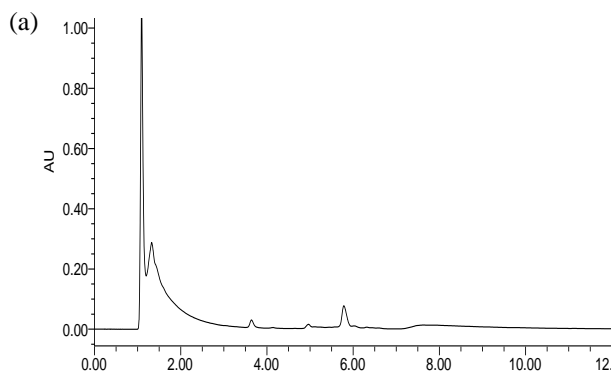168

(a)

(b)

233.1

(c)

177.0

169
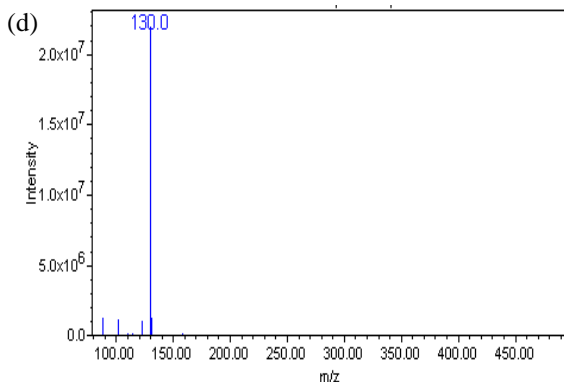
Figure 6.22. PGA-GG-AGM metabolite identification after 24 h in presence of cathepsin B. Panel (a) shows the chromatogram of PGA-GG-AGM degradation extract after 24 h in presence of cathepsin B. The tr for AGM is 5 min, 6min for G-AGM and 7 min for glutamic acid. Panel (b) shows the mass spectrum corresponding to the AGM peak retention time. Peak m/z 233,1, AGM [M+H$^+$]. Panel (c) shows the mass spectrum corresponding to the G-AGM peak retention time. Peak m/z 264,3, G-AGM [M+H$^+$]. Panel (d) shows the mass spectrum corresponding to the G-AGM peak retention time. Peak m/z 130,4, glutamic acid [M+H$^+$].

The LC-MS analysis confirmed that AGM, G-AGM and GG-AGM fragments were released from PGA-GG-AGM conjugate, also glutamic acid units were observed. For the PGA-X-Dox family, MALDI experiments were also carried out to identify the main metabolites after incubation with cathespin B.

As it can be seen in figure 6.18. and figure 6.19., the kinetics of drug release and the degradation of the polymer mainchain were directly influenced by the linker used. For example, PGA-AGM conjugate showed an unusual degradation profile in comparison with PGA alone (Vicent and Pérez-Payá, 2006) achieving complete degradation only after 24 h, which corresponds to AGM release. This could be explained due to AGM 3D conformation as a non-planar molecule that could difficult the compactation of the expected unimollecular micelle to be formed giving as result a more open structure. Therefore the degradation of the PGA was first necessary to allow the access of cathepsin B and therefore to trigger drug release. Once again the polymer drug conjugate conformation is a key parameter to achieve and understand an efficient control on drug release

170

kinetics. Regarding linker evaluation, the –G- for AGM with a 60% of drug released seems to be an adequate candidate for our first combination. Furthermore, with PGA-G-AGM similar degradation profile was achieved when compared to the parent PGA (Vicent and Pérez-Payá, 2006). For the PGA-Y-Dox family, the linker offering the greatest rate of drug release was –GG- with only 20% of drug released after 96 h.

6.6.2. Kinetics of drug release from the combination conjugates.

6.6.2.a. Drug release kinetics.

As it was already proved with the SANS experiment, the conjugation of both drugs in the same polymeric backbone induced a dramatic change in the solution conformation in comparison with PGA and the single conjugates. The degradation of the combination conjugates was performed in presence of cathepsin B and the results were always compared with the single conjugates.

(a)

171

(b)

(c)

172

(d)

(e)
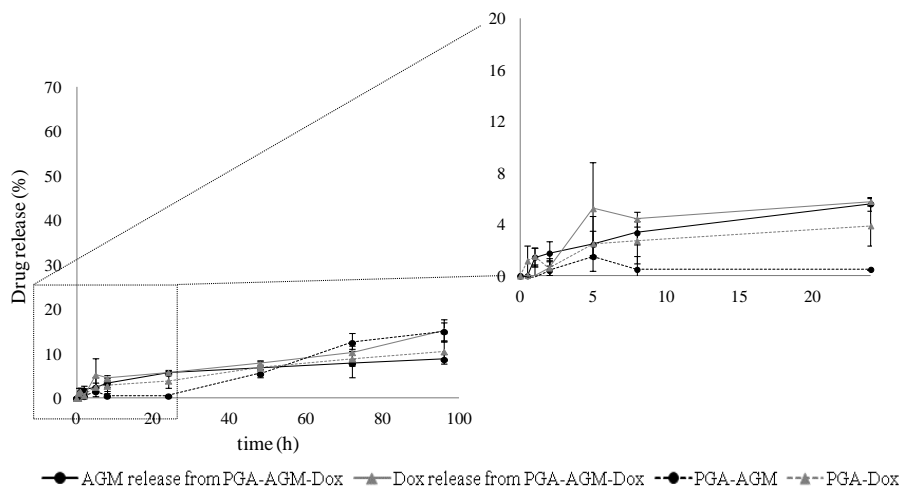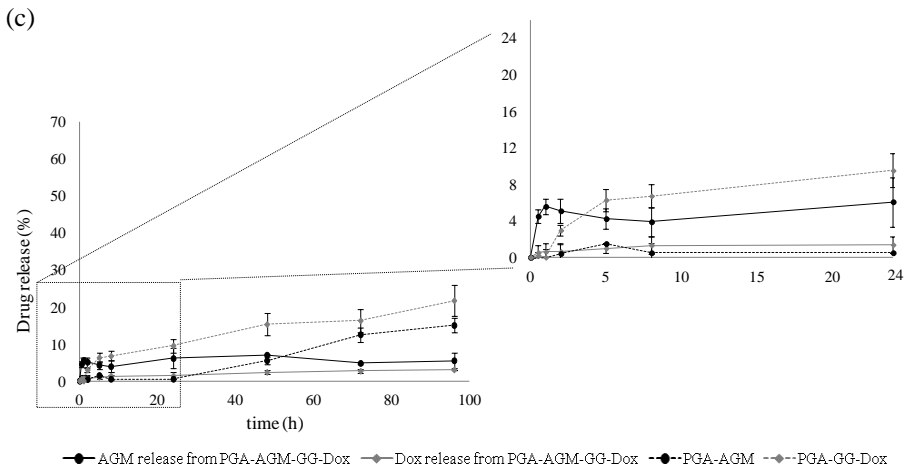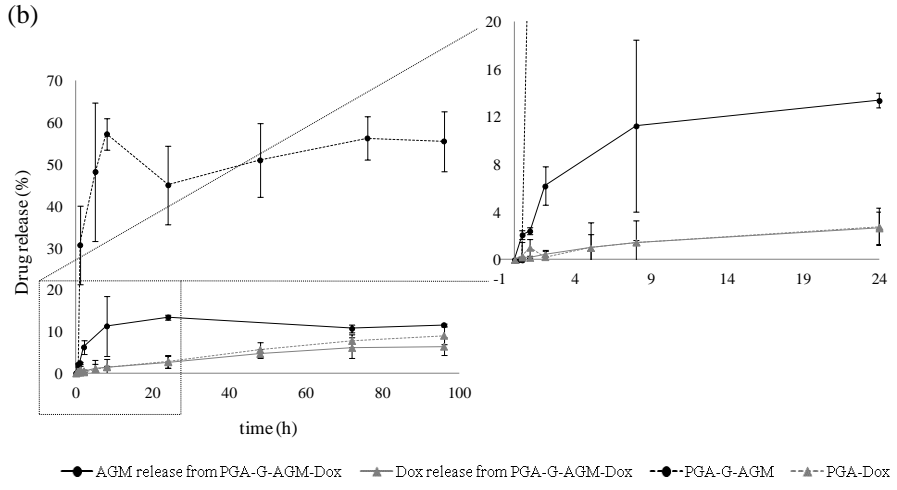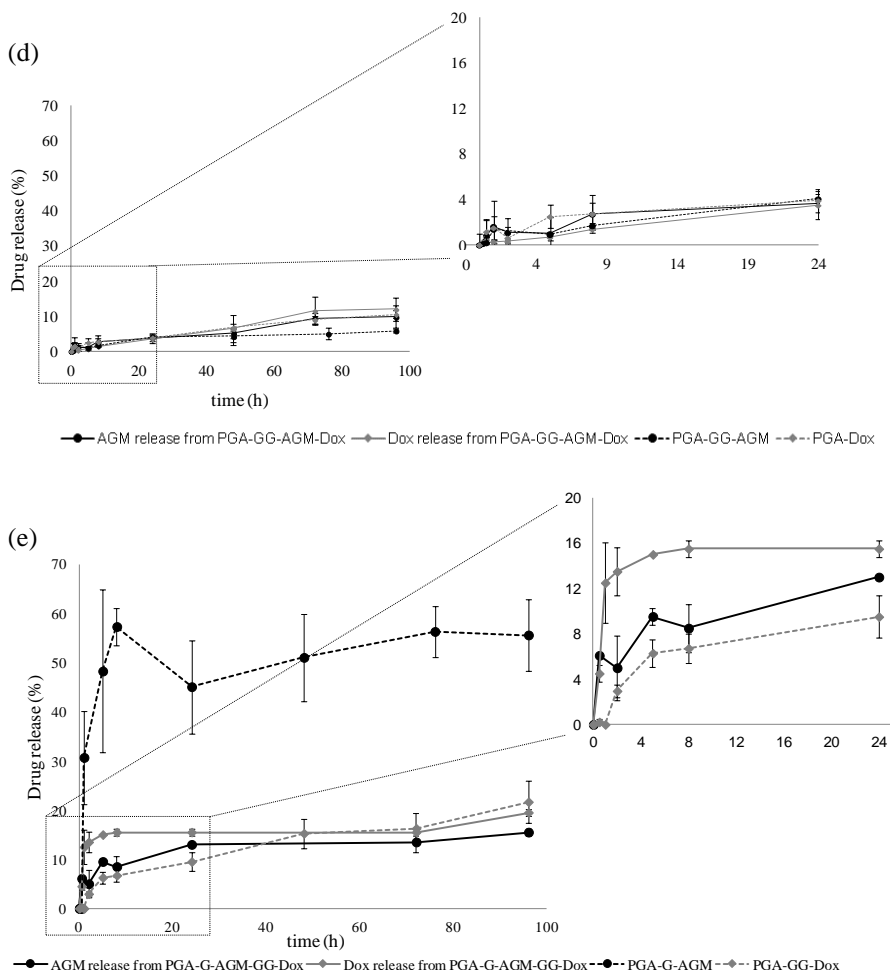
Figure 6.23. Drug release kinetic profile from the combination conjugates synthesised. Panel (a) shows the comparison of AGM and Dox release from PGA-AGM-Dox vs PGA-Dox and PGA-AGM. Panel (b) shows the comparison of AGM and Dox release from PGA-G-AGM-Dox vs PGA-Dox and PGA-G-AGM. Panel (c) shows the comparison of AGM and Dox release from PGA-AGM-GG-Dox vs PGA-GG-Dox and PGA-AGM. Panel (d) shows the comparison of AGM and Dox release from PGA-GG-AGM-Dox vs PGA-Dox and PGA-GG-AGM. Panel (e) shows the comparison of AGM and Dox release from PGA-G-AGM-GG-Dox vs PGA-GG-Dox and PGA-G-AGM. An ANOVA Analysis was performed in order to evaluate the significance between the data. * $P < 0,05$, ** $P < 0,01$, *** $P < 0,001$. Data is expressed as mean $\pm$ SD (n = 3).

173

Table 6.2. Statistical analysis data of drug release.

P value	PGA-G-AGM-GG-Dox							
	0,5 h	1h	2h	5h	8h	24h	72h	96h
PGA-G-AGM	ns	ns	*	*	**	*	**	*
PGA-GG-Dox	*	**	*	**	*	ns	ns	ns

P value	PGA-AGM-Dox	PGA-G-AGM-Dox				
	24h	8 h	24 h	48 h	72h	96h
PGA-Dox	*	ns	ns	ns	ns	ns
PGA-G-AGM	NA	**	*	*	**	**

The degradation of each combination (continuous line) was compared with the single conjugate drug release (doted line). For the majority of the combinations, Dox release was not significantly different than that observed for the single conjugate. Except for PGA-G-AGM-GG-Dox, significant differences were observed in the beginning of the release, up to 8 h 14% of Dox liberation was achieved in comparison to 6% for the single conjugate. In addition, drug release was observed only after 1 h for the single conjugate in contrast with the release in the combination therapy that started from time zero. However after 48 h, the same rate of Dox release was achieved in both cases. Regarding the AGM liberation more differences were observed in the rate as well as in the kinetic profile. PGA-G-AGM-Dox and PGA-G-AGM-GG-Dox, presented similar drug release kinetics however a significant lesser amount of Dox was released around 15 % in both cases in contrast to the 55% obtained from the single conjugate. Regarding the combination with the AGM linked directly to the PGA (*i.e.* PGA-AGM-Dox and PGA-AGM-GG-Dox) the kinetic profile was different. In both cases, Dox release started from the beginning and not after 24 h, as it was observed with the single conjugate. A significant difference in the AGM release rate was also achieved only for the PGA-AGM-Dox up to 24 h. Regarding the last combination, PGA-GG-AGM-Dox no significant differences were observed on Dox or AGM release in comparison to the single conjugates.

6.6.2.b. Identification of the main Dox metabolite released by MALDI-Tof.

The release rate is not the only parameter to take into account as the metabolic profiling is also very important. Therefore Dox-bearing metabolites released from conjugate degradation were analysed by MALDI Tof.

Figure 6.24. MALDI-Tof spectrum of PGA-Dox conjugate after 24 h in presence of Cathepsin B. The peak m/z 656,0952 is the [M+H]$^+$ of Glu-Dox. The peak m/z 806,2994 is the [M+Na]$^+$ of GluGlu-Dox. The peak m/z 935,3424 is the [M+Na]$^+$ of GluGluGlu-Dox.

The main peaks obtained were, 656,09 m/z, 806,29 m/z and 935,34 m/z corresponding respectively to [Glu-Dox], [GluGlu-Dox + Na$^+$] and [GluGluGlu-Dox+ Na$^+$]. Peaks between 400 m/z and 450 m/z belong to the matrix. The release occurred only after polymer mainchain degradation, which was in fact the expected result from our design. MALDI-Tof experiment confirmed the release of Dox through the polymer mainchain cleavage as Glu-Dox, GluGlu-Dox and GluGluGlu-Dox were the main fragments observed.

Figure 6.25. MALDI-Tof spectrum of PGA-GG-Dox conjugate after 24 h in presence of cathepsin B. The peak m/z 543,4283 is the [M+H]$^+$ of Dox. The peak m/z 606,4573 is the [M+Na]$^+$ of GluNa-GluNa-GluNa-GluNa. The peak m/z 656,0290 is the [M+H]$^+$ of GlyGly-Dox.

Regarding the PGA-GG-Dox, first a release of GG-Dox was observed followed by free Dox release after 120 h. The release of Dox only after 120 h could result in a lower therapeutic effect in future *in vitro* and *in vivo* experiments.
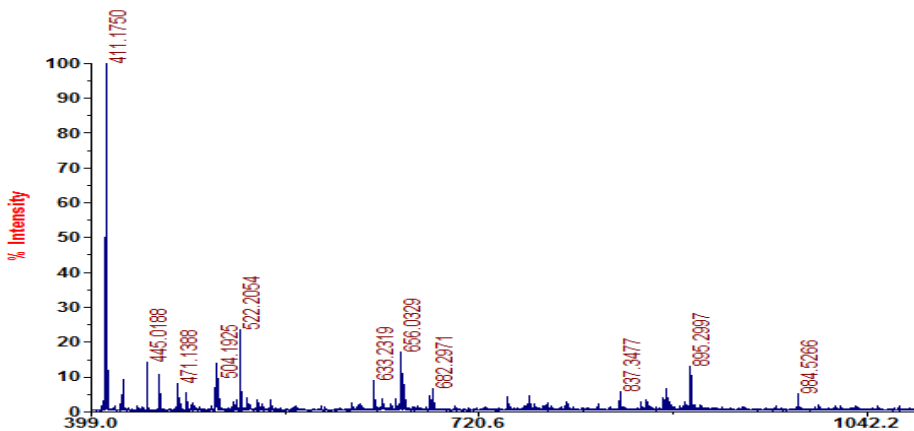
Figure 6.26. MALDI-Tof spectrum of PGA-G-AGM-GG-Dox conjugate after 72 h in presence of cathepsin B. The peak m/z 656,0390 is the [M+H]$^+$ of GlyGly-Dox. The peak m/z 682,2971 is the [M+Na]$^+$ of GlyGly-Dox.

176

Regarding the PGA-G-AGM-GG-Dox, release of GG-Dox was observed as in the single conjugate.
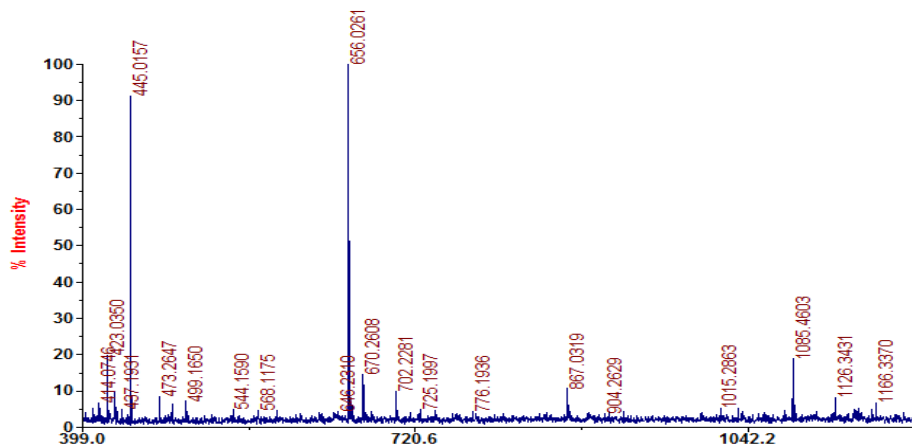
Figure 6.27. MALDI-Tof spectrum of PGA-GG-AGM-Dox conjugate after 24 h in presence of cathepsin B. The peak m/z 656,0261 is the [M+H]$^+$ of Glu-Dox.

More importantly main peaks obtained were, 656,09 m/z, corresponding to [Glu-Dox]. The release occurred only after polymer mainchain degradation, which was in fact the expected result from our design.
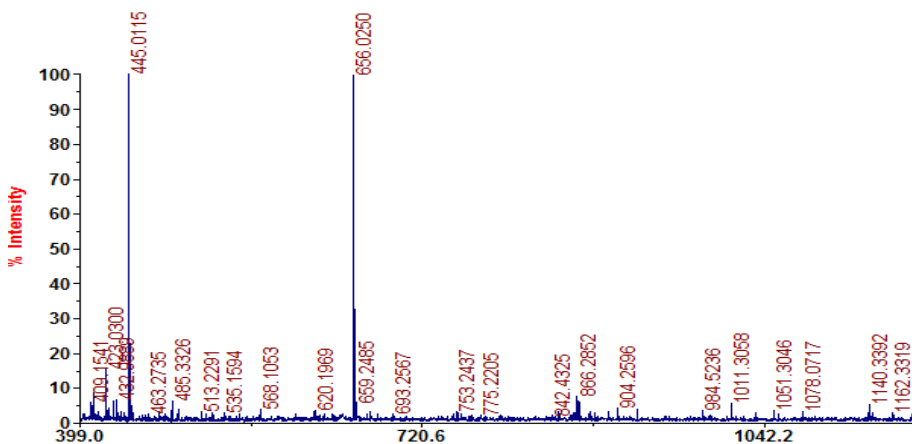
Figure 6.28. MALDI-Tof spectrum of PGA-AGM-GG-Dox conjugate after 24 h in presence of cathepsin B. Regarding the PGA-G-AGM-GG-Dox, a release of GG-

Dox was observed as in the single conjugate. The peak m/z 656,0290 is the [M+H]$^+$ of GlyGly-Dox.
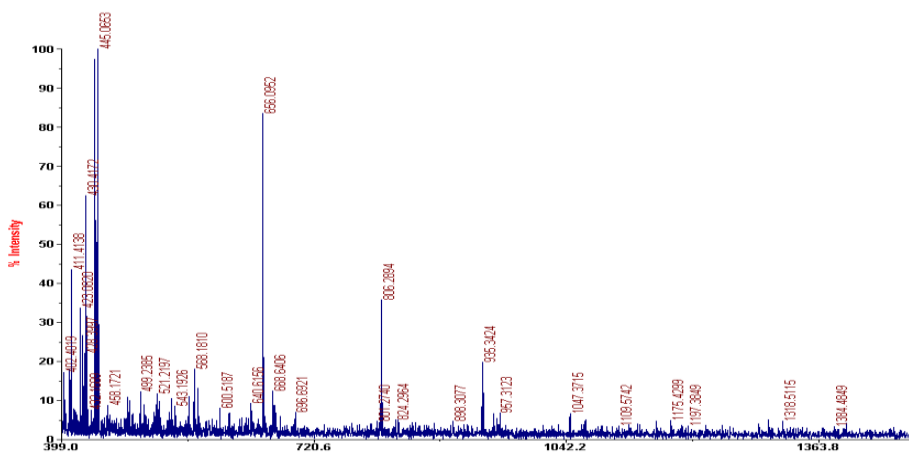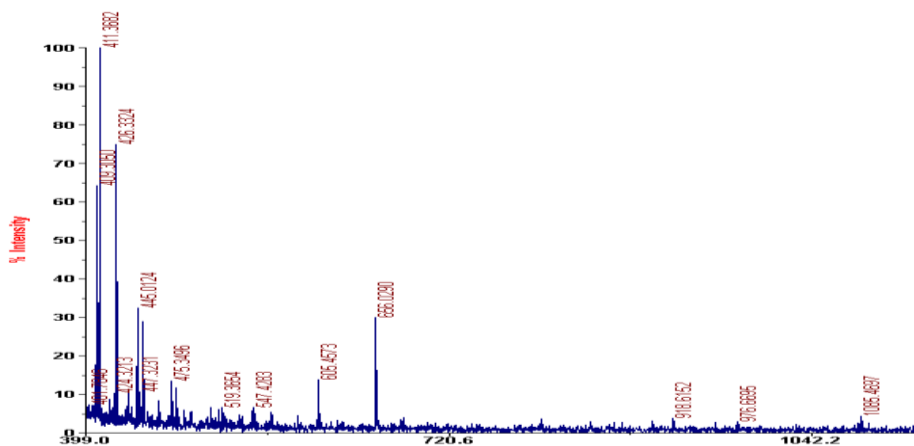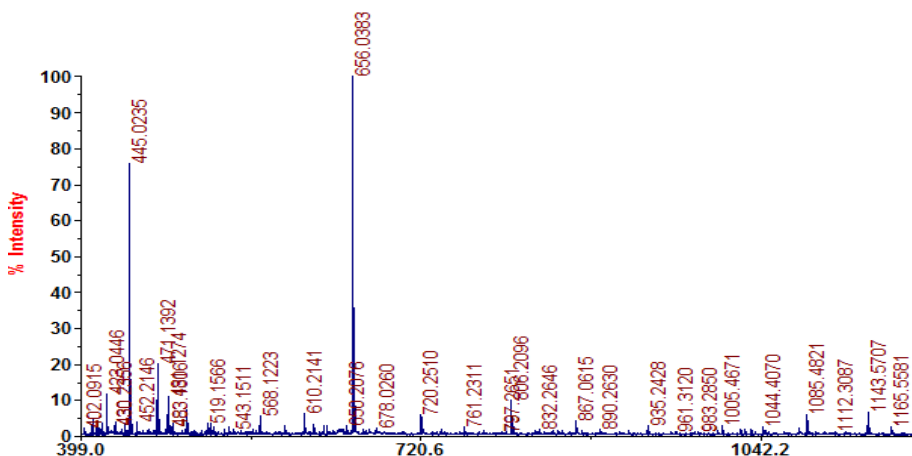

Figure 6.29. MALDI-Tof spectrum of PGA-AGM-Dox conjugate after 24 h in presence of cathepsin B. The peak m/z 656,0383 corresponds to the [M+H]$^+$ of Glu-Dox. The peak m/z 806,2096 is the [M+Na]$^+$ of GluGlu-Dox. The peak m/z 935,2428 is the [M+H]$^+$ of GluGluGlu-Dox.

More importantly main peaks obtained were, 656,09 m/z, 806,29 m/z and 935,34 m/z corresponding respectively to [Glu-Dox], [GluGlu-Dox + Na$^+$] and [GluGlu-Dox + Na$^+$]. Also in this case, the release occurred only after polymer mainchain degradation as expected.

To conclude, a clear time-dependent enzymatic drug release kinetics was observed for all conjugates tested as single agents or in combination. The greatest percentage of AGM release was observed for PGA-G-AGM conjugate with a 55% AGM released after 96 h. By LC-MS, it was determined that G-AGM was the main metabolite obtained up to 48 h in presence of cathepsin B, yielding free AGM already after 5 h. The highest Dox release was observed for PGA-GG-Dox with a 20% of GG-Dox found after 96 h yielding free Dox only after 120 h. In the combination conjugates, *i.e.* PGA-X-AGM-Dox there was not possible to make a direct correlation with the drug release data obtained for the single conjugates. PGA-X-AGM-Dox showed a release from the PGA backbone producing metabolites, such as, Glu-Dox and GluGlu-Dox. However, the

combination conjugate PGA-X-AGM-GG-Dox showed a release through the linker liberating GlyGly-Dox metabolite.

6.7. Biological evaluation of PGA-X-AGM-Y-Dox combination conjugates.

Regarding the literature encountered for HPMA copolymer-AGM-Dox (Greco et al., 2005; Vicent et al., 2005), the synergistic effect was observed when AGM was released first and subsequently Dox. In this study, the only combination conjugate showing a similar kinetic profile was PGA-G-AGM-Dox. To move a step further, *in vitro* tests were performed in human hormone dependent breast cancer cell line MCF7 Ca with a stable aromatase plasmid transfection as those performed with the model conjugate HPMA copolymer-AGM-Dox conjugate (Chapter 3).

(b)

Cell Viability (%)

Conc drug eq (mg/ml)

- - -◆- - - PGA G AGM   - -■- - PGA Dox   —▲— PGA G AGM Dox   —■— Dox   —■— PGA G AGM + PGA Dox

(c)

Cell Viability (%)

conc drug eq (mg.ml)

- - -■- - - PGA G AGM   —▲— PGA G AGM GG Dox   —■— Dox   - - -◆- - - PGA-GG-Dox   —■— PGA G AGM + PGA GG Dox
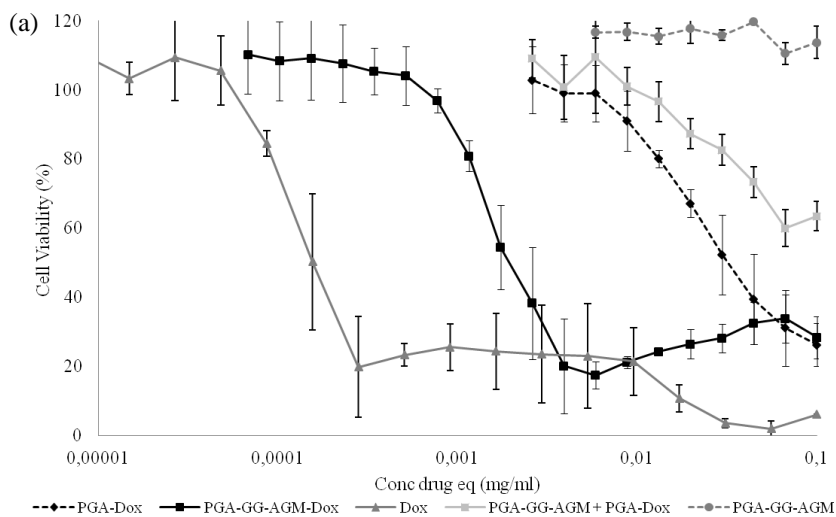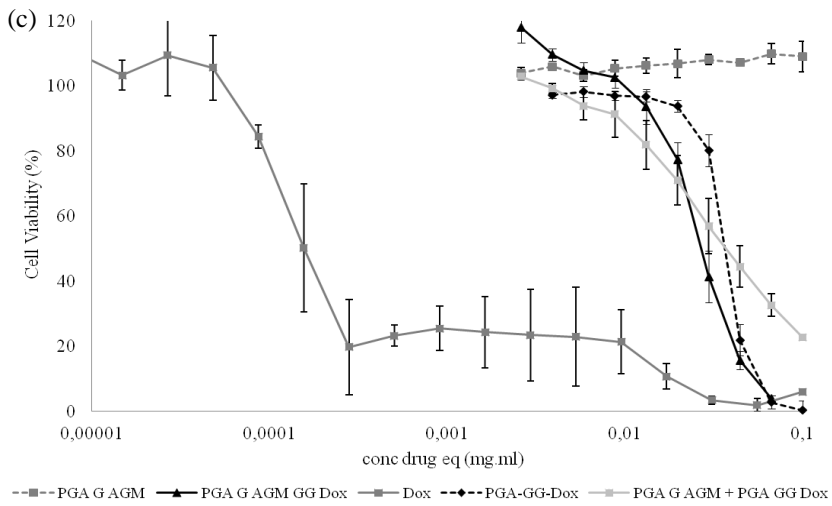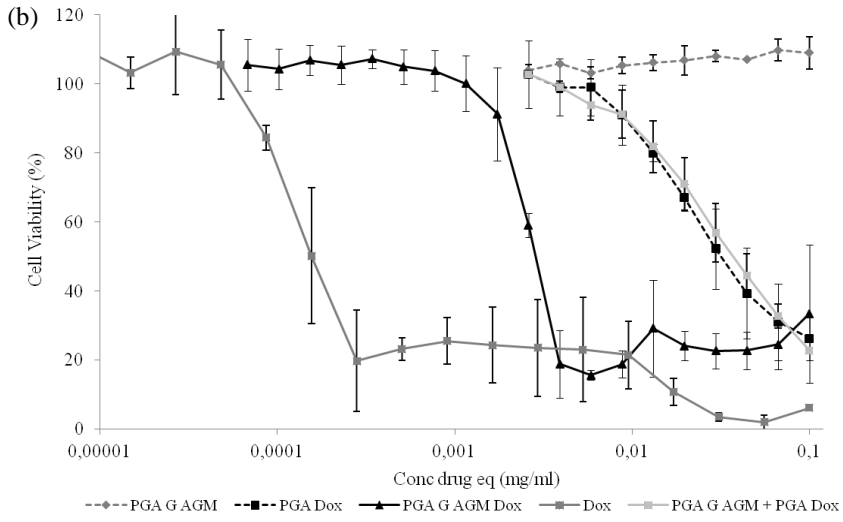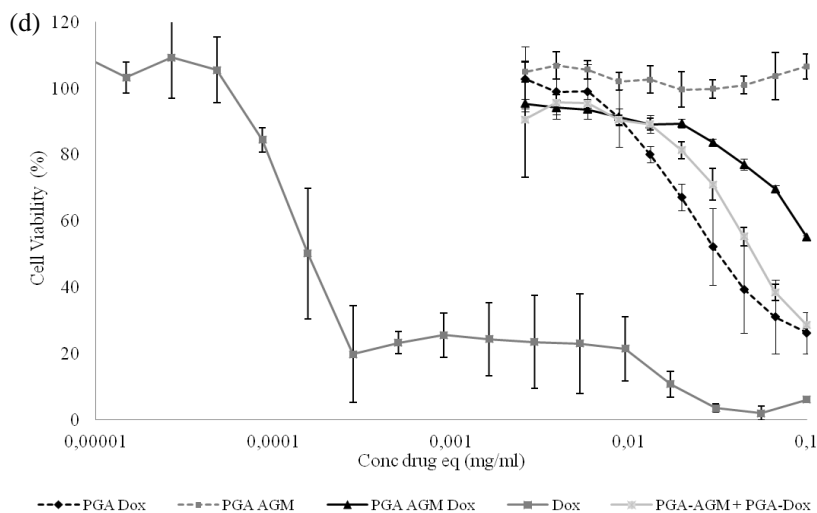
Figure 6.30. Effect of Dox and PGA conjugates family on MCF7 Ca cell viability after 72 h incubation. Panel (a) shows the cytotoxicity of PGA-GG-AGM-Dox in comparison with the single conjugates and their mixture. Panel (b) shows the cytotoxicity of PGA-G-AGM-Dox in comparison with the single conjugates and their mixture. Panel (c) shows the cytotoxicity of PGA-G-AGM-GG-Dox in comparison with the single conjugates and their mixture. Panel (d) shows the cytotoxicity of PGA-AGM-Dox in comparison with the single conjugates and their mixture. Data are expressed as mean ± SD where n = 3.

In order to evaluate the best combination conjugate synthesised based on its cytotoxic activity on MCF7 Ca, a comparative 72 h incubation MTT assay was performed between each designed polymer combination conjugate, the single conjugates, and the mixture of the single conjugates. As it could be seen in figure 6.30., three combination conjugates could already be discharged, PGA-AGM-Dox, PGA-AGM-GG-Dox and PGA-G-AGM-GG-Dox. Those combination conjugates presented lower toxicity or non-significant differences than the single conjugates against MCF7 Ca cells. In addition, PGA-AGM-GG-Dox presented no toxicity in the tested concentration range probably due to the low amount of Dox released. The two possible candidates with lower IC50 values than that for PGA-Dox were PGA-G-AGM-Dox and PGA-GG-AGM-Dox (figure 6.30.a. and figure 6.30.b.). Moreover by SANS, a comparison of the

solution conformation adopted by the four different combination conjugates was studied by looking at their scattering curves.
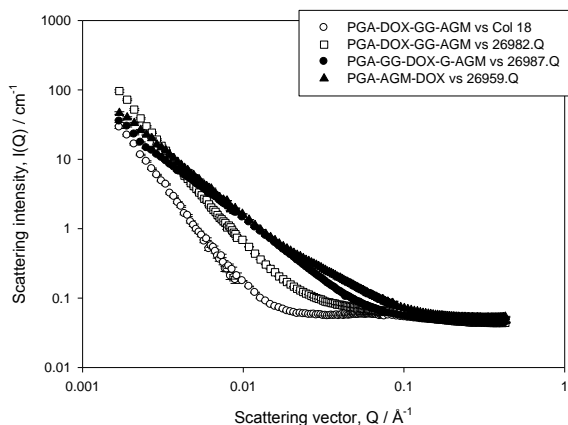
Figure 6.31. Comparison on combination conjugates scattering profile.

Remarkably, the conjugates presenting the best biological profile (PGA-G-AGM-Dox and PGA-GG-AGM-Dox, empty symbol lines) also presented similar scattering profiles and different from those not-biologically active. This could be a sign of a preferred conjugate solution conformation to achieve synergism. PGA-G-AGM-Dox seemed to be more compact than the other due to its higher Q value. In order to find out the final conjugate solution conformation capable of inducing better biological profile in breast cancer models further SANS studies are being performed looking for a clear correlation between conformation and the cell death results achieved against MCF7 Ca cells.

6.8. *In vivo* evaluation of PGA-X-AGM-Y-Dox combination conjugates.

Due to the experimental difficulties to perform an orthotopic animal model with MCF7 Ca cells as described in chapter 4, and in order to evaluate our conjugate in a representative model with functional immune system that also allowed the comparison with the previous studied model conjugate HPMA copolymer-AGM-Dox, a 4T1 metastatic murine model was used (see details in chapter 4).

(a)

(b)
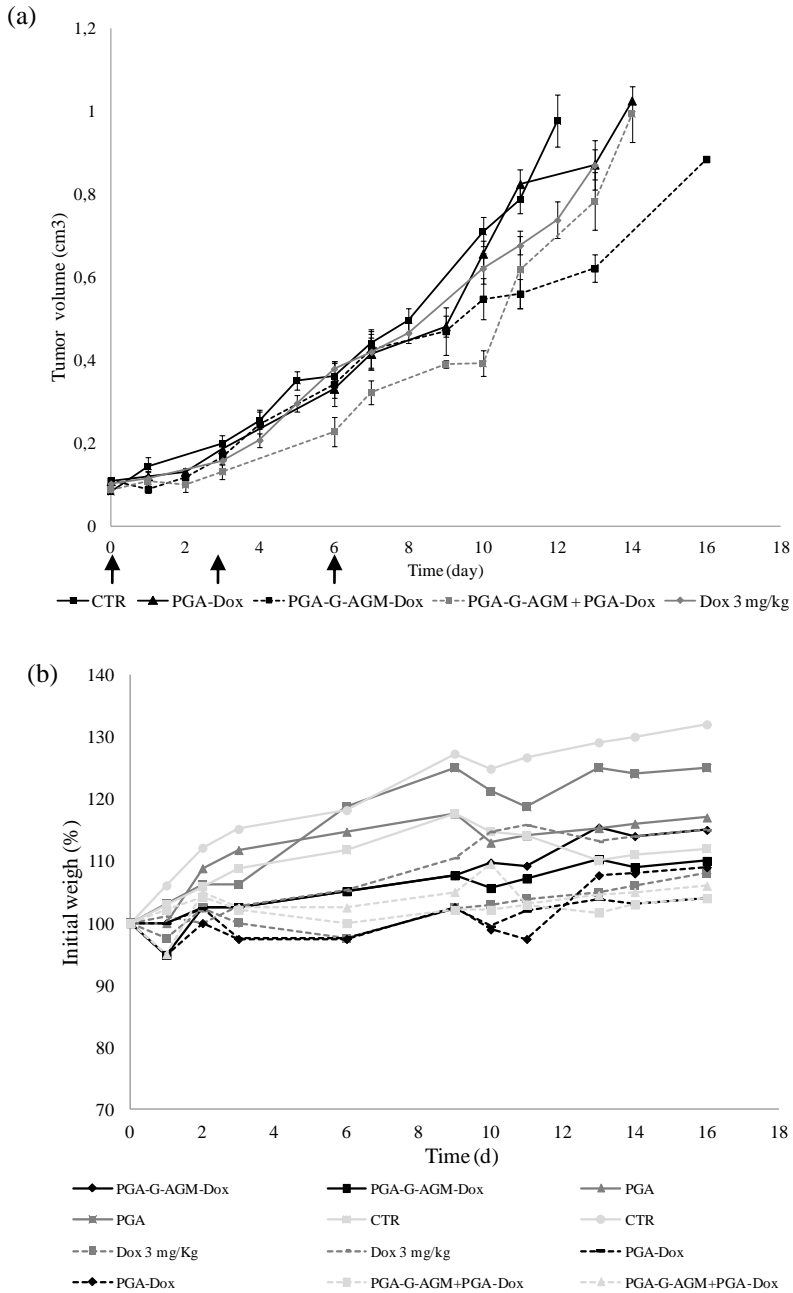
Figure 6.33. *In vivo* evaluation of PGA-G-AGM-Dox conjugate in 4T1 orthotopic murine model. Panel (a) shows the tumour growth with and without treatment, Ctr,

PGA-Dox, PGA-G-AGM-Dox and PGA-G-AGM + PGA-Dox. Results are expressed as mean ± SEM where n = 6 animals per group. The injection of treatments was performed on days 0, 3 and 6 as indicated by the arrows. Panel (b) shows the animals weight during the experiment. The weight progression of 2 animals is shown as example.

Table 6.2. Significance of PGA conjugates and free Dox in the 4T1 murine model

	d 7	d 9	d 10	d 11	d 13	
P value	2	2	2	1	1	4
1	*	*	*	NA	NA	ns
2	NA	NA	NA	*	*	ns
3	ns	ns	ns	**	***	ns
4	ns	ns	ns	ns	*	NA
5	ns	ns	ns	ns	*	***

1- PGA-G-AGM-Dox, **2-** PGA-G-AGM + PGA-Dox and **3-** PGA-Dox. **4** − CTR. **5** − Dox. The total Dox content was represented (PGA conjugate + free Dox, analysed by HPLC looking at aglycone, see Materials and Methods) (n = 4). Significances calculated by one-way ANOVA. P*** < 0,001, P* *< 0,01, P* < 0,05, ns: non significance. The statistics at T = 0 d to T = 6 d showed non significance.

PGA conjugates were injected intravenously at 5 mg/kg, 3 times every 3 days following the same strategy as described in chapter 4. Due to Dox toxicity as previously explained, only 3 mg/kg was injected as free Dox treatment, corroborating the better therapeutic outcome of the Dox conjugates in comparison to the toxic free drug. As it can be seen in figure 6.33.a., none significant differences for tumour volume were observed with all treatments compared to the control group up to day 10, except for PGA-G-AGM+PGA-Dox treatment, which showed an early significant down-regulation of tumour volume. However, after day 10, an interesting antitumor effect was observed with PGA-G-AGM-Dox presenting significantly better activity than PGA-G-AGM+ PGA-Dox, and consequently than the other treatments. Furthermore, treatment with PGA-G-AGM-Dox was capable to constrain the tumour growth in contrast with the other treatments. Regarding PGA-Dox, significant differences were observed when compared with the control group after day 11, however, its effect was similar to that observed with free Dox. PGA as a carrier

was also evaluated and non-differences with the control were achieved. None toxicity was observed regarding the weight evolution and the animal behaviour (figure 6.33.b.).

6.9. Discussion.

In order to design an efficient PGA-AGM-Dox combination conjugate, firstly, a family of PGA-X-AGM conjugates based on different peptide linkers was synthesised, characterised and fully evaluated. Two linkers were used with drug loadings around 5 mol% and free drug content lower than 1 wt%. The Mw of all conjugates was set to be around 19 000 Da. The PDI was determined to be the same as the PGA carrier due to the synthetic approach used, a post-polymerisation modification. Regarding the polymer degradation experiment, some differences were observed in terms of degradation kinetics. PGA-AGM conjugate showed a fast degradation to reach a 100% Mw loss of the starting conjugate only after 24 h. One of the explication of this phenomenon could be the change in the solution conformation of the conjugate after AGM conjugation. This conjugate did not showed any side-chain linkers so a quite compact structure could result from the conjugation of the AGM and could favor the degradation in some specific site of the PGA main chain. This hypothesis was confirmed by the AGM release which occured only after 24 h when the PGA mainchain was degraded. For the PGA-G-AGM a totally different release profile was observed. The use of -G- as linker generated a more expanded structure and allowed better enzyme accessibility. Moreover regarding the AGM release, first a fast liberation was observed up to reaching a plateau after 10 h. Possibly a change in the conjugate solution conformation occurred during the degradation process. The same conclusion could be drawn for PGA-GG-AGM. To confirm our hypothesis further studies evaluating the solution conformation of conjugates have been carried out by SANS including a cathepsin B degradation study. Regarding the kinetics of drug release, a clear time dependent drug release was observed in presence of the lysosomal enzyme cathepsin B directly correlated with the linker. The linker allowing the greater rate of drug release was the –G- reaching 55% of AGM released, first as –G-AGM that was

transformed in AGM after 5 h. Consequently, it was selected as the best candidate to be part of the combination conjugate.

In parallel, a family of PGA-Y-Dox were successfully synthesised and characterised. The same linkers were selected. Around 5 mol% Dox loading was achieved with a free drug content always lower than 0,4 wt%. The Mw was determined to be around 25 000 Da. The PDI were not achieved due to problems with Dox retention in the GPC column inducing calculation errors, however, due to the synthetic approach followed (post-polymerisation modification) a PDI approximately of 1,2 would be expected. Regarding the polymer degradation, both PGA-Y-Dox conjugates showed a slower degradation profile in comparison to PGA-Na. The presence of Dox could induce a π-π stacking phenomena (Gu et al., 2011; Hynek et al., 2012) resulting in the stability of the complex. Based on the MS experiment, Dox was released from PGA-Dox as Glu-Dox and Glu-Glu-Dox as described for the Opaxio® (Singer et al., 2003; Singer, 2005). For PGA-GG-Dox, drug release occurred through -GG-Dox first, and transformed into Dox only after 120 h. Our first idea was to evaluate and select Dox and AGM linkers from the evaluation of the single conjugates. Regarding the drug release and metabolite identification from the single conjugate, the two selected linkers were –G- for AGM and –GG- for Dox. However the final combination conjugate showed a different drug release profile in comparison with the parent single conjugates possibly due to the adopted solution conformation that compromised drug release kinetics and therefore therapeutic output.

Consequently, a family of 5 different combinations were synthesised playing with the linkers studied in the single conjugate without any prior rational. The drug loading was around 5 mol% for both drugs and the Mw around 25 600 Da. For the same reason than PGA-Y-Dox the PDI was not determined but expected to be around 1,2. Regarding drug release kinetics, most of the Dox release was not changed in comparison to the single conjugate. However, regarding the AGM drug, differences in drug release profile were observed. For the combination bearing –G- as linker for the AGM, the kinetic profile presented the

same scattering curve shape however the amount released was 3 times less after 96 h. For the combination with AGM linked directly to the polymer the kinetic profile changed and AGM release started from t0 achieving the same rate after 96 h. Drug release from the combination PGA-GG-AGM-Dox conjugate was the same than the one observed with the single conjugate.

Importantly, the kinetics of drug release for the model HPMA copolymer-AGM-Dox conjugate showed first the release of AGM and then Dox (Vicent et al., 2005). The combinations showing the same profile were PGA-G-AGM-Dox and PGA-AGM-GG-Dox, in fact those showing better performance. The PGA-AGM-GG-Dox was discharged because of its only 2% of Dox release after 96 h.

Once the drug release kinetics from the different conjugates were fully analysed, an *in vitro* test was performed in MCF7 Ca cells to evaluate the cytotoxic activity of the combination conjugates. It was confirmed that PGA-GG-AGM-Dox and PGA-G-AGM-Dox presented a synergistic effect in comparison to the PGA-Dox regarding cytotoxic activity. Moreover, both conjugates presented a clear different solution conformation when studied by SANS in comparison with the other non-biologically active combination conjugates.

Finally, the selected PGA-G-AGM-Dox conjugate was evaluated in a 4T1 orthotopic breast cancer murine model trying to achieve *in vivo* proof of antitumour activity. After day 10, PGA-G-AGM-Dox was capable to stop tumour growth in comparison to the control and with significantly better performance than the PGA-G-AGM+PGA-Dox. The results obtained with this PGA conjugate could be understood and related to the kinetics of Dox release. The drug release from PGA-G-AGM-Dox was low in comparison to HPMA conjugate explaining the lower antitumour effect. The faster rate of AGM release from PGA-G-AGM single conjugate could explain the greater early antitumour effect of the combination of the single conjugates. Indeed, separately AGM release achieved a 60% in 5 h when in the combination conjugate 15%. One hypothesis could be that somehow AGM was turning the 4T1 tumour cells more sensitive to Dox treatment, therefore for a future design would be important to secure a fast AGM release before any free Dox is present in the

cell. After day 10, the benefits of the combination of the single conjugates in comparison to the combination conjugate disappeared demonstrating the importance to secure the delivery of both drugs in the same tumour cell, only possible with the combination conjugate.

An experiment is currently ongoing with a higher conjugate dose 10 mg/kg. Moreover, a new design of PGA-G-AGM-Dox with higher AGM content is also being performed as this fact could enhance the AGM effect in tumour cells and consequently, could induce an earlier tumour inhibition.

6.9.1. HPMA copolymer-AGM-Dox versus PGA-G-AGM-Dox combination conjugates.

In order to understand better the design of efficient combination conjugates it was decided to carry out an *in vitro* and *in vivo* comparison between the results obtained with PGA-G-AGM-Dox and the model conjugate HPMA copolymer-AGM-Dox. Regarding MCF7 Ca cell viability inhibition, the IC50 obtained were 0,0038 mg/mL and 0,002 mg/mL Dox equivalent for PGA-G-AGM-Dox and HPMA copolymer-AGM-Dox, respectively, much lower for the model conjugate (figure 6.34.). However, the synergism seemed to be greater for the PGA conjugate with a CI of 0,21 in comparison to a CI 0,27 for the HPMA conjugate
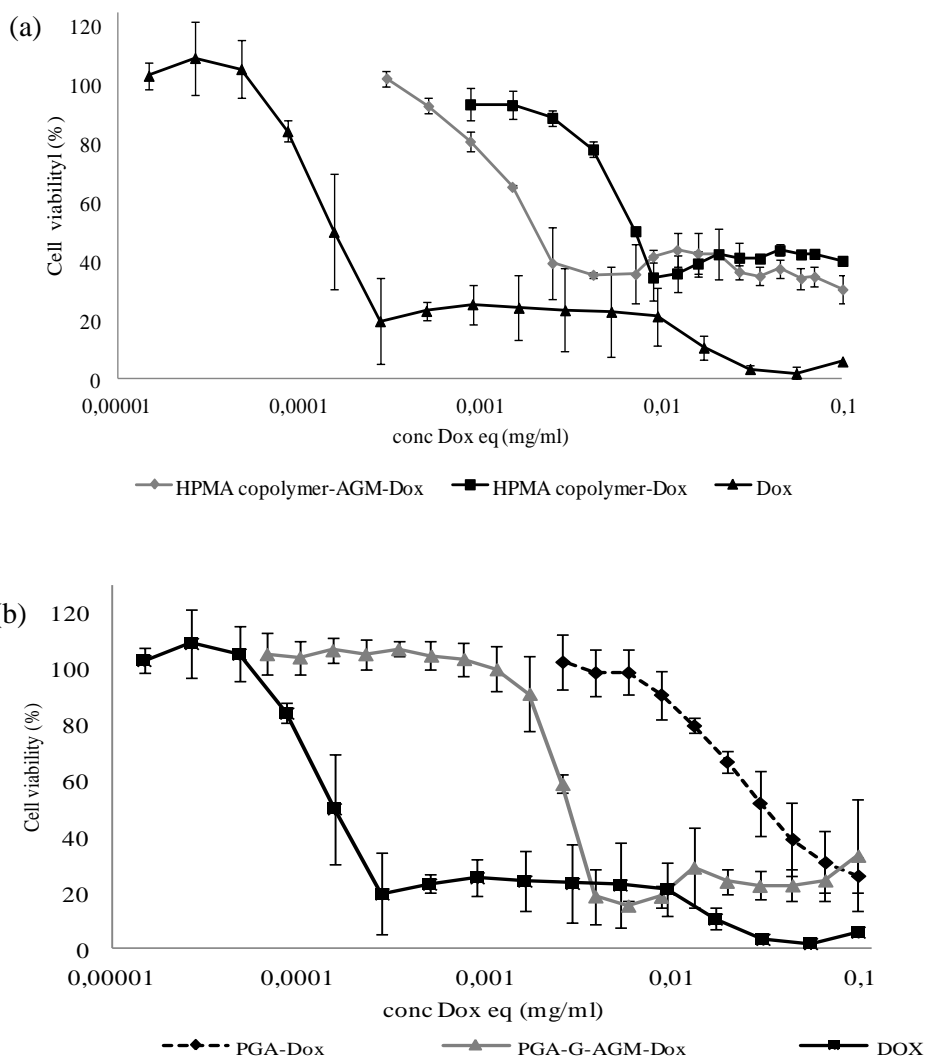
Figure 6.34. Comparison between HPMA conjugate and the best candidate of PGA conjugates on cell viability inhibition. Panel (a) shows cell death analysis in MCF7 Ca cell line induced by HPMA conjugates. Panel (b) shows cell death analysis in MCF7 Ca cell line induced by PGA-G-AGM-Dox family. Data are expressed as mean ± SD where n = 3.

When both combination conjugates were compared in the 4T1 *in vivo* mice model, HPMA conjugate showed greater efficiency than the selected PGA

189

combination conjugate (figure 6.35.) probably due to a greater and faster drug release kinetics (figure 6.36.). Indeed a 20% drug release was achieved from HPMA copolymer after 5 h whereas to reach those levels with PGA conjugate the period required was 96 h. Therefore, in an aggressive tumour model such as 4T1, to enhance the performance of PGA conjugates its design and administration schedule have to be optimised. PGA-G-AGM-Dox combination conjugate is a good starting point as significant differences on tumour growth inhibition have been already achieved but it is believed that a faster and greater AGM release from the PGA carrier could significantly enhance this value. Experiments are ongoing in this respect.
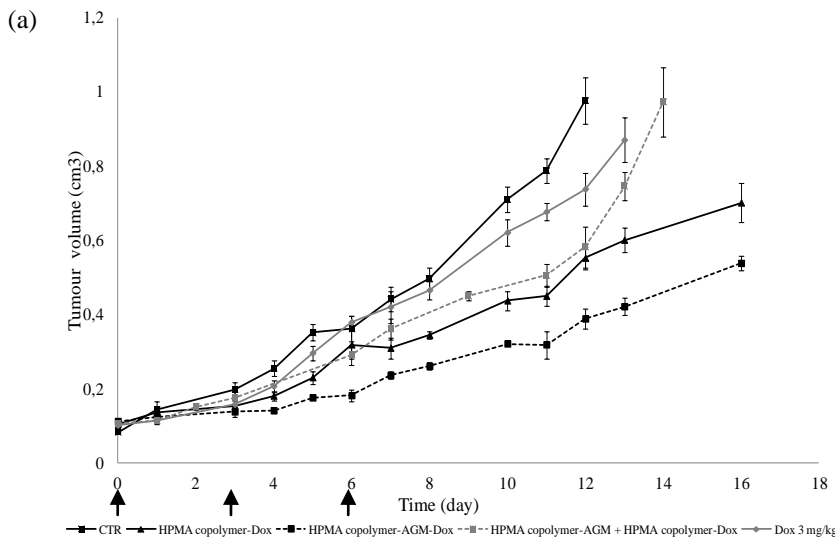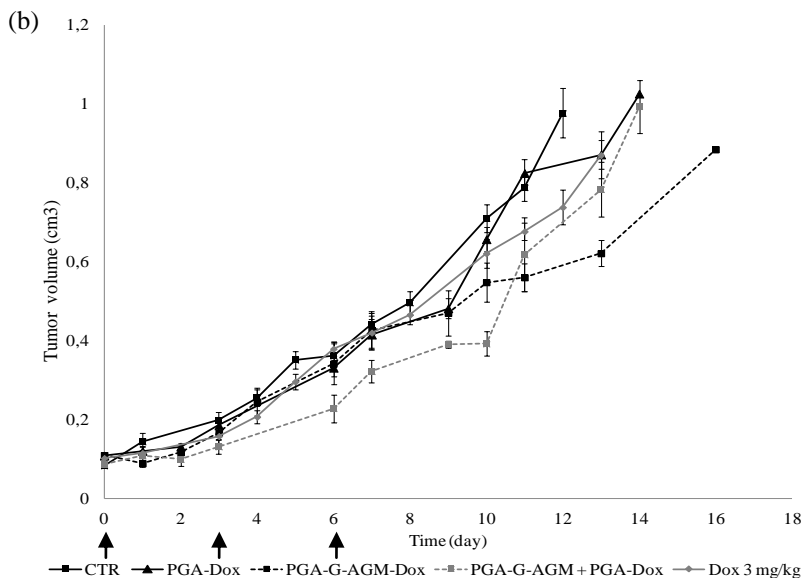
Figure 6.35. Evaluation of tumour growth in 4T1 orthotopic mice model. Panel (a) shows HPMA conjugates effect on tumour growth. Panel (b) shows PGA conjugates effect on tumour growth. Arrows indicate injection schedule and results are expressed as mean ± SEM where n = 6 animals per group. Treatment administration was performed on days 0, 3 and 6.

191

(b)
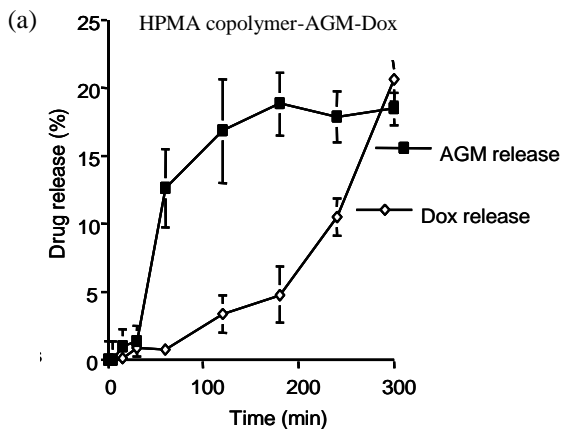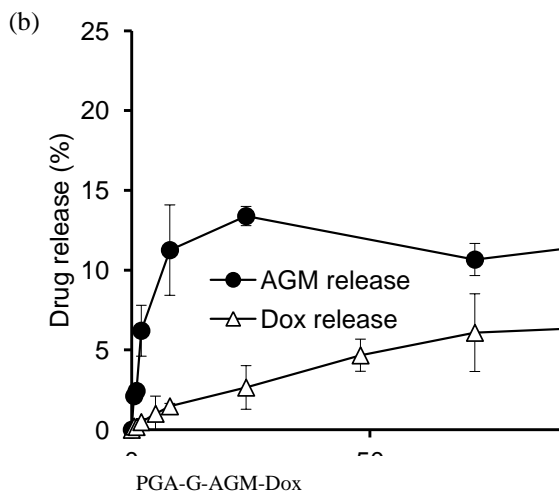
PGA-G-AGM-Dox

Figure 6.36. Comparison of AGM and Dox release kinetic profiles when both drug are linked to either HPMA copolymer or PGA as polymer carrier. Panel (a) shows the drug release from PGA-G-AGM)-Dox. Panel (b) shows the drug release from HPMA copolymer-AGM-Dox. Results are expressed as mean ± SD where n = 3 experiments.

6.10. Bibliography.

Barz, M., Luxenhofer, R., Zentel, R. and Vicent, M.J. (2011). «Overcoming the PEG-addiction : well-defined alternatives to PEG, from structure-property relationships to better defined therapeutics. » Polym. Chem. 2: 1900-1918.

Chipman, S. D., F. B. Oldham, Pezzoni, F.B. and Singer, J.W. (2006).Biological and clinical characterization of paclitaxel poliglumex (PPX, CT-2103), a macromolecular polymer-drug conjugate." Int J Nanomedicine 1(4): 375-383.

Conejos-Sanchez, I., Duro-Castano., Birke, A., Barz, M., and Vicent, M.J. (2013) Polymer Chemistry *in press.*

Deladriere, C., Lucas, R., and Vicent, M.J. (2011). Future trends, challenges and opportunities with polymer-based combination therapy in cancer, Wiley-VCH. 3: Chap4.

Devetzi, M., Scorilas, A., Tsiambas, E., Sameni, M., Fotiou, S., Sloane, B.F., and Talieri, M. (2009). Cathepsin B protein levels in endometrial cancer: Potential value as a tumour biomarker. Gynecol Oncol 112(3): 531-536.

Duncan, R. and Gaspar, R. (2011). Nanomedicine(s) under the microscope. Mol Pharm 8(6): 2101-2141.

Gaspar, R. and Duncan, R. (2009). Polymeric carriers: preclinical safety and the regulatory implications for design and development of polymer therapeutics. Adv Drug Deliv Rev 61(13): 1220-1231.

Gu, Y.J.; Cheng, J.; Jin, J.; Cheng, S.H. and Wong, W.T. (2011). "Development and evaluation of pH-responsive single-walled carbon nanotube-doxorubicin compkexes in cancer cells." Int. J. nanomedicine 6:2889-2899.

Greco, F., Vicent, M.J., Penning, N.A., Nicholson, R.I. and Duncan, R. (2005). "HPMA copolymer-aminoglutethimide conjugates inhibit aromatase in MCF-7 cell lines." J Drug Target 13(8-9): 459-470.

Giménez, V., James, C., Armiñán, A., Schweins, R., Paul, A., and Vicent, M.J. (2012). "Demonstrating the importance of polymer-conjugate conformation in solution on its therapeutic output: Diethylstilbestrol (DES)-polyacetals as prostate cancer treatment." J Control Release 159(2):290-301.

Hynek, D.; Krejcova, L.; Zitka, O.; Adam, V.; Trnkova, L.; Sochor, J., Stiborova, M.; Eckschlager, T.; Hubalek, J. and Kizek, R. (2012). "Electrochemical study of doxorubicin interaction with different sequences of single stranded oligonucleotides, PartI." Int. J. Electrochem. Sci.,7:13-33

http://www.celltherapeutics.com/pdf/OPAXIO_facts-4pg.pdf (2008). "Opaxio"

Langer, C.J., O'Byrne, K.J; Socinski, M.A., Mikhailov, S.M., Leśniewski-Kmak, K., Smakal, M., Ciuleanu, T.E., Orlov, S.V., Dediu M, Heigener D, Eisenfeld AJ, Sandalic L, Oldham FB, Singer JW and Ross HJ. (2008). Phase III trial comparing paclitaxel poliglumex (CT-2103, PPX) in combination with carboplatin versus standard paclitaxel and carboplatin in the treatment of PS 2 patients with chemotherapy-naive advanced non-small cell lung cancer. J Thorac Oncol 3(6): 623-630.

O'Brien, M.E., Socinski, M.A., Popovich, A.Y., Bondarenko, I.N., Tomova, A., Bilynsky, B.T., Hotko, Y.S., Ganul, V.L., Kostinsky, I.Y., Eisenfeld, A.J., Sandalic, L., Oldham, F.B., Bandstra, B., Sandler, A.B. and Singer, J.W. (2008). "Randomized phase III trial comparing single-agent paclitaxel Poliglumex (CT-2103, PPX) with single-agent gemcitabine or vinorelbine for the treatment of PS 2 patients with chemotherapy-naive advanced non-small cell lung cancer." J Thorac Oncol 3(7): 728-734.

Paz-Ares, L., Ross, H., O'Brien, M., Riviere, A., Gatzemeier, U., Von Pawel, J., Kaukel, E., Freitag, L., Digel, W., Bischoff, H., García-Campelo, R., Iannotti, N.,

Reiterer, P., Bover, I., Prendiville, J., Eisenfeld, A.J., Oldham, F.B., Bandstra, B., Singer, J.W., and Bonomi, P. (2008). Phase III trial comparing paclitaxel poliglumex vs docetaxel in the second-line treatment of non-small-cell lung cancer. Br J Cancer 98(10): 1608-1613.

Sabbatini, P., Sill, M.W., O'Malley, D., Adler, L., Secord, A.A. and Gynecologic Oncology Group Study. (2008). A phase II trial of paclitaxel poliglumex in recurrent or persistent ovarian or primary peritoneal cancer (EOC): a Gynecologic Oncology Group Study. Gynecol Oncol 111(3): 455-460.

Singer, J. W. (2005). "Paclitaxel poliglumex (XYOTAX, CT-2103): a macromolecular taxane." J Control Release 109(1-3): 120-126.

Singer, J.W., Baker, B., De Vries, P., Kumar, A., Shaffer, S., Vawter, E., Bolton, M., and Garzone, P. (2003). Poly-(L)-glutamic acid-paclitaxel (CT-2103) [XYOTAX], a biodegradable polymeric drug conjugate: characterization, preclinical pharmacology, and preliminary clinical data. Adv Exp Med Biol 519: 81-99.

Vicent, M.J., Greco, F., Nicholson, R.I., Paul, A., Griffiths, P.C. and Duncan, R. (2005). Polymer therapeutics designed for a combination therapy of hormone-dependent cancer. Angew Chem Int Ed 44(26): 4061-4066.

Vicent, M. J. and Perez-Paya, E. (2006). Poly-L-glutamic acid (PGA) aided inhibitors of apoptotic protease activating factor 1 (Apaf-1): an antiapoptotic polymeric nanomedicine. J Med Chem 49(13): 3763-3765.

Chapter 7. Hight Trough Put screening to find new combination.

7.1. Introduction.

As it has been previously described AGM and Dox drug combination within the same polymer backbone showed very promising results for the treatment of breast cancer as demonstrated firstly by its cytotoxic activity *in vitro* against breast cancer cells, and secondly acting as antitumor therapy administered in an *in vivo* orthotopic breast cancer model (Chapter 4). However, AGM belongs to a first generation aromatase inhibitors (AI) with a non-specific mode of action and most probably if substituted with a more advanced AI the antitumour effects already achieved could be even enhanced. In fact, AGM not only acts on aromatase enzyme, but it also blocks other P-450 enzymes like 11-β-hydroxylase, involved in the biosynthesis of corticosteroids. Therefore, patients treated with AGM need to be supported by simultaneous administration of cortisol (Njar and Brodie, 1999) (figure 7.1.).
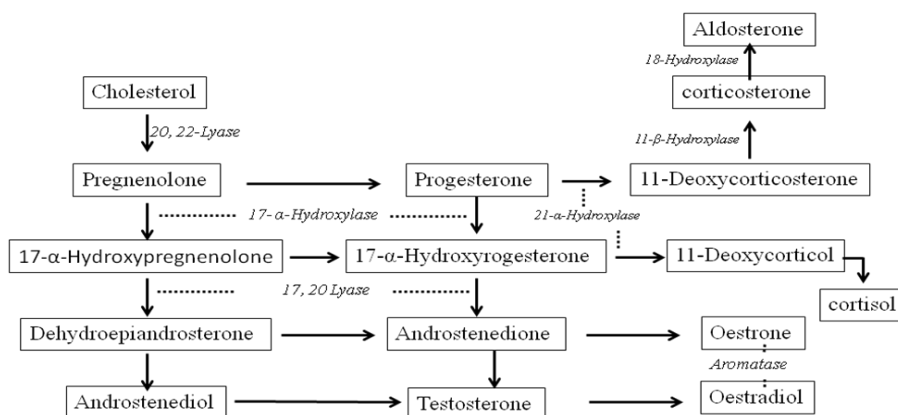
Figure 7.1. Steroid genesis pathways (Njar and Brodie, 1999).

Nowadays, new generation AIs have been developed with higher selectivity and potency than AGM, such as Letrozole, Anastrozole and Exemestane (Exe) (Jordan, 2003). Apart from AI, other endocrine treatments, such as Tamoxifen, with a mechanism of action based on oestrogen receptor blockade, have been also successfully used in the clinics for the treatment of hormone dependent breast cancer (Jordan and Brodie, 2007; Zilli et al., 2009; Rao and Cobleigh, 2012). In the case of tamoxifen the clinical activity was

found mostly in pre-menopausal woman (Bowles et al., 2012; Su et al., 2012) although it also demonstrated important activity in post-menopausal patients (Bowles et al., 2012). On the other hand, other chemotherapeutic drugs than Dox have been also described for breast cancer treatment, such as Paclitaxel (PTX), (Jeansonne et al., 2011) and 5- Fluorouracil (5-FU) (Tan and Swain, 2001; Alvarez et al., 2012). Therefore, trying to increase the combination therapy armory and benefiting of the already developed technological platform (Chapter 6), our aim along this last chapter was to find new drug combinations with antitumour synergistic potential that could allow the design of advanced PGA-based combination conjugates. To reach this goal in a systematic but efficient manner, a high throughput screening (HTPS) approach was implemented using 4 chemotherapeutic drugs and 3 endocrine therapy agents, which were selected from the current clinical treatments for advanced breast cancer.
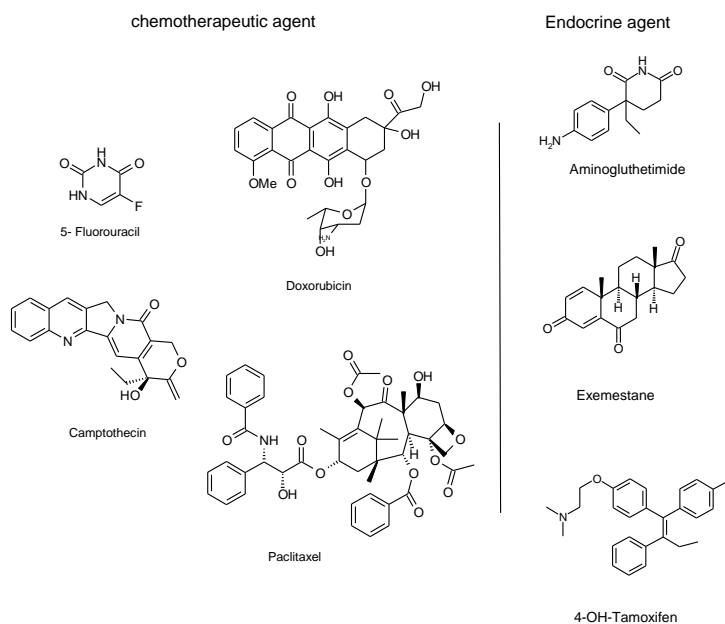
Figure 5.2. Chemotherapeutic and Endocrine agent chemical structures selected to performed the HTPS experiment.

The 4 chemotherapeutic drugs chosen were Camptothecin (CPT), PTX, Dox and 5-FU, whereas AGM, Exe and 4-OH-Tamoxifen (4 OH) were used as endocrine agents. Dox, PTX and the endocrine agents mechanism of action was already described in the introduction chapter. With respect to 5-FU, it could be said that is a thymidylate synthase inhibitor that blocked the synthesis of the pyrimidine thymidine, a nucleoside required for DNA replication. Therefore, cell cycle arrest and apoptosis are induced as a direct consequence of blocking the cell's abilities to synthesise DNA (Liu et al., 2000; Alvarez et al., 2012). CPT can be considered as a cytotoxic quinoline alkaloid inhibitor of the DNA enzyme topoisomerase I and therefore apoptosis inductor (Liu et al., 2000).

In the experimental screening platform design, the cell viability of the 7 different drugs at 3 different concentrations, either alone or in the different possible combinations was evaluated against MCF7 (ER+) and MDA MB231 (ER-) cell lines. MCF7 is a hormone dependent breast cancer cell line. On the other hand MDA MB 231 is a breast cancer cell line oestrogen receptor negative, used here as our negative control. The concentration inhibiting 50% of cell viability (IC50) was evaluated for each single compound in both cell lines MCF7 and MDA MB 231. Then, each chemotherapeutic agent was tested at 3 serial concentrations and combined with each endocrine agent also at 3 different concentrations for both cell lines. In all cases, the 3 concentrations selected for the drugs were their IC50 and concentrations inducing 35% and 70% cell death (IC35 and IC70, respectively).

7.2. IC50 evaluation for each compound.

To determine the IC50 of all compounds, cells were seeded onto 96 well plates (P 96) at 10 000 cells/well for MCF7 and 20 000 cells/well for MDA MB 231. After 24 h for MCF7 and 48 h for MDA MB 231, cells were incubated for 72 h with serial dilutions of the different compounds (n = 6) and cell viability was determined by MTS assays (chapter 3, see material and methods for more detailed explanation). Appropriate control cells were treated identically. Each plate was then read at a wavelength of 496 nm being the

absorbance directly proportional to the number of living cells in culture. Cell viability was expressed as a percentage of the viability of untreated control cells.

In order to determine the rate of significance, the raw data (n = 6) obtained for each experiment (n = 3) was evaluated in comparison to the standard (untreated control cells). The level of statistical significance was determined by analysis of variance (ANOVA) followed by Dunnett's *t*-test for multiple comparisons.

7.2.1. Determination of IC50 value in MCF7.

The concentrations evaluated for IC50 calculation are summarised in the following table.

Table 7.1. Concentrations evaluated for each compound in MCF7 cells to determine their IC50 value.

	AGM	Exe	4 OH	PTX	CPT	Dox	5-FU
[a]Conc (µM)	4000	6	20	18	3,7	13,5	20
	1300	2	13.5	12	2,7	9	15
	440	0,6	8	6	1,7	6	7,5
	140	0,2	6,6	3	0,7	4	6,6
			6	1,5		2	6
				0,22		0,22	3,7

a: Concentration tested to determine the IC50.

199
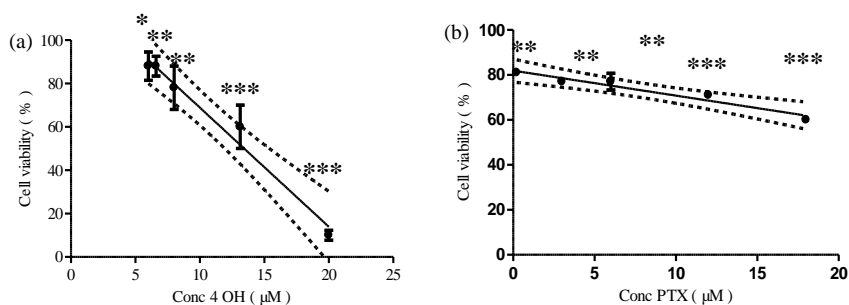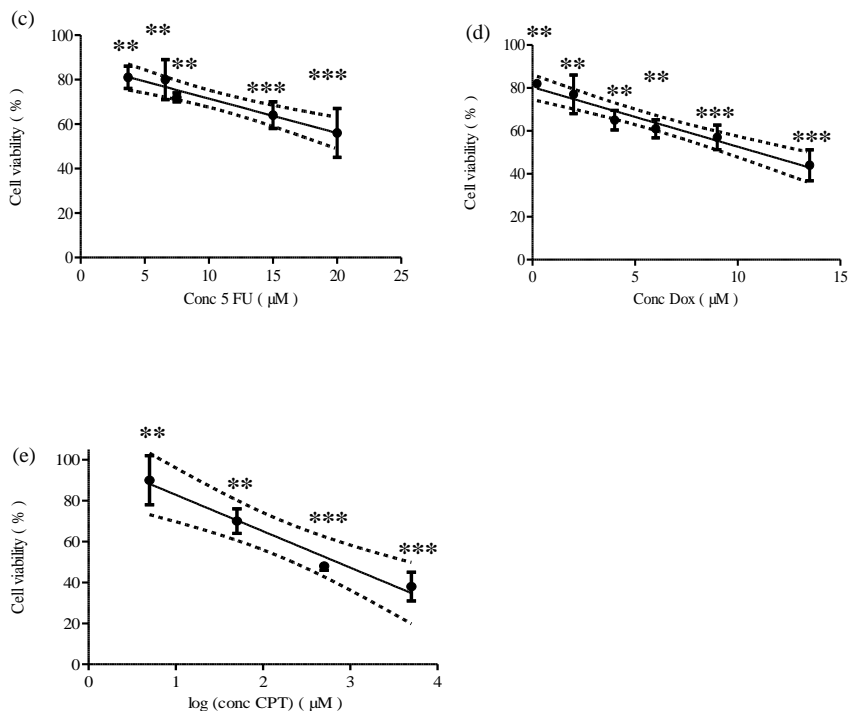
Figure 7.3. Determination of IC50 value for each compound in MCF7 cell line. Panel (a) shows the IC50 of 4 OH (IC50 = 13 μM, R^2 = 0,927), panel (b) shows the IC40 of PTX (IC40 = 18 μM, R^2 = 0,93), panel (c) shows the IC 50 of 5-FU (IC50 = 23,9 μM, R^2 = 0,947), panel (d) shows the IC50 of Dox (IC50 = 11 μM, R^2 = 0,95) and panel (e) shows the IC50 of CPT (IC50 = 0,7 μM, R^2 = 0,94). Results are expressed as mean ± SD where at least n=4 experiments per group and significances calculated by one-way anova and P*** < 0,001, P* *< 0,01, P* < 0,05 in comparison to cell control without treatment.

The IC50 obtained for AGM and Exe were higher than 1000 μM. This result could be explained due to the fact that both compounds are not cytotoxic agents but cytostatics. Therefore, the IC50 of cell survival for AGM and exemestan was not determined, however based on literature (Vicent et al., 2005; http://www.pfizer.ca/en/our_products/monograph/123 2009) the concentrations selected for both compounds were the concentration needed to inhibit 100 % of aromatase enzyme activity. For AGM the value was 0,862 μM (Vicent et al., 2005) and for exemestane, the value was 0,033 μM (http://www.pfizer.ca/en/our

_products/monograph/123 2009). Moreover, 5-FU IC50 was quite high regarding the other IC50 values.

As already described in the introduction chapter, the selection of the drug(s) to be conjugated to a polymer carrier in the design of an anticancer conjugate strongly depends on its potency. Therefore, chemotherapeutic drugs with high IC50 values could be abandoned as important amounts of the resulting conjugate should be administered to the patient in order to reach the adequate doses. Consequently, 5-FU (IC50 = 23,9 μM) was not viable for our design and was not considered for further studies. It is important to note that, due to the poor solubility of PTX only concentrations that resulted in a 40% cell death in the MCF7 cell line were reached being the highest PTX concentration 18 μM offereing results non-significantly different to 12 μM concentration which was here considered as IC50. The same study was performed against MDA MB 231 cells.

7.2.2. Determination of IC50 value in MDA MB 231 cell.

The same statistic analysis was done for data obtained with the drugs tested on MDA MB 231 cells. The concentrations used to determine IC50 values are described in the following table.

Table 7.2. Concentrations tested for each compound to determine the IC50 value in MDA MB 231 cell line.

	AGM	Exe	4 OH	PTX	CPT	Dox	5-FU
^aConc (μM)	4000	6	20	12	4	2	240
	1300	2	13,5	6	2	1	120
	440	0,6	8	3	1	0,5	60
	140	0,2	6	1,5	0,5	0,25	30
				0,375			

a: Concentration tested to determine the IC50.

The resulting cell viabilily curves are shown in figure 7.4.
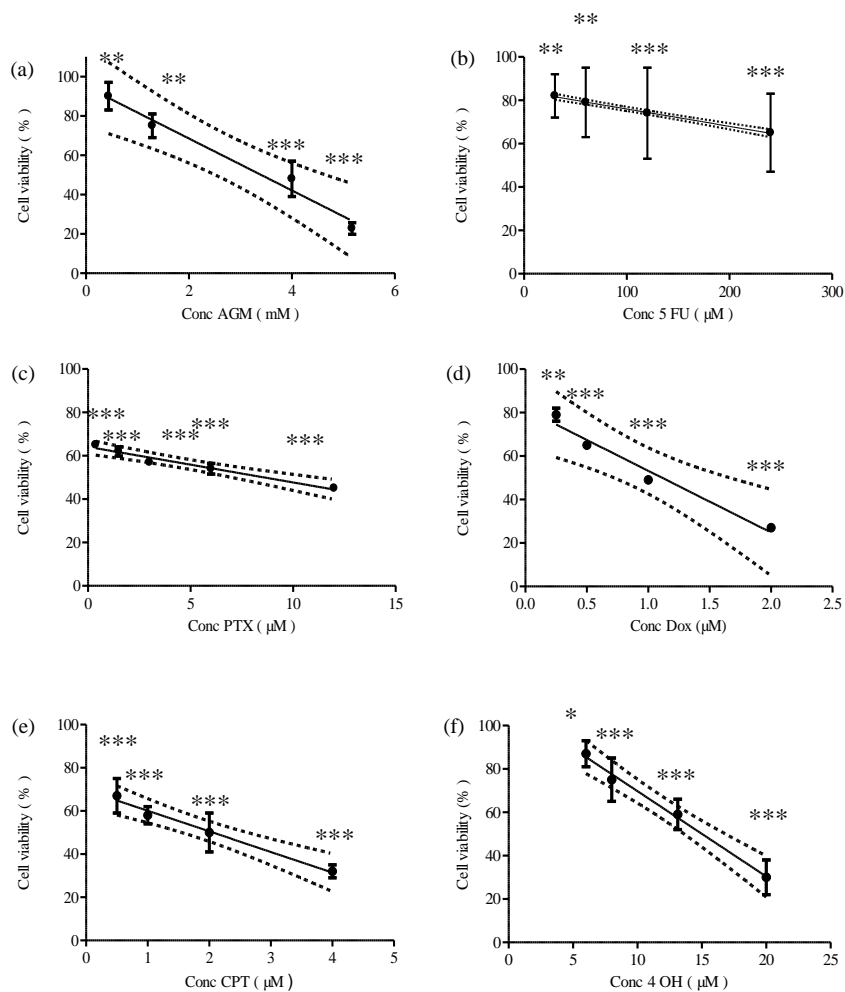
Figure 7.4. Determination of the IC50 value for each compound in MDA MB 231 cell line. Panel (a) shows the IC50 of AGM (IC50 = 3,78 mM, R^2 = 0,9328), panel (b) shows the IC50 of 5-FU (IC50 = 425 µM, R^2 = 0,9976); panel (c) shows the IC50 of PTX (IC50 = 7,6 µM, R^2 = 0,947), panel (d) shows the IC 50 of (Dox IC50 = 1,078 µM, R^2 = 0,9394), panel (e) shows the IC 50 of CPT (IC50 = 2,058 µM, R^2 = 0,9857) and panel (f) shows the IC50 of 4 OH (IC50 = 15 µM, R^2=0,9936). Results are expressed as mean ± SD where n = 4 experiments per group and significances calculated was done by one-way anova and P*** < 0,001, P* *< 0,01, P* < 0,05.

202

In MDA MB 231 cells, an IC50 value was able to be reached for AGM (3738 µM) but not for Exe. However, to keep coherence within the study the AGM concentration used for the HTPS combination studies was the same as in MCF7 cells, following the same pattern chosen for the selected aromatase enzyme inhibitors. Finally, as in the MCF 7 cells, the 5-FU IC50 was very high (450 µM) and therefore this compound was not taken further.

Table 7.3. Summary of the IC50 values obtained with selected compounds in both cell lines.

	IC50 (MCF7)	IC50 (MDA MB 231)
Dox	11 µM	1,1 µM
CPT	0,7 µM	2,1 µM
5-FU	> 20 µM	425 µM
PTX	> 18 µM*	7,6 µM
4 OH	15 µM	15 µM
Exe	> 1000 µM	> 1000 µM
AGM	> 3738 µM	3402 µM

 * Concentration inducing only 40 % of cell death as the IC50 was not reached.

7.3. Evaluation of drug combinations

As described above, in order to identify possible synergic combinations (chemo ± endocrine therapy) a HTPS experiment was performed with 3 different drug concentrations: (i) concentration inducing 70% cell death (IC70, Conc 1), except in the case of PTX where IC40 in MCF7 cells or IC60 in MDA MB 231 cells was used instead due to solubility issues, (ii) the IC50 concentration (Conc 2) and, (iii) the concentration triggering 35% cell death (IC35, Conc 3). The PTX in MCF7 cells induced only 40% cell death therefore Conc 1 and Conc 2 induced the same cell death and Conc 3 was equivalent at 90 % of cell survival.

Table 7.4. Concentration chosen for new combination in MCF 7 and MDA MB 231 cell lines.

	MDA MB 231		MCF7	
	Conc	Cell death	Conc	Cell death
Dox 1 (IC70)	2 μM	70 %	22 μM	75 %
Dox 2 (IC50)	1 μM	50 %	11 μM	50 %
Dox 3 (IC35)	0,5 μM	35 %	2,2 μM	25 %
CPT 1 (IC70)	4 μM	70 %	5 μM	70 %
CPT 2 (IC50)	2 μM	50 %	0,7 μM	50 %
CPT 3 (IC35)	0,5 μM	33 %	0,05 μM	30 %
PTX 1 (IC60)	12 μM	60 %	18 μM	40 %
PTX 2 (IC50)	7,6 μM	50 %	12 μM	40 %
PTX 3 (IC35)	0,7 μM	35 %	2,4 μM	15 %
AGM 1	4,3 μM	0 %	4,3 μM	0 %
AGM 2	0,86 μM	0 %	0,862 μM	0 %
AGM 3	0,172 μM	0 %	0,172 μM	0 %
Exe 1	0,164 μM	0 %	0,164 μM	0 %
Exe 2	0,033 μM	0 %	0,033 μM	0 %
Exe 3	0,006 μM	0 %	0,006 μM	0 %
4 OH 1 (IC70)	20 μM	70 %	18 μM	90 %
4 OH 2 (IC50)	15 μM	50 %	15 μM	50 %
4 OH 3 (IC25)	8 μM	25 %	10 μM	20 %

7.3.1. Evaluation of new combinations in MCF7 cell line.

For each chemotherapeutic agent concentration, the combination with the three endocrine agents at all concentrations was evaluated. The aim was to find new synergisms, drug combinations capable of enhancing the antitumour activity if compared with the parent single drugs.

Surprisingly, in both cell lines, only the combination of a chemotherapeutic agent with 4 OH showed synergism. A careful statistic analysis was carried out to evaluate if the differences observed in cell viability with the designed combination in comparison to the single drug were significant. The level of statistical significance was determined by analysis of variance (ANOVA) followed by Dunnett's t-test for multiple comparisons. P*** < 0,001, P** < 0,01, P* <0,05, ns non-significative.
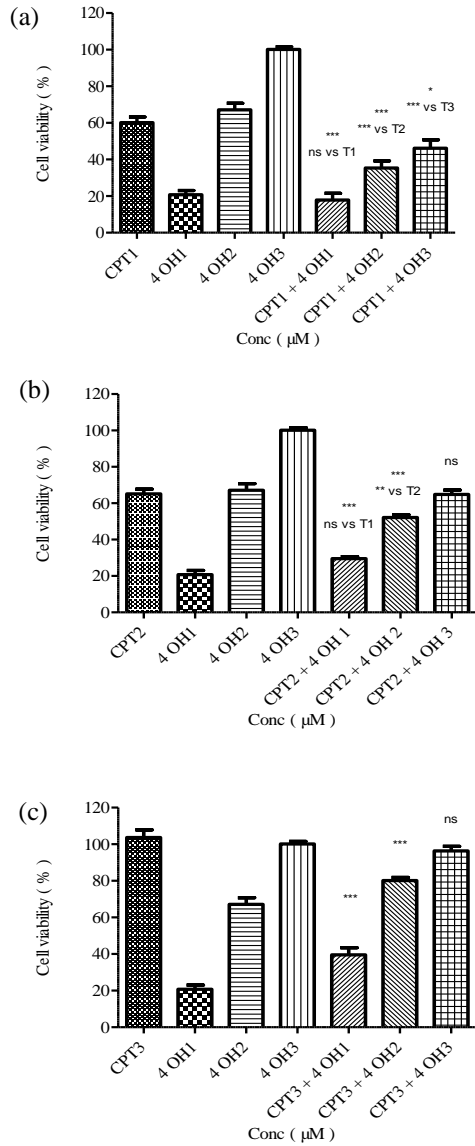
Figure 7.5. Evaluation of the combination formed by CPT with 4 OH in MCF 7 cell line. CPT1 = 5 μM, CPT2 = 0,7 μM and CPT3 = 0,05 μM. 4 OH1 = 18 μM, 4 OH2 = 13 μM and 4 OH3 = 10 μM. Panel (a) shows the effect of CPT1 and 4 OH1, 4 OH2 and 4 OH3 on cell viability alone and in combination. Panel (b) shows the effect of CPT2 with 4 OH1, 4 OH2 and 4 OH3 on cell viability alone and in combination. Panel (c) shows the effect of CPT3 with 4 OH1, 4 OH2 and 4 OH3 on

cell viability alone and in combination. Results are expressed as mean ± SD where n = 3 experiments per group and significances calculated by one-way ANOVA, P*** < 0,001, P* < 0,05.

As it can be seen in figure 7.10., the first star represented the significance of the combination compared to the single chemotherapeutic agent. And the second level of stars represented the significance of the combination vs. 4 OH. For example, in figure 7.5.a., the cytotoxicity induced with the combination CPT1 + 4 OH1 in comparison with CPT1 was significant (P***). However, the combination CPT1 + 4 OH1 in comparison with 4 OH1 alone was not significant (ns). Following our criteria, this combination was considered not synergistic as significant differences should be obtained with both single drugs.

Whereas the cell viability obtained for all 4 OH concentrations was in good agreement with our previous results (IC50 determination), the values obtained for CPT differed from those expected. Unfortunately, a possible experimental error could take place here but we decided to move forward with IC40 as CPT1, IC60 as CPT2 and IC50 as CPT3 instead of IC70, IC50 and IC35 and in any case explore possible synergisms. Taking these modifications into account, the combinations inducing a greater cell death were: (i) CPT1 (5 µM) + 4 OH2 (13 µM) (*** / ***) with 40% cell viability and (ii) CPT2 (0,7 µM) + 4 OH2 (13 µM) (* / ***) with a resulting 50% cell viability. In both cases the cell survival achieved with the combination was significantly lower than that with the single treatments however, CPT1 + 4 OH2 showed the best significance and therefore selected as possible drug combination for future conjugations.

Figure 7.6. Evaluation of the combination Dox with 4 OH in MCF7 cell line. Panel (a) shows the effect of the combination of Dox at Dox1 = 22 μM with different concentrations of 4 OH, 4 OH1 = 18 μM, 4 OH2 = 13 μM and 4 OH3 = 10 μM. Panel (b) shows the effect of the combination of Dox at Dox2 = 11 μM with different concentrations of 4 OH, 4 OH1 = 18 μM, 4 OH2 = 13 μM and 4 OH3 = 10 μM. Panel (c) shows the effect of the combination of Dox at Dox3 = 2,2 μM with

different concentrations of 4-OH, 4 OH1 = 18 μM, 4 OH2 = 13 μM and 4 OH3 =10 μM. Results are expressed as mean ± SD where n = 3 experiments per group and significances calculated by one-way ANOVA and ns: non significant, $P^{***} < 0,001$, $P^* < 0,05$.

As it can be seen in figure 7.6. several Dox + 4 OH combinations showed possible synergisms. These are summarised in Table 7.5.

Table 7.5. Possible synergistic combinations for Dox and 4 OH obtained after data mathematical treatment.

Combination	Cell viability (%)
Dox1 + 4 OH1	10% (***/***)
Dox1 + 4 OH2	12% (***/***)
Dox2 + 4 OH2	30% (***/***)
Dox3 + 4 OH2	35% (***/***)
Dox3 + 4 OH3	50% (***/***)

Although all 5 combinations showed in Table 7.5. demonstrated similar significances, looking at possible combination conjugates as clinical candidates and to prevent side toxicities due to the use of high Dox doses our selected combinations in this case were Dox3 (2,2 μM) + 4 OH2 (13 μM) and Dox2 (11 μM) + 4 OH2 (13 μM).

208

Figure 7.7. Evaluation of the combination of PTX with 4 OH in MCF7 cell line. Panel (a) shows the effect of the combination of PTX at PTX1 = 18 μM with different concentrations of 4 OH, 4 OH1 = 18μM, 4 OH2 = 13μM and 4 OH3 = 10μM. Panel (b) shows the effect of the combination of PTX at PTX2 = 12 μM with different concentrations of 4 OH, 4 OH1 = 18 μM, 4 OH2 = 13 μM and 4 OH3 = 10 μM. Panel (c) shows the effect of the combination of PTX at PTX3 = 2,4 μM with different concentrations of 4 OH, 4 OH1 = 18 μM, 4 OH2 = 13 μM and 4 OH 3 = 10 μM. Results are expressed as mean ± SD where n = 3 experiments per group and significances calculated by one-way ANOVA and ns: non significant, P*** < 0,001, P* < 0,05.

PTX was the chemotherapeutic agent showing better results upon combination with 4 OH in MCF7 cells. As mentioned aboved it was not able to achieve PTX IC50 value due to solubility issues, however with the presence of even the smallest concentration of 4 OH its cytotoxic potential was significantly enhanced. The best possible combinations after mathematical treatment are shown in Table 7.6.

209

Table 7.6. Possible synergistic combinations for paclitaxel and 4-OH-Tamoxifen.

Combination	Cell viability (%)
PTX1 + 4 OH1	10% (**/***)
PTX1 + 4 OH2	20% (***/***)
PTX2 + 4 OH1	10% (**/***)
PTX2 + 4 OH2	25% (***/***)
PTX3 + 4 OH2	45% (**/***)

The combinations with the highest PTX concentration, PTX1 (18 μM), were very efficient but even with PTX2 (12 μM) similar results could be achieved being more beneficial as lower PTX doses would be required for the same therapeutic output. The combination PTX3 (2,4 μM) + 4 OH2 (13 μM) induced 45% cell viability with a really low PTX concentration.

Summarising, in MCF7 cells the best drug combinations encountered and therefore selected for future polymer conjugate design were: CPT1 (5 μM) + 4 OH2 (13 μM) (*** / ***), CPT2 (0,7 μM) + 4 OH2 (13 μM), Dox3 (2,2 μM) + 4 OH2 (13 μM) (*** / ***), PTX2 (12 μM) + 4 OH1 (18 μM) and PTX3 (2,4 μM) + 4 OH2 (13 μM) and PTX2 + 4 OH2 (*** / ***).

7.3.2. Evaluation of new combinations in MDA MB 231 cell line.

As seen for MCF7 cells, in the case of MDA MB 231 cell line only combinations of chemotherapeutics with 4-OH showed synergisms if compared with the parent single compounds. Therefore only the results obtained with 4 OH are shown here.
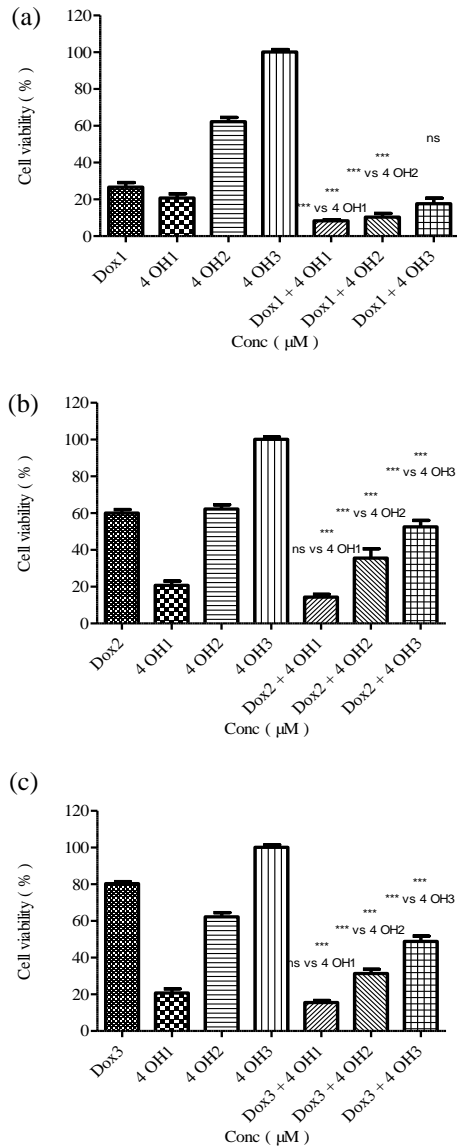
Figure 7.8. Evaluation of the combination PTX with 4 OH in MDA MB 231 cell line. Panel (a) shows the effect of the combination of PTX at PTX1 = 12 μM with different concentrations of 4 OH, 4 OH1 = 20 μM, 4 OH2 = 15 μM and 4 OH3 = 8 μM. Panel (b) shows the effect of the combination of PTX at PTX2 = 7,6 μM with
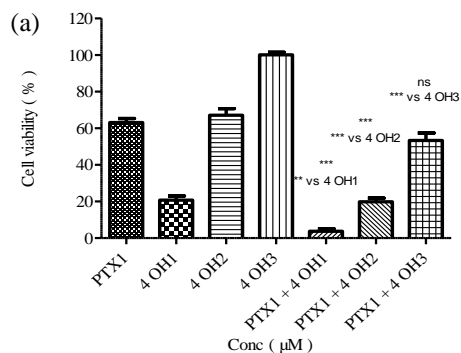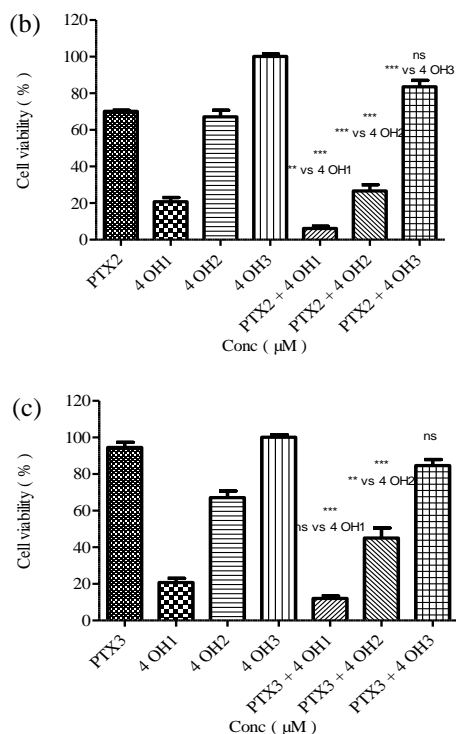
different concentrations of 4 OH, 4 OH1 = 20 μM, T4 OH2 = 15 μM and 4 OH3 = 8 μM. Panel (c) shows the effect of the combination of PTX at PTX3 = 0,7 μM with different concentrations of 4 OH, 4 OH1 = 20 μM, 4 OH2 = 15 μM and 4 OH3 =8 μM. Results are expressed as mean ± SD where n = 3 experiments per group and significances calculated by one-way ANOVA and ns: non significant, $P^{***} < 0,001$, $P^* < 0,05$.

Data obtained with single drugs was in good agreement with our previous data. In this case the selected combinations are shown in Table 7.7.

Table 7.7. Possible combinations for paclitaxel and 4-OH-Tamoxifen after mathematical treatment in MDA MB 231 cell line.

Combination	Cell viability (%)
PTX1 + 4 OH1	10% (***/**)
PTX1 + 4 OH2	20% (***/**)
PTX1 + 4 OH3	50% (**/***)
PTX2 + 4 OH1	10% (***/*)
PTX2 + 4 OH2	20% (***/**)
PTX2 + 4 OH3	50% (*/***)
PTX3 + 4 OH1	15% (***/**)

Summarising, the best choice was found to be the combination PTX 2 (7,6 μM) + 4 OH 2 (15 μM) showing a 80% cell death in comparison with the parent single drugs with only a 50%. An even better combination could be PTX3 (0,7 μM) + 4 OH1 (20 μM) with the induction of a 85% cell death with a low PTX concentration.

212
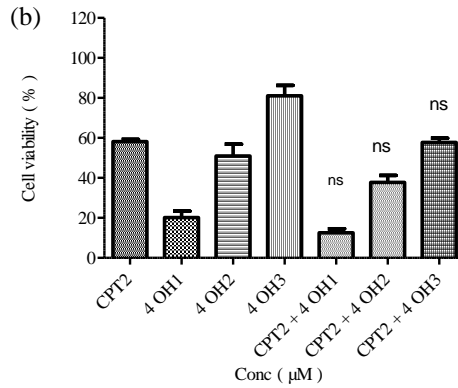
Figure 7.9. Evaluation of the combination CPT with 4 OH in MDA MB 231 cell line. Panel (a) shows the effect of the combination of CPT at CPT1 = 4 μM with different concentrations of 4 OH, 4 OH1 = 20 μM, 4 OH2 = 15 μM and 4 OH3 = 8 μM. Panel (b) shows the effect of the combination of CPT at CPT2 = 2 μM with different concentrations of 4 OH, 4 OH1 = 20 μM, 4 OH2 = 15 μM and 4 OH3 = 8 μM. Panel (c) shows the effect of the combination of CPT at CPT3 = 0,5 μM with different concentrations of 4 OH, 4 OH1 = 20 μM, 4 OH2 = 15 μM and 4 OH3 =8 μM. Results are expressed as mean ± SD where n = 3 experiments per group and significances calculated by one-way ANOVA and ns: non significant, P*** < 0,001, P* < 0,05.

With camptothecin, the only combination which showed a significant synergistic effect was CPT1 (4 μM) + 4 OH1 (20 μM) (*** / *). Nevertheless, the result was obtained with the highest concentration of both drugs, and comparing with

the effect obtained from 4 OH1 alone the difference was not so significant. Therefore, CPT1 + 4 OH1 was not selected.

(a)

Cell viability (%)

Conc (μM)

(b)

Cell viability (%)

Conc (μM)

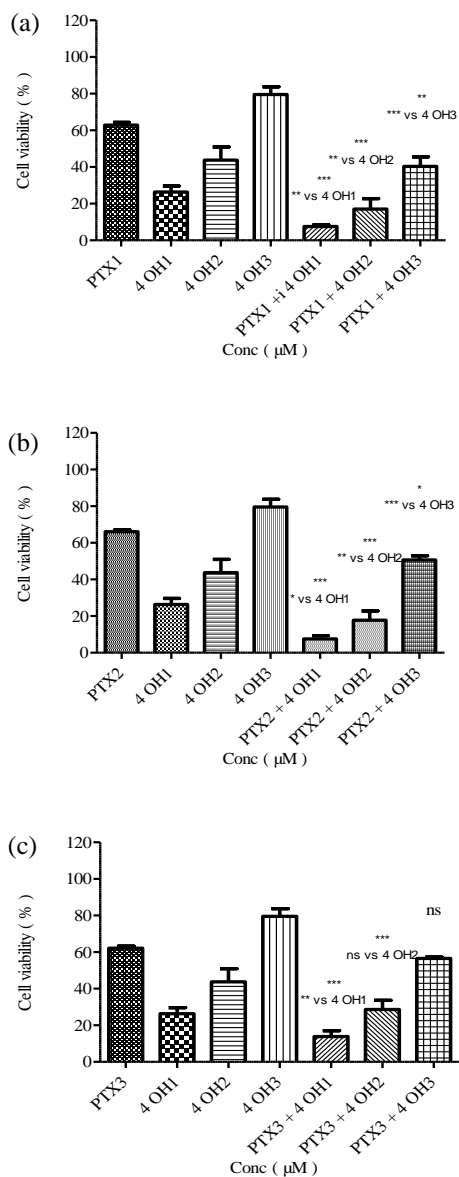(c)

Cell viability (%)

Conc (μM)
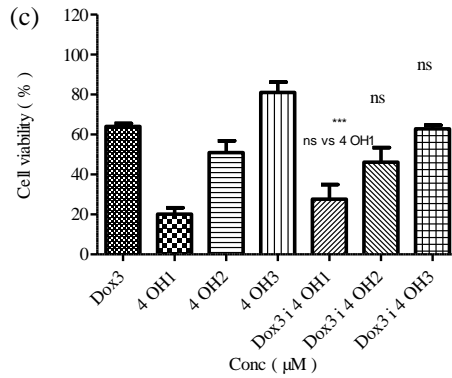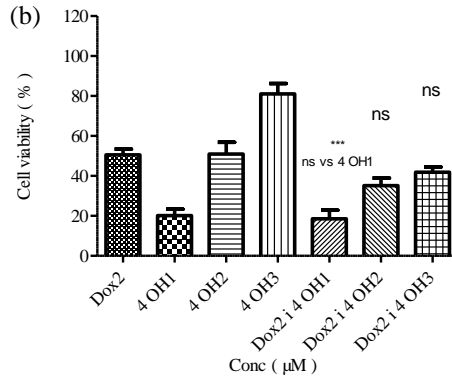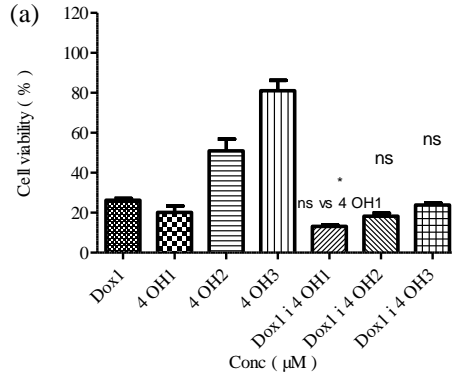
Figure 7.10. Evaluation of the combination of Dox with 4 OH in MDA MB 231 cell line. Panel (a) shows the effect of the combination of Dox at Dox1 = 2 μM with different concentrations of 4 OH, 4 OH1 = 20 μM, 4 OH2 = 15 μM and 4 OH3 = 8 μM. Panel (b)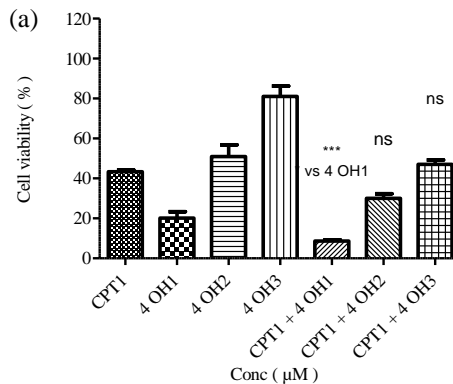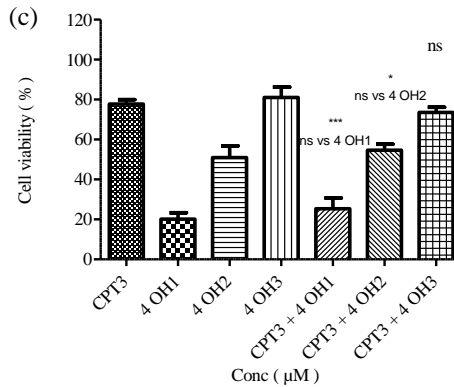 shows the effect of the combination of Dox at Dox2 = 1 μM with different concentrations of 4 OH, 4 OH1 = 20 μM, 4 OH2 = 15 μM and 4 OH3 = 8 μM. Panel (c) shows the effect of the combination of Dox at Dox3 = 0,5 μM with different concentrations of 4 OH, 4 OH1 = 20 μM, 4 OH2 = 15 μM and 4 OH 3 = 8 μM. Results are expressed as mean ± SD where n = 3 experiments per group and significances calculated by one-way ANOVA and ns: non significant, $P*** < 0,001$, $P* < 0,05$.

The combination of Dox and 4 OH did not give any benefit if compared with the single drugs in MDA MB 231. This cell line seems to be highly responsive to Dox being this the possible explanation (Dox1 and Dox2).

To conclude, in MDA MB 231 cells we were not able to identify any outstanding combination with AGM or Exe due to the absence of aromatase enzyme in this cell line, the small concentration used (reported concentration needed to inhibit the aromatase enzyme) and their non cytotoxic behaviour against MDA MB 231 cells. Unexpectedly, 4 OH was cytotoxic against MDA MB 231 cells (ER-) and more importantly, in combination with PTX cytotoxic synergism was observed. The best combination achieved and selected for future polymer conjugation were PTX2 (7,6 μM) + 4 OH2 (15 μM) (*** / **) and PTX3 (0,7 μM) + 4 OH1 (20 μM) (*** / **).

7.4. Discussion

In order to find new drug combinations for the future design of PGA-based combination conjugates, an HTPS experiment including four different chemotherapeutics and three different endocrine agents was performed in two different cell lines MCF7 (ER +) and MDA MB 231 (ER-). The chemotherapeutics chosen were Dox, PTX, CPT and 5-FU and as endocrine agents AGM, Exe and 4 OH were selected. Firstly, the IC 50 value for each drug was determined. Exe and AGM were cytostatic compounds, therefore, their IC50s were not reach (> 1000 μM for Exe and > 3738 μM for AGM). In this case, the concentration chosen for further experiments was that reported in

literature as the one required to achieve the inhibition of 100% of the aromatase enzyme activity, 0,862 μM for AGM and 0,033 μM for Exe. Within the chemotherapeutics, 5-FU showed a high IC50 and therefore discharged for further studies. Due to solubility issues the IC50 for PTX was not reached and the maximum concentration used for the combination studies was that only triggering 40% cell death in MCF7 cells. Once the IC50 values were identified, three different concentrations for each drug were chosen to proceed with the combination studies (IC70, IC50 and IC35; concentrations showing a 70%, 50% and 35% cell death, respectively). Each selected concentration of the chemotherapeutic agent was combined with all concentrations of the endocrine agent and the effect on cell death was studied. In all cases, only combinations with the ER blocker 4 OH showed significant cytotoxicities if compared with the parent single drugs. This was expected as for the ER+ character of MCF7 cells. Even if MCF7 possess a basal expression of aromatase enzyme (Greco et al., 2007), this is not sufficient to observe AI effects as it could be in the transfected MCF7 Ca cell line (these studies are ongoing). Surprisingly, in the ER- MDA MB 231 cell line a cytotoxic behaviour for 4 OH was also observed. In the ATCC web site (http://www.atcc.org), the MDA MB 231 cell line is described as ER-, epidermal growth factor receptor (EGFR) positive and transforming growth factor alpha (TGF- α) receptor positive. Taking into account the bibliography on ER negative breast cancer cell lines, the 4 OH could be involved in other pathways apart from ER and also the cross-talk between EGFR and ER (Nicholson and Gee, 2000) could play a role here. It has been already described that 4 OH is capable to inhibit cell proliferation via up-regulation of growth factor (TGF- β) and (TGF- α) involved in growth inhibition (Butta et al., 1992; MacGregor Schafer et al., 2001) and down-regulation of the potent mitogen IGF II which promoted cell proliferation (Seeger et al., 2003). 4 OH also induced apoptosis by inhibiting kinase C protein involved in oncogene transcription and by binding calmodium, a calcium binding protein involved in several physiological processes such as inflammation or apoptosis (Gelmann, 1996). All these reported results could explained our data of 4 OH in MDA MB 231 cells.

The best identified anticancer combinations in MCF 7 cell line were (i) CPT1 (5µM) + 4 OH2 (13 µM) with a 70 % cell death, (ii) CPT 2 (0,7 µM) + 4 OH2 (13 µM) with a 50 % cell death, (iii) PTX 2 (12 µM) + 4 OH 1 (18 µM) with a 90% cell death, (iv) PTX 3 (2,4 µM) + 4 OH 3 (10 µM) with a 30 % cell death, and (v) Dox 3 (2,2 µM) + 4 OH 2 (13 µM) with a 35 % cell death. Looking at possible risk-benefit ratios, those combinations involving lower chemotherapeutic concentration could offer benefits in front of the others. So, trying to choose the best of all of them we considered CPT2 + 4 OH2, PTX3 + 4 OH3 and Dox3 + 4 OH2 due to the high cell death percentage achieved with a low chemotherapeutic agent concentration. Another really efficient combination was PTX2 + 4 OH1 with a 90% cell death using only PTX IC60 concentration. Therefore, our first choice for PGA-based combination conjugate design would be PTX2 + 4 OH1 in a ratio 1:1,3. This combination was ratified in MDA MB 231 cells.

7.5. Bibliography.

Álvarez, P., Marchal, J.A., Boulaiz, H., Carrillo, E., Vélez, C., Rodríguez-Serrano, F., Melguizo, C., Prados, J., Madeddu, R., and Aranega, A. (2012). "5-Fluorouracil derivatives: a patent review." Expert Opin Ther Pat 22(2): 107-123.

Bowles, E.J., Buist, D.S., Chubak, J., Yu, O., Johnson, J., Chestnut, J., and Boudreau, D.M. (2012). "Endocrine therapy initiation from 2001 to 2008 varies by age at breast cancer diagnosis and tumor size." J Oncol Pract 8(2): 113-120.

Butta, A., MacLennan, K., Flanders, K.C., Sacks, N.P.M., Smith, I, McKinna, A, Dowsett, M, Wakefield, L.M., Sporn, M.B., Baum, M., and Colletta A.A. (1992). "Induction of transforming growth factor beta 1 in human breast cancer in vivo following tamoxifen treatment." Cancer Res 52(15): 4261-4264.

Gelmann, E. P. (1996). "Tamoxifen induction of apoptosis in estrogen receptor-negative cancers: new tricks for an old dog?" J Natl Cancer Inst 88(5): 224-226.

Greco, F., Vicent, M.J., Gee, S., Jones, A.T., Gee, J., Nicholson, R.I., and Duncan, R. (2007). "Investigating the mechanism of enhanced cytotoxicity of HPMA copolymer-Dox-AGM in breast cancer cells." J Control Release 117(1): 28-39.

http://www.atcc.org.

http://www.pfizer.ca/en/our_products/monograph/123 (2009). "AROMASIN (exemestane)."

Jeansonne, D.P., Koh, G.Y., Zhang, F., Kirk-Ballard, H., Wolff, L., Liu, D., Eilertsen, K. and Liu, Z. (2011). "Paclitaxel-induced apoptosis is blocked by camptothecin in human breast and pancreatic cancer cells." Oncol Rep 25(5): 1473-1480.

Jordan, V. C. (2003). "Antiestrogens and selective estrogen receptor modulators as multifunctional medicines. 2. Clinical considerations and new agents." J Med Chem 46(7): 1081-1111.

Jordan, V. C. and Brodie, A.M. (2007). "Development and evolution of therapies targeted to the estrogen receptor for the treatment and prevention of breast cancer." Steroids 72(1): 7-25.

Liu, L.F., Desai, S.D., Li, T.K., Mao, Y., Sun, M., and Sim, S.P. (2000). "Mechanism of action of camptothecin." Ann N Y Acad Sci 922: 1-10.

MacGregor Schafer, J., Liu, H., Levenson, A.S., Horiguchi, J., Chen, Z., and Jordan, V.C. (2001). "Estrogen receptor alpha mediated induction of the transforming growth factor alpha gene by estradiol and 4-hydroxytamoxifen in MDA-MB-231 breast cancer cells." J Steroid Biochem Mol Biol 78(1): 41-50.

Nicholson, R. I. and Gee, J.M. (2000). "Oestrogen and growth factor cross-talk and endocrine insensitivity and acquired resistance in breast cancer." Br J Cancer 82(3): 501-513.

Njar, V.C. and Brodie, A.M. (1999). "Comprehensive pharmacology and clinical efficacy of aromatase inhibitors." Drugs 58(2): 233-255.

Rao, R.D. and Cobleigh, M.A. (2012). "Adjuvant endocrine therapy for breast cancer." Oncology (Williston Park) 26(6): 541-547, 550, 552 passim.

Seeger, H., Diesing, D., Gückel, B., Wallwiener, D., Mueck, A.O., and Huober, J. (2003). "Effect of tamoxifen and 2-methoxyestradiol alone and in combination on human breast cancer cell proliferation." J Steroid Biochem Mol Biol 84(2-3): 255-257.

Gu, R., Jia, W., Zeng, Y., Rao, N., Hu, Y., Li, S., Wu, J., Jin, L., Chen, L., Long, M., Chen, K., Chen, L., Xiao, Q., Wu, M., Song, E., and Su, F. (2012). "A comparison of survival outcomes and side effects of toremifene or tamoxifen

therapy in premenopausal estrogen and progesterone receptor positive breast cancer patients: a retrospective cohort study." BMC Cancer 12(1): 161.

Tan, A.R. and Swain, S.M. (2001). "Adjuvant chemotherapy for breast cancer: an update." Semin Oncol 28(4): 359-376.

Vicent, M.J., Greco, F., Nicholson, R.I., Paul, A., Griffiths, P.C., and Duncan, R. (2005). "Polymer therapeutics designed for a combination therapy of hormone-dependent cancer." Angew Chem Int Ed Engl 44(26): 4061-4066.

Zilli, M., Grassadonia, A., Tinari, N., Di Giacobbe, A., Gildetti, S., Giampietro, J., Natoli, C., Iacobelli, S. and Consorzio Interuniversitario Nazionale per la Bio-Oncologia (CINBO). (2009). "Molecular mechanisms of endocrine resistance and their implication in the therapy of breast cancer." Biochim Biophys Acta 1795(1): 62-81.

Chapter 8. General discussion.

8.1. Discussion.

Statistics recently reported (www.cancerresearchuk.org/cancer-info/cancerstats/reports/about-cancerstat-reports) state that the number of people who will get cancer during their lifetime will increase to nearly half the population by 2020, mostly due to the ageing population. Breast cancer is one of the most common cancers in women and although more patients are now surviving this disease compared to 20 years ago, in advanced stages (III and IV) the 5-year survival rate achieved is still really low ($\approx 20\%$). Therefore, more efficient therapeutic approaches are still needed and we believe nanomedicine and in particular polymer therapeutics could offer significant clinical benefits. Different types of breast cancer have been described (Luminal A, B, HER2 + and the triple negative); however this study was focused on hormone dependent breast cancer (Luminal A and B) as it is one of the most common.

Due to the molecular complexity of cancer combination approaches are required. The discovery of new molecular targets and the subsequent development of novel anticancer agents are opening new possibilities for drug combination therapy as anticancer treatment. Polymer–drug conjugates are well established for the delivery of a single therapeutic agent, but only in very recent years their use has been extended to the delivery of multi-agent therapy. The use of polymer-drug conjugates in combination therapy represents an important opportunity to enhance tumour response rates. These early studies revealed the therapeutic potential of this application but raised new challenges (namely, drug loading and drug ratio, characterisation, and development of suitable carriers) that need to be addressed for a successful optimisation of the system (Greco and Vicent, 2009).

The first polymer drug combination conjugate HPMA copolymer-AGM-Dox was described by Dr Vicent et al, showing higher cytotoxic effects in breast cancer cells than the parent HPMA copolymer-Dox conjugate, thus confirming the necessity to move from single drug to combination therapy (Vicent et al., 2005; Greco et al., 2005; Greco et al., 2007). In a first stage of this project and in order to confirm the synergistic effect of HPMA copolymer-AGM-Dox on cell viability inhibition observed in cell models, two *in vivo*

orthotopic breast cancer models were stablished, fully characterised (regarding vasculature, growth rate and histological parameters) and used to achieve *in vivo* proof of concept for anticancer synergism with combination conjugates. This approach would also help us to elucidate those mechanisms responsible for drug synergism and consequently, it would help in the design of novel generation of polymer-based combination conjugates.

Two different breast cancer animal models were stablished in order to carry out these studies, both of them orthotopic but with very different behaviour in order to represent better clinical situations: (i) a post menopausal human MCF7 Ca cells induced model (Yue et al., 1994; Brodie et al., 2007) and (ii) an aggressive metastatic murine 4T1 model (Aslakon and Miller, 1992; Yang et al., 2004; Tao et al., 2008). The transfected MCF7 Ca human tumour cell line induced slow and heterogeneous growing tumours in ovarectomised nude mice treated daily with hormone-replacement therapy to mimic postmenopausal patient situation. The evaluation of single drug conjugate HPMA copolymer-Dox, combination drug conjugate HPMA copolymer-AGM-Dox and free Dox in this model, demonstrated greater efficiency in comparison to free Dox regarding tumor growth inhibition and toxicological profiling. However, no differences between both cojugates were observed. With the 4T1 model, the idea was to reproduce breast tumours at advanced stages in a fully immunocompetent environment. 4T1 *in vivo* tumour model has been described to metastasize in lung, bone, liver and brain as occurs in human breast cancer patients (Tao et al., 2008; Gao et al., 2011). In this fast growing aggressive model a significant difference on tumour growth was obtained with both conjugates in comparison to control and free Dox. Furthermore, tumour growth inhibition achieved by both conjugates was statistically analysed, and HPMA copolymer-AGM-Dox combination conjugate proved to be more efficient reducing tumour growth than HPMA copolymer-Dox conjugate. These results confirm *in vitro* data and importantly, allowed to achieve *in vivo* proof of concept for antitumour synergism with polymer-drug combination conjugates. Conjugate whole body biodistribution and half-life were also studied together with compound toxicological profile. Both conjugates showed greater tumour

accumulation than the free Dox, being the drug better retained in the tumour with the combination conjugate maybe due to a slightly greater half-life. Important heart accumulation observed by free Dox was completely diminished upon conjugation in good agreement with data already reported (Vassey et al., 1994) and clearly explaining the better toxicological profile obtained with the conjugates.

Once *in vivo* proof was achieved, the molecular mechanisms responsible for the observed antitumour synergim were also studied trying to better understand the parameters that would help us in the future design of polymer-based combination conjugates. This was performed looking at key protein expression in 4T1 tumour tissues with and without treatments at 2 different time points; end of the experiment (16 days) and at 48 h after the last treatment injection (8 days) trying to correlate with data in cell models. It is important to point out that pharmacokinetics play a major role in this complex process, not only at the whole organism level (EPR effect) but also at cellular level (uptake and drug release kinetics). When comparing free drug with polymer conjugates and also cell data with *in vivo* data we have to be aware that it is not easy to select all time points for study and to draw final conclusion. In any case, we believe the results obtained here under the parameters considered represent some of the key mechanisms responsible for the antitumour activity differences observed.

First, cell death signalling pathways were explored. At short-term both conjugates and free Dox seems to induce tumour cell death by a mix mechanism using both apoptosis and autophagy. However, at long-term autophagy is the main mechanism involved in cell death when animals are treated with the combination conjugate HPMA-copolymer-AGM-Dox in contrast to HPMA copolymer-Dox conjugate where apotosis plays a major role. A difference was also obtained when looking at proteins involved in the angiogenic and proliferative pathways. HPMA-copolymer-AGM-Dox induced from early stage an inhibition of VEGF protein expression as a result of two main phenomena: (i) the oestrogen reduction induced by AGM due to the relation between oestrogen levels and VEGF expression (Kazi and Koos, 2007; Koos, 2010; Koos, 2011) and, (ii) the inhibition on p-Akt protein expression and consequently the down

regulation of p-Akt target genes including VEGF protein expression (Pore et al., 2004; Pore et al., 2006). At long-term, VEGF inhibition was observed for all compounds studied (conjugates and free Dox). Importantly, preliminary results looking at iNOS protein expression seemed to indicate that HPMA copolymer-AGM-Dox combination conjugate is also involved in cell migration and dissemination in a greater manner than the single HPMA copolymer-Dox conjugate or free Dox. Consequently, the greater antitumour effect observed with the HPMA copolymer-AGM-Dox combination conjugate in comparison to the single HPMA copolymer-Dox conjugate, could be justified on one side by the different Dox tumour accumulation observed for the combination conjugate that could induce a faster and longer-lasting antitumour effect. On the other hand, looking at the molecular mechanisms involved, the combination conjugate showed a stronger inhibition on the proliferative-metastatic processes modulated by angiogenesis (Kazi and Koos, 2007; Koos, 2010; Koss, 2011) and this effect was complemented by a major role of autophagy *vs.* apoptosis. These features could clearly enhance its antitumour efficiency in comparison with the single conjugate. More mechanistics studies are ongoing trying to corroborate these statements and to better understand this complex process.

Despite the good results achieved with the model combination conjugate HPMA copolymer-AGM-Dox, some limitations need also to be considered. Biopersistent carriers, such as PEG or HPMA copolymers, present disadvantages if chronic parenteral administration and/or high doses are required. Preclinical evidence of intracellular vacuolation with certain PEG-protein conjugates (Knop et al.,2010) is raising awareness of the potential advantage of biodegradable polymers regarding safety benefit apart from the possibility to use higher molecular weight carriers allowing PK optimisation (Barz et al., 2011). Taking this into account and aiming to move a step further with our polymer-based combination strategy, we substituted the non-biodegradable HPMA copolymer by the multivalent, biodegradable poly-L-glutamic acid (PGA) as carrier. Due to its intrinsic characteristics, PGA presents a more favourable pharmacological profile as already demonstrated in the clinics with Opaxio[TM] (PGA-Paclitaxel conjugate, Cell Therapeutics Inc.) in phase III

clinical trial and recently designated as orphan drug in combination with radiotherapy for glioblastoma (Singer et al., 2003; Oldham et al., 2006; http://www.celltherapeutics.com/pdf/OPAXIO_facts-4pg.pdf.2008).

In Chapter 6, the synthesis, characterisation and biological evaluation of a family of PGA-AGM-Dox derivatives have been described including three different subfamilies: PGA-X-AGM, PGA-Y-Dox and PGA-X-AGM-Y-Dox. After their structural evaluation and cell viability inhibition analysis against MCF7 Ca and 4T1 cell lines, two combination candidates ratify the synergism of AGM + Dox cocktail and as in the case of HPMA copolymer-AGM-Dox conjugate, they also demonstrated the importance of conjugate solution conformation and, consequently, of the drug release kinetics. The selected candidates were PGA-G-AGM-Dox and PGA-GG-AGM-Dox, with IC50 values of 0,0038 and 0,0042 mg/mL Dox equivalent, respectively against MCF7 Ca cells and CI values of 0,21 and 0,22, respectively. Then, PGA-G-AGM-Dox combination conjugate was evaluated *in vivo* to explore its antitumor activity versus PGA-Dox single conjugate using the same protocol followed for HPMA copolymer-AGM-Dox in the 4T1 mice tumour model. Due to the slower drug release kinetics of the PGA-G-AGM-Dox in comparison to the HPMA copolymer-AGM-Dox conjugate none significant differences on tumour volume were observed with all treatments compared to the control group up to day 10, except for PGA-G-AGM+PGA-Dox group, which showed an early significant down-regulation of tumour volume. However, after day 10, an interesting antitumor effect was observed with PGA-G-AGM-Dox presenting significantly better activity than PGA-G-AGM+PGA-Dox group, and consequently than the other treatments.The differences observed could be explained by a faster and greater AGM release from PGA-G-AGM in comparison to PGA-G-AGM-Dox. Indeed separately AGM release achieved 60% after 5 h when in the combination conjugate only 15% AGM was achieved at the same time. It has been already reported that AGM molecular mechanism is directly related with angiogenesis modulation in tumours (Kazi and Koos, 2007; Koos, 2010; Koss, 2011), this could easily justify the better performance at early stages of the PGA-G-AGM + PGA-Dox combination. However, the presence of both drugs in the same cell

225

could be only secured by means of PGA-G-AGM-Dox combination conjugate and this is the reason of its enhanced long-term antitumour activity. In order to improve the results obtained so far it is clear that a faster and greater AGM release combination conjugate should be designed. Ongoing experiments are directed towards this aim.

Once a clinical relevant platform was designed, as a final approach towards more efficient conjugates, novel drug combinations were evaluated to replace AGM-Dox. Our aim here was to find new drug combinations with antitumour synergistic potential that could allow the design of advanced PGA-based combination conjugates. To reach this goal in a systematic but efficient manner, a high throughput screening (HTPS) approach was implemented using 4 chemotherapeutic drugs (Dox, PTX, CPT and 5-FU) and 3 endocrine therapy agents (AGM as control, 4 OH and Exe), which were selected from the current clinical treatments for advanced breast cancer. *In vitro* evaluation was performed in two cell lines MCF7 (ER+) and MDA MB 231 (ER-). In MCF7, the better combination were PTX (2,4 µM) and 4 OH (10 µM) inducing 70% cell death, Dox (2,2 µM) and 4 OH (13 µM) with a 65% cell death. Another really efficient combination was the PTX (12 µM) and 4 OH (18 µM), which triggered a 90% cell death only with the IC60 PTX concentration. Those drug combinations in the adequate ratio (*i.e.* PTX + 4 OH, 1 : 1,5) are currently being the based of novel PGA-based combination conjugates.

8.2. Bibliography.

Aslakson, C. J. and Miller, F.R. (1992). "Selective events in the metastatic process defined by analysis of the sequential dissemination of subpopulations of a mouse mammary tumor." Cancer Res 52(6): 1399-1405.

Brodie, A., Sabnis, G., and Macedo, L. (2007). "Xenograft models for aromatase inhibitor studies." J Steroid Biochem Mol Biol 106(1-5): 119-124.

Gao, Z.G., Tian, L., Hu, J., Park, I.S., and Bae, Y.H. (2011). "Prevention of metastasis in a 4T1 murine breast cancer model by doxorubicin carried by folate conjugated pH sensitive polymeric micelles." J Control Release 152(1): 84-89.

Greco, F. and Vicent, M. J., (2009). "Combination therapy: opportunities and challenges for polymer-drug conjugates as anticancer nanomedicines." Adv Drug Deliv Rev 61(13): 1203-1213.

Kazi, A. A. and Koos, R. D. (2007). "Estrogen-induced activation of hypoxia-inducible factor-1alpha, vascular endothelial growth factor expression, and edema in the uterus are mediated by the phosphatidylinositol 3-kinase/Akt pathway." Endocrinology 148(5): 2363-2374.

Kazi, A.A., Molitoris, K.H. and Koos, R.D. (2009) "Estrogen rapidly activates the PI3K/AKT pathway and hypoxia-inducible factor 1 and induces vascular endothelial growth factor A expression in luminal epithelial cells of the rat uterus." Biol Reprod. 81(2):378-387.

Koos, R. D. (2010). "HIF-1's role in estrogen-induced VEGF expression : Implications for both normal and pathological cell proliferation." Bio of reprod. 83: 199.

Koos RD. (2011). "Minireview: Putting physiology back into estrogens' mechanism of action." Endocrinology. 152(12):4481-8.

Pore N, Liu S, Shu HK, Li B, Haas-Kogan D, Stokoe D, Milanini-Mongiat J, Pages G, O'Rourke DM, Bernhard E and Maity A. (2004) "Sp1 is involved in Akt-mediated induction of VEGF expression through an HIF-1-independent mechanism." Mol Biol Cell. 15(11):4841-4853.

Pore N, Jiang Z, Gupta A, Cerniglia G, Kao GD and Maity A. (2006) "EGFR tyrosine kinase inhibitors decrease VEGF expression by both hypoxia-inducible factor (HIF)-1-independent and HIF-1-dependent mechanisms." Cancer Res. 66(6):3197-3204.

Tao, K., Fang, M., Alroy, J., and Sahagian, G.G. (2008). "Imagable 4T1 model for the study of late stage breast cancer." BMC Cancer 8: 228.

Yang, J., Mani, S.A., Donaher, J.L., Ramaswamy, S., Itzykson, R.A., Come, C., Savagner, P., Gitelman, I., Richardson, A., and Weinberg, R.A. (2004). "Twist, a master regulator of morphogenesis, plays an essential role in tumor metastasis." Cell 117(7): 927-939.

Yue, W., Zhou, D., Chen, S., and Brodie, A. (1994). "A new nude mouse model for postmenopausal breast cancer using MCF-7 cells transfected with the human aromatase gene." Cancer Res 54(19): 5092-5095.

Chapter 9. Conclusions.

9.1. Conclusions.

- Two breast cancer *in vivo* mice models from MCF7 Ca human cell line and 4T1 murine cell line were established, optimised and fully characterised.

- *In vivo* proof of concept for synergism was achieved with HPMA copolymer-AGM-Dox conjugate, showing significant differences in tumour growth inhibition if compared with free Dox, the single conjugate (HPMA copolymer-Dox) or the combination of single conjugates (HPMA copolymer-AGM + HPMA copolymer-Dox). Important tumor recurrence in the first 5 days of treatment was also achieved for the combination conjugate in comparison to Dox in the MCF7 Ca model.

- Differences in the molecular mechanisms responsible for antitumour activity were observed for HPMA copolymer-AGM-Dox conjugate if compared with HPMA copolymer-Dox conjugate. Two days after the last injection, HPMA copolymer-AGM-Dox triggered a significant inhibition of proteins involved in angiogenesis pathways (VEGF) in comparison to HPMA copolymer-Dox and Control and therefore triggered the tumour inhibition growth before than the HPMA copolymer-Dox. This was complemented with a different cell death mechanism (autophagy *vs*. apoptosis) at long-term treatment.

- A more clinically relevant combination platform has been achieved based on the use of PGA as carrier. Three families PGA-X-AGM, PGA-Y-Dox and PGA-X-AGM-Y-Dox conjugates were successfully synthesised, fully characterised and evaluated in cell culture.

- A direct relation between solution conformation and *in vitro* activity was demonstrated for the PGA-based combination conjugates.

- The best candidate, PGA-(G-AGM)$_{5mol\%}$-(Dox)$_{5mol\%}$, was selected for *in vivo* evaluation and showed a significant inhibition on tumour growth in 4T1 mouse model 10 days after the first injection when compared to the other groups.

- New drug candidates were evaluated by means of a cell-based HTPS experiment in order to identify novel synergistic drug combinations. The best combination found was PTX + 4 OH in a ratio of 1,15 : 1.

Annexe I. Objectives, Methodology and Conclusions of the Project in Spanish.

1. Objetivos de la Investigación.

Los conjugados poliméricos son nanoconstrucciones multicomponente presentes actualmente en clínica como terapia anticancerígena, tanto como agentes únicos, como formando parte de combinaciones. Estos nanoconjugados tienen el potencial de mejorar farmacológicamente el tratamiento de tumores sólidos, debido a una acumulación pasiva en el tumor (efecto 'EPR') y a un diferente mecanismo de internalización celular y posterior liberación del fármaco(s). La transferencia de conjugados polímero-proteína a uso clínico rutinario, y el desarrollo clínico de conjugados polímero-fármaco anticancerígeno sitúa a los conjugados poliméricos como una de las primeras clases de nanomedicinas con potencial terapéutico antitumoral ya demostrado. La experiencia obtenida con los primeros nanoconjugados en clínica, ha proporcionado las bases para el desarrollo de polímeros conjugados más sofisticados de segunda generación con propiedades terapéuticas mejoradas. El desarrollo de nuevos portadores poliméricos biodegradables con propiedades mejoradas, la utilización de terapia de combinación o el diseño de conjugados dirigidos a nuevas dianas moleculares son algunas de las aproximaciones a seguir para conseguir conjugados más específicos y efectivos considerados de segunda generación. La propiedad de multivalencia que poseen los polímeros nos permite la conjugación de varios compuestos activos en el mismo esqueleto polimérico, la combinación del modulador activo con un citotóxico, otra sustancia activa o un residuo dirigente puede aumentar marcadamente el valor terapéutico de estas macromoléculas. En este sentido, el punto de partida de la presente propuesta es un nuevo concepto establecido por nosotros en 2005 con el desarrollo de HPMA copolimero-AGM-Dox, basado en la terapia de combinación (terapia endocrina + quimioterapia dentro de la misma matriz polimérica) para el tratamiento de cáncer de mama hormono-dependiente (Vicente et al., 2005). El valor terapéutico de esta nueva estrategia ha sido previamente demostrado en modelos celulares, lo que implicaría una clara aplicación potencial en el tratamiento de tumores hormono-dependientes en mujeres postmenopáusicas.

En el presente proyecto, se plantea corroborar la actividad antitumoral del nanoconjugado de combinación HPMA copolimero-AGM-Dox utilizando

232

modelos *in vivo*, así como elucidar las bases moleculares responsables de su destacada actividad anticancerígena. La comprensión del mecanismo de acción molecular nos permitirá el diseño futuro de nanoconjugados de combinación con propiedades mejoradas. En una segunda etapa se propone mejorar el valor terapéutico de esta nueva terapia de combinación mediante la utilización de un polímero biodegradable como portador, ácido poli-L-glutámico (PGA), desarrollando un nuevo conjugado de combinación PGA-AGM-Dox y evaluando su actividad antitumoral en modelos *in vitro* e *in vivo*. La etapa final de la presente tesis doctoral consiste en el desarrollo de un cribado farmacológico utilizando 5 quimio agentes y 3 agentes de terapia hormonal para evaluar su actividad citotóxica en las líneas celulares de cáncer de mama con el objetivo de seleccionar una combinación sinérgica de fármacos con mayor potencial citotóxico que AGM-DOX, que sirva de base para el desarrollo de futuras terapias de combinación.

1.1. Antecedentes.

Para comprobar la hipótesis de partida se desarrolló un conjugado modelo HPMA copolímero-AGM-Dox que transporta una combinación de terapia endocrina (inhibidor de aromatasa (AGM) y quimioterapia (Dox) para el tratamiento de cáncer de mama (figura 1.) (Greco, et al., 2005; Vicent et al., 2005; Greco et al., 2006). Su diseño se basó en dos observaciones principalmente: (i) el copolímero HPMA copolímero-Dox (PK1, FCE28068) es un conjugado en fase clínica II con demostrada actividad en pacientes con tumores de mama quimioresistentes (Vasey et al., 1999) y (ii) los inhibidores de aromatasa pueden actuar de forma sinergíca con quimioterapia (Johnston and Dowsett, 2003). La elección de AGM (inhibidor de aromatasa de primera generación) se debió principalmente a que presenta una funcionalización adecuada para ser conjugado al polímero y está disponible comercialmente, por tanto, AGM fue considerado como el fármaco adecuado en esta primera fase de prueba de concepto (Goss and Strasser, 2001; Pool and Paridaens, 2007).
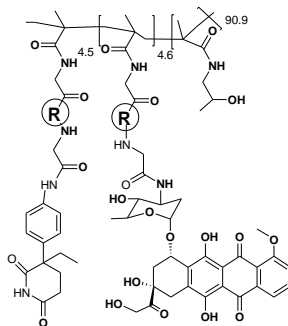
Figura 1. Estructura del conjugado de combinación HPMA copolímero-AGM-Dox.

El conjugado de combinación (HPMA copolímero-AGM-Dox) mostró un aumento muy marcado de citotoxicidad frente a modelos celulares de cáncer de mama positivos en receptores de estrógenos (ER+) (MCF7 y MCF7 Ca (transfectada de forma estable con el gen humano aromatasa (Yue et al., 1994)) en comparación a la actividad citotóxica obtenida con los conjugados individuales por separado (HPMA copolímero-Dox) o una mezcla simple de ambos (HPMA copolímero-Dox + HPMA copolímero-AGM) (Figura 2). Además, experimentos llevados a cabo con una familia de conjugados sintetizados que contienen AGM (los primeros conjugados con terapia endocrina descritos), confirmaron que era necesaria la liberación de AGM para conseguir la inhibición del enzima aromatasa (Greco et al., 2005; Greco et al., 2007).
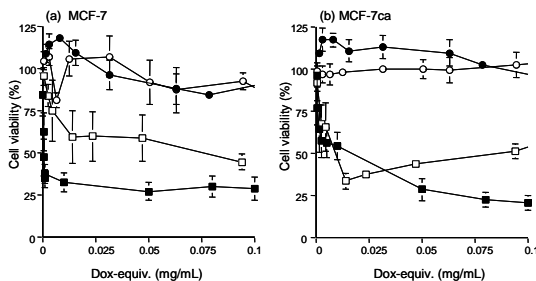
Figura 2. Comparación de la actividad citotoxica de HPMA copolímero-AGM-Dox y mezcla de conjugados simples en células MCF7 (Panel a) y en células MCF7 Ca

234

(panel b). —■— Dox; —□— HPMA copolímero-AGM-Dox; —•— HPMA copolímero-Dox + HPMA copolímero-AGM; —○—HPMA copolímero-Dox.

En una segunda fase se evaluó el mecanismo de acción de HPMA copolímero-Dox y HPMA copolímero-AGM-Dox para entender el efecto sinérgico de citotoxicidad únicamente observable cuando los dos fármacos se hallan covalentemente unidos a la misma matriz polimérica. En este sentido, se analizaron exhaustivamente las diferencias en el tráfico intracelular (unión e internalización celular, mecanismo de endocitosis con diferentes inhibidores de rutas endocíticas y fagocitosis) y en la cinética de liberación de fármaco (transporte lisosomotrópico) (Greco et al., 2005; Vicent et al., 2005; Greco et al., 2006).
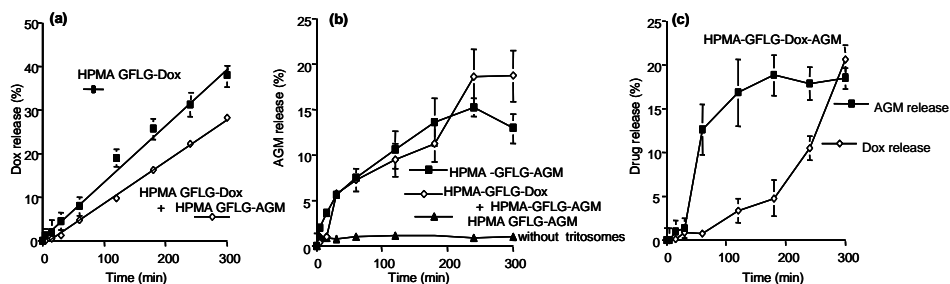
Figura 3. Perfil de liberación de Dox y AGM de los diferentes conjugados de HPMA en presencia de enzimas lisosomales de rata (tritosomas).

Por otra parte, estudios preliminares de posibles diferencias en el mecanismo de acción molecular también se realizaron mediante técnicas de immunohistoquímica (Greco et al., 2007). Los resultados obtenidos sugieren que el aumento de actividad obtenido con el conjugado de combinación es debido principalmente a la diferente cinética de liberación intracelular de los fármacos (Figura 3). Al hallarse en la misma matriz polimérica poseen un perfil de liberación distinto en comparación a los conjugados simples, este cambio en la cinética de liberación induce un aumento de apoptosis celular en las células MCF7 y MCF7 Ca a través de la disminución de la proteína anti-apoptótica Bcl-2 (Greco et al., 2007).

De los datos obtenidos hasta ese momento, era evidente que el conjugado de combinación HPMA copolímero-AGM-Dox muestra un aumento en la actividad antitumoral *in vitro* y que mecanismos moleculares complejos parecen ser los responsables de este efecto sinergístico.

Esta aproximación nos ofrece, claramente, una nueva oportunidad para el tratamiento de cáncer de mama metastático quimioresistente. Además de aumentar la actividad del citotóxico, esta plataforma tecnológica es de aplicación sistémica intravenosa (muy adecuada para el tratamiento de metástasis con elevada angiogénesis) y su mecanismo de internalización celular es diferente evitando mecanismos de resistencia como la sobreexpresión de la p-glicoproteína en membrana celular.

En consecuencia, a la vista de los resultados preliminares obtenidos con HPMA copolimero-AGM-Dox como potente agente antitumoral en modelos *in vitro*, en este proyecto de tesis doctoral se pretende (i) completar el estudio del mecanismo de acción molecular del conjugado de combinación HPMA copolímero-AGM-Dox y evaluar su potencial terapéutico en modelos animales. De este modo podríamos definir el potencial antitumoral de esta terapia de combinación polimérica para el tratamiento de pacientes con cáncer de mama.

La especificidad tumoral debido al efecto EPR depende de la concentración en plasma del polímero circulante, de este modo, portadores poliméricos no-biodegradables tales como el copolímero HPMA o polietilenglicol (PEG) (Mw<40 000 g/mol para asegurar una eliminación renal efectiva), tienen un perfil farmacocinético menos favorable. Por este motivo, una vez demostrada la actividad *in vivo* del conjugado HPMA copolímero-AGM-Dox se propone (ii) mejorar el valor terapéutico de esta nueva terapia de combinación mediante la utilización de un polímero biodegradable como portador, ácido poli-L-glutámico y finalmente (iii) el desarrollo de un cribado farmacológico utilizando 5 quimio agentes y 3 agentes de terapia hormonal en las líneas celulares MCF7 y MDA-MB 321 con el objetivo de seleccionar una combinación sinérgica de fármacos con mayor potencial citotóxico, que sirva de base para el desarrollo de futuros polímeros de conjugados.

2. Metodología.

2.1. Síntesis de conjugados.

2.1.a. PGA-OSucc síntesis y purificación.

Para la síntesis de PGA-AGM, se requiere la activación previa de los grupos carboxílicos. Debido a la pobre reactividad de la amina aromática AGM, una clásica activación de diimida no fue suficiente para el acoplamiento. Los grupos carboxílicos de PGA fueron activados primero por grupo succinimico. PGA (3,55 mmol, 471.4 mg) se disolvió en di-metil-formamida (DMF) anhidra (5 mL), los grupos succínicos (2,33 mmol, 268.4 mg) se añadió hasta alcanzar un máximo del 60% de la activación del grupo carboxílico. Cuando el medio de reacción era completamente transparente, N, N'-diisopropil carbodiimine (DIC) (2,33 mmol, 350 μL) y una cantidad catalítica de 4, dimetilaminopiridina (DMAP) fueron añadidos. La reacción se dejó durante 36 h. El DMF se evaporó por alto vacío y el PGA-OSucc se precipitó por Chloroformo (CHCl$_3$) / acetona (4/1). El producto se purificó mediante lavado con éter (x3) en baño de ultrasonidos (5 min cada uno). El rendimiento fue de 77% y la tasa de activación fue de 41%.

2.1.b. PGA-AGM síntesis y purificación.

PGA-OSucc (0,52 mmol, 91,3 mg) se disolvió en DMF anhidro (5 mL), a continuación, AGM (0,026 mmol, 6 mg) y una cantidad catalítica de DMAP fue añadida. El pH se controló y se ajustó con N, N-diisopropiletilamina (DIEA) a pH 8. La reacción se dejó reaccionar durante 36 h a temperatura ambiente (RT). El DMF se evaporó a vacío elevado y el polímero conjugado se precipitó con acetato de etilo (AcOEt) / acetona 4/1 a 4 ° C. PGA-AGM sal sódica se realizó mediante la adición de bicarbonato de sodio (NaHCO$_3$) 1 M (0,58 mmol, 285 μL). La etapa de purificación por cromatografía de exclusión por tamaño (SEC) se llevó a cabo con el fin de evitar el exceso de sal y el resto de productos que no habían reaccionado. Si una cantidad de DMAP libre se detectó por UV, una diálisis frente a H$_2$O se realizó. Después de la liofilización, el rendimiento de la reacción fue del 60% (60 mg).

2.1.c. PGA-G-AGM síntesis y purificación.

Para realizar PGA-G-AGM, se require la síntesis previa de G-AGM.

G-AGM: Fluorenilmetiloxicarbonilo glicina (Fmoc-G) (0,65 mmol, 193,24 mg) se disolvió en DMF anhidro (5 mL). La activación con DIC (0,975 mmol, 153 µL) se realizó durante 5 min y después se añadió el 1-hidroxibenzotriazol (HOBt) (0,975 mmol, 132 mg). Después de 10 minutos, AGM (0,65 mmol, 147 mg) fue finalmente añadido. El pH se controló y se ajustó a pH 8 con DIEA. La reacción se dejó reaccionar durante 36 h a temperatura ambiente. El DMF se evaporó a vacío elevado y Fmoc-G-AGM se purificó por extracción liq / liq. Fmoc-G-AGM se disolvió en AcOEt (10 mL) y se extrajo con NaHCO3 (3x10 mL). A continuación la fase orgánica se lavó con ácido clorhídrico (HCl) 1 M (3x10 mL), se secó sobre sulfato de sodio (Na$_2$ (SO4)) y se evaporó para producir 90% de un producto blanco. La etapa de desprotección se realizó con piperidina al 20% en AcOEt durante 1 h. La purificación del producto se realizó por columna C18. Las condiciones cromatografías iniciales fueron: agua (H$_2$O) / acetonitrilo (ACN) (30:70). La purificación se controló por TLC (G-AGM Rf: 0, Fmoc Rf: 0,83 con hexano: EtOAc 1:4). El protocolo de detección utilizizado fue doble: UV y tinción Nihindrina. El rendimiento de la reacción fue del 70% (0,46 mmol, 125 mg).

PGA-G-AGM: La síntesis de PGA-G-AGM se realizó mediante el siguiente protocolo. PGA (0,51 mmol, 80,3 mg) se disolvió en DMF anhidro (5 mL), DIC (0,808 mmol, 126,2 µL) fue añadido y después de 5 min HOBt (0,808 mmol, 109 mg). Después de la activación de los grupos de ácido carboxílico por DIC y HOBt, G-AGM (0,0269 mmol, 7,8 mg) se añadió. El pH se controló y se ajustó a pH 8 con DIEA. La reacción se monitorizó por TLC y se dejó reaccionar 36 h a temperatura ambiente. El DMF se evaporó a vacío elevado y el polímero conjugado de fármaco se precipitó por CHCl$_3$/Acetone 4/1 a 4 ° C con agitación media hora y media hora sin agitación. PGA-G-AGM sal de sodio se obtiene mediante la adición de NaHCO$_3$ 1 M (0,51 mmol, 250 µL). La etapa de purificación (Diálisis y columna G25) se llevó a cabo con el fin de evitar el

238

exceso de sal y eliminar el fármaco libre. Después de la liofilización, el rendimiento de la reacción fue del 60%.

2.1.d. PGA-GG-AGM síntesis y purificación.

En este caso, la síntesis previa de GG-AGM también era necesaria, sin embargo Fmoc-GG no estaba disponible comercialmente, por lo tanto Fmoc-GG se sintetizó en un paso anterior.

Fmoc-GG: GG (0,28 mmol, 37,8 mg) se disolvió en una solución de NaHCO3 (10%) (1,6 mL), después se añadió dioxano (0,9 mL) y la reacción se enfrió en hielo. Una vez alcanzada la temperatura adecuada, cloruro de fluorenilmetiloxicarbonilo (Fmoc-Cl) (0,28 mmol, 80 mg) fue cuidadosamente añadido gota a gota. La reacción se dejó reaccionar durante 4 horas en un baño de hielo y durante la noche a temperatura ambiente. Fmoc-GG se purificó por extracción liq / liq. La fase acuosa se extrajo con AcOEt (3x5 mL), a continuación seacidificó con HCl (1 M) hasta pH 2 y se extrajo con EtOAc (3x5 mL). La fase orgánica se recogió, se secó sobre Na2 (SO4) y se evaporó para producir 81% de un producto blanco.

La síntesis GG-AGM y PGA-GG AGM-se llevaron a cabo siguiendo el mismo procedimiento descrito anteriormente para G-AGM y PGA-G-AGM.

2.1.e. PGA-DOX síntesis y purificación.

PGA (0,51 mmol, 80,3 mg) se disolvió en DMF anhidro (5 mL), a continuación, DIC (0,808 mmol, 126,2 µL) fue añadido y después de 5 min HOBt (0,808 mmol, 109 mg) se añadió también como sólido. Después de 10 min, Dox.HCl (0,0269 mmol, 14 mg) se añadió. El pH se controló y se ajustó a pH 8 con DIEA. La reacción se controló por TLC y se dejó reaccionar durante 36 h a temperatura ambiente (TA). DMF se evaporó mediante vacío elevado y el polímero conjugado de droga se precipitó usando CHCl3/Acetone 4 / solución de 1 hora a 4 ° C con agitación y media hora sin agitación media. PGA-Dox sal de sodio se obtuvo por adición de $NaHCO_3$ 1 M (0,51 mmol, 250 µL). La purificación se realizó del mismo modo que los conjugados PGA-X-AGM.

2.1.f. PGA-G-Dox síntesis y purificación.

G-Dox: Bz-G (0,083 mmol, 31,8 mg) se disolvió en DMF anhidro (5 mL), a continuación se adicionó DIC (0,124 mmol, 20 μL) y después de 5 min HOBt (0,124 mmol, 22 mg) se añadió también como sólido. Después de 10 min de activación, Dox, HCl (0,083 mmol, 45,5 mg) fue finalmente incorporado. El pH se controló y se ajustó con DIEA para conseguir pH 8. La reacción se dejó reaccionar durante 36 h a TA. El DMF se evaporó a vacío elevado. El gránulo seco se disolvió en MeOH y la purificación se realizó por cromatografía RP-(C18) con 10 mL de 2-propanol/H_2O (12:88) (v / v), 10 mL de 2-propanol/H_2O (29 : 71) (v / v) y luego 20 mL de MeOH (pH 3,2). El procedimiento de purificación se controló por TLC a través de un sistema de detección de doble fijado en $\lambda = 254$ nm y $\lambda = 366$ nm. Entonces, la desprotección se llevó a cabo en H2 Pd / Cact durante la noche. La solución se filtró a través de celita y con un filtro de 0,2 micras. Después de la eliminación de MeOH, con un rendimiento de 50% fue alcanzada.

PGA-G-Dox se sintetizó siguiendo el mismo procedimiento utilizado para PGA-Dox.

2.1.g. PGA-GG-Dox síntesis y purificación.

La síntesis de GG-Dox y PGA-GG-Dox se llevaron a cabo siguiendo el protocolo descrito para el G-Dox y PGA-Dox, respectivamente.

2.1.h. síntesis y purificación de los conjugados de combinación.

*PGA-AGM-Dox:*PGA-OS (0,259 mmol, 85,45 mg) se disolvió en DMF anhidro (5 mL). Una cantidad catalítica de DMAP se añadió y el pH se ajustó a 8 con DIEA. A continuación se adicionó, AGM (0,027 mmol, 6.3mg). La reacción se controló por TLC y se dejó reaccionar durante 36 h a TA. Entonces se añadió DIC (0,036 mmol, 5,7 μL) y después de 5 min HOBt (0,036 mmol, 4.9 mg). Después de la activación de los grupos de ácido carboxílico por DIC y HOBt, se añadió a continuación Dox (0,024 mmol, 13,6 mg), se ajustó el pH a 8 con DIEA y la reacción se dejó reaccionar durante 36 h más a TA. El DMF se evaporó a vacío elevado y el polímero conjugado precipitó por adición de 5 mL

de CHCl3: acetona (1:1). PGA-AGM-Dox sal sódica se obtuvo mediante la adición de NaHCO3 1 M (0,51 mmol, 250 μL). La purificación se realizó del mismo modo que los conjugados PGA-X-AGM.

PGA-X-AGM-Y-Dox: El PGA se disolvió en DMF anhidro (5 mL). DIC (1,5 eq de X-AGM) se añadió y, después de 5 min el HOBt (1,5 eq de X-AGM). Siguiendo a la activación de los grupos ácido carboxílico mediante DIC y HOBt, se añadió X-AGM, el pH se ajustó a 8 con DIEA y la reacción se dejó reaccionar durante 36 h a TA. El DMF se evaporó a vacío elevado y el polímero conjugado precipitó por adición de 5 mL de CHCl$_3$: acetona (1:1). PGA-X-AGM-Y-Dox sal sódica se obtuvo mediante la adición de NaHCO$_3$ 1 M (0,51 mmol, 250 μL). La purificación se realizó del mismo modo que los conjugados PGA-X-AGM.

2.2. Caracterización de los conjugados

2.2.a. Determinación de la carga de fármaco total y el contenido de fármaco libre en el conjugado sintetizado.

X-AGM y AGM fueron utilizados como un estándar para producir una curva de calibración. Se disolvió en MeOH grado HPLC para tener una solución stock de 1 mg/mL. Este se diluyó entonces para producir una gama de concentración (0-65 μg/mL para AGM y 0-65 μg/mL de X-AGM). La absorbancia UV de cada muestra se determinó entre 200-400 nm.

La otra posibilidad para evaluar la cantidad total de carga de fármaco consiste en la cuantificación del fármaco que no ha reaccionado. El primer paso fue realizar la curva de calibración de HPLC utilizando las soluciones añadidas para la curva de calibración UV. A continuación, el precipitado de AcOEt/acetona (4/1) obtenido después de la precipitación del polímero conjugado de fármaco, se evaporó, se disolvió en 10 mL de HPLC, y se inyectó en HPLC. La carga de fármaco se determinó de manera indirecta usando RP18 columna (125x4mm), con un flujo de 1mL/min y usando un gradiente de elución [A: H$_2$O +0,1% TFA

milliQ, disolvente B: ACN +0,1% TFA]. El tiempo total de análisis fue de 25 min y con el gradiente siguiente: t = 0 A 90%, t = 4 Un 90%, t = 19 A 10%, t = 21 A = 90%, t = 25 A = 90%, t = 40 A 0%, t = 42 A 0%. Un estándar interno (estradiol) se usó para la cuantificación del AGM. El tiempo de retención fue de 2 min para GG-AGM, 6 min para G-AGM y 5 min para AGM.

Para evaluar la carga de fármaco libre, 100 μL de una concentración conocida de polímero conjugado de fármaco se añadió con 100 μL de bicarbonato sódico y 100uL de estradiol (1 μg/mL) como patrón interno. X-AGM libre y estradiol se extrajo a fondo con una mezcla de AcOEt / Isopropyl alcohol 4/1 (10s x 3). La capa orgánica superior se recuperó cuidadosamente y se secó a través de flujo de N2. El residuo seco se disolvió en 100 μL de grado HPLC ACN. En paralelo para construir una curva estándar, los mismos puntos utilizados para la determinación de la carga de fármaco total se utilizaron para hacer la curva HPLC estándar. 100 μL de cada punto se añadió a una mezcla de 100 μL de bicarbonato, 100μL de estradiol y 700 μL de agua MilliQ y después se extrajo con AcOEt / alcohol isopropílico (4/1) como se ha descrito antes. La cantidad de fármaco libre se determinó por HPLC usando el mismo método descrito para la carga de fármaco no directa. El tiempo de retención fue de 2 para GG-AGM, 6 min para G-AGM, 5 min para AGM y 12 min para el estradiol.

2.2.b. Determinación de Dox total y libre por HPLC.

Para determinar la carga de fármaco total de PGA-Y-Dox conjugado, 100 μL de una concentración conocida del polímero se añadió a una solución de ácido (1 mL de HCl 2 M). 100 μL de Dau (1 μg/mL) se utilizó como estándar interno. La solución se dejó 30 minutos a 80 ° C. Después de enfriar hasta TA, 360uL de 5M de NaOH se añadió para neutralizar el pH. Dox aglicona se extrajo con una mezcla de $CHCl_3$/Isopropyl 4/1 (30 x 3). La capa acuosa superior se retiró cuidadosamente y la fase orgánica se secó usando flujo de N2. El residuo seco se disolvió en 100 μL de MeOH grado HPLC. En paralelo el mismo proceso se llevó a cabo con una mezcla de Y-Dox y daunorrubicina (DAU) para construir una curva estándar. Los estándares se disolvieron en 1 mL de MeOH grado HPLC para dar 100 μg/mL de solución madre de la que se preparó un intervalo

de concentración (5-100 µg/mL). La cantidad de fármaco total liberado se determinó por HPLC utilizando columna RP18 (125x4 mm), con un flujo de 1mL/min y usando un gradiente de elución [A: 2-propanol/H_2O 12:88 (v/v), disolvente B: 2-propanol/H_2O 29:71 (v/v)] se ajustó a pH 3,2 con ácido fosfórico. Tiempo total fue de 25 min y el perfil del gradiente utilizado fue: t = 0% A 0, t = 1 A 60%, t = 3 A 60%, t = 8 A = 0%, t = 18 A = 0%, t = 20 Un 100%, t = 20 A 100%. Mediante detección por fluorescencia (λ excitación = 485nm y λ emisión = 560 nm) se supervisaron los estándares internos Dox y Dau. El tiempo de retención (tr) fue de 15 min para aglicona Dox y 20 min para aglicona Dau.

Para evaluar la carga de fármaco libre, 100 µL de una concentración conocida de conjugado se añadió a 100 µL de NaHCO3 y 100 µL de Dau (1 µg/mL) como patrón interno. La Dox libre y la Dau se extrajo con alcohol CHCl3/Isorpopyl 4/1 (30x3). La capa acuosa superior se retiró cuidadosamente y la fase orgánica se seco a través de flujo de N2. El residuo seco se disolvió en 100 µL de MeOH grado HPLC. En paralelo el mismo proceso también se llevó a cabo con una mezcla de Dox y Dau para construir una curva estándar. Los estándares se disolvieron en 1 mL de MeOH grado HPLC para tener una solución madre de 100 µg/mL de la cual se preparó un intervalo de concentración (0-65 µg/mL). La cantidad de fármaco libre se determinó por HPLC utilizando columna RP18 (125x4 mm), con un flujo de 1mL/min y usando un gradiente de elución [A: 2-propanol/H_2O 12:88 (v/v), disolvente B: 2 -propanol/H_2O 29:71 (v / v)], a continuación se ajustó a pH 3,2 con ácido fosfórico. El tiempo total fue de 42 min y el perfil de gradiente utilizado fue: t = 0% A 0, t = 1% A 0, t = 26 A 100%, t = 27 A = 50%, t = 37 A = 50%, t = 40 A = 0%, t = 42 A 0%. Para cuantificar la Dox y la Dau se utilizó la detección por fluorescencia El Tr fue de 20 min para Dox y 30 min para Dau. Para evaluar la carga de fármaco de manera indirecta se utilizó el mismo procedimiento que el desarrollado para PGA X AGM.

2.2.c. Peso Molecular (MW) determinación por GPC.

Para evaluar la masa del conjugado, 100 μL de 3 mg/mL exactamente PGA-G-Dox solución se inyectó en GPC utilizando dos columnas TSK Gel en serie G2500 PWXL y PWXL G3000 con Viscoteck TDA detector 302 en serie con una detección UV. La fase móvil usando es PBS 0,1 M.

2.2.d. Small angle neautron scattering (SANS).

Los experimentos de SANS se realizaron en el reactor HFR 57 MW (High-Flux Reactor) en el Instituto Max Von Laue-Paul Langevin (ILL) de Grenoble, Francia. Los conjugados se disolvieron a 10 mg/mL en D_2O y los experimentos de dispersión se realizaron a 37 °C, condiciones que imitan la conformación en el cuerpo. Todos los experimentos se realizaron en células de cuarzo de 2 mm con la medición de tiempos de 1 h por muestra.

2.3. Estabilidad en plasma de conjugado y cinética de la liberación del fármaco en presencia de la catepsina B.

2.3.a. Cinética de liberación de fármaco en presencia de catepsina B.

PGA-X-AGM, PGA-Y-Dox y PGA-X-AGM-Y-Dox (3 mg/mL) se incubaron (37 ° C) en una solución de acetato sódico (20 mM, pH 6), DTT (5 mM) y EDTA (2 mM). Para comenzar la degradación 5 unidades de catepsina B (100 μL) eran adicionadas. Alícuotas de los conjugados (150 μL) se tomaban de forma consecutiva en momentos seleccionados (0, 0,5, 1, 2, 5, 8, 24, 48, 72, 96 h) horas hasta dos semanas, y se congelaban inmediatamente en nitrógeno líquido hasta realizar el ensayo de HPLC. Para los experimentos control se reproducía el mismo ensayo pero sin conjugados.

Una vez recopiladas las muestras, se descongelaron y se añadieron a tubos de polipropileno, completando hasta 1 mL con H_2O incluyendo 100μL de Dau (1 μg/mL) como patrón interno y 100 μL de tampón de formiato de amonio (pH 8,8), seguido por la adición de una mezcla de CHCl3: isopropanol 4 : 1 (5 mL). A continuación las muestras fueron extraídas a fondo con el vórtex (3x30s). La capa acuosa superior se retiró cuidadosamente y el disolvente se evaporó bajo

N$_2$. El residuo seco se disolvió en 100 μL de metanol para análisis por HPLC. La cantidad de liberación de fármaco de conjugados se determinó mediante HPLC utilizando el método descrito para el fármaco libre, y los metabolitos liberados fueron identificados por MALDI-TOF. En un volumen de 30 μL las muestras sin ningún tipo de preparación se inyectaron en GPC para seguir el perfil de degradación del polímero.

2.3.b. Estabilidad en plasma.

Los conjugados (3 mg/mL) se incubaron a 37°C en suero recién extraído de ratones Balb/c hasta 24 h. En las horas programadas se recogieron alícuotas de 100 μL a los cuales se añadió 100 μL de MeOH con el fin de precipitar las proteínas del suero y recuperar el fármaco libre. Después de la centrifugación (12000 g, 5 min), los sobrenadantes se analizaron por HPLC como se informó anteriormente.

2.3.c. Identificación de metabolitos por MS.

Los metabolitos X-AGM se identificaron utilizando un sistema UPLC-MS de Waters. El método fue optimizado masa capilar (kV) 3,50, el cono (V) 20, Extractor (V) 6, RF Lente (V) 0,2. La temperatura de la fuente era 120 ° C y la temperatura de desolvatación era de 380 ° C. Desolvatación Gas y el cono de gas eran respetablemente 950 y 50 L / H. El parámetro analizador y detector era lo normal para este tipo de masa ZQ. El método UPLC era 90/10 H$_2$O + 0,1% de ácido fórmico / ACN ácido fórmico 0,1% a 10/90 H$_2$O + 0,1 ácido fórmico / ACN ácido fórmico + 0,1% en 15 min. Las condiciones iniciales se recuperaron en 2 minutos y el sistema se equilibró en 4 min. Después de 20 μL de filtración de la muestra, se inyectó. Este sistema tenía una doble detección por UV (DAD), λ = 268 nm se utilizó en este caso y el TIC de masa.

Para los metabolitos Y-Dox, el Pm es mayores, en consecuencia un experimento de MALDI-TOF se realizó. La matriz utilizada fue α-ciano-4-hydroxucinnamic ácido, se extrajo con un láser pulsado a 337 nm. La adquisición se realizo en modo reflectron.

2.4. Ensayos *in vitro*.

2.4.a. Cultivo celular.

Para los ensayos *in vitro* las siguientes líneas celulares inmortalizadas fueron utilizadas: MCF7, MCF7 Ca, 4T1 (cáncer de mama metastásico de origen murino) y MDA-MB 231 (cáncer de mama humano ER-). La línea celular MCF7 Ca es el resultado de la transfección estable del gen de la aromatasa humana en MCF7 (cáncer de mama humano hormono dependiente). La línea MCF7 Ca fue generosamente proporcionada por la Universidad de Cardiff. Las células se cultivaron en placas P100 con el medio adecuado suplementado con suero bovino fetal (SBF) (10%) a 37 °C y 5% CO_2. Para MCF7 Ca, el SBF utilizado fue previamente tratado con el fin de imitar las condiciones post-menopáusicas añadiendo una alícuota de estradiol a una concentración final de 10^{-9} M para el cultivo celular. En todos los casos, el medio celular se cambiaba cada dos días para inducir el crecimiento celular. Una vez alcanzada una confluencia celular de 70-90%, después de retirar el medio, y lavar las células con PBS, se añadía 1 mL de tripsina durante 5 min a 37 ºC, las células despegadas se recuperaban con 9 mL de medio libre y se centrifugaban durante 5 min a 200 g a TA. El sobrenadante se retiraba cuidadosamente y a continuación las células se resuspendían en medio fresco. Tras el recuento celular utilizando una cámara de Neubauer, las células fueron sembradas en placas de P100 a 40.000 cels/mL o a 20.000 cels/mL para alcanzar la confluencia después de una o dos semanas, respectivamente.

2.4.b. Preparación de SBF empobrecido en estrógeno.

Con el fin de cultivar MCF7 Ca imitando las condiciones hormonales de mama en mujeres postmenopáusicas, el SBF fue previamente tratado para eliminar la mayoría de los factores de crecimiento y hormonas de origen y posteriormente se adicionó un nivel de hormona control al medio final. Para ello, el SBF (500 mL) se desactivó a 56ºC durante 30 min. Una vez a temperatura ambiente, se ajustó a pH 4,2 con HCl (5 M) y se equilibró a 4 °C. A continuación una

suspensión de carbón (25 mL) preparada añadiendo 18 mL de H_2O dd, 0,2 g de carbón Norit A y 0,01 g de dextrano 80.000 era añadida al SBF frío durante16 horas a 4 °C. Posteriormente se centrifugó (40 min a 12.000 g) y por filtración gruesa se separó el carbón vegetal. El pH se reajustó a 7,2 con NaOH (5 M) y el SBF obtenido era esterilizado por filtración con filtros Millipore de 0,2 micras y alicuotado en recipientes universales a -20°C. Finalmente, para el cultivo de células MCF7 Ca, una alícuota de estradiol (concentración final 10^{-9} M) se adicionó al medio de cultivo conteniendo 10% de SBF pretratado.

2.4.c. Ensayo de MTS para la determinación de la viabilidad celular.

Para poder realizar ensayos de viabilidad celular, en primer lugar se realizó una curva de crecimiento para todas las líneas celulares de cáncer de mama utilizadas. Las concentraciones de siembra celular óptimas para los ensayos de citotoxicidad fueron determinadas. 50 μL de las concentraciones seleccionadas de MCF7 Ca (4000cels/pocillo), 4T1 (2000 cels/pocillo) y MDA MB 231 (10000 cels/pocillo) se sembraron en placas transparentes de 96 pocillos (P96). Transcurridas 24 h en el caso de MCF7 Ca y 4T1cells y 48 h para MDA MB231, se adicionaron a los cultivos celulares diluciones seriadas de los conjugados poliméricos o compuestos libres (50 μL) (n = 6) y se incubaron durante 72 h a 37ºC y 5% de CO_2 con el fin de evaluar los posibles efectos citotóxicos. Las células control fueron tratadas idénticamente, añadiendo medio sin compuestos. La viabilidad celular se determinó procediendo posteriormente al ensayo colorimétrico del MTS [3 - (4,5-dimetiltiazol-2-il) -5 - (3-carboximetoxifenil) -2 - (4-sulfopheyl) 2H-tetrazolio], siguiendo instrucciones del fabricante (Cell Titer 96® AQ_{ueous} Non-Radioactive Cell Proliferation Assay Technical Bulletin *TB169,* Promega Corporation). 10 ul de solución de MTS se añadió a cada pocillo, y las células se incubaron durante otras 2 h a 37°C, CO_2 5%. Las células vivas y metabólicamente activas son capaces de reducir el MTS a formazano, un producto soluble en el medio de cultivo, la absorbancia del formazano puede medirse a 490 nm y es directamente proporcional al número de células vivas en el cultivo. El efecto citotóxico se obtiene al comparar

directamente el resultado obtenido en las células no tratadas (control) frente a las células tratadas con los compuestos.

El mismo sistema de determinación de viabilidad celular fue utilizado para el desarrollo de la plataforma de cribado (HTPS). Sin embargo, en este caso las líneas celulares MCF7 y MDA MB 231 se cultivaron con antibiótico P/S (1%), con el fin de evitar cualquier posible contaminación durante la utilización del robot TECAN (condiciones no estériles controladas), imprescindible para la dispensación de los compuestos y sus combinaciones en las placas de 96 pocillos.

2.5. Ensayos *in vivo*.

2.5.a. Modelo de tumor en ratones atímicos con células MCF7 Ca.

Todos los experimentos con animales se realizaron de acuerdo con las directrices establecidas por el Consejo de las Comunidades Europeas (86/609/ECC) y por el Real Decreto Español 1201/2005. Todos los procedimientos experimentales fueron aprobados por el Cuidado de Animales institucional. Ratones atímicos hembra Balb/c de 4-6 semanas de edad se adquirieron de Harlan (Europa). Los animales fueron alojados en un entorno libre de patógenos bajo condiciones de control. La ovariectomía se realizó bajo sevofluorano 1 semana antes de la inoculación de células. Las células MCF7 Ca se resuspendieron en matrigel y 10 millones de células en una alícuota de 100 μL se inyectaron en cada animal, en la tercera mama. Comenzando un día después de la inoculación de células, los animales recibían 100 μL de androstenodiona subcutánea (0,1 mg/ratón/día). La evolución del crecimiento tumoral se supervisaba dos veces a la semana midiendo el volumen del tumor con un calibrador para calcular el tamaño de los tumores. En el momento en que los tumores alcanzaban el tamaño máximo autorizado, los ratones se sacrificaban y el tumor era extirpado para realizar estudios histológicos y de vascularización.

Posteriormente al proceso de optimización del modelo *in vivo*, los conjugados de polímero se ensayaron con el fin de evaluarse su actividad antitumoral. Por

tanto, 10 millones de células MCF7 Ca fueron inyectados en la tercera mama. Una vez que el tamaño del tumor alcanzaba $0,2$ cm^3, los conjugados se inyectaban por vía intravenosa 3 veces cada 3 días y el peso del animal y el tamaño del tumor eran evaluados dos veces a la semana. Cuando el tumor alcanzó el tamaño máximo autorizado, corazón, hígado, riñón y bazo se extrajeron, se pesaron y se fijaron para continuar con análisis histológicos. En paralelo, los tumores fueron congelados en hielo seco para el análisis de expresión de proteínas mediante western blot.

2.5.b. Modelo de tumor inducido por células 4T1.

Ratones hembra Balb/c de 4-6 semanas fueron comprados en Harlan Inc. (Europa). Los animales fueron alojados en un entorno libre de patógenos bajo condiciones de control. Dos concentraciones diferentes de células 4T1 ($5x10^5$ y 10^6 células) fueron inyectadas en la tercera mama. El crecimiento del tumor se siguió cada día. Una vez que el tamaño límite del tumor era alcanzado (1cm^3), los ratones se sacrificaban y los órganos principales y el tumor se extraían con el fin de realizar estudios histológicos y vascularización.

En una segunda etapa, con el fin de testar la actividad antitumoral de los conjugados de polímero en el modelo murino 4T1, $5x10^5$ células fueron inyectadas en la tercera mama. Transcurridos 8 días el tamaño del tumor alcanzó $0,1$ cm^3 y a continuación los conjugados se inyectaban por vía intravenosa 3 veces cada 3 días y el peso de los animales así como el tamaño del tumor se evaluó cada día. Cuando el tumor alcanzó el tamaño máximo autorizado 1 cm^3, corazón, hígado, riñón y bazo se extrajeron, pesaron y se fijaron para realizar estudios histológicos y el tumor fue congelado para el análisis de expresión proteica mediante western blot.

2.5.c. Análisis de la vascularización del tumor.

Los tumores desarrollados en ambos modelos *in vivo* se retiraron y se analizaron para evaluar la vascularización y el poder de penetración de nuestros

compuestos. Diferentes tamaños de tumor se desarrollaron en 10 ratones y cuando el tamaño del tumor alcanzó de 0,1 a 0,5 cm3, una solución de BSA-azul de Evans se inyectó por vía intravenosa. Una hora después de la inyección, los ratones se sacrificaron y el tumor, así como varios órganos se extrajeron. El tumor fue puesto en 1 mL de formamida durante 48 h a 60 °C con el fin de extraer el azul de Evans. La cuantificación se realizaba entonces en UV a 620 nm.

2.5.d. Análisis toxicológico: Evaluación hepática en sangre.

La sangre extraída de corazón se centrifugó a 4000 g durante 10 minutos para obtener el plasma. El plasma fue enviado a Analitica Clínica Veterinaria Lab (ACVLAB) para evaluar las características de las diferentes enzimas implicadas en el daño hepático como transaminasa glutámico oxalacética (GOT), transaminasa glutámico piruvato (GPT), lactato deshidrogenasa (LDH) y fosfatasa alcalina (ALP).

2.5.e. Análisis histológico.

El tumor fue retirado de los animales control después de la optimización de ambos modelos *in vivo*. A continuación los tumores se lavaron en PBS y se fijaron en paraformaldehído (PFA) durante una noche. El exceso de PFA se eliminó por lavado con PBS a través de una fuerte de agitación (200 rpm) durante 20 min 3 veces. Finalmente, las muestras se almacenaron en una solución de PBS con 0,05% de azida sódica. Con el fin de incluir las muestra en parafina, una deshidratación previa de las muestras a través de 2 min de incubación en baños de alcohol de concentración creciente (30%, 50%, 70%, 96% y 2 baños de 100%) se llevó a cabo, seguido por 2 lavados en xileno de 1 min para incluir finalmente la muestra en parafina. A continuación, el bloque de parafina se redujo a un grosor de 4 micras y se instaló en Superfrost Plus portaobjetos de vidrio para proceder a la tinción hematoxilina-eosina.

La hematoxilina tiene un profundo color azul-morado y tiñe los ácidos nucleídos de las células mediante una reacción compleja. La eosina es de color rosa y tiñe las proteínas forma no específica. En un tejido típico, los núcleos están teñidos

en azul, mientras que el citoplasma y la matriz extracelular tienen diferentes grados de tinción de color rosa. Para la tinción de hematoxilina-eosina, en primer lugar los cortes de 4 micras se desparafinaron con xileno y posteriormente las muestras se rehidrataron con una batería de etanoles decreciente (100%, 95%, 70%, 50%, 30%, agua destilada). A continuación se sumergieron en 2 baños de agua de 5 min seguido de baño de hematoxilina 2 min y 2 lavados de agua de 5 min. Posteriormente los portaobjetos se incubaron 3 min en carbonato de litio y HCl al 0,25% en etanol al 70% para eliminar el exceso de tinción hematoxilina. Después de 2 lavados en agua durante 5 min, los cortes se incubaban en un solución fresca de eosina-floxina (0,35% de eosina, 1,1% de floxin a 2%, 83 mL de alcohol absoluto, 3,3 mL de agua destilada y ácido acético 450 µL) durante 6 min. Para finalizar, los cortes se lavaron hasta eliminar los restos de tinción y se deshidrataron de nuevo con diferentes baños en alcohol de graduación creciente. Tras el baño con etanol absoluto, los cortes se lavan con xileno y se montan con el medio de montaje no acuoso Eukitt.

2.5.f. Inmunodetección por Western blot.

Las proteínas contenidas en los tumores extraídos de los ratones después de 16 días de tratamiento en el modelo 4T1 se separaron mediante electroforesis en geles de poliacrilamida-SDS (dodecilsulfato sódico). De este modo las bandas de proteína obtenidas según su peso molecular eran posteriormente transferidas a membranas que permiten su inmunodetección. Para ello, los tumores extraídos se homogeneizaron en tampón RIPA (150 mM NaCl, 1% de NP40, 0,5% de desoxicolato de sodio, 0,1% SDS, 50 mM Tris PH8, 50 mM NaF, 100µM Na3VO4 y la tableta de cóctel inhibidor de la proteasa), seguido de 15 min en agitación a 4 °C, una serie de tres sonicaciónes 5 s y 1 h a 4 °C en agitación. A continuación, la solución obtenida se centrifugó durante 20 min a 13.500 g, 4 ℃ y los niveles de proteína contenida en el sobrenadante se determinaron mediante el ensayo de Bradford. 100 µg de proteína se mezclaron con tampón de muestra desnaturalizante 5xSDS y se hirvió durante siete minutos a 95 °C. Dependiendo del peso molecular de la proteína que se requiere analizar, se seleccionaba un porcentaje u otro de acrilamida, en este caso las proteínas se separaron a través de geles de 8% a 15% SDS-PAGE. Después de la electroforesis, las proteínas se

transfirieron a membranas de PVDF (Amersham Pharmacia Biotech, UK). Posteriormente las membranas se bloquearon en 5% de leche desnatada durante 2 h, y se incubaron durante la noche a 4 ºC con los siguientes anticuerpos primarios: beta-actina y α-tubulina (Sigma), bax, (Santa Cruz Biotechnology), caspasa 3, Beclin-1, LC3B, pAKT, Bcl2 y VEGF (Cell Signaling), iNOS (Cayman Chemical) y HIF1α (BD Biosciences Pharmingen). El exceso de anticuerpos se retiró por lavado de las membranas en PBS/0,1% de Tween 20. Seguidamente las membranas se incubaron durante 1 h con anticuerpos secundarios específicos para el primario a detectar y marcados con peroxidasa (cabra anti-IgG de ratón, asno anti-IgG de conejo y conejo anti IgG de cabra) (1:5000) (Santa Cruz Biotechnology Inc., Santa Cruz, CA, EE.UU.). Después de 3 lavados en PBS/0,1% de Tween 20, la inmunodetección se realizó mediante el sistema de detección por quimioluminiscencia intensificada ECL Western Blot (Amersham Pharmacia Biotech, Reino Unido), de acuerdo con las instrucciones del fabricante. Los niveles relativos de proteína se cuantificaron por densitometría con el programa Scion Image. Los resultados fueron normalizados utilizando β-actina como referencia.

2.5.g. Análisis estadístico.

Los resultados procedentes de ensayos *in vitro* han sido expresados como media ± SD (n = 3). Los resultados obtenidos de cada experiencia *in vivo* han sido expresados como media ± SEM (n = 4).

El análisis estadístico se ha realizado mediante el programa informático GraphPad Prism 5.

Los valores obtenidos de las experiencias se analizaron empleando ANOVA simple y el método de la *t* de Dunnett para comparaciones múltiples. Este método permite comparar los valores medios obtenidos para varios grupos problema respecto a un único grupo control en un mismo experimento, teniendo en cuenta el error asociado a las comparaciones múltiples (Dunnett, 1964). La significatividad respecto a la diferencia entre los grupos tratados y el control es (*) cuando el valor de *t* obtenido es mayor que el tabulado para un margen de confianza del 95% ($p < 0,05$), (**) cuando es mayor del 99% ($p < 0,01$) y (***)

cuando es mayor del 99,9% (p < 0,001). No empleamos símbolo indicativo cuando la diferencia respecto al grupo control no es significativa.

3. Conclusión.

- Dos modelos *in vivo* de cáncer de mama han sido establecidos, optimizados y caracterizados a partir de dos líneas celulares inmortalizadas, MCF7 Ca humanas y 4T1 murinas.

- La prueba de concepto de sinergismo ha sido demostrada con HPMA copolímero-AGM-Dox, mostrando una diferencia significativa en la inhibición del crecimiento del tumor en comparación con Dox, HPMA copolímero-Dox o la combinación HPMA copolímero-AGM + HPMA copolímero-Dox. Ambos conjugados han ejercido una disminución importante del volumen tumoral en comparación con Dox en el modelo *in vivo* inducido utilizando la células humanas MCF7 Ca.

- Se han establecido diferencias en el mecanismo molecular responsable del efecto antitumoral obtenido con ambos conjugados HPMA copolímero-AGM-Dox y HPMA copolímero-Dox. HPMA copolímero-AGM-Dox indujo una inhibición significativa de las proteínas involucradas en angiogenesis (VEGF) desde el segundo dia después de la última inyección, en comparación con HPMA copolímero-Dox y el control. Por lo tanto, HPMA copolímero-AGM-Dox presentaba un efecto inhibidor tumoral temprano en comparación con HPMA copolímero-Dox. Este mecanismo se completa a largo plazo con la inducción de autofagia por HPMA copolímero-AGM-Dox frente al efecto apoptótico generado por HPMA copolímero-Dox.

- Una plataforma de combinación mas revelante para una aplicación clínica crónica ha sido desarrollada utilizando PGA como portador. Tres familias PGA-X-AGM, PGA-Y-Dox y PGA-X-AGM-Y-Dox han sido sintetizadas, caracterizadas y evaluadas en cultivo celular.

-Una relación directa entre la conformación en solución y la actividad *in vitro* ha sido demostrada por los conjugados PGA de combinación.

253

- El mejor candidato, PGA-(G-AGM)$_{5mol\%}$ - (Dox)$_{5mol\%}$, fue seleccionado para su evaluación *in vivo* y mostró un retraso significativo en el crecimiento tumoral en el modelo de ratón 4T1, 10 días después de la primera inyección en comparación con los otros grupos.

- Nuevos candidatos (quimioterapia + terapia endocrina 2ª generación) han sido evaluados *in vitro* a través de una plataforma de cribado con el objetivo de identificar una combinación de fármacos con mayor efecto sinérgico. Esto permitirá sintetizar conjugados de combinación con mayor eficacia en etapas posteriores. La mejor combinación encontrada ha sido (PTX, 4-OHT) en la relación (1,15:1).

4. Bibliografia.

Goss, P.E. and Strasser K.(2001). Aromatase Inhibitors in the Treatment and Prevention of Breast Cancer. J. Clin. Oncol. 19(3): 881-894.

Greco, F., Vicent, M. J., Gee, S., Jones, A.T., Gee, J., Nicholson, RI., and Duncan, R. (2007). "Investigating the mechanism of enhanced cytotoxicity of HPMA copolymer-Dox-AGM in breast cancer cells." J Control Release 117(1): 28-39.

Greco, F., Vicent, M.J., Penning, N.A., Nicholson, R.I. and Duncan, R. (2005). "HPMA copolymer-aminoglutethimide conjugates inhibit aromatase in MCF-7 cell lines." J Drug Target 13(8-9): 459-470.

Johnston, S. R. and Dowsett, M., (2003). Aromatase inhibitors for breast cancer: lessons from the laboratory. Nat Rev Cancer 3(11): 821-831.

Poole, R. and Paridaens, R. (2007). The use of third-generation aromatase inhibitors and tamoxifen in the adjuvant treatment of postmenopausal patients with hormone-dependent breast cancer: evidence based review. Current Opinion in Oncology. 19(6): 564-572.

Vasey, P.A., Kaye, S.B., Morrison, R., Twelves, C., Wilson, P., Duncan, R., Thomson, A.H., Murray, L.S., Hilditch, T.E., Murray T., Burtles, S., Fraier, D., Frigerio, E., and Cassidy, J. (1999). "Phase I clinical and pharmacokinetic study of PK1 [N-(2-hydroxypropyl)methacrylamide copolymer doxorubicin]: first member of a new class of chemotherapeutic agents-drug-polymer conjugates. Cancer Research Campaign Phase I/II Committee." Clin Cancer Res 5(1): 83-94.

Vicent, M. J., Greco, F., Nicholson, R.I., Paul, A., Griffiths, P.C., and Duncan, R. (2005). "Polymer therapeutics designed for a combination therapy of hormone-dependent cancer." Angew Chem Int Ed Engl 44(26): 4061-4066.

Yue, W., Zhou, D., Chen, S. and Brodie, A. (1994). "A new nude Mouse model for postmenopausal breast cancer using MCF-7 cells transfected with human aromatase gene." Cancer research 54: 5092-5095.

Annexe II. Tumour Node Metastasis (TNM) nomenclature.

TNM	Criteria
T1 m1c	The tumour is 0.1cm across or less
T1 a	The tumour is more than 0.1 cm but not more than 0.5 cm
T1 b	The tumour is more than 0.5 cm but not more than 1 cm
T1c	The tumour is more than 1 cm but not more than 2 cm
T2	The tumour is more than 2 cm, but no more than 5 cm across
T3	The tumour is bigger than 5 cm across
T4 a	The tumour has spread into the chest wall
T4 b	The tumour has spread into the skin and the breast may be swollen
T4c	The tumour has spread to both the skin and the chest wall
T4 d	Inflammatory carcinoma – this is a cancer in which the overlying skin is red, swollen and painful to the touch

TNM	Criteria
N1	Cancer cells are in the upper levels of lymph nodes in the armpit but the nodes are not stuck to surrounding tissues
N2 a	There are cancer cells in the lymph nodes in the armpit, which are stuck to each other and to other structures
N2 b	There are cancer cells in the lymph nodes behind the breast bone (the internal mammary nodes), which have either been seen on a scan or felt by the doctor. There is no evidence of cancer in lymph nodes in the armpit
N3 a	There are cancer cells in lymph nodes below the collarbone
N3 b	There are cancer cells in lymph nodes in the armpit and behind the breast bone
N3 c	There are cancer cells in lymph nodes above the collarbone

TNM	Criteria
cMo (i+)	It means there is no sign of the cancer on physical examination, scans or X-rays but cancer cells are present in blood, bone marrow, or lymph nodes far away from the breast cancer – the cells are found by laboratory tests
M1	It means the cancer has spread to another part of the body

Annexe III. Breast cancer stage.

Breast cancer stages	Classification TNM
Stage 1	T1,N0,M0
Stage 2 A	(T0,N1,M0), (T1,N1,M0), (T2,N0,M0)
Stage 2 B	(T2,N1,M0), (T3,N0,M0)
Stage 3 A	(T0,N2,M0), (T1,N2,M0), (T2,N2,M0), (T3,N1,M0), (T3,N2,M0)
Stage 3 B	(T4,N0,M0), (T4,N1,M0), (T4,N2,M0)
Stage 3 C	Any T,N3,M0
Stage 4	Any T,any N, any M